Isolation Of New Alleles Of Phytochrome Genes Of Tomato

(*Solanum lycopersicum*)

Thesis Submitted For The Degree Of

Doctor Of Philosophy

By

Sherinmol Thomas

2013

Department Of Plant Sciences

School Of Life Sciences

University Of Hyderabad

Hyderabad-500 046

India

Enrollment No. **07LPPH06**

ISOLATION OF NEW ALLELES OF PHYTOCHROME GENES OF TOMATO (*Solanum lycopersicum*)

SHERINMOL THOMAS

UNIVERSITY OF HYDERABAD
Department of Plant Sciences
School of Life Sciences
Hyderabad-500 046
India

UNIVERSITY OF HYDERABAD

DEPARTMENT OF PLANT SCIENCES

SCHOOL OF LIFE SCIENCES

UNIVERSITY OF HYDERABAD

CERTIFICATE

This is to certify that the thesis entitled "ISOLATION OF NEW ALLELES OF PHYTOCHROME GENES OF TOMATO (*Solanum lycopersicum*)" is based on the results of the work done by **Ms. Sherinmol Thomas** for the degree of **Doctor of Philosophy** under my supervision. This work has not been submitted for any degree or diploma of any other University or Institution.

HEAD

DEPARTMENT OF PLANT SCIENCES

PROF R P SHARMA

SUPERVISOR

DEAN

SCHOOL OF LIFE SCIENCES

DEPARTMENT OF PLANT SCIENCES

SCHOOL OF LIFE SCIENCES

UNIVERSITY OF HYDERABAD

DECLARATION

I hereby declare that the work presented in this dissertation has been carried out by me under the supervision of **Prof R P Sharma** and that this has not been submitted for a degree or diploma in any other university.

DATED : June 2013

PLACE : Hyderabad **SHERINMOL THOMAS**

PROF R P SHARMA

SUPERVISOR

To,
My Beloved Parents
and
Husband.....

ॐ

पूर्णमदः पूर्णमिदं पूर्णात्पुर्णमुदच्यते।

पूर्णस्य पूर्णमादाय पूर्णमेवावशिष्यते ॥

(ईशावास्योपनिषत्)

(pūrṇamadaḥ pūrnamidam pūrṇāt pūrṇamudacyate,

pūrṇasya pūrṇamādāya pūrṇamevāvaśiṣyate.

Īśāvāsyopaniṣat)

Aum

That is the whole; this is the whole

From wholeness emerges wholeness

wholeness coming from wholeness

wholeness still remains

ACKNOWLEDGEMENT

I would like to express my sincere gratitude to Prof R P Sharma (Acting Dean, School of Life Sciences), my supervisor, for his constant support, encouragement, scientific inspiration and the immense freedom he provided during the course of my research work.

I am very much thankful to Dr. Y Sreelakshmi, for her constant support, constructive criticism and timely advice, which made the completion of my PhD.

I would also like to thank Prof. Ramanadham(former Dean, School of Life Sciences), Prof A S Raghavendra (former Dean, School of Life Sciences), Prof A R Reddy (Head, Dept of Plant Sciences), Prof A R Podile (former Head, Dept of Plant Sciences) and Prof P B Kirti (former Head, Dept of Plant Sciences) for providing me with the opportunity to utilise the facilities of the School and Department.

I am very fortunate that I have friends like Hameeda CK, Sivaja S Nair, Greeshma Justin John, Rosmin Paul, Kavya Bakka and Rajitha Venugopal who always poured mental support on me when I was descended. My affectionate thanks to them.

My special thanks to Dr. Sheeba Sudheer for her timely support and encouragement.

I would like to express my sincere gratitude to Chaitanya Ch, Suresh Kumar Gupta, Rachana P, Mickey Hanjabam and Shalini Mahadev for extending support.

I am very much thankful to all the former and present post-doctoral, doctoral and project students of RPS group for making my stay at university a memorable one.

Sincere thanks to my parents, my brothers and my sisters for their love and continuous support from the very beginning to the end of this work. Words fall short in expressing my appreciation for what they have endured.

I would like to thank Prof. Klaus J Appenroth and Fr. Joy Palakkunnel for their lovely comradeship.

I would also like to thank University Grants Commission (UGC), Government of India, for the award of research fellowship.

Finally, I thank you Sunil for your "Presence" in my life.

Hyderabad **SHERINMOL THOMAS**

June, 2007

TABLE OF CONTENTS

LIST OF FIGURES

LIST OF TABLES

ABBREVIATIONS

ACC	1-Aminocyclopropyl-1-carboxylic acid
At	*Arabidopsis thaliana*
au	*aurea*
AV	Arka Vikas
bp	Base pairs
BSA	Bovine Serum Albumin Fraction V
cm	Centimeter
cry	*cryptochrome*
cv	cultivar
D	Dark
DAG	Day(s) after germination
dNTP	deoxy-nuclotide triphosphate
EDTA	Ethylene diamine tetra acetic acid
EMS	Ethyl Methyl Sulfonate
FR	Far red light
fri	*far-red insensitive*
g	gram
hr	hour
IAA	Indole acetic acid
IR	Infra-Red
Kb	kilo base pairs
kD	Kilo Dalton
LRF	Lateral root formation

mM	Millimolar
PAT	Polar Auxin transport
PCR	Polymerase chain reaction
PDA	Personal Data Assistants
PHYA	Phytochrome A
PHYA	Phytochrome A gene
PHYB1	Phytochrome B1
PHYB1	Phytochrome B1 gene
PHYE	Phytochrome E
PHYE	Phytochrome E gene
PHYF	Phytochrome F
PHYF	Phytochrome F gene
R	Red Light
rpm	Revolutions per minute
SDS	Sodium dodecyl sulphate
TIBA	2,3,5-triiodobenzoic acid
TILLING	Targeting Induced Local Lesions In Genomes
tri	*temporary red insensitive*
UV	Ultra-violet Light
v/v	volume/volume
w/v	weight/volume
WL	White light
WT	Wild Type
yg	*yellow green*

1. INTRODUCTION

Plants have evolved an extraordinary degree of developmental plasticity to optimize their growth and metabolism in response to the changing environmental conditions. Among the environmental conditions, light is one of the important factors that is continually monitored by the plants. To sense different features of light such as quality, quantity, direction, and duration of photoperiod and also to integrate these signals to initiate the appropriate physiological and developmental response, plants evolved a diverse set of photoreceptors (Möller *et al.,* 2002; Montgomery and Lagarias, 2002). In higher plants, there are four families of such photoreceptors, classified by the wavelength of light they perceive: the phytochrome family of photoreceptor which perceive red/far-red light (600-750 nm), and cryptochromes and phototropins which perceive blue/UVA (320-500 nm) and UVR8 (280-320 nm) which senses UV-B (Briggs and Christie, 2002; Rizzini *et al.,* 2011).

Among these photoreceptors, phytochromes play a key role in regulating a wide variety of photoresponses of plants, including seed germination, leaf and stem development, circadian rhythms, shade avoidance and induction of flowering (Rockwell *et al.,* 2006, Smith *et al.,* 2000). Phytochromes are chromoproteins with ca 120-KD molecular mass having covalently attached linear tetrapyrrole chromophore (Rockwell *et al.,* 2006). *In vivo* phytochromes can form homodimers and/or heterodimers. One of the distinguishing characters of phytochrome is the photochromicity between two distinct forms. Depending on quality of light phytochrome can exist in two forms, a Pr form which is physiologically inactive, and absorbs red light (R) and an active Pfr form which absorb, far-red light (FR). Having two distinct forms endows phytochrome with the capacity to sense the relative amounts of R and FR in Nature (Smith and Whitelam, 1990).

In higher plants phytochromes are encoded by a small gene family (Quail, 1991), comprising of two distinct classes, light-labile and light-stable species. In tomato, light-labile phytochrome species that predominates in etiolated plant tissue is encoded by the *PHYA* gene

and the gene product is referred to as PHYA. Other phytochrome genes in tomato encode the apoproteins of light-stable phytochrome species, which include PHYB1, PHYB2, PHYE, and PHYF (Pratt *et al.*, 1997).

The role of different phytochromes and their interactions with other photoreceptors in regulating photomorphogenic response have been facilitated by the isolation and physiological charecterization of photomorphogenic mutants (von Arnim and Deng, 1996; Fankhauser and Chory, 1997; Quail, 1997). The characterization of different phytochrome mutants and transgenic lines generated using site-directed mutagenesis and similar other techniques, have shown that different alleles of the same phytochrome species are immensely useful for dissection of the role of different domains of phytochrome (Zhang *et al.*, 2013).

Phytochrome protein comprises of several domains such as N-terminal photosensory PAS, GAF, and PHY domain and a C terminal regulatory histidine kinase or histidine kinase-related domain (HKRD) (Rockwell *et al.*, 2006). Though functions of many of these domains are inferred from homology studies with other proteins, to unravel their specific biological activities in light signalling, specific mutations are needed in each of the domains. Availability of domain specific mutations would help to assign the biological functions of the respective domains of the phytochrome. In addition to this, domain specific mutations can also provide information about roles of the domain in dimerization with the same phytochrome species polypeptide or with other phytochrome species polypeptide as phytochrome exist *in vivo* as homo and/or heterodimer.

The present study was undertaken to analyse how the defect in different domains of these two phytochrome genes may alter the physiological responses mediated by light. Considering the importance of different domains of phytochrome on its biological activity, we attempted to isolate an allelic series of *Phytochrome A* and *B1* mutants through reverse genetic strategy

TILLING (Targeting Induced Local Lesions In Genomes). A related technique EcoTILLING was also used to find out the natural variants of these two phytochrome genes present in natural accessions and to analyse the altered light responses imparted by them. Finally, we also analysed the sequence diversity in phytochrome genes.

2. LITERATURE REVIEW

As sessile organisms, plants have evolved an extraordinary degree of developmental plasticity to cope with the ever-changing environmental conditions that challenge the plant throughout its life cycle. Light is one of the most important environmental factors that regulate plant growth and development. Light plays a primary role in multiple responses in the plant life cycle, including seed germination, seedling de-etiolation, phototropism, shade avoidance, circadian rhythms and flowering time (collectively termed as photomorphogenesis). Plants have evolved an array of photoreceptors, each responding to specific regions of the light spectrum, to detect the presence or absence of light in addition to the duration, wavelength and intensity of incident light. In higher plants, there are four families of such photoreceptors, classified by the wavelength of light they perceive: the phytochrome family of photoreceptor which perceive red/far-red light (600-750 nm), and cryptochromes and phototropins which perceive blue/UVA (320-500 nm) and UVR8 (280-320 nm) which senses UV-B (Briggs and Christie, 2002; Rizzini *et al.*, 2011).

2.1 Plant Photoreceptors

2.1.1 The Blue Light Photoreceptors: Cryptochromes and Phototropins

A number of blue light mediated responses have been observed in plants, which include phototropism, stomatal opening, inhibition of hypocotyl growth, and the induction of several gene expressions. Cryptochromes and phototropins are the two plant photoreceptors mediate the blue light–induced responses in plants.

Cryptochrome: In plants the cryptochrome family of UV-A/blue light photoreceptors, participate in several physiological process, ranging from photomorphogenesis to entrainment of the circadian clock. Their functions include inhibition of hypocotyl elongation (Ahmad and Cashmore, 1993; Lin *et al*., 1998), anthocyanin accumulation (Ahmad *et al*., 1995), cotyledon expansion (Botto *et al.,* 2003), flowering time (Guo *et al.,* 1998; Mockler *et al.,* 1999;

Giliberto *et al.,* 2005) and also the circadian clock (Devlin and Kay, 1999; Millar, 2003). The cryptochromes families of photoreceptors are structurally similar to DNA photolyases (Ahmad and Cashmore, 1993; Lin *et al.,* 1998), but most of them do not possess any DNA photolyase activity. DNA photolyases are flavoproteins found in microbes involved in blue/UVA-dependent repair of DNA damage (Sancar, 2000; Lin, 2002). DNA photolyases have an amino terminal photolyase homology region (PHR) noncovalently binding a primary/catalytic FAD chromophore (Flavin Adenine Dinucleotide) and a second light-harvesting chromophore, a pterin or deazaflavin (Lin *et al.,* 1995; Sancar, 2003). Although there is no detectable photolyase activity, cryptochromes contains an FAD and a pterin (methenyltetrahydrofolate, MTHF) chromophore (Lin *et al.,* 1995; Malhotra *et al.,* 1995). In addition to this, most plant cryptochromes have a distinctive carboxy-terminal domain (Lin and Shalitin, 2003).

Phototropin: Phototropins (phot1 and phot2) that absorb UV-A/blue light have been suggested to play an important role in phototropism, chloroplast movement, leaf expansion, and stomatal opening (Takemiya 2005). The molecular characterization of an *Arabidopsis* mutant impaired in phototropism, *nph1* (*NONPHOTOTROPIC HYPOCOTYL 1*), led to the identification of phototropin1 (Huala *et al.,* 1997). Phototropins are members of a larger family of proteins known as the LOV domain family (Crosson *et al.,* 2003). The LOV domain acts as a *l*ight, *o*xygen or *v*oltage sensor domain (Huala *et al.,* 1997; Taylor and Zhulin, 1999; Crosson et *al.,* 2003). The phototropin family of photoreceptors contains two repeated LOV (Light, Oxygen, and Voltage) domains (designated as LOV1 and LOV2) in contrast to other LOV domain family members (Huala *et al.,* 1997; Crosson *et al.,* 2003). Light sensing function of these photoreceptors is mediated by LOV domain. The ability of the phototropins to function as near-UV/blue light receptors is derived from the association of a single flavin mononucleotide (FMN) with each LOV domain and the unique photocycle it undergoes in

dark and light states (Crosson *et al.,* 2003; Kennis *et al.,* 2003; Liscum *et al.,* 2003). Photoexcitation of the LOV domain results in receptor autophosphorylation and an initiation of phototropin signalling by phototropins.

2.1.2 UV-B Receptor: The UVR8

Though UV-B radiation represents a very small fraction of the sunlight that reaches the earth surface (290-320 nm), it is an important signal in plants which elicit a variety of response including cellular damage (Baker *et al.,* 1997; Sullivan and Rozema, 1999), induction of flavonoid (Beggs and Wellman, 1994), inhibition of hypocotyl elongation (Ballaré *et al.,* 1991), stomatal opening (Eisinger *et al.,* 2003), and phototropism (Baskin and Iino, 1987; Eisinger *et al.,* 2003; Shinkle *et al.,* 2004). The UV RESISTANCE LOCUS 8 (UVR8) in Arabidopsis has been recently established to be a UV-B photoreceptor (reviewed by Heijde and Ulm, 2012). UVR8 is a β-propeller protein localised both in the cytoplasm and the nucleus and its abundance is unaffected by UV-B or other light qualities (Favory *et al.,* 2009; Kaiserli and Jenkins, 2007). However, upon UV-B irradiation, the constitutive UVR8 levels in cell are redistributed, resulting in the accumulation of this molecule in the nucleus (Kaiserli and Jenkins, 2007).

2.1.3 The Red/Far Red Light Receptors: Phytochromes

Plant phytochromes are members of a wide spread family of red/far-red responsive photosensors that are found also in cyanobacteria (cyanobacterial phytochromes Cph1 and Cph2) as well as in purple and nonphotosynthetic bacteria (bacteriophytochromes; BphP) and even fungi (fungal phytochromes; Fph family) (Montgomery and Lagarias, 2002; Blumenstein *et al.,* 2005; Froehlich *et al.,* 2005; Karniol *et al.,* 2005). Members of the phytochrome family proteins share a common architecture consisting of an N-terminal photosensory region with three conserved domains (termed P2 or PAS domain, P3 or GAF

domain, and P4 or PHY domain) and a C-terminal regulatory histidine kinase or histidine kinase related domain (HKRD) (Montgomery and Lagarias, 2002; Rockwell *et al*., 2006). Plant phytochromes are different from other members of the phytochrome family in that they have an additional N-terminal extension termed P1 known to inhibit dark reversion (Vierstra, 1993) and two additional regulatory PAS domains important for nuclear localization (Rockwell *et al*., 2006).

2.2 Phytochrome Structure

In solution, phytochromes are homo/hetero dimers of two 120-KD proteins, each covalently attached to a linear tetrapyrrole (phytochromobilin) via a thioether linkage to a unique cysteine. The phytochrome chromoprotein can be divided into two globular domains: an amino-terminal chromophore binding photosensory (signal input) domain and a carboxy terminal domain believed to act as a regulatory, dimerization, and signal output domain. The N-terminal photosensory domain consists of three conserved domains termed P2 (PAS domain), P3 (GAF domain), and P4 (PHY domain) (Rockwll *et al*., 2006; Montgomery and Lagarias, 2002; Wu and Lagarias, 2000). Plant phytochromes have an additional N-terminal extension termed P1 (NTE), which is known to inhibit dark reversion (Vierstra, 1993). A conserved cysteine residue present in the P3 domain forms a thioether linkage with the A ring of phytochromobilin and also autocatalyzes the bilin ligation reaction (Kendrick and Kronenberg, 1994; Wu and Lagarias, 2000). The role of P4 domain is to interact with the D ring of the chromophore to maintain its extended linear conformation in the Pr form and to stabilize the Pfr form (Montgomery and Lagarias, 2002). The carboxy-terminal half of phytochrome can be divided into two subdomains: a PAS-related domain (PRD) containing two PAS domains (Bolle *et al*., 2000) and a histidine kinase-related domain (HKRD), which belongs to the ATPase/kinase GHKL (gyrase, Hsp90, histidine kinase, MutL) superfamily

(Chen *et al.*, 2004; Montgomery and Lagarias, 2002; Yeh and Lagarias, 1998). The standard phytochromes structure thus consist of a PAS-GAF-PHY N-terminal photosensory module typically combined with a C-terminal HKRD module (Rockwell *et al.*, 2006)

The understanding of phytochrome structure and photochemistry was greatly benefited through crystallographic studies conducted in *Deinococcus radiodurans.* A major breakthrough occurred when a 2.5 Å crystal structure for the BV (biliverdine) -bound P2/PAS and P3/GAF domains of DrBphP, the BphP was unveiled. The P2 and P3 domains adopt PAS and GAF folds. crystallographic studies along with biochemical studies confirms that the BV chromophore is covalently attached to Cys24, and is deeply buried within a conserved pocket in the P3/GAF domain and the interface between the PAS and GAF domains is formed by a deep trefoil Knot (Rockwell *et al.,* 2006). This knot is formed from sequence lying between Cys24 and the P2/PAS domain, which passes through a "lasso" formed by P3/GAF sequence between the fourth and fifth strands of the central GAF β sheet (Wagner *et al*., 2005). The trefoil knot is centered on the conserved amino acids within the N-terminal sequence element required for both bilin assembly and for interaction with the B-ring carboxylate of the biliverdin chromophore. Mutations in the PAS and GAF of plant phytochromes result in altered function as these mutations might affect the proper folding of these domains (Rockwell *et al.,* 2006).

2.3 Phytochrome Gene Family

In the model plant species, *Arabidopsis thaliana* phytochrome family includes five phytochromes designated *PHYA* to *PHYE.* The five phytochromes are classified based on their light stability into two groups (Sharrock and Quail, 1989), Type I (light labile) and type II (light stable). PHYA is a type I phytochrome, which degrades fairly rapidly upon exposure to red or white light, while type II or light stable phytochromes which includes PHYB-E are

stable upon light exposure. In dark grown seedlings PHYA is found to be abundant, whereas, its level drops rapidly upon exposure to red (R) or white (W) light. Among the other type II phytochrome members, PHYB1 is found to be the most abundant one (Quail, 1997; Sharrock and Clack, 2002). Phylogenetic studies reveal that duplication occurred during the evolution of early seed plants resulted in formation of *PHYA*/*C* and *PHYB*/*D*/*E* lineages. This lineage in turn diverged into *PHYA* and *PHYC,* and *PHYE* and *PHYB*/*D*, which finally resulted in *PHYB* and *PHYD* (Mathews *et al.*, 1995; Mathews and Sharrock, 1997; Alba *et al.*, 2000). Sequence analysis shows that *PHYB* and *PHY*D polypeptides are about 80% identical and are somewhat more related to *PHYE* than to either *PHYA* or *PHYC* (about 50% identity).

2.4 Pr and Pfr Forms of Phytochrome

Physiological and biochemical analysis proves that phytochrome exist *in vivo* in two photoreversable forms. Phytochromes are synthesized in a relatively stable Pr form that shows maximum absorbance at 666 nm. Upon light exposure Pr form is converted back to the Pfr form which is considered as the biologically active form. Pfr shows maximum absorbance at 730 nm and is phototransformed back to Pr upon FR light absorption (Quail, 1997). The photoconversion of phytochrome involves the isomerization of the chromophore and conformational changes of the apoprotein that results in differential exposure of specific domain (Casal *et al*., 2003).

2.5 Phytochrome Mutants

The elucidation of molecular nature of photoreceptors has been conducted largely through the physiological and molecular genetic studies of photomorphogenic mutants (von Arnim and Deng, 1996; Fankhauser and Chory, 1997). The isolation and characterization of photomorphogenic mutants have led to the identification of various light signaling components and contributed significantly to our understanding of how light signals are

transmitted in plants. The forward or reverse genetic approaches along with extensive efforts using genetic, molecular and photobiological techniques have led to the identification putative roles for several loci in the regulation of development.

To unravel the roles of the different phytochrome species, mutants deficient in one specific type of phytochrom*e* are required. Three types of phytochrome mutants have been identified so far, which include (a) mutants with defect in the biosynthesis of the common phytochrome chromophore (b) mutants that lack a light labile phytochrome (phytochrome A) (c) mutant that are deficient in light stable, Phytochrome B1-like protein (Van Tuinen *et al.,* 1995b).

Chromophore mutants are characterized by reduced levels of spectrophotometrically detectable phytochrome in dark-grown seedlings (Koornneef *et al.,* 1985) as they are unable to synthesize the chromophore of phytochrome. Mutations in the chromophore biosynthesis pathway affect all phytochrome species and these mutants have been used extensively in physiological research studies (Kendrick *et al.,* 1994; Migge *et al.,* 1998; Terry and Kendrick 1999; Terry *et al.,* 2001).

Phytochrome A (phyA) mutants in various plant species are characterized by their failure to de-etiolate in continuous FR light (absence of a FR-HIR for hypocotyl inhibition and the rather normal phenotype in WL. Similarly, characterization of phytochrome B (phyB) deficient mutants in various species revealed that they have difficulty de-etiolating in continuous red light. Additionally adult plant tissues exhibited a reduction in chlorophyll content. A large-scale screen for Arabidopsis phytochrome B (phyB) mutants identified 14 novel missense mutations in the N terminal moiety. Analysis of these new mutations revealed that each subdomain has an important function. Analysis on the spectral properties of these mutants enabled them to be classified into two principal classes: light-signal perception mutants (those with defective spectral activity), and signaling mutants (defective in

intracellular signal transfer). Most of the spectral mutants were found in the GAF and PHY subdomains. On the other hand, the signalling mutants tend to be located in the N-terminal extension and PLD. These observations indicate that the N-terminal extension and PLD are mainly involved in signal transfer, but that the C-terminal GAF and PHY subdomains are responsible for light perception (Oka *et al.,* 2008).

More recently, Su and Lagarias (2007) reported the isolation of a new class of plant phytochrome mutants that exhibit light-independent signalling activity. These mutants are reported to have a dominant gain-of function activity caused by mutation of a conserved GAF domain Tyr residue (Y^{GAF}). Y^{GAF} mutants of Arabidopsis phyA and phyB exhibited a light-independent activation of gene expression, and general R/FR insensitivity with a COP (Constitutive photomorphogenesis) phenotype. The above study clearly demonstrates the critical role of the conserved GAF domain in coupling light perception with downstream signaling.

2.6 Phytochrome Mutants in Tomato

Tomato is an important crop and an excellent model system with extensive genome data available. Tomato is considered as a model species complimentary to Arabidopsis, to characterize the entire phytochrome family to make general conclusion about the roles played by phytochrome in higher plants by its individual members (Kendrick *et al.,* 1997). Although multiples genes encoding apo-phytochrome have been identified in higher plants, in tomato only phyA and phyB deficient mutants have been isolated so far.

Chromophore Mutants

Chromophore mutants of tomato have also been isolated which are either lacking or deficient in phytochrome. These include the *aurea* (*au*) mutant (Koornneef *et al.,* 1985) and the *yellow green-2* (*yg-2*) mutant (Koornneef *et al.,* 1985; Buurmeijer *et al.,* 1987).

***aurea* (*au*) mutant:** The tomato *au* mutant (Koornneef *et al.,* 1985) are characterised by yellow-green leaves of the adult plant which are slightly juvenile in appearance. Young seedlings of *au* mutants exhibit a reduction in hypocotyl growth inhibition in white light (Koornneef *et al.,* 1985), with reduced chlorophyll and chloroplast development (Koornneef *et al.,* 1985; Neuhas *et al.,* 1993), and reduction in anthocyanin content (Adamse *et al.,* 1989). Moreover, *au* mutants show a reduced germination in darkness compared to wild type (Koornneef *et al.,* 1985). Although mutant seedlings contain about 20% of wild type levels of PHYA (Sharma *et al.,* 1993) there is no spectrophotometrically detectable phytochrome (Koornneef *et al.,* 1985) in etiolated seedlings of the *aurea* mutant. Subsequently Terry and Kendrick (1996) proposed that the *aurea* mutant is deficient in phytochrome chromophore synthesis. Muramoto *et al.,* (2005) showed that *aurea* mutant is defective in phytochromobilin synthase, required for chromophore biosynthesis confirming that the deficiency of phytochrome is not due to a mutation in the *PHYA* structural gene.

***yellow green-2 (yg-2)* mutant:** The *yg-2* mutant is characterized by elongated hypocotyl, reduced chlorophyll and anthocyanin level and reduced germination (Koornneef *et al.,* 1985; Buurmeijer *et al.,* 1987). It is a recessive mutant, which is phenotypically similar to aurea mutant (Koornneef et al., 1985), but unlike the *aurea* mutant, older *yg-2* seedlings have been shown to accumulate spectrophotometrically detectable phytochrome (Koornneef *et al.,* 1985). The *yg-* mutant was also proposed to be a phytochrome chromophore deficient mutant (Terry and Kendrick, 1996) like the *aurea* mutant where the phenotype is not a consequence of a mutation in the *PHYA* gene.

***far-red insensitive* (*fri*) mutant:** *fri* mutant is characterized by its failure to de-etiolate in continuous FR light (absence of a FR-HIR) for hypocotyl inhibition and the rather normal phenotype in WL. The *fri* mutant of tomato was isolated, from an EMS (Ethyl methane sulphonate) treated tomato population, on the basis of slightly longer hypocotyls than WT

under low fluence rates of red light. Genetic, spectrophotometric, immunochemical and physiological investigations led to the conclusion that the *fri* mutant is deficient in phyA (van Tuinen *et al.,* 1995a). Additionally genetic mapping of the *FRI* loci and RFLP mapping of *PHYA* indicated that both the *FRI* loci and *PHYA* are located in the same chromosome (van Tuinen *et al.,* 1997). At genomic level *fri* mutant harbours a base substitution which changes a consensus AG/ to TG/ at the 3' end of the intron between exon 1 and 2 resulted in an aberrant processing of the pre-mRNA (Lazarova *et al.,* 1998a).

***temporarily-red light insensitive* (*tri*) mutant:** *tri* mutants are characterized by a long hypocotyl and small cotyledons compared to wild type under low fluence RL, a phenotype typical of phyB mutants of other species (Kendrick *et al.,* 1994). The mutants are only insensitive to R during the first two days after transfer from darkness irrespective of their physiological age (van Tuinen *et al.,* 1995b). Unlike other phyB mutants, *tri* mutants are not dramatically taller than the WT and exhibit a strong shade-avoidance response. The molecular analysis of *tri* alleles revealed that these mutants had normal levels of *PHYA, PHYB2, PHYE* and *PHYF* but there is reduction in *PHYB1* transcript levels than that observed in wild type, indicating that the *tri* alleles were defective in *PHYB1* (Kerckhoffs *et al.,* 1995). The four putative *PHYB1* mutants were subsequently confirmed to harbour mutations at different regions of the *PHYB1*gene (Lazarova *et al.,* 1998b). The allele tri^1 contains a premature stop codon while tri^2 and tri^4 encode proteins truncated at their C-termini. The tri^3 allele has an amino acid substitution from valine to phenylalanine (Lazarova *et al.,* 1998b).

***PHYB2* mutants:** Mutants defective in *PHYB2* gene were isolated from a γ-mutagenised population of *phyA phyB1* lines (Kerckhoffs *et al.,* 1999). Two putative mutant lines were isolated based on their elongated hypocotyls and reduced anthocyanin content as compared to the *phyA phyB1* double-mutant parent. Molecular analysis revealed that both of them were

allelic and both mutations resulted in truncated PHYB2 apoproteins lacking a substantial portion of the C-terminal region (Kerckhoffs *et al.,* 1999).

2.7 Physiological Response Controlled by Phytochrome

Light perceived by phytochrome influences the growth and development throughout the life cycle of plants. The variety of different phytochrome response observed in plants is enormous, in terms of response and fluence. Fluence is the amount of light required to induce a response and is defined as the number of photons absorbed per unit surface area (mol m^{-2}). Each phytochrome response has a characteristic range of light fluences over which the magnitude of the response is proportional to the fluence. Phytochrome responses have been divided into different classes based on the amount of light required to induce the response. These include low fluence responses (LFRs), very low fluence responses (VLFRs), and high irradiance responses (HIRs) (Nagy and Schafer, 2002; Chen *et al.,* 2004).

LFRs include most of the classic Red/Far-red photoreversible responses, such as promotion of seed germination and the regulation of leaf movements. LFR spectrum consists of a main peak for stimulation in the red and a major peak for inhibition in the far red. VLFR are irreversible response with a characteristic action spectrum which exhibit broad peak in the red and blue region (Shinomura *et al.,* 1996).VLFR response are sensitive to a broad spectrum of light between 300 nm and 780 nm. Phytochrome responses of third type are termed high irradiance responses (HIRs) which require prolonged or high frequency intermittent illumination and usually are dependent on the fluence rate of light (Nagy and Schafer, 2002; Casal *et al.,* 2003; Casal *et al.,* 2002; Shinomura *et al.,* 1996). Genetic studies and mutant analysis reveal that type I phytochrome is responsible for the VLFR and FR HIR while type II phytochrome are responsible for LFR and R-HIR.

2.7.1 Phytochrome and Germination

In many of the plants the germination of seeds are controlled by factors such as light and temperature. Phytochrome is the principle photoreceptor involved in germination. Mutant analysis indicates that loss of phytochrome has major impact on regulation of germination. The requirement of light in seed germination was first demonstrated by Caspary in 1860. Flint *et al.* (1935) showed that lettuce seed germination could be promoted by red light but inhibited by far red light. Later in 1952, Harry Borthwick explained the involvement of phytochrome in seed germination in the pioneering 'flip flop' experiment (Borthwick, 1952 b). In this experiment lettuce seeds were treated with alternating R and FR treatments and the efficiency of germination was analysed. There was 100% germination in these seeds which received R treatment at last. In contrast to this observation a markedly different response was observed in seeds receiving the FR treatment last, with much lower percentages of germination recorded (Borthwick *et al.*, 1952b). Borthwick's experiments thus could demonstrate that phytochromes operated reversibly in LFR mode.

Subsequent works on *Arabidopsis* have revealed that phyB is the photoreceptor mainly involved in red/far-red reversible (LFR) germination. Germination is also induced by low quantities of red or far-red light (VLFR) or continuous far-red light (far-red HIR) which are mediated through phyA (Casal and Sanchez, 1998).

The involvement of individual phytochrome mediated response and involvement of other phytochrome in seed germination has also been revealed using different photomorphogenic mutants. Comparisons and analysis of mutants deficient in phyA, phyB, and phyA/phyB have shown that phyB has a predominant role in regulating germination in R via the LFR mode whilst phyA mediates VLFRs in R and FR (Botto *et al.,* 1996; Shinomura *et al.,* 1996). Moreover phyA can promote germination in continuous FR in the HIR mode (Johnson *et al.*,

1994; Reed *et al.*, 1994; Hennig *et al.*, 2002). Observations of R/FR-reversible germination in *phyA phyB* double mutants suggested that phyA and phyB are clearly not the only phytochromes participating in light-induced germination and other phytochromes too play a role (Poppe and Schafer, 1997).

The analysis of mutant deficient in phyD and phyE revealed the additional roles of these phytochromes in seed germination. While only a minor role was observed for phyD deficiency, mutants deficient in phyE were found to be severely impaired in light induced germination and abolished R/FR reversibility (Hennig *et al.*, 2002). As in the case of *phyA* mutants, seed germination in *phyE* mutant was found to be severely impaired in blue light and abolished in FR. Moreover, the study revealed that phyE itself might operate as a FR photoreceptor in the regulation of germination. The severely impaired light induced germination of *phy A, phy B* and *phy E* mutants confirming the redundant interaction between these phytochromes (Hennig *et al.*, 2002).

2.7.2 Phytochrome and Shade Avoidance

One of the major threats to plant survival in natural environments is limitation of light through shading by neighbouring vegetation. Plants, which are grown in close proximity to each other, are in constant competition with their neighbours for the natural resources. Light is also one of the resources for which plants grown in close proximity compete to each other. Shade avoidance is one of the remarkable mechanisms that flowering plants have evolved to avoid shade to ensure their survival, which have probably contributed to their evolutionary success (Smith and Whitelam, 1997). In species, which exhibit shade avoidance, phytochromes perform a major role in the detection of shade and initiation of escape response. The photosynthetic pigments chlorophylls and carotenoids absorb light over most of the visible spectrum, and use this absorbed energy for photosynthesis. Therefore, the

reflected/transmitted light is depleted in R and B wavebands, and enriched with far-red and green wavebands resulting in a reduction in the ratio of R to FR (R:FR).This parameter can be defined as R(Franklin and Whitelam, 2004):

$$\text{FR ratio} = \frac{\text{photon irradiance between 655 and 665 nm}}{\text{photon irradiance between 725 and 735 nm}}$$

The R: FR ratio underneath of vegetation canopies are in the range of 0.05-0.7 (Smith, 1982). A reduction in R: FR ratio initiate a suite of developmental responses called the shade avoidance syndrome (Smith and Whitelam, 1997). Responses to shade are many and varied, and the term, shade avoidance syndrome is used to describe multiple responses to low R: FR syndrome. This include elongation of stem and petiole, large thinner leaves, retention of photosynthate in the shoot at the expense of root growth, increased apical dominance and at the extreme end of the syndrome is the inhibition of fruit and seed development and acceleration of flowering (Smith and Whitelam, 1997). Phytochromes are the major photoreceptors mediate the shade avoidance response by sensing the R: FR ratio. Plants are capable of sensing very small changes in R/FR and thus can warn the system for a potential shade threat. In this way reflected FR light provide a unique quantifiable signal that can initiate adaptive response before leaves are actually shaded (Ballare *et al.,* 1990).

Among phytochrome members, phyB is the principle phytochrome involves in the suppression of shade avoidance response. Arabidopsis mutant that lack functional phyB exhibit the so called ‘constitutive shade avoidance’ (Nagatani *et al.,* 1991; Somers *et al.,* 1991), which includes phenotype with dramatically elongated stem, early flowering and increased apical dominance under high R/FR (Smith and Whitelam, 1997). However, the observations of residual shade avoidance responses in Arabidopsis *phyB* mutant indicate that the involvement of other phytochrome species in this process. Subsequent analysis of Arabidopsis mutants, deficient in multiple phytochrome combinations demonstrates the

importance of phyB, phyD, and phyE in the regulation of shade avoidance (Devlin *et al.,* 1998, 1999).

2.7.3 Phytochrome in De-etiolation

Most of the plants, after germination, exhibit one of the two developmental patterns. Skotomorphogenesis is an etiolated development in darkness with a characteristic feature of having long stems (hypocotyls) and closed, unexpanded leaves (cotyledons) protected by an apical hook. The second one is the growth in light or photomorphogenesis is the de-etiolated development characterized by development characterized by short hypocotyls and open expanded cotyledons that are capable of photosynthesis (Sullivan and Deng, 2003). Etiolation is considered as an adaptation to life in the absence light. In natural environment, this adaptation allows the buried seeds to emerge through soil reach light, and switch to a developmental pattern optimal for photosynthesis (Frankhauser and Chory, 1997). The switch between skotomorphogenic growth and photomorphogenic growth or the successful establishment of photoautotrophy requires the sensitive detection of environmental cues.

The regulation of de-etiolation involves a complex interaction of several photoreceptor, including blue/UV light absorbing cryptochromes, the R and FR absorbing phytochromes (Nemhauser and Chory, 2002; Wang and Deng, 2002). Though various other components are involved in this complex process, phytochromes perform a variety of overlapping roles in seedling etiolation in combination with other photoreceptors. The skotomorphogenic phenotype of phyA mutants under continuous FR light is in contrast to the wild type counterpart, which exhibit a normal de-etiolated phenotype, confirms the unique role of phyA in mediating de-etiolation under FR-HIR (Dehesh *et al.,* 1993; Nagatani *et al.,* 1993; Parks and Quail, 1993; Whitelam *et al.,* 1993). Transcription profiling studies of WT and phyA mutant reveal under FR light there are more than about 800 genes changing their expression

pattern and thus they could be phyA regulated genes (Tepperman *et al.,* 2001). Mutant analysis of phytochrome B suggests that phyB is the major phytochrome regulating de-etiolation in WL an R and the mutants exhibited elongated hypocotyl, reduced cotyledon expansion, and reduced chlorophyll synthesis (Koornneef *et al.,* 1980; Nagatani *et al.,*1991; Somers *et al.,* 1991; Reed *et al.,* 1993) shows that phyB has a predominant role in de-etiolation under WL and R light.

2.7.4 Phytochrome in Flowering

The initiation of flowering or the transition of vegetative growth to reproductive growth is one of the major development switches in plant cycle. This transition to flowering in plants is controlled by environmental factors. Many plant species thus evolved the ability of flower initiation; in response to environmental factors like changes in day length (photoperiod) and temperature. Phytochromes are critical photoreceptor, which is involved in floral induction. A key function of phytochrome in plants is to involve the monitoring of day length or photoperiod, which together with temperature, provides plants with important seasonal information. Photoperiod is recognized as a major environmental factor of flowering time in many plants. Changes in day length are a predictable and reliable indicator of seasonal progression, which controls floral transition in many plants. The acceleration of flowering by long days (LD) in Arabidopsis involves the interaction of various photoreceptors and endogenous circadian oscillator (Yanovsky and Kay, 2002). The relative proportion of R:FR ratio, like photoperiod, provides a powerful signal that regulate flowering in plants. Phytochrome detects the altered R:FR ratios and it leads to the initiation of a syndrome response called shade avoidance (Smith and Whitelam, 1997). Acceleration of flowering is also a response, which could be induced by shade avoidance. In Arabidopsis acceleration of the onset of flowering is one of the major response induced by shade avoidance syndrome (Bagnall, 1993).The response thus has possible implications, as it helps in the survival of

cycle under unfavourable condition. Among the five members, phyB, phyD and phyE play some roles in the detection of R:FR ratio signal and thus in the initiation of shade avoidance (Whitelam *et al.,* 1998). From the physiological studies of phytochrome mutant in Arabidopsis, it is clear that phyB is the principle photoreceptor in shade detection and thus in the attenuated response to low R:FR (Goto *et al.,* 1991). The early flowering phenotype of phyB under altered R:FR clearly shows the involvement this photoreceptor in flowering in Arabidopsis. Mutants for either phyD or phy E have less obvious phenotypes, and their deficiency is more evident when phyB is also absent (Aukerman *et al.,* 1997; Devlin *et al.,* 1998; 1999).

2.7.5 Phytochrome and Roots

In seedlings, unlike shoots that grow upward, primary roots grow away from light and downward into the soil, where it is responsible for water and nutrients uptake (Hangarter, 1997). Though light exposure is usually limiting in the case of roots, a small amounts of light can always penetrate to sufficient depths in soil, and this light signal is sufficient to induce biological responses (Mandoli *et al.,* 1990). Tropism, a differential growth is one of the methods that plants exhibit to adjust their form in response to gravity or light. Though the influence of light on root growth have been less well characterized compared to other organs, the effect of light has been studied with respect to various physiological responses. Light promotes a positive gravitropic response in root (Lake and Slack, 1961), inhibit lateral roots in pea (Torrey, 1952), negative phototropism (Okada and Shimura, 1992; Liscum and Briggs, 1996) and inhibit root hair formation in Arabidopsis through a phytochrome mediated mechanism (Reed *et al.,* 1993). Moreover, in rice seedlings blue light has an inhibitory role in root growth through suppression of both cell elongation and division, while red or far-red light inhibited only cell elongation (Ohno and Fujiwara, 1967).

Photoreceptors like phytochrome (Wang *et al.,* 1993; Hall *et al.,* 2001; Salisbury *et al.,* 2007), phototropin (Sakamoto and Briggs, 2002) and cryptochrome (Usami *et al.,* 2007) have been found in roots, and it is well established that light can affect various aspects of root growth and development through these photoreceptors. Through mutational analysis of photoreceptor their roles in organ elongation and light-regulated gravitropic orientation for a variety of plant species has been established. In maize root, phyA is found to be the principle photoreceptor involved in modulating the gravitropic responses for far-red light-regulated processes (Parks and Spalding, 1999; Takano *et al.,* 2001; Hennig *et al.,* 2002). Both phyA and phyB are involved in the regulation of red-light mediated gravitropic responses (Liscum and Hangarter, 1993; Lu *et al.,* 1996; Poppe *et al.,* 1996; Robson and Smith 1996; Parks and Spalding, 1999). Though the exact role they play in gravitropic response is unknown, the other members of phytochrome family *viz.* phyC, phyD and phyE exhibit complex overlapping and distinct functions in red light mediated gravitropic response (Neff *et al.,* 2000).

2.8 Cellular Localization of Phytochromes

Phytochrome A, in dark grown seedlings, exists in the Pr form and it is localized to the cytocol of plant cells. Light induces the formation of Pfr form of phytochrome and the transformed molecule thus migrates to the nucleus, where it induces the formation of nuclear speckles. In white light (or light rich in red light) the process of migration of phyA and speckle formation is transient but in FR, the process is slow and the nuclear speckle formation would take at least 2 hours after irradiation (Kim *et al.,* 2000). This phenomenon reflects the spectral dependency of Pfr formation and under FR most of the phyA molecule would be in Pr form protected from degradation, only gradually exposed as the Pfr form and migrating to the nucleus. PhyB is also present in cytosol of dark grown seedlings, as in the case of

Phytochrome A and light induces the translocation of phyB into the nucleus (reviewed by Nagatani 2004**)**. In contrast to phyA, FR cancels the effect of R light induced nuclear localization and it clearly suggests that phyB migrates into nucleus only in the Pfr form. Other Phytochromes exhibit an opposite pattern of cellular localization. In dark phy C, phy D and phy E present in the nucleus and light treatment enhances speckle formation in the case of both phy E and phy C, but phy D rarely forms nuclear speckle formation (reviewed by Nagatani, 2004**)**.

2.9 Nuclear Localization of Phytochrome

Nucleo-cytoplasmic partitioning of proteins is a crucial step in the regulation of gene expression. In darkness, phytochrome accumulate in the cytoplasm in its inactive Pr form and upon light activation, phytochrome translocates from the cytoplasm into the nucleus (Sakamoto and Nagatani, 1996).

Biochemical and cytological investigations suggests that phytochrome has nuclear localization activity (Sakamoto and Nagatani, 1996). In dark grown Arabidopsis seedling, both phyA and phyB localize mainly in the cytoplasm in darkness. (Yamaguchi *et al.,* 1999; Kircher *et al.,* 1999; Kim *et al.,* 2000; Hisada *et al.,* 2000; Nagatani, 2004). According to the current model of light-dependent nuclear localization of phytochrome, in darkness, the amino-terminal domain of the Pr form retains phytochrome molecule in cytosol by suppressing the nuclear localization activity of the carboxy-terminal domain. The amino-terminal domain in the Pfr form stops suppressing the carboxy-terminal domain under light conditions, and results in the nuclear accumulation and speckle formation (Nagatani, 2004).

It was also experimentally proven that chromophore is not required for the retention of phytochrome in cytoplasm as phyB carrying a mutation that affect chromophore binding fails to accumulate in the nucleus (Kircher *et al.,* 1999). Mutant analysis also reveals that the

region including the PAS domains within the carboxyterminal appears to play an important role in nuclear speckle formation, as PAS domain mutant of phytochrome are known to reduce the signalling activity without affecting spectral activity (Quail *et al.,* 1995). But phytochrome carrying these mutants are localized in the nucleus suggests that, this region play a major role in the formation of speckles but may not be essential for the nuclear import of Phytochrome (Nagatani, 2004).

Evidences indicate that phytochrome transduces the light signal mainly in the nucleus. After light activation, PIF3 and phytochrome co-localize in nuclear speckle and PIF3, which binds to the promoter of several light regulated genes, continues the phytochrome initiated signalling cascade. Subsequently phytochromes form speckles in the nucleus (Yamaguchi *et al.,* 1999, Kircher *et al.,* 1999) but, the time course for speckle formation vary with different phytochromes. Phytochrome A mediated speckle formation is very fast (Kim *et al.,* 2000; Hisada *et al.,* 2000) while phytochrome B takes hours to form speckle (Yamaguchi *et al.,* 1999, Gil *et al.,* 2000). The number and size of speckle depends on the light condition and nature of treatment (Nagatani *et al.,* 2004). Along with PIF3, a few other factors like COP1 and cry2 has also been shown to localize with Phytochromes in the speckle (Mas *et al.,* 2000; Bauer *et al.,* 2004; Seo *et al.,* 2004).

2.10 Phytochrome Signal Transduction

The absorption of red light (R) by phytochrome molecule induces a chain of dramatic biochemical events in plants that culminate in major changes in plant growth and development. The cascade of events transduces the external light signal into critical adaptive changes, and thus the study of light induced signal transduction is an active and exciting area of research in biology. The entire event of signal transduction starts with formation of Pfr (biologically active far red light (FR)-absorbing form of phytochrome) from Pr (the R-

absorbing form of phytochrome). Though the Pfr formation can occur on a millisecond time scale, the transduction chain for phytochrome response thus formed can stretch out for many hours or even days (Mohr, 1983). It is well established that the involvement of protein kinase in phytochrome signal transduction (Trewavas and Gillroy, 1991). The finding that highly purified phytochrome has protein kinase activity closely associated with it (Wong *et al.,* 1989) suggests that phytochrome itself can bind to ATP.

The involvement of G-protein an early event required for stimulus response coupling (Trewavas and Gilroy, 1991) is well documented in various systems. They act as important players in signal transduction cascade by binding to key metabolic enzymes, in their GTP-activated form, and up-or down regulate their activity. The involvement of G-proteins in phytochrome signal transduction was first reported by Hasunuma *et al.,* (1987) in *Lemna* species. But, in Arabidopsis, mutant analysis of alpha and beta subunits of the heterotrimeric G protein indicate that heterotrimeric G protein is not directly involved in phytochrome mediated seedling photomorphogenesis (Jones *et al.,* 2003). On the other hand, there is evidence that at least some G-proteins regulate only a specific set of stimulus-response coupling pathways (Simon *et al.,* 1991). In that case, in plants there may be a G-protein specialized for transducing phytochrome responses, or even a different G-protein for different responses. The identification of a cytoplasmic localized calcium binding protein SUB1 suggests that the involvement of calcium in phytochrome signaling (Guo *et al.,* 2001). PhyA is required for the proper light regulation and posttranslational regulation.

2.11 Phytochrome and Transcription Regulation

Gene expression studies revealed that phytochrome responses are associated with alterations in gene expression (Delvin *et al.,* 2003; Ma *et al.,* 2001; Quail 2002; Tepperman *et al.,* 2001; Wang *et al.,* 2002). A number of transcription factors are essential for both phyA signalling

and Phytochrome mediated responses in plants. HY5, LAF1, and HFR1 are some of the major transcription factors, which are needed for phytochrome signalling. *CCA1* (circadian clock associated) and *LHY* (late elongated hypocotyl) were found to be some of the early targets of phytochrome-mediated responses in plants (Ballesteros *et al.,* 2001; Chattopadhyay *et al.,* 1998; Duek and Frankhauser *et al.,* 2003; Tepperman *et al.,* 2001). Signaling components like FAR1 (far-red impaired response) and FHY3 (far-red elongated hypocotyl), have been suggested to be related to transposases regulating transcription (Hudson *et al.,* 1999; Hudson *et al.,* 2003; Wang and Deng 2002). PIF3 (phytochrome interacting factor), binds preferentially to the Pfr form of Phytochromes (Ni *et al.,* 1998) and phytochrome PIF3 complexes have been shown to bind to a light-responsive G-box *cis*-element in vitro (Martinez-Garcia *et al.,* 2000). In *Arabidopsis* phytochrome interacting factors are members of a bHLH gene family (Heim *et al.,* 2003; Toledo-Ortiz *et al.,* 2003) and about six bHLH protein, which are closely related to PIF3 have also been implicated in phytochrome responses (Toledo-Ortiz *et al.,* 2003; Yamashino *et al.,* 2003). Various studies reveal that these transcription factors play positive or negative roles in light-induced signal transduction.

2.12 Ubiquitin-mediated Protein Degradation in phytochrome Signaling

In plants protein degradation and its regulation are important part in phytochrome mediated signal transduction. First, phyA colocalizes with the E3 ligase COP1 (COP1 is part of the light-dependent degradation machinery for phyA) in nuclear speckles and undergoes COP1-dependent ubiquitin-mediated degradation in the light. This step serves as a desensitizing mechanism for phyA function (Seo *et al.,* 2004; Sharrock and Clack, 2002). Later the downstream signaling components are subject to regulated protein degradation. PhyA signaling components like LAF1, HY5 were found to be the substrate of COP1 (Saijo *et al.,* 2003; Holm *et al.,* 2002). Another signalling component SPA1 (suppressor of *phytochrome*

A), was found to be a negative regulator of phyA signaling, and which is also directly interacts with COP1 (Hoecker *et al.,* 1999; Saijo *et al.,* 2003; Seo *et al.,* 2003). Two F-box proteins, EID1 (Empfindlicher ImDunkelroten licht 1) and AFR (attenuated FR response), play negative and positive roles in phyA signaling (Dieterle *et al.,* 2001; Harmon and Kay 2003).

2.13 Phytochromes and Hormones

The isolation and characterization of hormone signalling mutants has greatly helped in finding the roles of various hormones in signalling and how light signalling is integrated with hormone signalling (Chu *et al.,* 2005).

Auxin: Auxin play major role in various developmental processes and many of these processes are regulated through phytochrome action. The roles of auxin in root elongation, lateral root development and cell division and elongation (Chu *et al.,* 2005) has been well studied. Studies on auxin-regulated genes in combination with mutational analysis in Arabidopsis gave extensive insight into phytochrome-auxin crosstalk and interaction of auxin in phytochrome mediated light signalling (Møller *et al.,* 2002; Chu *et al.,* 2005).

Cytokinins: Cytokinins are involved in various developmental processes of higher plants that include cell division, inhibition of root growth, stimulation of de-etiolation etc….The studies that shows the presence of cytokinins and enzymes required for its metabolism in chloroplast provides a link between light signalling and cytokinins (Chu *et al.,* 2005; Eckardt *et al.,* 2002). The observation that cytokinins can rescue photomorphogenic response in pea lip mutant is also clearly indicating cytokinins role in light signalling. Response regulators like ARR4 (ARABIDOPSIS RESPONSE REGULATOR4) was found to interact with phytochrome B and plants overexpressing ARR4 showed enhanced sensitivity to red light while there observed delayed red light sensitivity when ARR4 has been knocked out. The involvement of

red light and cytokinins in ARR4 expression suggests its role in regulation of the crosstalk between light and hormones (Chu *et al.,* 2005).

Gibberellins: Though the exact role of GAs in phytochrome mediated light signalling is unclear, recent reports suggest that phytochrome and GA are closely interlinked. The GA signalling mutant *spy (spindly)* which has been isolated based on its spindly phenotype with light green leaves and long internodes resemble *phyB* mutant phenotype (Møller *et al.,* 2002; Chu *et al.,* 2005). RGA, a recessive suppressor of GA deficiency, encodes a protein, which is characterized as a member of GRAS protein family is demonstrated to localize to nucleus of plant cell. PAT 1, which is also a member of GRAS, was found to be involved in phytochrome signalling clearly showing the role of GRAS family protein in light signalling. Moreover, the member of GRAS family exhibit structural motif required for protein-protein interaction also strongly suggest the involvement of these group proteins in signal transduction. There are also cases where GA acts antagonistically to phytochromes. GA exhibits a positive effect in endoreduplication, while this phenomenon in Arabidopsis hypocotyl is under negative control of phytochrome. Similarly in contrast to phytochrome, GA induce early flowering in higher plants (Chu *et al.*, 2005).

ABA: ABA acts as a signalling molecule especially, when the plant is stressed (Xiong *et al.*, 2002). The response towards UV-B radiation in plants is operated mainly by the interactions between phytochrome signal system and ABA signal transduction pathway. By this mechanism, higher plants, their physiological and chemical reaction to the outside, thus reduce to the lowest extent of damage (Zhang *et al.,* 2002; Chu 2005).

2.14 TILLING

Targeting Induced Local Lesions in Genomes (TILLING) is a powerful technique which combines traditional mutagenesis with high through-put mutational screening to discover

induced lesions (McCallum *et al.,* 2000b). It enables the identification of single point mutations with the aid of a mismatch specific endonuclease CEL I. The strategy was applied successfully to a mutant collection of Arabidopsis and, since then procedure demonstrated its efficiency in the mutant collection of a large array of plant species includes rice (Till *et al.*, 2007b), maize (Till *et al.,* 2004), wheat (Slade *et al.,* 2005), *lotus* (Perry *et al*., 2003), pea (Triques *et al.,* 2007), tomato (Menda *et al.*, 2004; Saito *et al.,* 2011), barley (Talamè *et al.,* 2008), as well as animals like *Drosophila* (Winkler *et al.,* 2005) *Caenorhabditis elegans* (Gilchrist *et al.,* 2006), zebrafish (Wienholds *et al*., 2003b) and rat (Smits *et al*., 2004). Basic TILLING procedure consists of three steps: Developing a mutagenized population, (2) DNA pooling, and (3) mutation discovery (Till *et al.*, 2007b).

Traditional chemical mutagenesis methods, which include treatment of pollen or seeds with chemical mutagens such as EMS and MNU, which induce single nucleotide changes by alkylation of specific nucleotides, can be used for the development of mutagenized population. Chemical mutagenesis is reliable compared to other methods as it induces mutations that are high in density and are essentially randomly distributed throughout the genome (Greene *et al.,* 2003; Suzuki *et al.,* 2008). The selection of dosage of mutagen is crucial as a high dosage treatment may result in a high frequency of infertile plants. Plants arising from mutagenized seeds i.e., M_1 generation are chimeric in nature. M_2 generation in which mutations are stabilized can be used as a screening population for TILLING.

At first TILLING was based on protocol introduced by McCallum *et al.* (2000a), that successfully identified mutated alleles of a target gene. The protocol initially used a high throughput screening in which DNA samples are pooled to several fold followed by screening of the fragment of interest using a denaturing HPLC (dHPLC) platform for heteroduplex identification (McCallum *et al.,* 2000a). Later Colbert *et al.* (2001) modified the protocol to increase the sensitivity and throughput of the assay by introducing a digestion step where

PCR product is digested by an endonuclease at the mismatched position of the hetero duplex. Additionally they introduced a new platform of mutation detection by using a Li-COR electrophoresis system to run PCR product. The introduction of these modifications, to a great extent, increased the sensitivity and throughput of the assay.

2.15 Wild Tomato Species

The cultivated Tomato and its wild relatives belong to the large and diverse Solanaceae family also called Nightshades, which includes more than three thousand species. The *Lycopersicon* clade (Solanum sect. *Lycopersicon* previously known as genus Lycopersicon) consists of domesticated tomato (*Solanum lycopersicum*) and its 12 closest wild relatives (Peralta and Spooner, 2005). *S. ochranthum* and S. juglandifolium (belongs to *Solanum* sect. *Juglandifolia*), S. sitiens and *S. lycopersicoides* (belongs to sect. *Lycopersicoides*) are the closest outgroup species to the tomato clade. Charles Rick and colleagues made the first detailed studies on wild relatives of tomatoes as early in 1940's. The wild tomatoes and related nightshades are originated from the Andean region, including Peru, Bolivia, Ecuador, Colombia and Chile. Their growing environments of wild tomatoes range from sea level to sub alpine elevations, with some ecotypes adapted arid to rainy climate and others to extreme draught. The diversity of wild species, which is an outcome of their very large range of ecological conditions, also expressed at the morphological, physiological, sexual and molecular levels (Peralta and Spooner, 2005).

There are tremendous genetic potential locked up in wild tomatoes and that can be used effectively for crop improvement by searching for superior genes with the aid of modern technology. Domesticated species represent only a tiny fraction of the variability available among the wild relatives. Studies show that several useful traits which is found in wild tomato species, such as tolerance to drought and salinity (*S. pennellii*) (Dehan *et al.*, 1978; Shalata *et*

al., 1998), accumulation of health promoting phytochemicals (*S. habrochaites*), and resistance to multiple pathogens (*S. cheesmanii*, *S. lycopersicoides*, *S. neorickii* and *S.chilense*) can be introgressed into cultivated tomato (Venema, 1999; Stevens, 1986; Robert, 2001; Rick *et al.*, 1994).

3. MATERIALS AND METHODS

3.1 PCR Optimization

3.1.1 Standard Solutions and Reagents for the PCR

Nucleotides (dNTP) (Merck, Germany) were stored as a 100 mM stock solution (25 mM each dATP, dCTP, dGTP and dTTP). The standard 10X PCR buffer was prepared as described (Perkin-Elmer, Norwalk, CT, USA) and consisted of 500 mM KCl, 100 mM Tris- HCl, pH 8.3 (pH adjusted at 25°C) and 15 mM $MgCl_2$, 1% gelatin (w/v), 0.05% (v/v) Tween-20, 0.05% NP40 (v/v). In-house isolated *Taq* polymerase was used for PCR amplification. Bovine serum albumin (BSA), glycerol and polyvinylpolypyrrolidone (PVPP) were purchased from Sigma Chemical (St. Louis, MO, USA). Primers for TILLING were obtained commercially either from Biomer (Germany) or Sigma (St. Louis, MO, USA). Unless described the primers were used in a final concentration of 4 pmoles each. Both *phytochrome A* and *phytochrome B1* primers were used independently for PCR optimization. Genomic DNA was isolated using a protocol developed in our lab (Sreelakshmi *et al.*, 2009).

3.1.2 PCR Protocol

The basic PCR amplification reaction was carried out in 20 µl reaction volume consisting of autoclaved Milli-Q water, 1X PCR buffer [10 mM Tris, 5 mM KCl, 1.5 mM $MgCl_2$, 0.1% (w/v) gelatin, 0.005% (v/v) Tween-20, 0.005% (v/v) NP-40, (pH 8.3)], dNTP mixture (0.2 mM each), primer(s) (4 pmoles each), 6%(w/v) polyvinylpolypyrrolidone (PVPP), 1% (v/v) glycerol or BSA (20 mg/ml) (if used), *Taq* polymerase (0.18 µl /20 µl), and genomic DNA template (5 ng/20 µl). The components of the PCR can be added in any order; however, water is the first component to be added. The components were added to tubes placed on ice, and were mixed by vortexing followed by centrifuging the tubes in a tabletop centrifuge. Thereafter the tubes were transferred to Tetrad thermal cycler (M J Research Bio Rad) for PCR.

3.1.3 Analysis of PCR Products on Agarose Gel

The PCR products were separated by electrophoresis in stained ethidium bromide (0.5–1 mg/mL) containing agarose gel (1% (w/v)) (SeaKem LE, Rockland, ME, USA) in 1X TAE (0.04 M Tris-acetate; 0.001 M EDTA (pH 8.0)) buffer, at room temperature using 100-120 V current. The PCR products were visualized on the gel using an alpha imager gel documentation system.

3.1.4 Electrophoresis of PCR Product on Li-COR 4300 DNA Analyzer

After completion of PCR, the DNA (PCR products) was precipitated by the addition of 125 µl of cold absolute ethanol to the tubes. The tubes were then briefly incubated at -80°C followed by centrifugation at 4500 rpm in Sorvall SH-3000 rotor for 30 min. The precipitated pellet was washed with 70% (v/v) ethanol and excess ethanol was removed by keeping in a dry bath at 80°C. The pellet was finally suspended in 8 µl formamide loading buffer containing deionized formamide (37% (v/v)), 1 mM EDTA and 0.02% (w/v) bromophenol blue. The products were denatured by heating to 94°C for 2 min and then placed on ice. About 0.5 µl of the sample was loaded on a denaturing 6.5% (w/v) polyacrylamide gel and was electrophoresed in TBE buffer (89 mM Tris, 89 mM boric acid, 2 mM EDTA, pH 8.3) at 1500 V, 40 mA and 40 V setting in 4300 Li-COR DNA Analyser. The two TIFF images of 700 and 800 channels were imported to Adobe Photoshop software (Adobe Systems Inc.) and the gel was visually assessed for mutations.

3.2 TILLING

3.2.1 Plant Material and Consumables

The seeds of tomato (*Solanum lycopersicum*) *cv*. Arka Vikas (IIHR, Bangalore) or EMS mutagenized M_2 seeds of *cv.* M82 (Menda *et al.,* 2004) (originally obtained from Dani Zamir)

were used for this study. All the plasticware including deepwell plates (2 ml) were procured from Axygen Limited, India. The equipments used were capable of accommodating 96 well plasticwares: high-speed centrifuge (Evolution RC, Sorvall with SH-3000 swinging bucket rotor with capacity to centrifuge 4 deepwell plates at a time), 96 well pipettor (PP550 DS, Apricot Designs), Mini Beadbeater (BioSpec Products Inc.); PCR machine (DNA Engine Tetrad 2, MJ Research), 4300 DNA Analyzer (Li-COR Biosciences). Other equipments commonly used in molecular biology laboratory were horizontal gel electrophoresis system, gel documentation system (Alpha ImagerTM2200, Alpha Innotech), Nanodrop ND-1000 spectrophotometer, dry bath, water baths etc. All chemicals for DNA isolation were obtained from Sigma-Aldrich and the organic solvents used in the procedure were obtained from Qualigens Limited, India. Stock solutions for DNA isolation and TILLING were prepared in sterile MQ water (Milipore water purification system).

3.2.2 Development of EMS Mutagenized Populations

Seeds of tomato (*Solanum lycopersicum*) *cv*. Arka Vikas were used for mutagenesis using the following protocols as described below. Approximately 8000 tomato seeds (10-15 g) were imbibed in darkness in 500 ml double distilled water for 24 hours at 25 ± 2ºC in germination boxes (Koornneef *et al*., 1985). After draining excess water, the imbibed seeds were submerged in freshly prepared 60 mM (0.75% w/v) EMS (Ethyl Methane sulfonate) solution (500 ml) for 24 hours in dark with gentle shaking at 25±2°C. Following EMS treatment, the seeds were tied in a muslin cloth bag and were extensively washed under tap water for 8 hrs. Thereafter the seeds were over layered with blotting sheet. The seeds were then sown on nursery beds (2 m x 1 m) containing red loam sandy soil, in open field. To assure uniform spreading of seeds, the seeds were mixed with dry soil, sprinkled over the nursery bed and covered with a thin layer (~1 cm) of red loamy soil and vermiculite mixture. The nursery beds were covered with black polythene sheets until the seedlings begin to germinate. The nursery

beds were watered daily using a water sprinkler. A batch of 100 seeds was used as control and processed through the same procedures as described above without any EMS treatment. The three weeks old M_1 seedlings were transplanted from nursery bed to open field at a spacing of 1.3 m x 40 cm. The plants were watered using drip irrigation and M_2 seeds were collected. Each M_1 plant was labeled with a unique number for subsequent collection of M_2 seeds.

For growing M_2 plants, 10-15 seeds from each M_2 plants were treated with 2% sodium hypochlorite solution for 15-20 min, washed under running tap water, transferred to soilrite and were grown in individual paper cups in glass house. Two weeks old M_2 seedlings were transferred to clay pots and seedlings were grown up to an average height of 10 cm. Four individual seedlings (named as A, B, C and D) from each M_2 line was transplanted to open field and were grown to maturity. The seeds were extracted separately from four individual M_2 plants. The M_2 and M_3 seeds were Barcode labeled, catalogued and stored in -20°C freezers for long term storage. The same procedure was repeated later with an EMS solution of 120 mM (1.5% w/v) concentration.

3.2.3 Phenotyping and Data Analysis

The phenotype that are key indicators of the mutagenesis efficiency i.e, germination percentage and frequency of albinos and chimeric plants were recorded at the seedling stage of M_1 and M_2 populations. Each M_2 plant in the M_2 population was tagged with a unique plant-ID barcode label generated using BarTender v 7.5.1 Enterprise software (http://www.seagullscientific.com) and printed on synthetic polyester, non-erasable, tear proof paper using Zebra barcode printer (Zebra Technologies) (Vankadavath *et al.*, 2009). At different developmental stages of the plant, 15 major phenotype categories (Menda *et. al*., 2004) were recorded using a hand held Personal Digital Assistant (PDA). PDA has an inbuilt barcode laser scanner to identify barcode label tagged to the plants and customized software,

PHENOME, developed for large scale phenotypic data collection (Vankadavath *et al.,* 2009). For the different phenotypic variations observed, images were recorded using a digital camera (OLYMPUS CAMEDIA C-7070 wide zoom). All the recorded data and images were transferred to a central PC and analyzed to understand the effect of EMS mutagenesis on different developmental stages of tomato.

3.2.4 Extraction of DNA

Genomic DNA was extracted using a protocol developed in our lab (Sreelakshmi *et al.,* 2009). Young leaf tissue was harvested and placed in wells of deepwell plate or Eppendorf tube. The harvested tissue (80-100 mg/ 8 cotyledons) was disrupted mechanically with three steel balls of ~2 mm in diameter in Mini-Bead Beater for 2 min in the presence of 750 µl preheated (65°C) extraction buffer [(0.1 M Tris-HCl, pH 7.5; 0.05 M EDTA, pH 8.0; 1.25% (w/v) SDS) containing 0.2 M β-mercaptoethanol and 20 mg of insoluble polyvinylpolypyrrolidone (PVPP)]. The homogenate was then incubated at 65°C for 30 min for cell lysis. Contaminating RNA was removed by adding 4 µl RNase per well/tube from a 10 mg/ml stock and subsequent incubation for about 30 minutes at 37°C. Thereafter, proteins were precipitated by the addition of 400 µl of cold 6 M ammonium acetate and centrifuging at 4700 rpm in a swing out plate rotor (SH-3000) in Sorvall RC Evolution centrifuge for 30 minutes. Finally, the DNA was precipitated by adding equal volume of ice-cold isopropanol to the aqueous phase. After incubation at -20°C for at least 1 hour the precipitated DNA was collected by a centrifugation at 4700 rpm (SH-3000) for 30 minutes at 4°C.

The DNA pellet was washed twice with 70% (v/v) ethanol to remove traces of salts from the samples. The plates were then kept at 65°C for 10-15 min to dry the DNA pellet. To each well 200 µl TE (10 mM Tris, pH 7.5, 1 mM EDTA pH 8.0) supplemented with 3.2 µg/ml RNase, was added and the plates were kept at 4°C overnight for dissolving the DNA.

Thereafter, the plates were centrifuged at 4700 rpm at 4°C for 30 min to pellet any undissolved material. An aliquot from the supernatant (180 µl) was transferred to fresh 1 ml plate and stored at -80 °C. The concentration of DNA samples was first quantified by Nanodrop. The integrity of DNA was checked by agarose gels electrophoresis and quality was compared with a quantitative DNA ladder (Invitrogen, Carlsbad, CA.). The quantified DNA samples were then diluted to 5 ng/µl, vaccum dried, and stored at -20 °C for future use.

3.2.5 PCR for TILLING

The PCR was carried out in Tetrad Machine (Biorad) in 96-well microtiter plates. The primer sets for PCR amplification were designed using tomato gene sequences available in the NCBI GenBank (http://www.ncbi.nlm.nih.gov/).

The web-based tool CODDLE (http://proweb.org/coddle) was used to select the gene region for PCR amplification that may have the highest density of potentially deleterious mutations on treatment with chemical mutagens. Primers were designed by CODDLE using the Primer 3 software with melting temperatures ranging from 62 to 70° C and of length in the range of 25–32 nucleotides. 100 µM solution of each primer was prepared in TE buffer and aliquots were stored at -80°C to avoid repeated freeze–thaw cycles that could reduce fluorescent activity. The standard protocol of Colbert *et al.,* (2001) and Till *et al.,* (2006) were followed to detect SNPs.

A nested PCR strategy was used for better amplification of target from pooled DNA samples. The first PCR amplification was performed with a set of primers, designed from the flanking sequence of targeted genomic region and the diluted PCR product from the first PCR was used as a template for the second PCR. In the second PCR , a mixture of target specific inner primer with M13 overhangs, 5' fluorescent labeled M13 universal primers M13 F700 (5' TGTAAAACGACGGCCAGT 3') and M13 R800 (5' TGTAAAACGACGGCCAGT 3')

labeled with Infra-red dyes IRD700 and IRD 800 respectively were used to amplify the targeted region.

First step PCR amplification was performed in a volume of 20 µl with 2.5 ng DNA with an equal amount of reference (WT *cv*. AV) DNA. The reaction consisted of 5 µl of DNA template, 1X PCR buffer (10 mM Tris, 5 mM KCl, 1.5 mM $MgCl_2$, 0.1% (w/v) gelatin, 0.005% (v/v) Tween-20, 0.005% (v/v) NP-40, pH 8.8), 0.2 mM dNTPs, 0.18 µl *Taq* polymerase (in-house isolated), adjuvants: BSA (20 mg/ml) and 6% (w/v) PVPP and 3 pmoles each of first step forward and reverse primers. In the second step PCR reaction, 2 µl of two fold diluted first step PCR product was used as template and 3 pmoles of primers combined in a ratio of 3:2:4:1 (forward labeled: forward unlabeled: reverse labeled: reverse unlabeled) were used. The cycling conditions for amplification were 94°C-5 min, 35 cycles of 94°C-20 sec, 72°C-2 min followed by heteroduplex formation: 99°C-10 min, 80°C-20 sec, 70 cycles of 80°C-7 sec with a ramp of -0.3°C per cycle and held at 4°C.

3.2.6 Mismatch Cleavage Reaction

The mismatch cleavage reaction was performed in a total volume of 45 µl containing 20 µl of second PCR product, 1X CEL I digestion buffer (10 mM HEPES buffer pH 7.0, 10 mM KCl, 10 mM MgCl2, 0.002% (v/v) Triton X-100 and 10 µg/ml BSA) and CEL I enzyme at 1: 300 dilution (1 µl/ 300 µl CEL I digestion buffer). The mixture was incubated at 45°C for 15 min and then CEL I reaction was stopped by adding 10 µl stop solution (2.5 M NaCl, 75 mM EDTA, pH 8.0 and 0.5 mg/ml blue dextran). The DNA was precipitated by the addition of 125 µl of cold absolute ethanol and incubated at -80°C for 30 min. This was followed by centrifugation at 4500 rpm in a SH-3000 rotor for 30 min. The pellet was washed with 70% (v/v) ethanol, dried in a dry bath at 80°C and then suspended in 8 µl formamide loading buffer (37% (v/v) deionized formamide, 1 mM EDTA and 0.02% (w/v) bromophenol blue). The

PCR products were denatured by heating the plates/ tubes to 94°C for 2 min and then placed on ice. About 0.5 µl of the sample was loaded on a denaturing 6.5% (w/v) polyacrylamide gel. The samples were electrophoresed in TBE buffer (89 mM Tris, 89 mM boric acid, 2 mM EDTA, pH 8.3) at 1500 V, 40 mA and 40 V setting in 4300 Li-COR Analyzer. The two TIFF images obtained for 700 and 800 channels of Li-COR analyzer were analyzed in Adobe Photoshop software (Adobe Systems Inc.) and the gel was visually assessed for mutations. Mutations, which were visually discovered, were later on validated by analysis of target gene from mutant lines by PCR amplification and sequencing. The genomic DNA from homozygotes was reamplified and purified by a purification column (Bioserve) and outsourced for sequencing (Bioserve India).

3.3 EcoTILLING

3.3.1 Plant Materials and Growth Conditions

The accessions of tomato used for this study were obtained from NBPGR (National Bureau of Plant Genetic resources, http://www.nbpgr.ernet.in/), TGRC (Tomato Genetic Resource Center, University of California, Davis, http://tgrc.ucdavis.edu/), IIVR (Indian Institute of Vegetable Research, Varanasi, India, http://www.iivr.org.in) and Bejo Sheetal, Jalna, India (Table I, p-51). Prior to sowing, the seeds were surface sterilized in 2% (v/v) sodium hypochlorite. Seedlings were grown in plastic cup filled with Soilrite mixture. The cups were kept in large plastic trays filled with 1 cm of water. The seedlings were grown under white fluorescent light (100 µmol / m^2 / sec) in growth room at 25 ± 2°C until the harvest of leaf tissue.

3.3.2 Harvesting and DNA Isolation

Seedlings were harvested after full expansion of cotyledons, usually 7-10 days from germination. From each accession 100 mg cotyledon tissue was harvested and transferred to a single well of a 96-deep well plate. Genomic DNA samples were prepared from cotyledon tissue using a protocol as described earlier (Sreelakshmi *et al.,* 2009). The quality and quantity of DNA was assessed by running on a 1% (w/v) agarose gel with λ DNA ladder as a reference. The isolated DNA was diluted to final concentration of 2.5 ng/µl prior to PCR amplification.

3.3.3 PCR Amplification, SNP Detection and Confirmation

The standard protocol of Colbert *et al.* (2001) and Till *et al.* (2003, 2006) was followed to detect SNPs. Primers were designed to amplify approximately 800-1600 bp target region for 2 target genes. The sequence information for these genes was obtained from NCBI GenBank (http://www.ncbi.nlm.nih.gov/). The target regions in a given gene for SNP detection was ascertained by CODDLE software and primers were designed using Primer3 v.4 software. Nested PCR, a modification of standard PCR, which is based on two consecutive PCR reactions, was used to amplify targeted gene region. The first step PCR was carried out with a set of primers, designed from the flanking sequence of targeted genomic region. For next step appropriately diluted first step PCR product was used as a template in the second step. In the second step PCR, a mix of target specific inner primer with M13 overhangs and fluorescent labeled M13 universal primers M13 F700 (5' TGTAAAACGACGGCCAGT 3') and M13 - R800 (5' TGTAAAACGACGGCCAGT 3') labeled at 5′ end with IF dyes IRD 700 and IRD 800 respectively were used to amplify the targeted region (Table II, p-75).

First step PCR was performed in a volume of 20 µl with 2.5 ng genomic DNA with an equal amount of reference (WT AV) DNA. The reaction consisted of 5 µl of DNA template,

1X PCR buffer (10 mM Tris, 5 mM KCl, 1.5 mM $MgCl_2$, 0.1% (w/v) gelatin, 0.005% (v/v) Tween-20, 0.005% (v/v) Np-40, pH 8.8), 0.2 mM dNTPs, 0.18 µl *Taq* polymerase (in-house isolated) and 3 pmoles each of first step PCR forward and reverse primers. For second step PCR 2 µl of two fold diluted first step PCR product was used as template and 3 pmoles of primers combined in a ratio of 3:2:4:1 (forward labeled: forward unlabeled: reverse labeled: reverse unlabeled) were used.

After CEL-I digestion, second step PCR product was electrophoresed on a denaturing 6.5% (w/v) polyacrylamide gel at 1500 V, 40 mA and 40 V setting in 4300 Li- COR DNA Analyzer. The two TIFF images obtained in 700 and 800 channels were analyzed in Adobe Photoshop software (Adobe Systems Inc.) to visually assess for SNPs. The SNPs, which were detected on Li-COR were later validated by PCR amplification of gene from particular line and sequencing. The genomic DNA from accessions bearing SNP were reamplified and purified by a purification column (Bioserve) and sent for sequencing (Bioserve India).

3.4 Sequence Diversity of *PHY* Genes in Tomato Wild Relatives

3.4.1 Plant Materials and Growth Conditions

The Five wild *Solanum* species (*S. chilense;* S. *pimpinellifolium; S. habrochaites*; *S. pennellii*; *S. neorickii* and *S. cheesmanii*) were selected for this study along with tomato *S. lycopersicum* (*cv*. Ailsa Craig) (Table I, p-51). Seeds for these tomato accessions were obtained from the true-breeding monogenic stocks maintained by TGRC (University of California, Davis). The seeds were first surface sterilized with 2 % (v/v) sodium hypochlorite solution for 5-10 min at room temperature. Thereafter, the seeds were thoroughly washed under running tap water. Seeds were then sown in plastic cups filled with Soilrite mixture (Keltech Energies Limited, Karnataka, India) and were grown under continuous white light (100 µmol m^{-2} s^{-1}) at 25ºC. After fifteen days from sowing, seedlings were transferred to pots

and were grown in open field. Mature foliage leaves from each of the above accessions were used for RNA extraction. The collected tissue was either directly used for extraction or stored at -80°C for further experiment.

3.4.2 Primer Design

The structural and functional diversity of sequence in wild relatives of tomato was examined for phytochrome A, phytochrome B1, phytochrome E and phytochrome F (Table II, p-75). Primer 3 (http://frodo.wi.mit.edu/), a software for primer design was used to design primers suitable for target genes (Table III, p-89). The primers were designed by using the sequence of respective phytochrome gene obtained from Genebank. The primer pairs were selected in such a way that they amplified an amplicon of 800-900 bp size, which is an ideal size for sequencing. The properties of the primers such as Tm, GC content etc. were also checked with Oligocalc: oligonucleotide property calculator (http://www.basic. northwestern.edu/ biotools/oligocalc.html) or oligo analyzer: IDT (http://www.idtdna.com/analyzer/applications/ oligoanalyzer/) to rule out the possibility of hairpin or dimer formation between primer pairs.

3.4.3 Isolation of Total RNA

For total RNA isolation, the TRIzol reagent was used following instructions provided by the manufacturer (Invitrogen). Leaf tissues were homogenized to a fine powder in liquid nitrogen in a pre-cooled pestle and mortar. The homogenate was transferred to a 1.5ml Eppendorf tube. To 200 µg samples, 1 ml extraction buffer [TRIzol reagent: 38% (w/v) phenol] (USB Cooperation, Cleveland, Ohio, USA) was equilibrated to pH 4.0 with Tris-HCl buffer; 0.8 M guanidine thiocyanate; 0.4 M ammonium thiocyanate; 0.1 M sodium acetate (pH 5.0); 5% (w/v) glycerol] was added and samples were mixed by vortexing. Samples were then incubated for 5 min at room temperature. After incubation, 0.2 ml chloroform was added and tubes were subjected to vigorous vortexing. Thereafter tubes were incubated at room

temperature for 3 min followed by centrifugation at 10,000 rpm at 4°C for 15 min. After phase separation, the upper aqueous phase was carefully transferred into another Eppendorf tube and to it; 0.5 ml of isopropanol was added. After incubation at room temperature for 10 min, tubes were centrifuged (10,000 rpm; 4°C; 10 min) and the supernatant was discarded. The resulting pellet was washed with 75% ice-cold ethanol, and then re-centrifuged (10,000 rpm; 4°C; 10 min). Finally, the pellet was dissolved in 50 µl DEPC treated water. Total RNA concentration was determined by measuring absorbance at 260 and 280 nm. Samples were stored at -80°C until further use.

3.4.4 cDNA Synthesis

The cDNA for four phytochrome genes (*PHYA*, *PHYB1*, *PHYE* and *PHYF*) were amplified using the total RNA isolated from the respective plant tissue. Primers were designed for PCR using sequences in the NCBI database (Table II, p-75) (www.ncbi.nlm.nih.gov). The RNA samples were used to synthesise cDNA using SuperScript III reverse transcriptase (Invitrogen) following standard protocols. Gene-specific primers for *Phytochrome A*, *B1*, *E* and *F*, were designed to amplify full-length cDNA (Table III, p-89).

Amplification reaction was set up in a volume of 20 µl. The reaction consisted of 25 ng of template (cDNA), 1X PCR buffer (10 mM Tris, 5 mM KCl, 1.5 mM $MgCl_2$, 0.1% (w/v) gelatin, 0.005% (v/v) Tween-20, 0.005% (v/v) NP-40, pH 8.8), 2.5 mM dNTPs, 2.0 mM $MgCl_2$, 0.18 µl *Taq* polymerase (in-house isolated) and 3 pmoles of forward and reverse primers. PCR conditions were as follows: denaturation at 94°C for 2 min, followed by 35 cycles of 94°C for 20 s, 60°C for 45 s, and 72°C for 60 s. At the end, reactions were maintained at 72°C for 10 min followed by incubation at 4°C forever. Following amplification, the PCR products were visualized by electrophoresis on 1% (w/v) TAE-agarose gels stained with ethidium bromide.

3.4.5 Sequencing, Sequence Analysis, and Bioinformatics Tools

PCR products were sequenced using dideoxynucleotide chain termination method. DNA templates for sequencing reactions were purified with spin columns from Bioserve. Sequences were assembled using Chromas software (http://www.technelysium.com.au/chromaslite.html). Sequence analysis was done using multialin (http://multalin.toulouse.inra.fr/multalin/) which produced alignment of nucleotide sequences. The potential effect of SNPs on protein function was evaluated using the PARSESNP program, (http://www.proweb.org/-parsesnp/) which was used to find out the PSSM scores and SIFT values.

Position-specific scoring matrix (PSSM) is a commonly used representation of motif (patterns) in biological sequence. PSSMs enable the scoring of multiple alignments with sequences, structures etc. The conversion of a multiple alignment, such as a block, into a PSSM can use the multiple alignment sequence weights, the expected number of amino acids and the frequencies of unobserved amino acids (pseudocounts). SIFT (Sorting Intolerant From Tolerant) value can predict, whether an amino acid substitution affects the protein function. This prediction is based on the sequence homology and the physical properties of amino acids. For a SNP, a SIFT score < 0.05 and /or a PSSM score >10 is predicted to be damaging to the function of the encoded protein.

3.4.6 Tests of Neutrality

To test for deviations from the neutral equilibrium model of evolution, we performed Tajima's D (Tajima, 1989) analysis using the programs DnaSP (ver.5.0). In each locus, Tajima's D (Tajima, 1989) was calculated at all sites and at silent sites separately. Tajima's D is based on the discrepancy between the mean pairwise differences and Watterson's estimator (hw). In this analysis, negative values indicate an excess of low-frequency polymorphisms, whereas positive values indicate an excess of intermediate polymorphisms. DnaSP version

5.10 (Librado and Rozas, 2009) was used for carrying out statistical neutrality tests, and Tajima's D test (Tajima, 1989) was performed on each sequence. In addition, the nucleotide variation of each sequence was estimated as nucleotide diversity (Tajima, 1989).

3.4.7 Phylogenetic Analysis

We used Tree top-phylogenetic tree prediction from Gene Bee molecular biology service (http://www.genebee.msu.su/genebee.html) for analyzing the phylogenetic relationships between the sequences. Phylogenetic relationships were derived using the neighbor-joining method. Neighbor joining is a bottom up clustering method which uses distance measures to correct for multiple hits at the same sites and chooses a topology showing the smallest value of the sum of all branches as an estimate of a correct tree. This method computes the length of the branches of the tree and in each stage, two nearest nodes of the tree are chosen and defined as neighbors. This process is carried out until all the nodes are paired together.

3.4.8 Effect of R/FR Light on Seedling Phenotype

Surface-sterilized seeds were incubated in dark (D) for 72 h at 25°C on two layers of germination papers soaked with distilled water. The irradiation with continuous, R and FR (3 µmol/m^2/s) was started after emergence of the radicle. Seedlings used in all types of analyses were grown for 7 days after emergence under continuous broadband light.

3.5 Light Regulation of Lateral Root Formation (LRF) in Tomato

3.5.1 Plant Growth Conditions

Tomato seeds were surface sterilized in 2% (v/v) sodium hypochlorite for 15-20 min followed by washing under running tap water. Surface-sterilized seeds were germinated in dark at 25°C on two layers of germination papers soaked with distilled water. After emergence of the radicle, seeds were transferred to 1% agar plates. Plates were oriented vertically to allow roots

to grow on the surface of the media. Seedlings were grown in a culture room at 25 ± 1°C in continuous white light (100µmol m^{-2} s^{-1}). For experiments requiring specific light treatment, seedlings after radicle emergence, were irradiated with continuous, R (5 µmol/m^2/s) and FR (3 µmol/m^2/s). The root length was measured after 7 days of growth on vertical agar plates. For application of pharmacological inhibitors, seedlings after radicle protrusion were transferred on agar containing the concerned chemical/inhibitors. The effect of the following chemicals 0.5 µM TIBA (polar auxin transport inhibitor) or 20-80 µM ACC (ethylene substrate) were examined on root length.

3.5.2 Excision of Root Tips from Seedlings

Root tips were excised at desired time intervals with a sterilized blade while the seedlings were still on the plates. The plates were re-sealed and placed in the growth room for additional 3 to 5 days (based on the experiment). At the end of this period, numbers of lateral roots formed were counted.

4. RESULTS

4.1 PCR Optimization

The optimization of PCR is one of the most important requisite for successful TILLING. PCR is carried out using a set of stringent primers design, which includes high Tm and high GC content. In addition, since we used an in-house purified *Taq* polymerase, it also required rigorous optimization compared to commercially available *Taq* polymerase such as TAKARA-ex-*Taq*. Initial optimization for PCR was carried out using unlabeled primers. The parameters which were optimized included varying units of *Taq* polymerase, amount of Mg^{2+} ions, effect of monovalent salt concentration, amount of template (DNA) and effect of PCR additives (for more yield and specific product) in the PCR reaction. One of the major factors influencing PCR was the type of cycling conditions (i.e., touchdown versus straight cycles). Second level of optimization required achieving a proper balance between ratios of IR dye labeled primers and unlabeled primers. A cocktail of 3 pmoles of forward and reverse primers combined in a ratio of 3:2:4:1(forward labeled: forward unlabeled: reverse labeled: reverse unlabeled) was found to be most optimal for PCR amplification.

Based on a set of optimization experiments, a final protocol was derived for TILLING PCR, which included several modifications to overcome most of the commonly encountered problems related to PCR.

In current study, three different sets of primers (two sets for *phytochrome A viz* set A and set B and one set for *phytochrome B1*) were optimized (Table I). To save time, initial PCR optimization was carried out using set A primer of *phytochrome A*. Subsequently the same optimized protocol of PCR was also applied to two other primers used in this study.

Table I. The primer sequences for amplification of *phytochrome A* (*phyA*) and *phytochrome B1* (*phyB1*) gene used in TILLING. Two sets of primers were used for *phytochrome A* and one set of primer was used *for phytochrome B1*. The precise sequence of phytochrome gene amplified by respective primer set is indicated in the table.

Sl. No	Primers	Region amplified (bp to bp)	Product size (bp)	Sequence (Forward) 5′-3′	Sequence (Reverse) 5′-3′
1	*PhyA (set A)*	2684 to 4104	1420	ACACGTCAACA AGGAACTGGAA TTGGAAAATC	CTGATCAATTTG GCTGGTGTTCT GAGTGGA
2	*PhyA (set B)*	1304 to 2708	1402	AGGTAGAGGCT TTACGATAAATC ATCC	AATTCCAGTTCC TTGTTG ACGTGTATG
3	*PhyB1 (set A)*	3041 to 3908	868	CATCACAAGGT CAAGCTCAATCT TCAGG	TCCACAATCATT CTCACCCTGTCC TGC

4.1.1 Optimization of PCR using *Phytochrome A* (set A) Primers

Optimization with unlabeled primers: Since agarose electrophoresis is more cost effective to detect PCR product, initial PCR optimization were carried out using unlabeled primer. Following modifications were attempted to optimize PCR using unlabeled primers:

i) Gradient PCR

ii) Optimization of cycling parameters

iii) Optimization of ratio of reaction components

iv) Use of different adjuvants.

Gradient PCR: Using tomato genomic DNA, a gradient PCR was set up for *Phytochrome A* (set A) primer with a temperature gradient ranging from 62ºC to 70ºC. Analysis of PCR products on agarose gel electrophoresis showed that temperature of 62°C was most optimal for annealing resulting in sharp band of PCR products (Fig. 1). Taking above result in

account, 62ºC was chosen as the temperature for *phytochrome A* (set A) primer set for further PCR optimization.

Optimization of PCR Cycling Conditions: Even though annealing at 62ºC resulted in better PCR amplification with unlabeled primers, when PCR product were electrophoresed on a Li-COR DNA analyser used for TILLING, we found that simple straight cycle PCR was insufficient and did not yield a satisfactory PCR amplification for visualization on Li-COR machine (Fig. 2). Therefore as a next step, we optimized the PCR cycling parameters to attain a better amplification for TILLING. Initial modifications which included variations in the annealing time and extension time during cycling did not improve the PCR product formation.

To overcome this we adopted a different method of PCR, *viz* touchdown PCR, where cycling conditions were altered. A touchdown program was used where annealing temperature was progressively lowered from 70ºC to 60ºC by 1ºC every cycle followed by 10 additional cycles at 60ºC. Using above touchdown program for PCR with *Phytochrome A* primer (Set A), a 3 fold better PCR amplification was attained compared to normal straight cycle PCR. Moreover agarose gel electrophoresis revealed that PCR product band was sharper compared to straight cycle PCR (Fig. 3).

Use of adjuvants: PVPP, glycerol and BSA: Several studies recommend glycerol as an adjuvant to improve efficiency and also specificity of PCR, when used at a suitable concentration. Addition of glycerol in PCR mixture enhanced the yield of amplification; however, we observed that increasing the concentration of glycerol could also lead to decrease in PCR specificity (Fig. 4). Compared to glycerol, inclusion of BSA (20 mg/ml) was found to be a better alternative. Inclusion of BSA increased the efficiency of the PCR without leading to nonspecific PCR product formation. The enhancing effect of BSA on PCR yield

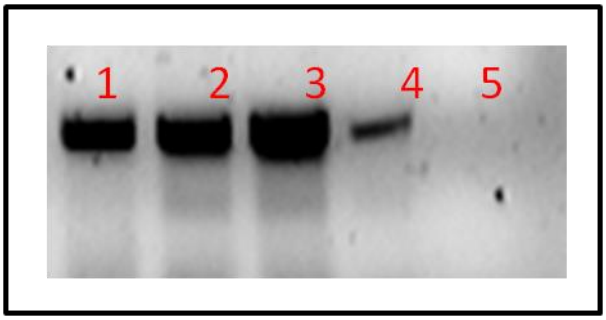

Figure 1. Determination of optimal annealing temperature for PCR using *phytochrome A* (setA) primer. A gradient PCR was carried out with a temperature gradient ranging from 60ºC to 65ºC. Lane 1: 60ºC, lane 2: 61ºC, lane 3: 62ºC, lane 4: 63 ºC and lane 5: 64 ºC. The optimal annealing temperature was found to be 62ºC (lane 3). The following cycling parameters were selected: denaturation 20 s, 30 cycles of annealing (40 s) and extension (2 min).

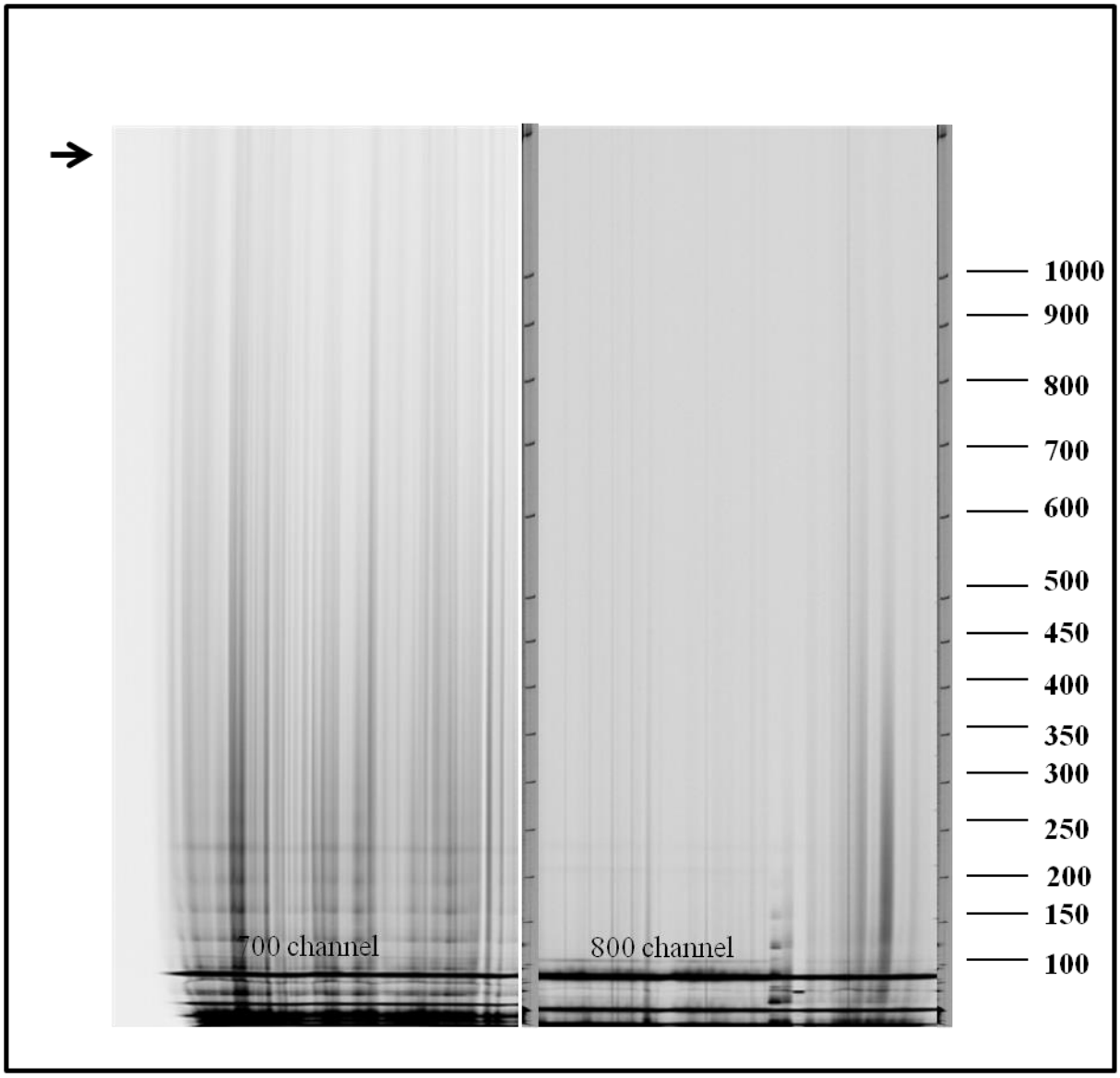

Figure 2. Li-COR gel images showing amplification profile for a 1.4-kb region of *Phytochrome A* gene (amplified using primer set A). Note that the PCR product is not visible (Arrow). The size (bp) of the marker is indicated on right side of the image. The following cycling parameters were selected: denaturation 20 s, 30 cycles of annealing 40 s and extension 2 min, *and Taq* polymerase 0.4 units.

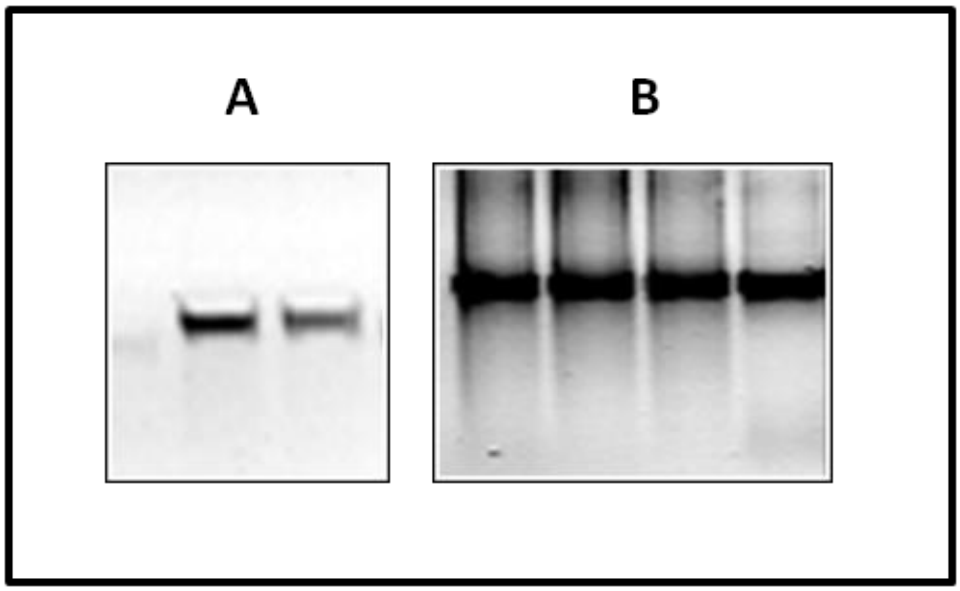

Figure 3. Comparison of PCR cycling conditions for amplification of a 1.4-kb *Phytochrome A* gene region (amplified using primer set A). (A) Straight (normal cycling), and (B) touchdown cycling. Note that compared to straight cycle more efficient PCR amplification is obtained with touchdown cycling. The following cycling parameters were selected for straight cycle: denaturation 20 s, 30 cycles of annealing 40 s, and extension 2 min. For touchdown cycle: denaturation 20 s , 22 cycles of annealing 40 s, and extension 2 min with initial annealing at 70 ºC for 40 s with a temperature decrement of 1ºC after each cycles for 8 cycles.

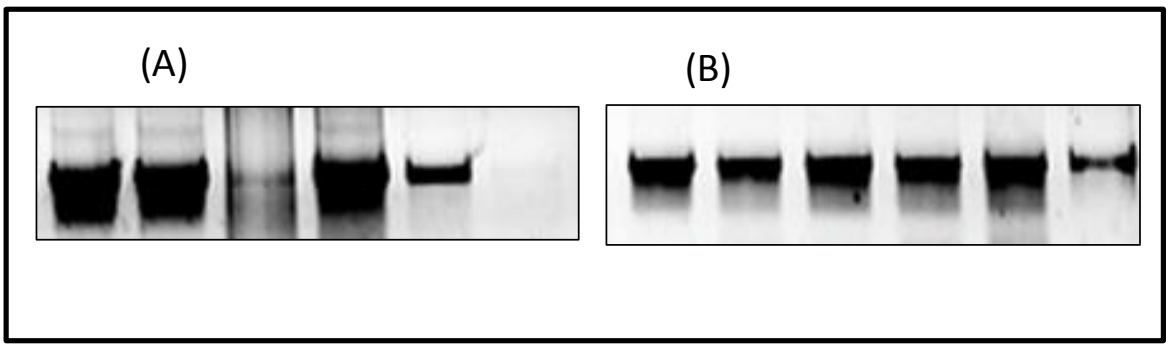

Figure 4. Effect of 1% (w/v) glycerol on PCR amplification of a 1.4-kb *Phytochrome A* gene region (amplified using primer set A . (A) 1% (w/v) glycerol, and (B) without 1% (w/v) glycerol. Though there was an increased PCR product formation in the presence of glycerol, there is also a decreased specificity and lack of consistency (A). A touchdown cycle with following cycling parameters was used for amplification: denaturation 20 s, annealing 40 s, extension 2 min, *Taq* polymerase 0.4 units. An initial annealing at 70ºC for 40 s with a temperature decrement of 1ºC after each cycles for 8 cycles.

was more obvious when it was used along with 6% (w/v) PVPP. It is likely that inclusion of PVPP may have removed phenolics which co-purifies with plant genomic DNA (Fig. 5).

Optimization with labeled primer: After achieving improved PCR amplification with unlabeled primer, we next optimized PCR combining fluorescently labeled with unlabeled primer using standard protocol of TILLING. Surprisingly the same PCR combinations which yielded optimal amplification with unlabeled primer, were found to be suboptimal as these did not yield a good profile of PCR product on Li-COR DNA analyzer (reaction with labeled primer) (Fig. 6). In view of this, PCR optimization was further continued by modifying various reaction components to suite for TILLING.

Optimization of Reaction Components

To overcome the inconsistency of PCR reaction and to attain better reproducibility, further optimization was attempted by again varying the concentration of various PCR reaction components. As described above the parameters which were tested included units of *Taq* polymerase, amount of Mg^{2+} ions and amount of dNTP in the PCR.

Amount of *Taq* polymerase: On testing different concentrations of *Taq* polymerase (In-house isolated) optimal enzyme amount was found to be around 0.18 µl for a 20 µl reaction volume (Fig. 7). Though a range of *Taq* amount from 0.1 to 0.4 µl led to better PCR amplification (data not shown), a mid-range, 0.18 µl *Taq* /20 µl, was selected for PCR as it resulted in maximum consistency for formation of PCR product.

Amount of $MgCl_2$: Most PCR protocols recommend a concentration of about 1.5 mM magnesium chloride, along with dNTP concentrations of about 2.5 mM each. To examine the influence of magnesium chloride, a PCR was performed, by keeping a fixed concentration of dNTP (2.5 mM) and a stepwise increment of magnesium chloride from 1.5–2.5 mM (Fig. 8).

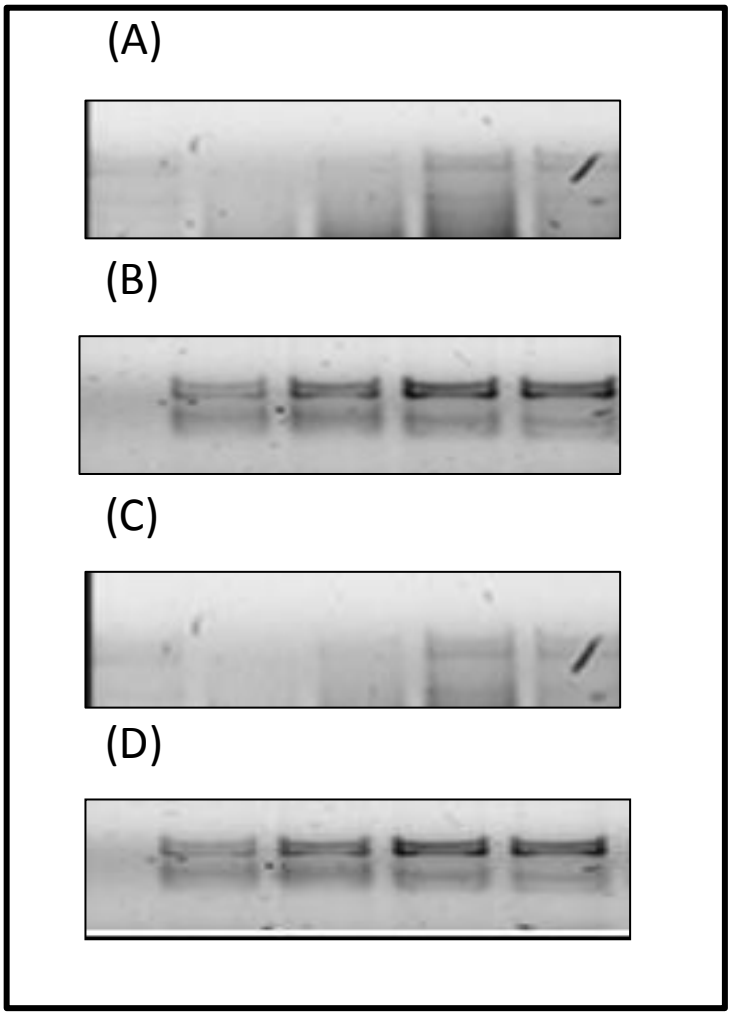

Figure 5. Effect of BSA (20 mg/ml) and PVPP (6% w/v) on PCR amplification of a 1.4-kb *Phytochrome A* gene region (amplified using primer set A). (A) control, (B) 20 mg/ml BSA, (C) 6% (w/v) PVPP, and (D) 6% (w/v) PVPP + 20 mg/ml BSA. Note the inclusion of BSA (20 mg/ml) increased the efficiency of the PCR without undesired nonspecific PCR product formation. When used in combination with 6% (w/v) PVPP the enhancing effect of BSA was further increased (D). A touch down cycle with following cycling parameters was used for amplification: denaturation 20 s, annealing 40 s, extension 2 min, and *Taq* polymerase 0.4 units. An initial annealing at 70ºC for 40 s with a temperature decrement of 1ºC after each cycles for 8 cycles.

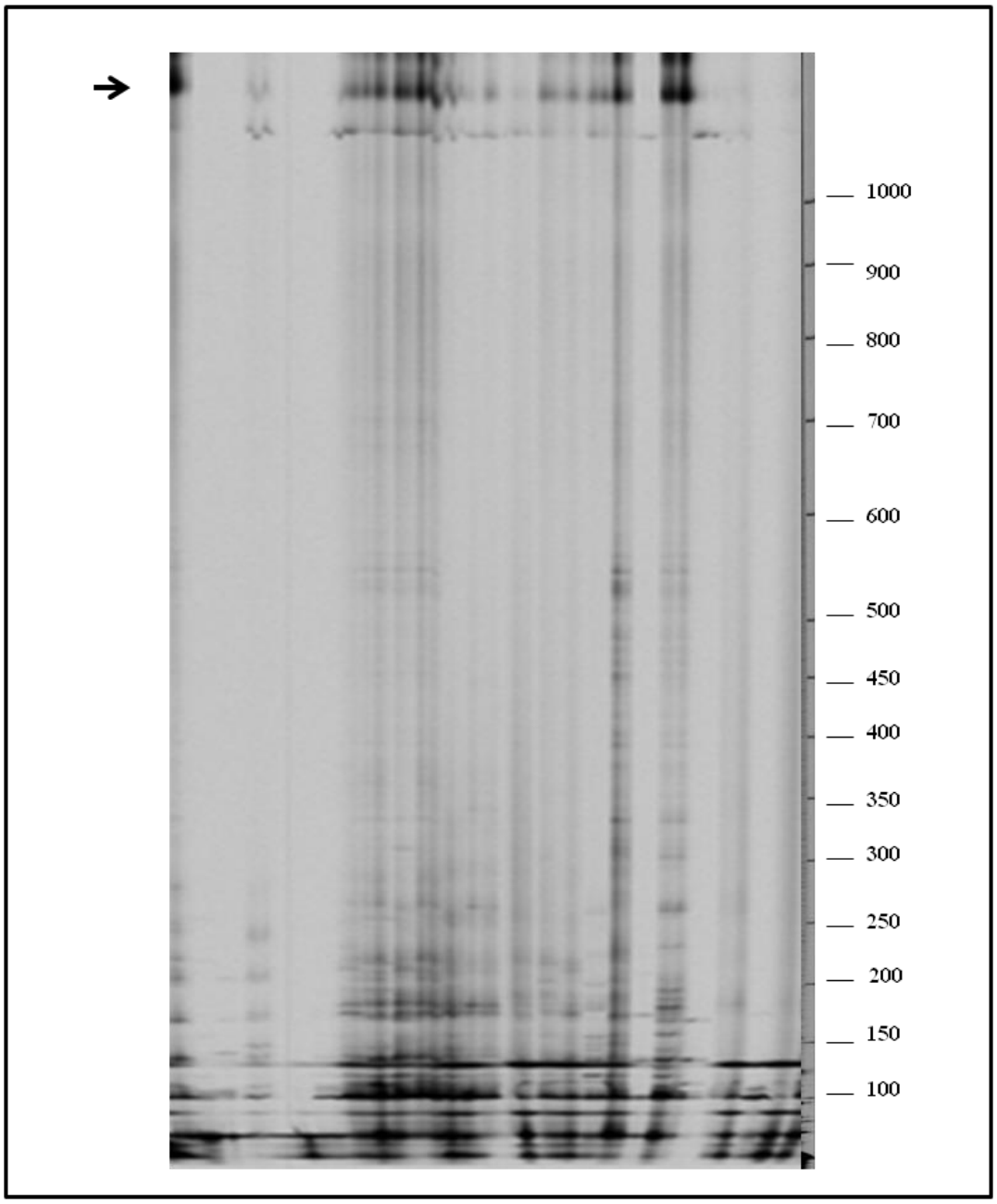

Figure 6. A Li-COR image showing PCR amplification of a 1.4-kb *Phytochrome A* gene region (amplified using primer set A). A touchdown cycle was used and adjuvants (BSA(20 mg/ml) and 6% (w/v) PVPP) were added in the reaction mix. Note the absence of a PCR product (arrow). Only 700 channel is shown here. The size (bp) of the marker is indicated on right side of the image.

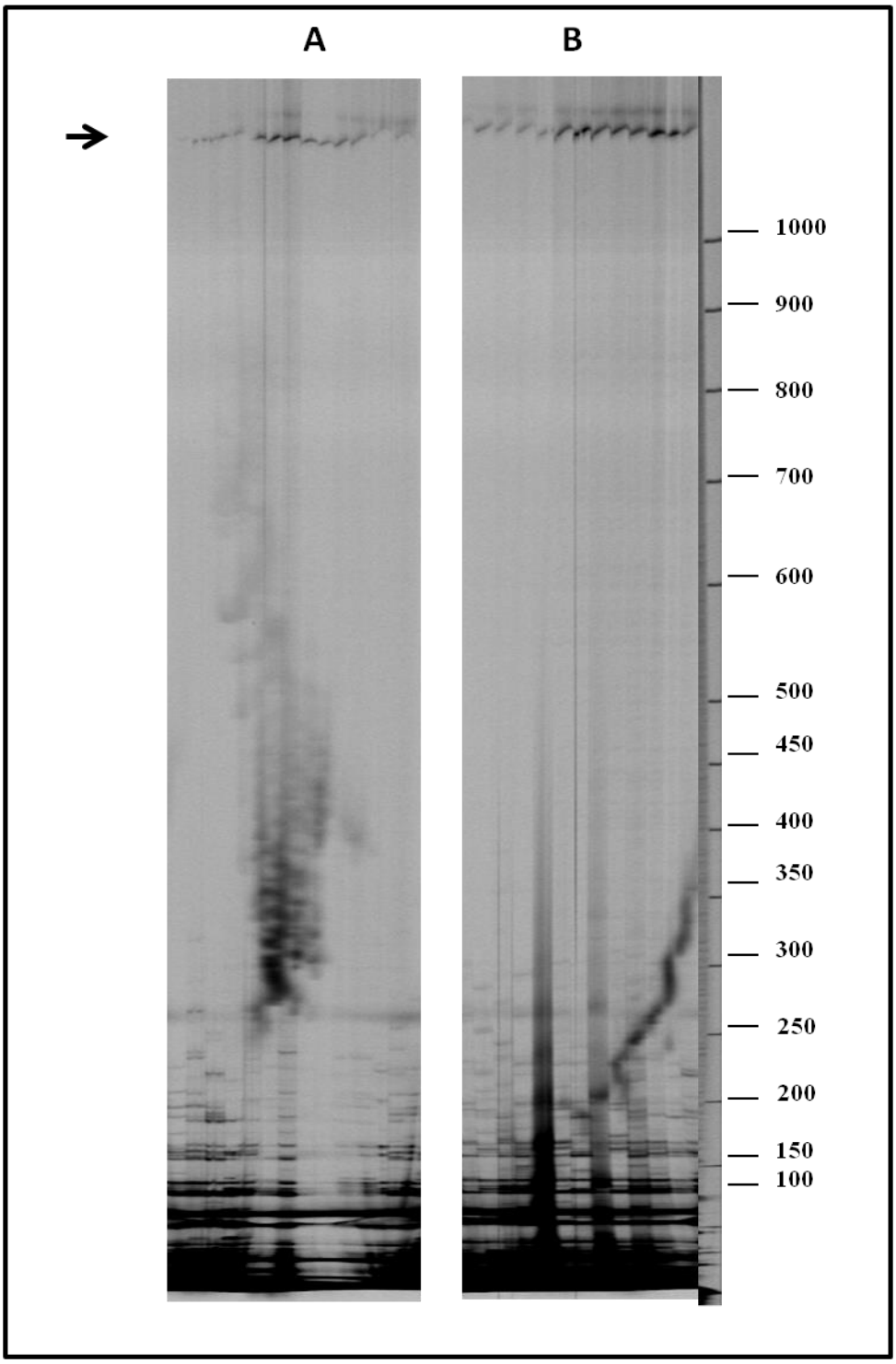

Figure 7. A representative Li-COR image showing effect of concentration of *Taq* polymerase on amplification of 1.4-kb *phytochrome A* gene region (amplified using primer set A. (A) 0.10 µl *Taq*, and (B) 0.18 µl *Taq*. Note an increased amplification with 0.18 *Taq*. A touchdown cycle was used and adjuvants (BSA (20 mg/ml) and 6% (w/v) PVPP) were added to the reaction mix.(only 700 channel is shown). The size (bp) of the marker is indicated on right side of the image.

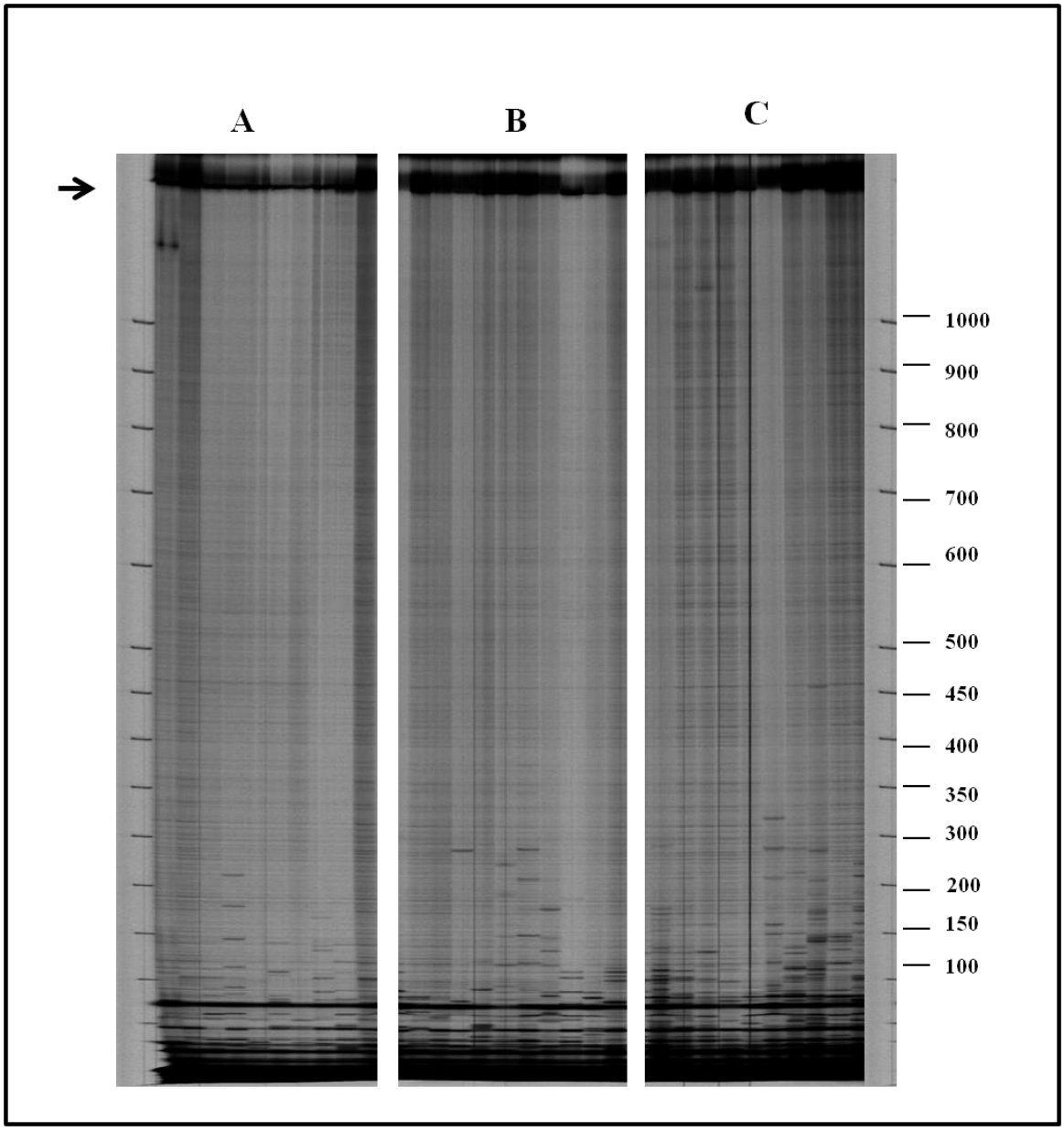

Figure 8. Representative Li-COR gel images showing optimization of $MgCl_2$ concentration for amplification of 1.4-kb *Phytochrome A* gene region (amplified using primer set A). The full-length PCR product is visible as a dark line at the top of each wells (top arrow). Amplifications with three different $MgCl_2$ concentrations are shown. (A) 1.5 mM, (B) 2 mM, and (C) 2.5 mM. Note a robust and specific *phytochrome A* amplification in panel B. A touchdown cycle was used and adjuvants BSA (20 mg/ml) and 6% (w/v) PVPP) were added in the reaction mix (only 700 channel is shown). The size (bp) of the marker is indicated on right side of the image.

Our results showed that at high concentrations (~2.5 mM $MgCl_2$), the PCR amplification resulted in more specific product. At this concentration, there was almost 2-fold increase in products formation compared to the standard $MgCl_2$ concentration.

Amount of dNTP: The effect of varying dNTP concentration in a TILLING PCR was tested by maintaining constant concentration of other reaction components. On testing two different dNTP concentrations (2.5 mM and 3 mM) it was found that both concentrations led to good yield of PCR product. Since both the concentrations were giving good yield, the lower concentration of dNTP (2.5 mM) was selected for TILLING reactions (Fig. 9).

Nested PCR

A modification of standard PCR, Nested PCR, which basically employs two consecutive and independent PCR reactions, was used to amplify gene targets for TILLING. This two-step PCR or nested PCR was employed to increase the sensitivity of the technique and also to reduce nonspecific amplifications. In the TILLING reaction where pooled DNA is used as the template, nested PCR plays an important role by increasing specific product formation. The first step of PCR amplification was carried out using a set of unlabeled primers, designed from the flanking sequence of targeted genomic region. After completion of first step PCR the diluted first step PCR product was used as a template for the second step PCR (Fig. 10).

Using these combinations, a protocol was derived for *phytochrome A* (set A) primer for TILLING PCR. For the nested reaction the first step PCR was carried out using a straight cycle. First step PCR amplification was performed in a volume of 20 µl with 5 ng DNA (1:1 ratio of reference: mutant sample). The reaction mixture consisted in final volume of 5 µl of the DNA template, 1X PCR buffer (10 mM Tris, 5 mM KCl, 1.5 mM $MgCl_2$, 0.1% (w/v) gelatin, 0.005% (v/v) Tween-20, 0.005% (v/v) NP-40, pH 8.8), 0.2 mM dNTPs, 0.18 µl *Taq* polymerase and 3 pmoles each of first step unlabeled forward and reverse primers.

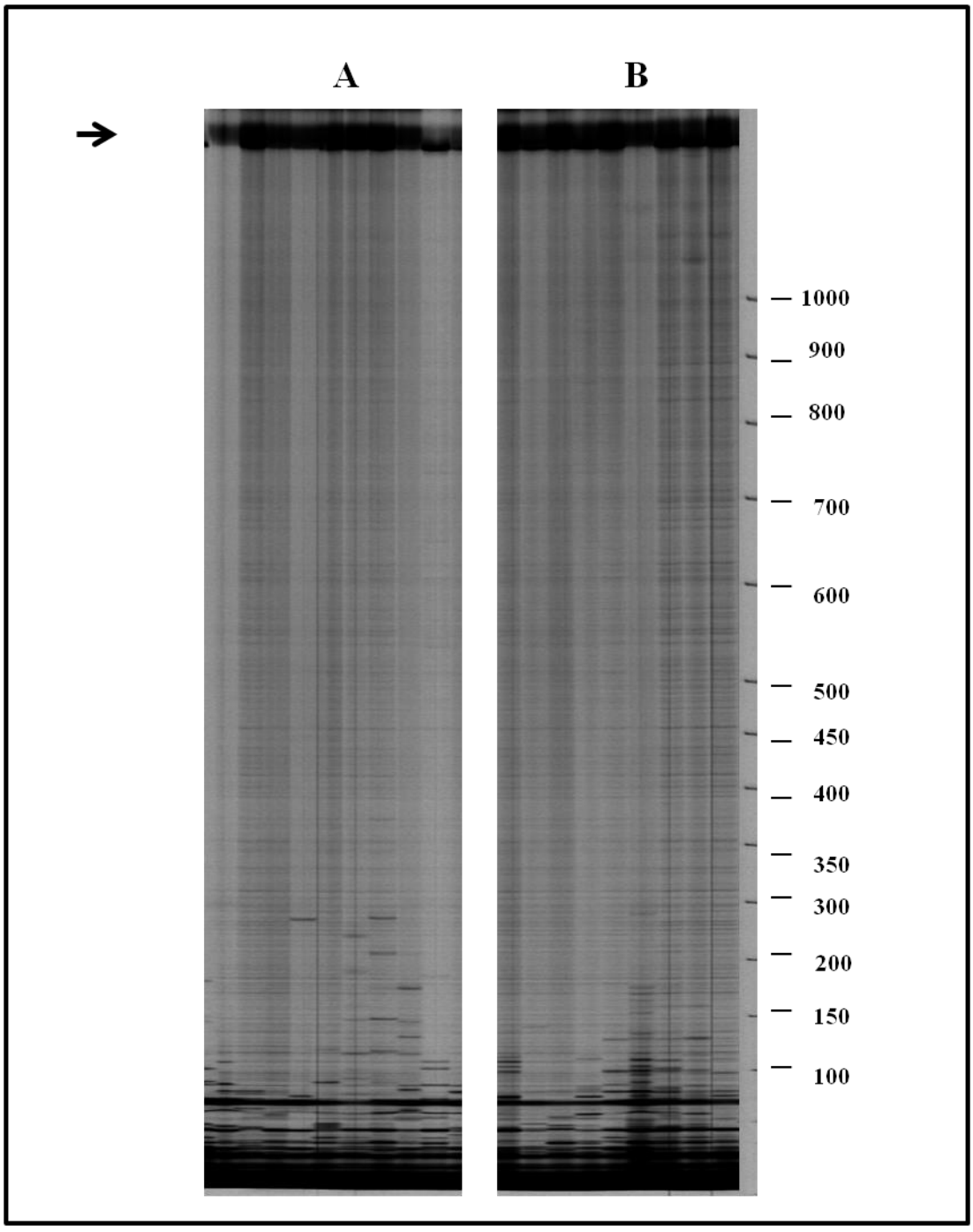

Figure 9. Representative Li-COR gel images showing optimization of dNTP concentration for a 1.4-kb *Phytochrome A gene region* (amplified using primer A). The full-length PCR product is visible as a dark line at the top of each wells (top arrow). Amplification with two different dNTP concentrations (2.5mM and 3 mM) was shown. (A) 2.5 mM and (B) 3 mM. A touchdown cycle was used and adjuvants (BSA(20 mg/ml) and 6% (w/v) PVPP) were added in the reaction mix (only 700 channel is shown). The size (bp) of the marker is indicated on right side of the image.

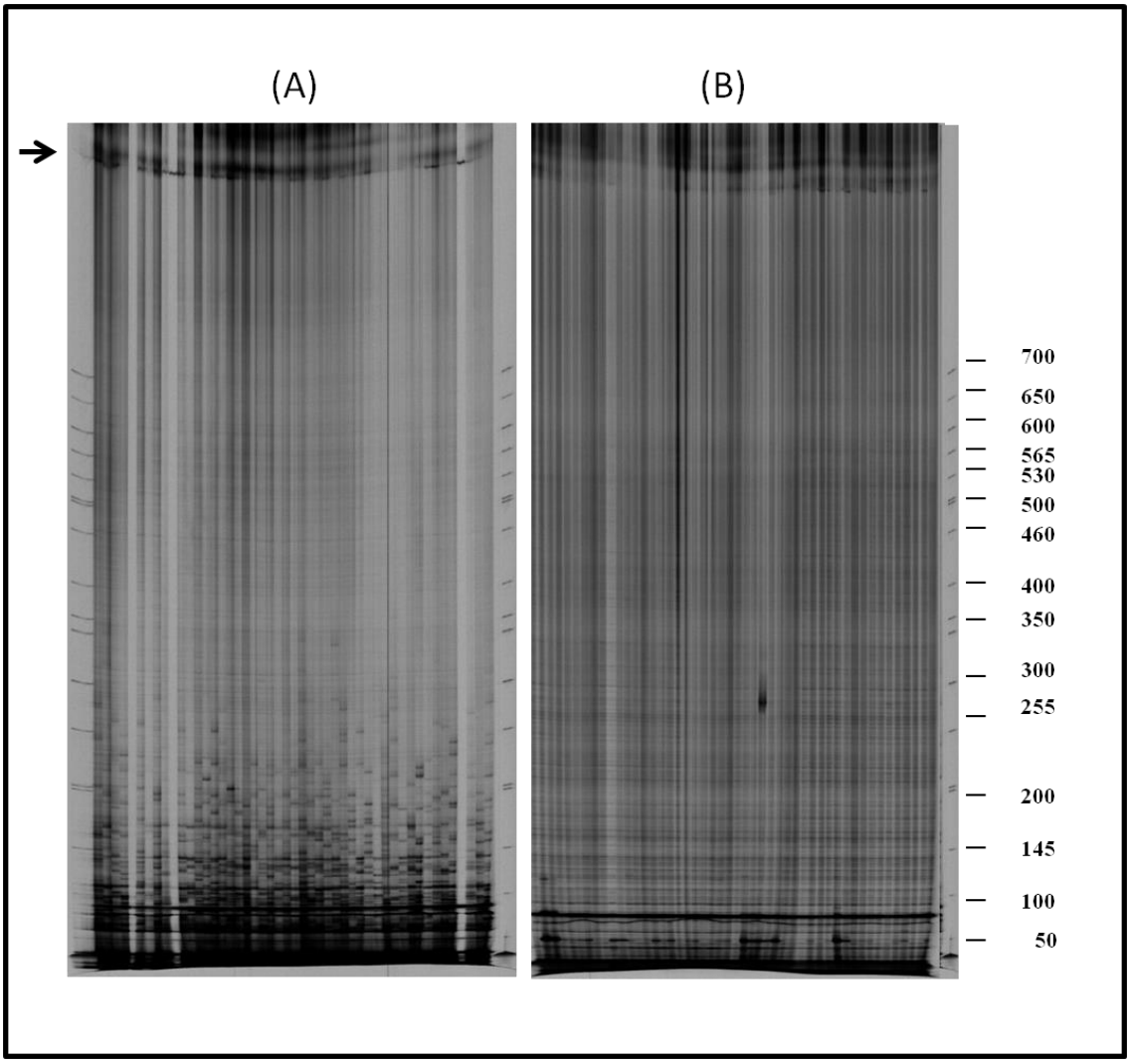

Figure 10. Representative Li-COR gel images showing improvement of amplification profile for a 1.4-kb *Phytochrome A gene region* (amplified using primer set A with nested PCR). The full-length PCR product is visible as a dark line at the top of each of the 48 wells (top arrow). (A) Normal PCR and (B) nested PCR. A touchdown cycle was used and adjuvants (BSA (20 mg/ml) and 6 % (w/v) PVPP) were added in the reaction mix. Only 700 channel is shown. The size (bp) of the marker is indicated on right side of the image.

This was followed by the second step PCR reaction where an aliquot of 2 µl of two fold diluted first step PCR product was used as template. Here 3 pmoles of unlabeled and labeled primers combined in a ratio of 3:2:4:1 (forward labeled: forward unlabeled: reverse labeled: reverse unlabeled) were used. In contrast to straight cycle used for first step PCR, for second step PCR touchdown cycle with following parameters were used for amplification: denaturation for 20 s, annealing at 60ºC 40 s, extension 2 min, *Taq* polymerase 0.4 µl with an initial annealing temperature set at 70ºC for 40 s followed with a temperature decrement of 1ºC after each cycles for 8 cycle). The reaction mixture consisted of 1X PCR buffer (10 mM Tris, 5 mM KCl, 1.5 mM $MgCl_2$, 0.1% (w/v) gelatin, 0.005% (v/v) Tween-20, 0.005% (v/v) NP-40, pH 8.8), 0.2 mM dNTPs, 0.18 µl *Taq* polymerase (in-house isolated) and adjuvants: BSA(20 mg/ml) and 6% (w/v) PVPP (Fig. 11).

4.1.2 PCR Optimization for *Phytochrome B1*

A very similar series of steps for optimization that were used for *Phytochrome A* (set A) primers was also carried out for *Phytochrome B1* primer. The parameters which were optimized included units of *Taq* polymerase, amount of Mg^{2+} ions, effect of monovalent salt concentration, amount of 10X buffer added into the reaction mixture for PCR (0.8X-1.5 X) and effect of additives (for more yield and specific product) on the PCR reaction. The effect of cycling conditions was also checked. It was found that touchdown cycle is also well-suited for *Phytochrome B1* amplification. Subsequently, nested PCR strategy was also optimized for the amplification of *Phytochrome B1* (Fig. 12). Second level of optimization was carried out using with labeled primers. The reaction was optimized in a reaction volume of 20 µl, with 5 ng of DNA. The reaction consisted of 5 µl of template,1X PCR buffer (10 mM Tris, 5 mM KCl, 1.5 mM $MgCl_2$, 0.1% (w/v) gelatin, 0.005% (v/v) Tween-20, 0.005% (v/v) NP-40, (pH 8.8), 0.2 mM dNTPs, 0.18 µl *Taq* polymerase (in-house isolated) and 3 pmoles of primers

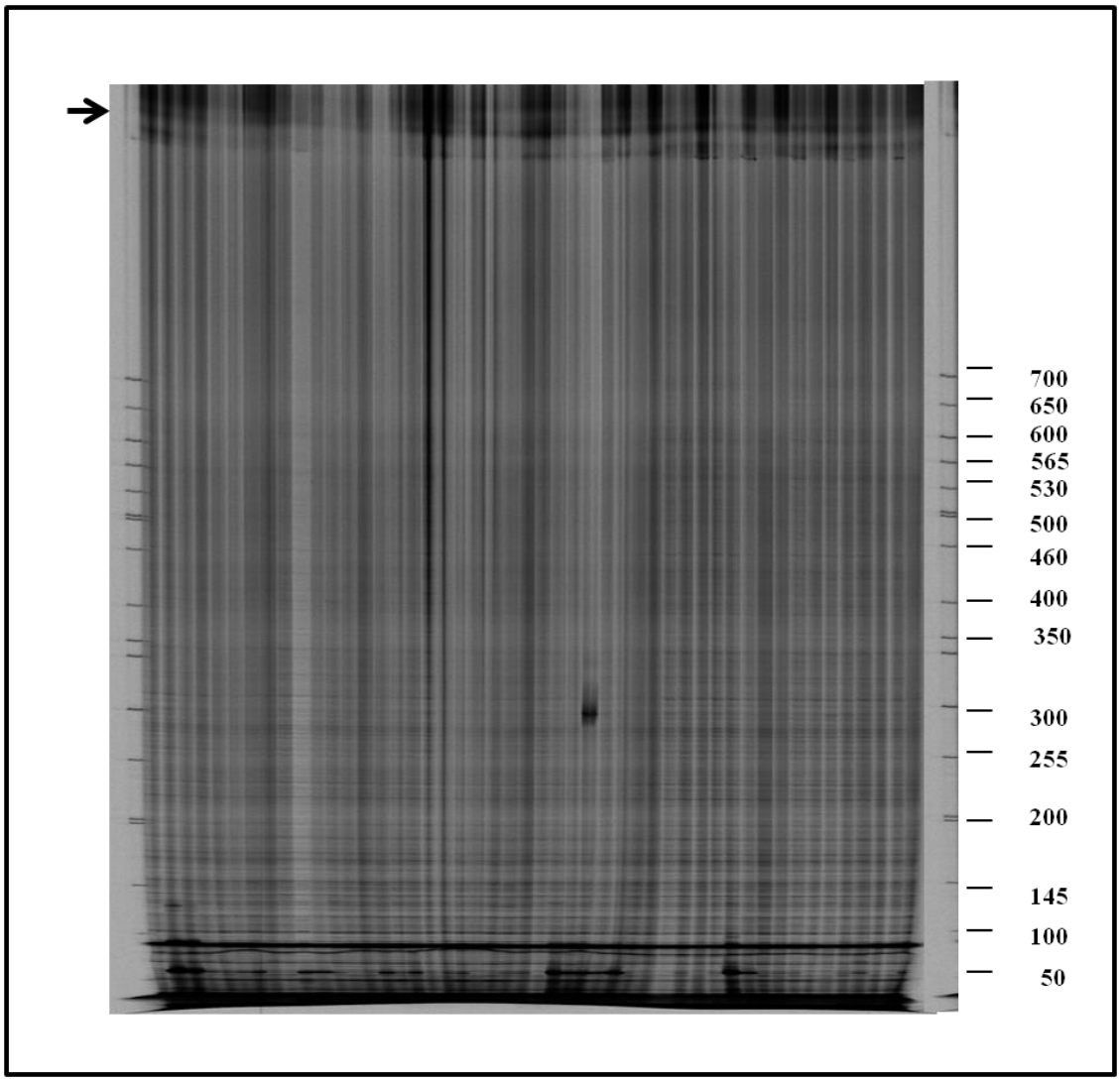

Figure 11. Representative Li-COR gel images showing an amplification profile for a 1.4-kb *Phytochrome A gene region* (amplified using primer set A). The full-length PCR product is visible as a dark line at the top of each of the 96 wells (top arrow). A touchdown cycle was used and a reaction mix consisted of 5 ng of template, 1X PCR buffer, 0.2 mM dNTPs, 0.18 µl *Taq* polymerase (in-house isolated) and 3 pmoles of primers cocktail and adjuvants (BSA(20 mg/ml) and 6% (w/v) PVPP) was used for this reaction (only 700 channel is shown). The size (bp) of the marker is indicated on right side of the image.

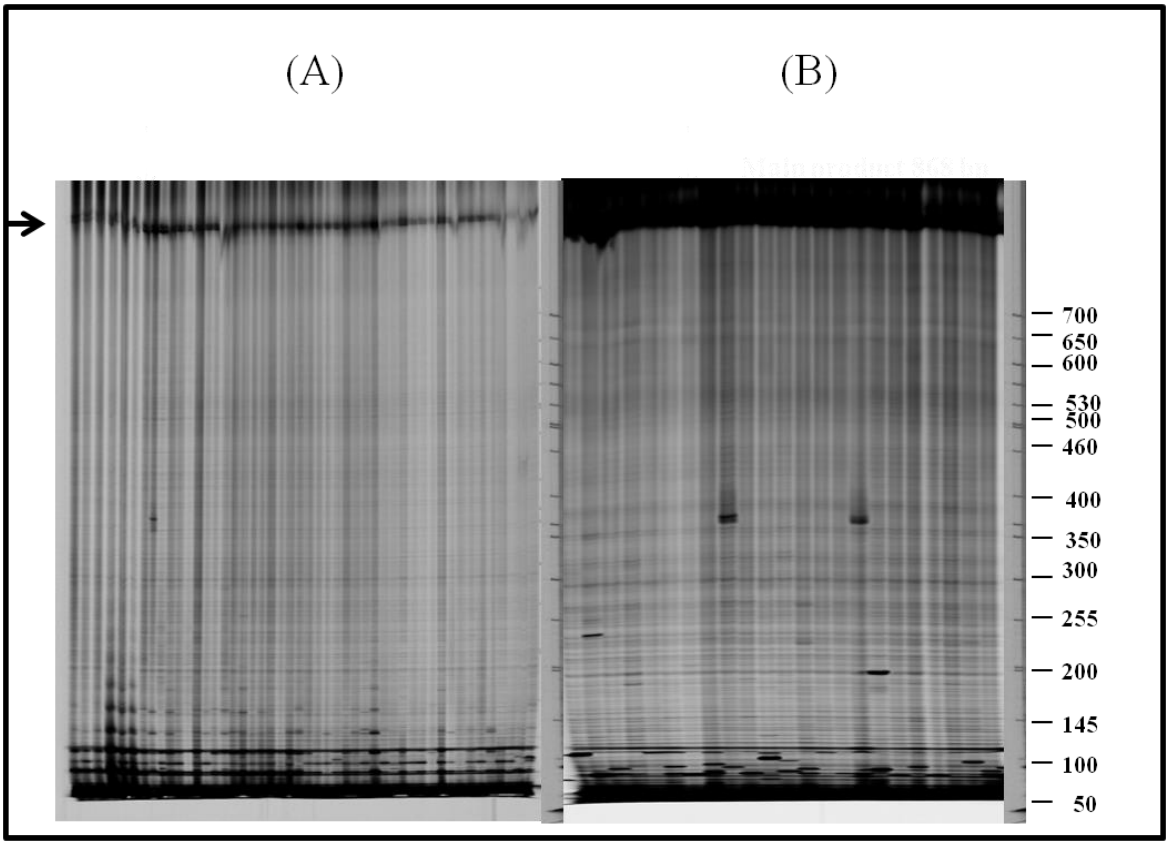

Figure 12. Representative Li-COR gel images showing improvement of amplification profile for a 868-bp *Phytochrome B1 gene region* (amplified using *phytochrome B1* primer set B) with nested PCR. The full-length PCR product is visible as a dark line at the top of each of the 48 wells (top arrow). (A) Normal PCR and (B) nested PCR. A touchdown cycle was used and adjuvants (BSA(20 mg/ml) and 6 % (w/v) PVPP) were added in the reaction mix. Only 700 channel is shown. The size (bp) of the marker is indicated on right side of the image.

combined in a ratio of 3:2:4:1 (forward labeled: forward unlabeled: reverse labeled: reverse unlabeled) (Fig. 13).

4.1.3 PCR Optimization for *Phytochrome A* Primer (set B)

The composition used for *Phyochrome A* (for set B primer) consisted of 5 µl of genomic DNA template, 1X PCR buffer (10 mM Tris, 5 mM KCl, 1.5 mM $MgCl_2$, 0.1% (w/v) gelatin, 0.005% (v/v) Tween-20, 0.005% (v/v) NP-40, pH 8.8), 0.2 mM dNTPs, 0.18 µl *Taq* polymerase (in-house isolated) and 3 pmoles of primers combined in a ratio of 3:2:4:1 (forward labeled: forward unlabeled: reverse labeled: reverse unlabeled) (Fig. 14).

4.2 TILLING

4.2.1 High Throughput Mutation Detection Platform

In general, TILLING identifies mutation using a mismatch specific endonuclease that specifically cleaves at the mutation point by recognizing mismatches in double stranded DNA molecule (McCallum *et al.,* 2000b). Adopting the efficient point mutation discovery method described for Arabidopsis TILLING project (Till *et al.,* 2003), we used a Li-COR DNA analyzer based mutation detection protocol. In addition to Arabidopsis, the Li-COR based TILLING has also been successfully carried out in several other organisms.

Basically, the TILLING procedure can be divided into a number of steps (Fig. 15). Genomic DNA is first extracted from a mutagenized population. Screening for mutations starts with PCR amplification of the target sequence of up to~1.5 kb using gene-specific infrared dye-labeled primers. Ideally the forward primer is labeled (5'-end) with an IR dye (IR Dye 700) that fluoresce at ~700 nm (IR Dye 700) and the reverse primer is labeled with the IR Dye 800, which fluoresce at ~800 nm. After performing PCR, the amplified products are denatured and annealed to form heteroduplexes between mutant and wild-type DNA strands.

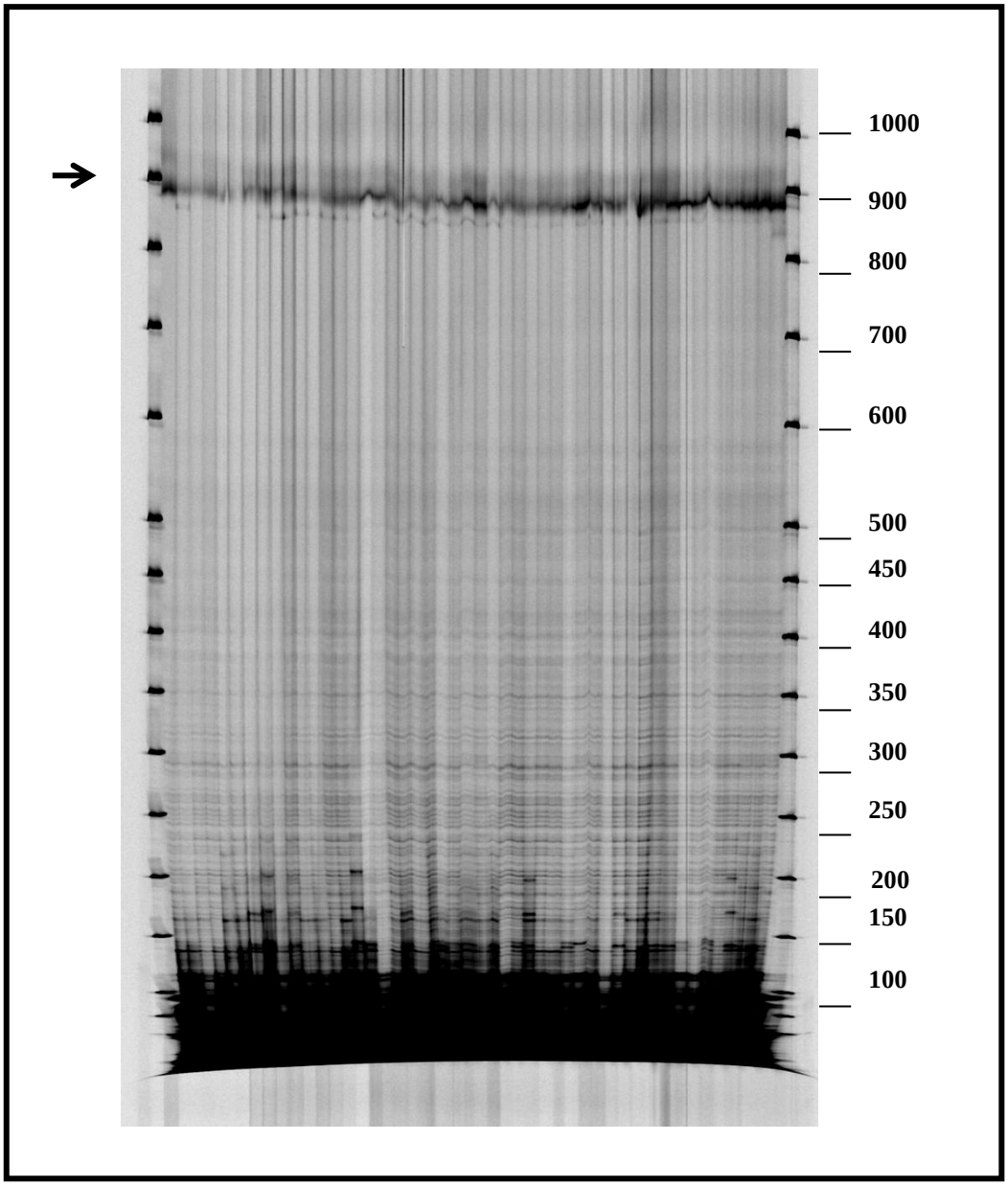

Figure 13. Representative Li-COR gel images showing an amplification profile for a 868-bp *Phytochrome B1 gene region* (amplified using *Phytochrome B1* set A primer). The full-length PCR product is visible as a dark line at the top of each of the 96 wells (top arrow). A touchdown cycle was used and a reaction mix consisted of 5 ng of template, 1X PCR buffer, 0.2 mM dNTPs, 0.18 µl *Taq* polymerase (in-house isolated) and 3 pmoles of primers cocktail and adjuvants (BSA(20 mg/ml) and 6% (w/v) PVPP) was used for this reaction. Only 700 channel is shown. The size (bp) of the marker is indicated on right side of the image.

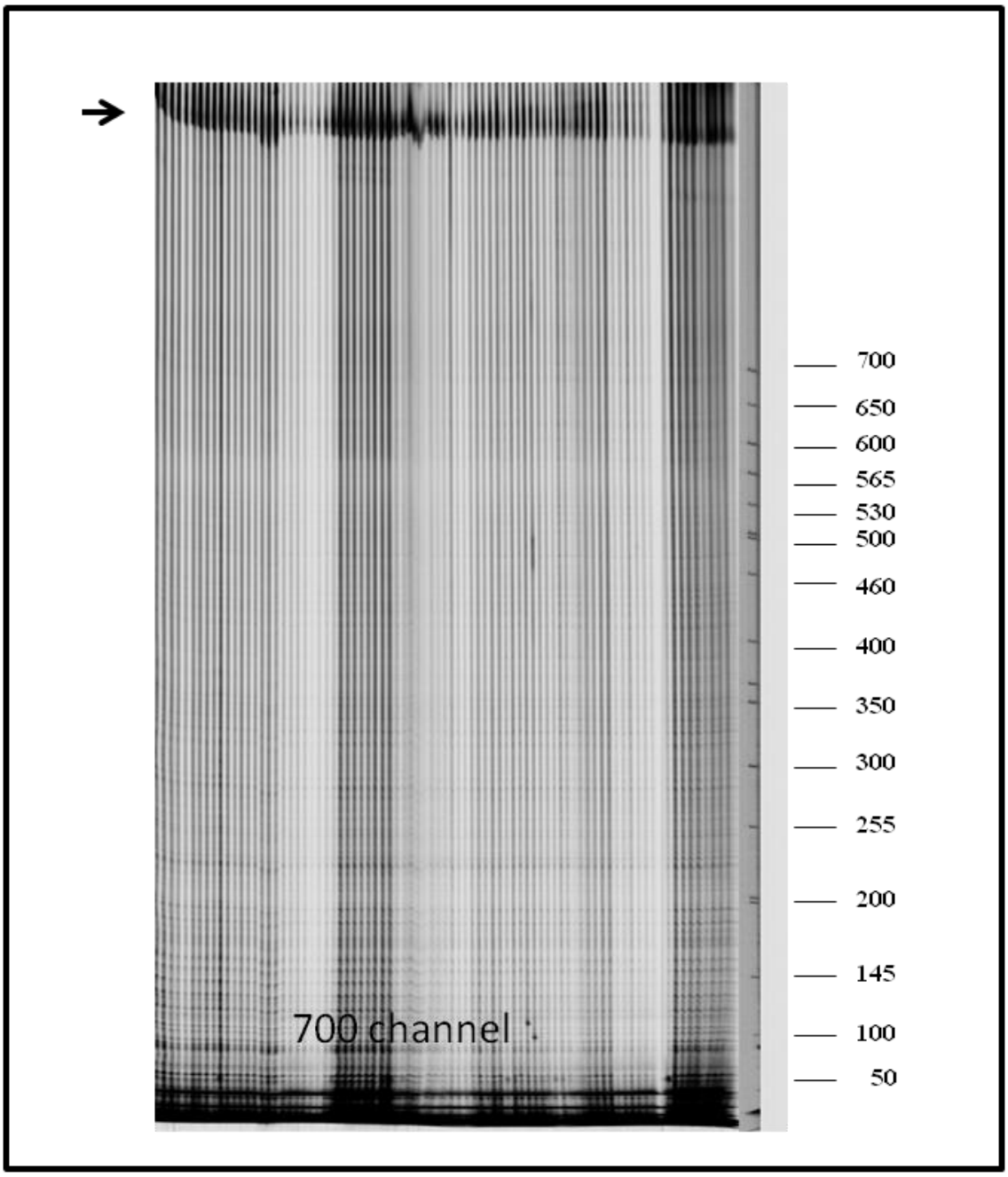

Figure 14. Representative Li-COR gel images showing an amplification profile for a 1402-bp *Phytochrome A gene region* (amplified using *Phytochrome A* set B. The full-length PCR product is visible as a dark line at the top of each of the 96 wells (top arrow). A touchdown cycle was used and a reaction mix consisted of 5 ng of template, 1X PCR buffer, 0.2 mM dNTPs, 0.18 µl *Taq* polymerase (in-house isolated) and 3 pmoles of primers cock tail and adjuvants (BSA(20 mg/ml and 6% (w/v) PVPP) was used for this reaction. Only 700 channel is shown. The size (bp) of the marker is indicated on right side of the image.

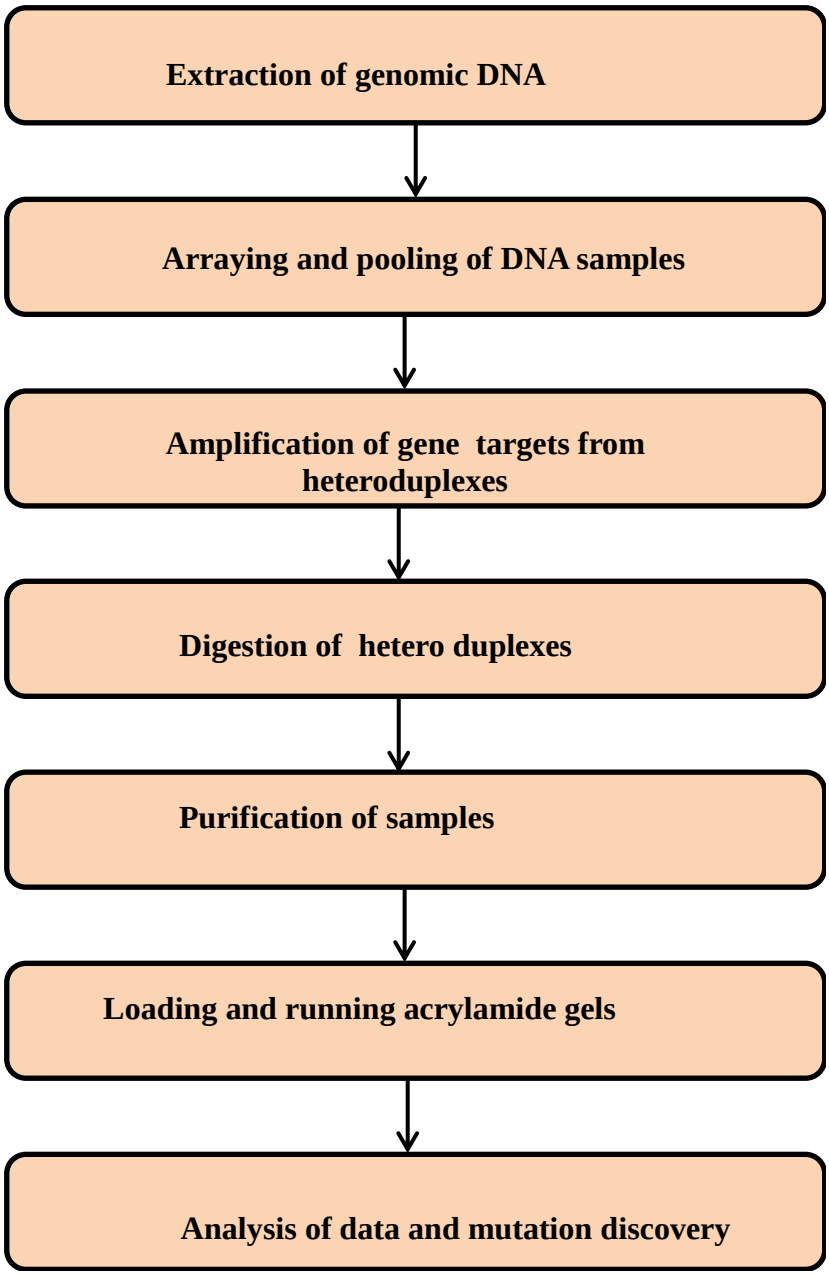

Figure 15. The major steps for high-throughput mutation discovery by TILLING (Till *et al.*, 2006). The procedure consists of (i) extraction of genomic DNA (ii) Arraying and pooling of DNA samples (iii) PCR amplification using fluorescently labeled gene-specific primers followed by the generation of heteroduplexed molecules by denaturing and annealing polymorphic amplicons, (iv) enzymatic cleavage of mismatched regions in heteroduplexed fragments, (v) sample purification and volume reduction, (vi) polyacrylamide denaturing gel electrophoresis, and (vii) data analysis to discover polymorphic samples.

Single-strand specific nuclease CEL-I is then used to digest mismatched base pairs (Fig. 16). After purification of the cleaved DNA, an aliquot of each sample is loaded onto a denaturing polyacrylamide slab gel (Till *et al.,* 2006), in Li-COR DNA analyzer system to visualize fluorescently labeled DNA. The two TIFF images of 700 and 800 channels obtained in Li-COR DNA analyser are analyzed in Adobe Photoshop software (Adobe Systems Inc.) and the migration pattern of PCR fragment on gel is visually assessed for mutations (Sreelakshmi *et al.,* 2009). In samples bearing mutation, using standard DNA sequencing methods, the exact nucleotide change leading to mutation in genomic DNA is determined.

4.2.2 Tomato TILLING

To set up TILLING for tomato, we used an M_2 population consisting of ~10,000 tomato lines. The key steps in the TILLING procedure (Fig. 17) were,

i) Generation of mutagenized population of Tomato

ii) Pooling and genomic DNA isolation

iii) Polymerase chain reaction (PCR) amplification of genes of interest and subsequent screening for induced mutations and, finally

iv) Production of selfed progeny to obtain homozygous mutant lines for the gene of interest

v) Confirmation of linkage phenotype with genotype by genetic segregation.

4.2.3 Production of Arka Vikas Mutant Population

TILLING, a reverse genetic high throughput approach, aims to identify mutations in a gene or genes of interest from a mutagenized population. Mutagenesis is often accomplished by

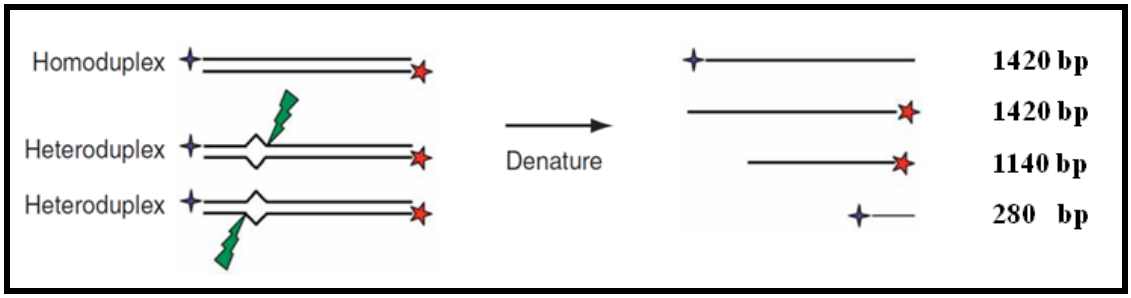

Figure 16. Schematic diagram of enzymatic mismatch cleavage. PCR is performed using 5′ IR Dye-labeled primers. The forward primer is labeled with IRDye 700 (blue four-point star) and the reverse with IRDye 800 (red five-point star). Heteroduplexed DNA molecules are formed by denaturing and annealing amplified fragments. Mismatched regions are cleaved by treatment with a single-strand specific nuclease (green lightning bolts). Products are denatured and fragments are size-fractionated using denaturing polyacrylamide gel electrophoresis and visualized using a Li-COR DNA analyzer. The molecular weight of the cleaved IRDye 700 fragment (1140 bp in this example) plus the IRDye 800 cleaved fragment (280 bp) equals the molecular weight of the full-length PCR product (1420 bp). The molecular weights of the two fragments provide the position of the nucleotide change (Till *et al.*, 2006).

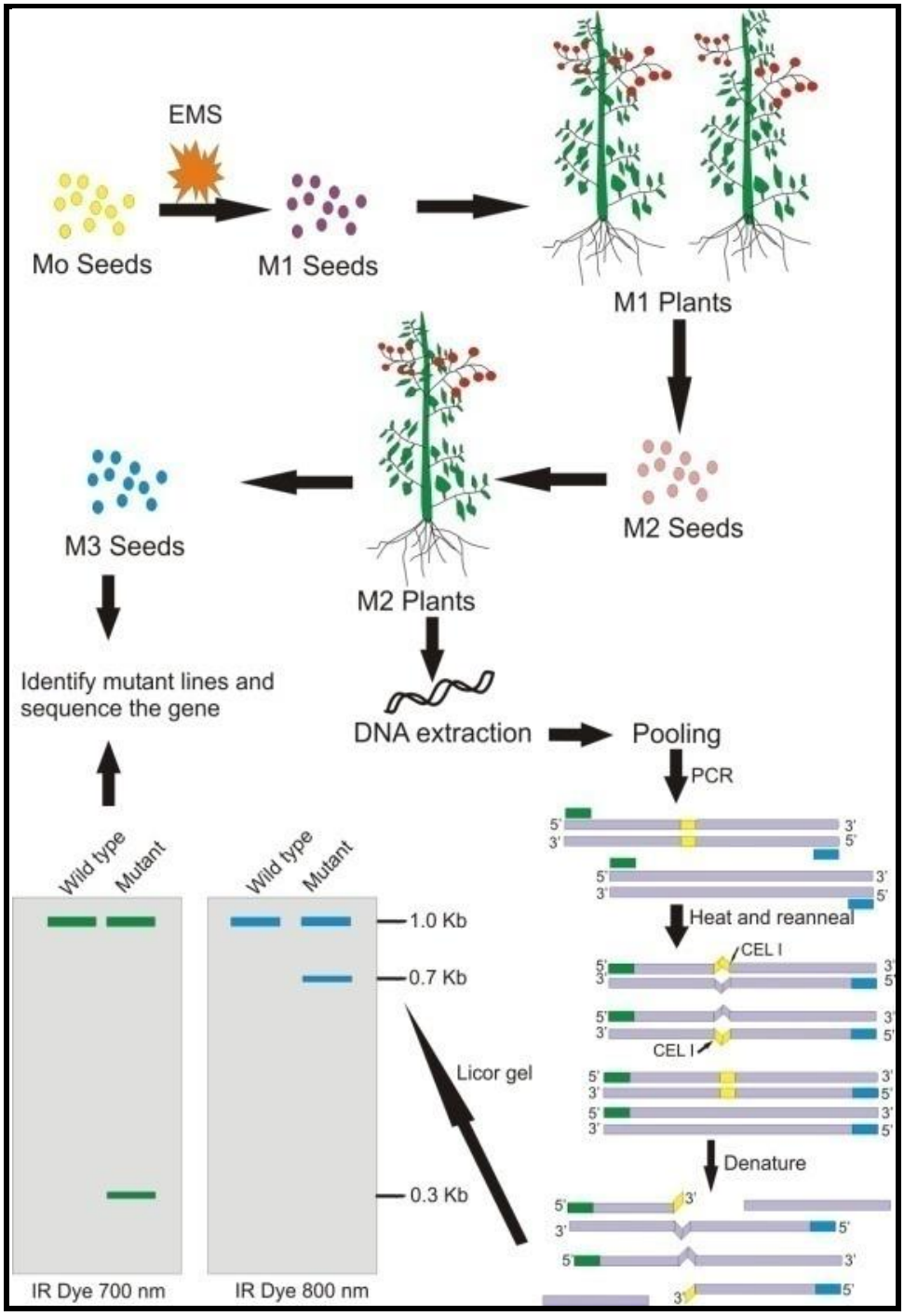

Figure 17. Establishment of Tomato EMS mutant library. Tomato *cv.* Arka Vikas seeds were EMS mutagenized. From the self-fertilized field grown M_1 plants M_2 seeds were collected. DNA extracted from the M_2 plants was used for TILLING assay. Eight fold pooled DNA was amplified with fluorescent labeled primers and mismatch cleavage was done with a mismatch specific endonuclease CEL1. Mutants, which shows variable length of fragments after mismatch cleavage was detected on a LI-COR 4300 DNA analyzer.

treating seeds with a chemical mutagen such as EMS. Most plant species are well suited for this strategy as plants can be self-fertilized and mutagenized seeds can be stored for long periods. One of the commonly used mutagen for raising mutagenized population is ethyl methane sulphonate (EMS). EMS typically produces transition mutations because it alkylates G residues and these alkylated G residue pair with T instead of the conventional base pairing with C. In our experiments, we used Arka Vikas cultivar, which is an Indian cultivar of tomato commonly grown in South India. It completes its reproductive cycle within four months, permitting three successive generations in a year under greenhouse conditions.

To deduce the impact of chemical mutagenesis with EMS, lethality was determined for a number of different concentrations of EMS. Based on the previous reports of the Lethal Dose (LD) values and saturation of mutations in tomato (Menda *et al.,* 2004), initially a mutagenized population of plants treated with 60 mM (0.75% w/v) EMS was raised after treating the seeds of Arka Vikas (M_0) as the starting material. The seeds of M_1 plants showed 40% reduction in germination (Table II) compared to control untreated seeds under standard greenhouse conditions, which directly indicated the effectiveness of EMS treatment. Out of the total germinated seedlings, nearly 83% of M_1 plants survived when grown in open field with drip irrigation.

The frequency of phenotypic variations observed in 60 mM-EMS treated M_2 population of Arka Vikas was lower as compared to the 0.5% EMS treated population of *cv*. M-82 (Menda *et al.,* 2004). To augment improved mutation detection, we raised another M_2 population with stronger dosage of mutagen (120 mM EMS) (Table II). After germination, seedlings from individual M_2 lines were scored for the number of albinos and yellow green seedlings obtained along with wild type phenotype. Segregation ratios of albino/yellow phenotype at seedling stage for individual M_2 lines were used to ascertain the number of germ cell in tomato. We used this data for determining the efficiency of mutagenesis. Many abnormal

phenotypes were observed in field grown 120 mM EMS treated M_2 Arka Vikas population. The phenotypes were recorded using PDA and stored in a database for future forward genetic analysis.

Table II. Comparative survival percentage of 60 mM and 120 mM EMS treated populations.

EMS conc.	Lethality	No. of M_1 plants survived
60 mM	40%	4000
120 mM	53%	3000

4.2.4 Phenotyping for Plant Architecture Variation.

From nearly 12,000 M_2 plants planted in the field, about 10,000 plants survived. During the vegetative and reproductive growth, these plants were repeatedly evaluated for aberrant phenotypes distinct from wild-type *cv*. Arka Vikas. The phenotypes related to architectural variation were organized into plant size, plant habit, internodal length, leaf width, leaf colour, leaf size, leaf complexity, leaf texture, flowering and flower morphology. The characters used to describe the phenotypes were selected from the plant phenotype ontology and from previous investigations of systematic phenotyping of the mutant tomato collection (Menda *et al.*, 2004). We used an electronic hand held device Personal Data Assistant (PDA) with specifically designed PC compatible software PHENOME in combination with an in built barcode laser scanner to record phenotype data of each plant in M_2 population. The digitally recorded data under 10 categories (described above) were analysed.

Interestingly several alterations in plant architecture were observed in 120 mM M_2 lines. In the field grown M_2 population many plants showed phenotypes distinct from cultivar Arka Vikas. Frequency of the phenotype variations was calculated and overall distribution of

different phenotype was expressed as a percentage of total number of variation. Fig.18 shows that most drastic effect of mutagenesis was on leaf phenotype where all classes combined together consisted of ~88% of total variations. The most abundant variations were in leaf texture (33%) followed by leaf size (17%), leaf width (13% and leaf colour (11%). Compared to this only 7% plants showed variations related to flower morphology. We also found several M_2 plants with drastically increased or decreased height and profuse branching (Fig. 19). Some of the distinct phenotypes which are related to leaf morphology like wiry leaf, needle like leaf tip (Fig. 20) and leafy inflorescence were also observed (Fig. 21). Our analysis showed that phenotypes related to leaf morphology are the most frequent type of change observed as a consequence of mutagenesis in our population.

4.2.5 NEATTILL (Nucleic Acid Extraction from Arrayed Tissue for TILLING)

We developed a novel strategy involving pooling of tissue prior to extraction of DNA which is advantageous, especially, while handling large number of plants. The merits of this method includes,

i) It causes an 8 fold reduction in number of DNA preparations to be handled

ii) It reduces the number of steps and

iii) It also reduces the chances of contamination by nucleases.

The suitability for different tissues of tomato was examined with respect to quality of genomic DNA isolation. We first selected leaf tissue as the material for DNA isolation. We found that DNA isolated from mature leaves was of inferior quality due to the presence of secondary metabolites (especially, anthocyanins and polyphenolics). We next opted for emerging juvenile leaves, which have less secondary metabolites as a tissue material for DNA

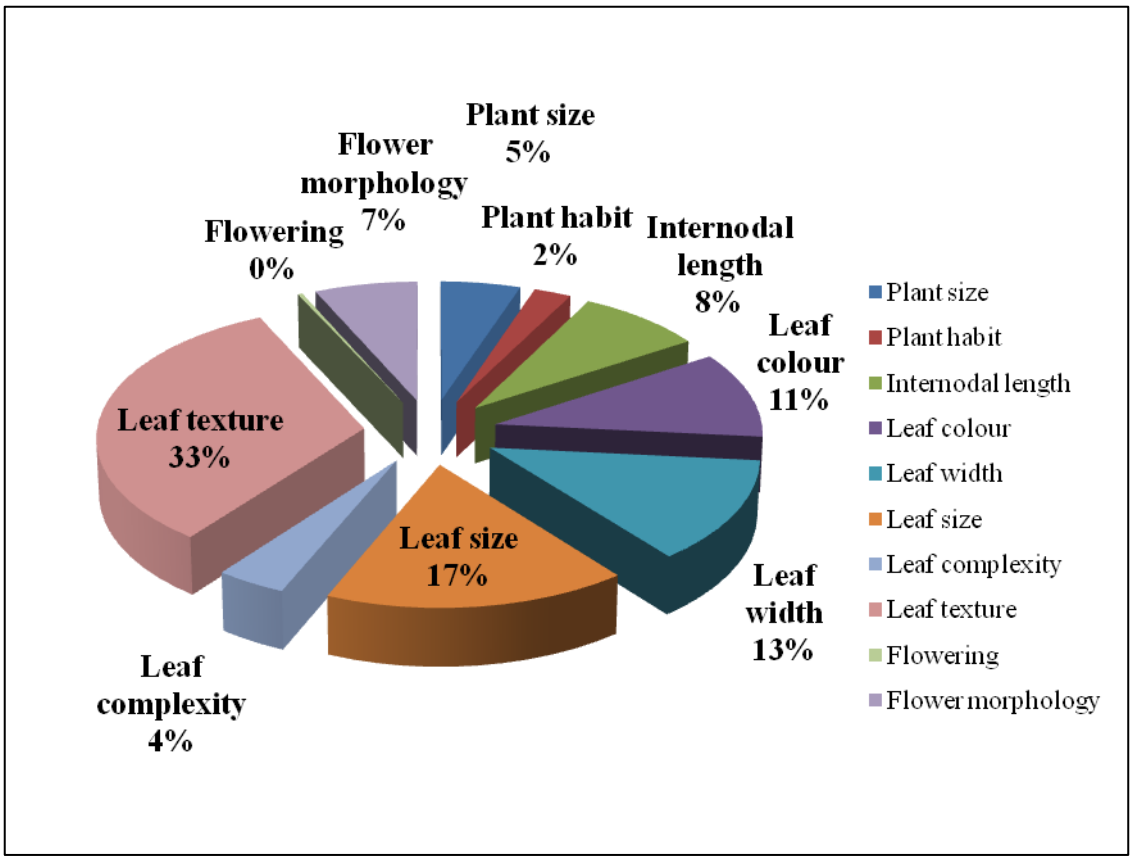

Figure 18. Classification of visible mutant phenotypes of the tomato M_2 population. The pie diagram shows per cent distribution of 10 phenotypic categories (which include mutant lines with variations in plant architecture, leaf morphology and inflorescence) in M_2 plants.

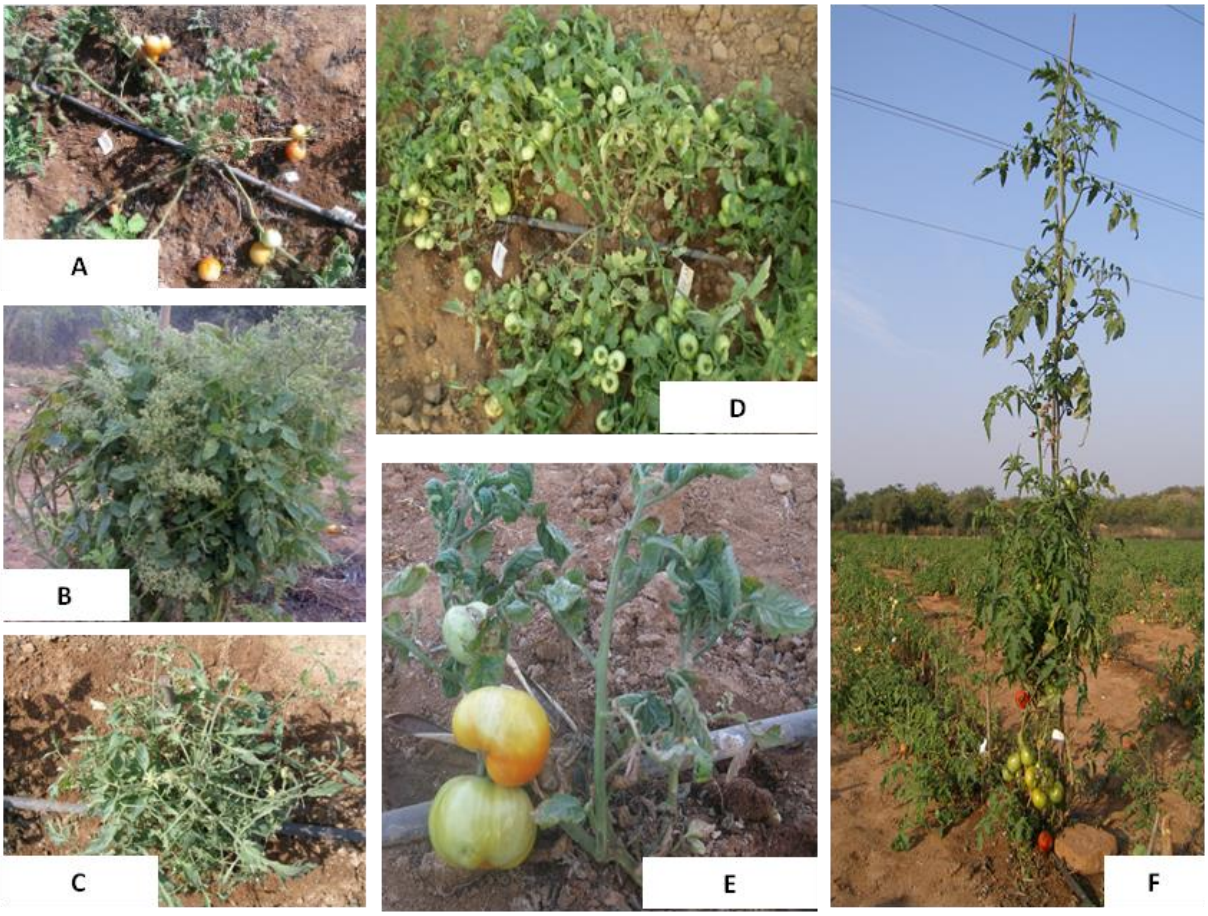

Figure 19. Representative pictures of tomato M_2 lines affected for plant architecture. (A) Rosette (AVM_2 120 mM 880C), (B) bushy (AVM_2 120 mM 510C), (C) stunted (AVM_2 120 mM 230D), (D) profuse branching (AVM_2 120 mM 459D), (E) stunted with less branching (AVM_2 120 mM 1498A), and (F) tall (AVM_2 120 mM 17A). The number in parenthesis indicates the respective M_2 line number.

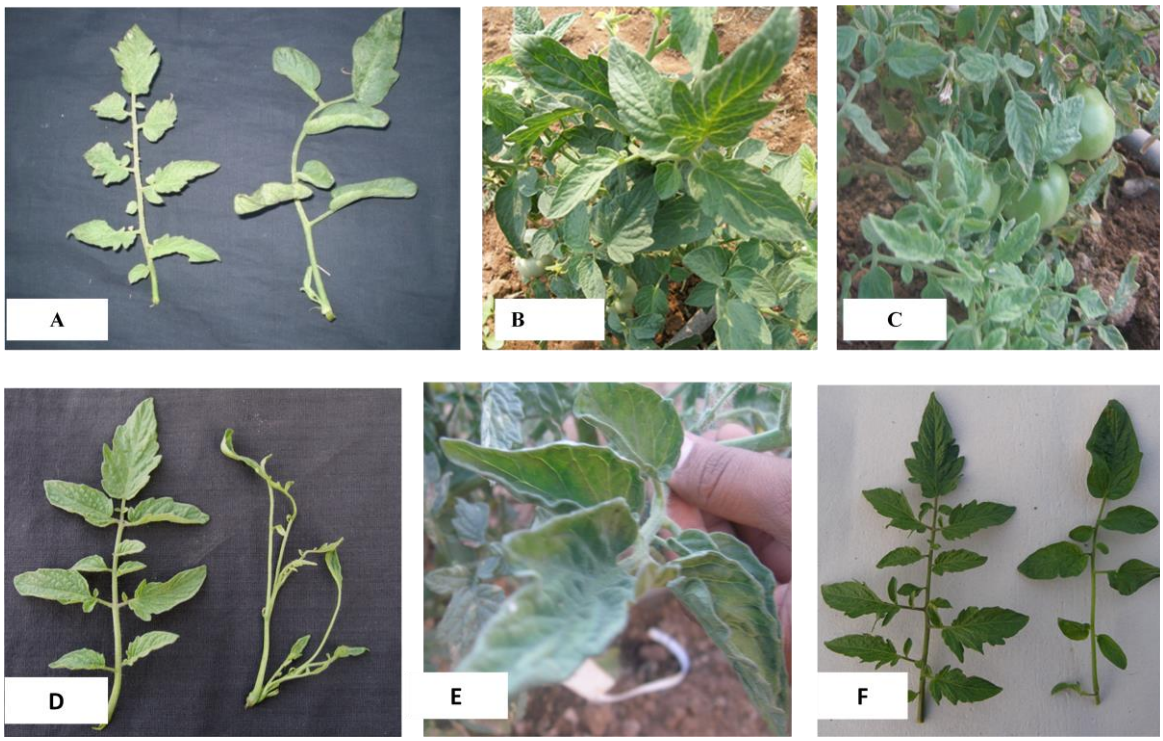

Figure 20. Representative pictures of tomato M_2 lines affected for leaf morphology (A) Leaves with no serration (AVM_2 120 mM 484C), (B) broad sized leaves (AVM_2 120 mM 1459 B), (C) small sized leaves (AVM_2 120 mM 2138 A), (D) wiry leaves (AVM_2 120 mM 230 D), (E) leathery leaves (AVM_2 120 mM 2230 B), (F) leaves with no serrations (AVM_2 120 mM 25 A). The number in parenthesis indicates the respective M_2 line number.

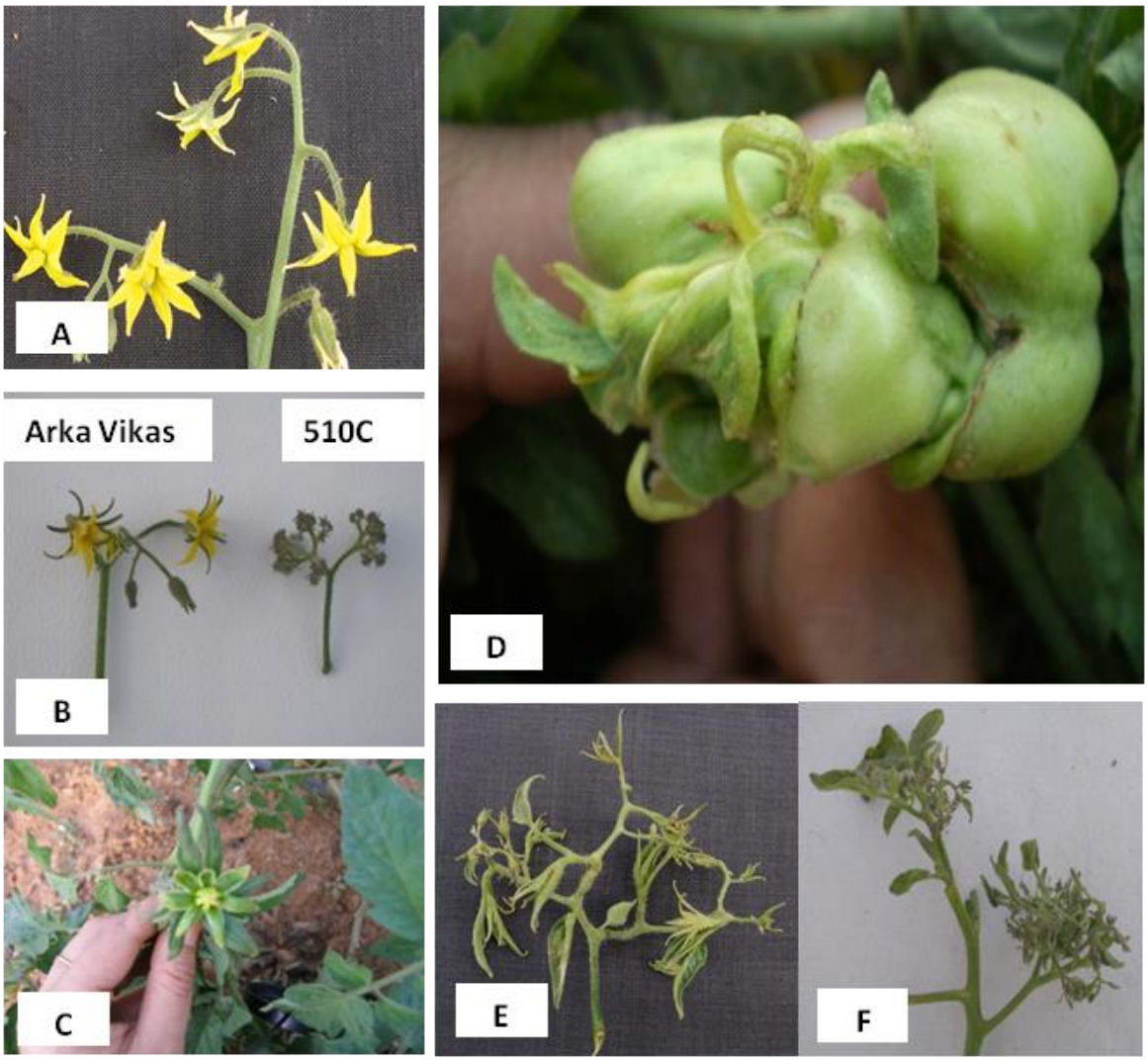

Figure 21. Representative pictures of tomato M_2 lines affected for inflorescence. (A) Dark yellow flower (AVM_2 120 mM 246C), (B) abnormal inflorescence (AVM_2 120 mM 510C), (C) sepaloid flowers(AVM_2 120 mM 620B), (D) abnormal inflorescence (AVM_2 120 mM 484C), (E) large sepals (AVM_2 120 mM 2270A), and (F) abnormal inflorescence (AVM_2 120 mM 107B). The number in parenthesis indicates the respective M_2 line number.

isolation. On comparing different tissues, we found that high quality DNA can be isolated from young cotyledons with minimal interference from secondary metabolites.

For isolation of genomic DNA, tomato cotyledon/leaves of almost equal weight or size were selected to ensure that the DNA from each individual plant is equally represented. The total amount of tissue to be harvested for DNA extraction was determined by the overall volume available for tissue homogenization and processing in the deep well plate and sample weight/extraction buffer ratio. Eight equal sized cotyledons of tomato were taken per well (weighing about 80-100 mg). The above weight was close to the optimal weight that could be homogenized in 2 ml volume of individual wells of deep well plates.

For pooling of cotyledons, 8 seedlings per mutant line were germinated in 96 well plates and one seedling per line was pooled. The cotyledon arraying strategy (Fig. 22) simultaneously generated a row and a column plate each carrying 768 mutant lines. The placement of the two cotyledons of a single seedling in the row and column plates led to direct identification of the precise mutant line during mutation screening from 8-fold pools. In other words, for every mutant pool identified in a plate (e.g. row) during screening, the exact mutant line was subsequently identified while screening its complementary plate (column). Once a mutation was identified, seeds from the M_2 seed packet of that mutant line were sown. The individuals were then examined for the presence of mutation and were sequenced (Sreelakshmi *et al.*, 2009).

The described NEATTILL protocol involves germination of seedlings, arraying of cotyledons, extraction of DNA, quantification and equalization in approximately two weeks time (germination: 7-12 days; arraying of cotyledons: 1 day; extraction of DNA: 1 day; quantification and equalization: 1 day). The arraying, DNA extraction, quantification and

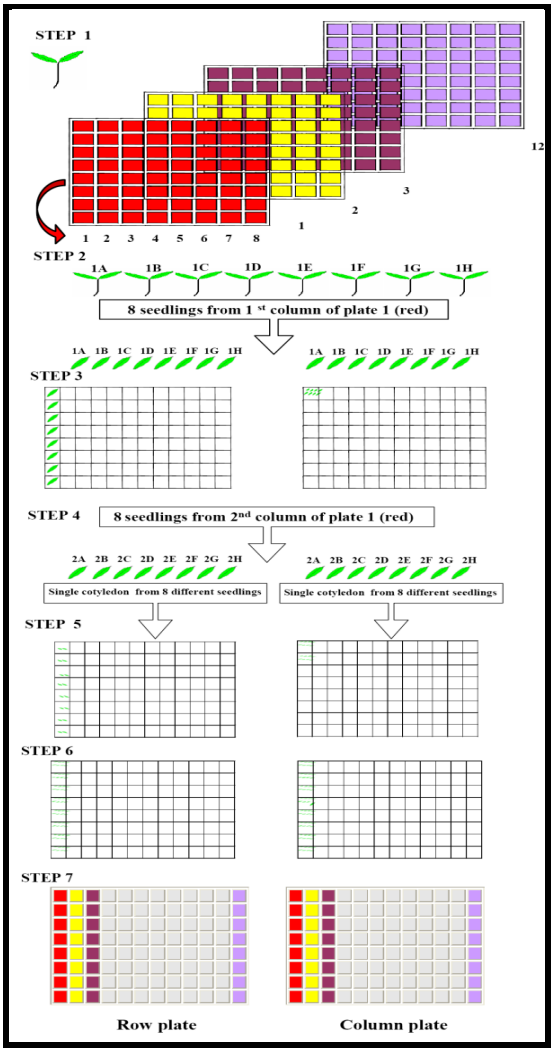

Figure 22. Two-dimensional pooling of the cotyledons in 96-well plates. Step 1: Twelve 8 × 8 grids were prepared (as depicted by numericals 1, 2, 3.....12 and colored red, yellow, brown.... lavender, respectively,). Step 2: The eight seedlings arrayed in column 1 of the first grid were removed and arranged linearly. The right and the left cotyledons of the seedlings were excised and arranged in the same order as present in the column of the grid from which they were removed. Step 3: In two new deepwell plates, the cotyledons were placed in the wells as shown in the Figure. One set of cotyledons was placed in 1A-1H wells in the ROW plate whereas the other set of cotyledons was placed in 1A well of COLUMN plate. Step 4: Eight seedlings from 2A-2H of plate 1 (red colored) were removed and their cotyledons excised as in step 2. Step 5: One set of cotyledons was placed in 1A-1H of ROW plate whereas the other set was put in 1B well of COLUMN plate. Step 6: Similarly the seedlings were removed from columns 3, 4, 5, 6, 7 and 8 and pooled as described steps 2 and 3 in different wells. After pooling the seedlings of eight columns, both the ROW and COLUMN plate had eight cotyledons each in 1A-1H wells. Step 7: The whole procedure was repeated for the second, third....twelveth grid (as shown with yellow, brown....lavender colors in Figure) to generate eight pooled ROW and COLUMN plates.

equalization merely takes 3-4 days time. DNA from about 3072 samples (four 96 deep well plates) can be conveniently isolated by this protocol in 6-7 hours of time. Since all reagents and consumables can be directly purchased and prepared in-house compared to the commercial kits and reagents (Qiagen, DNAzol) this protocol is more economical.

4.2.6 Evaluation of High Throughput DNA Isolation

NEATTILL (Sreelakshmi *et al.,* 2009) for genomic DNA isolation from arrayed tissues involved inclusion of several important steps. Applying NEATTILL to isolate DNA from pooled tissue we found that the DNA yield and quality was suitable to permit PCR reaction for high throughput TILLING applications. It is already known that plant phenolics which are retained in the DNA preps even after DNA isolation would interfere with PCR amplifications. The above method included several steps that could remove the phenolics during tissue homogenization such as inclusion of PVPP and β-mercaptoethanol. To evaluate the above steps, the untreated and treated DNA preparations were checked for quality by amplifying actin gene fragment as control (Fig. 23). The preparations which included β-mercaptoethanol (which acts as a strong reductant by breaking intramolecular disulphide bonds in proteins and prevents oxidation of polyphenols) and PVPP (which helps in removal of polyphenols) during homogenization resulted in better PCR amplification. The above protocol also included treatment with RNase to remove contaminating RNA in DNA preparations.

4.2.7 Reverse Genetic Screening

For molecular screening for detection of mutations, a CEL-I-based heteroduplex assay was used, coupled with gel electrophoresis on Li-COR DNA sequencers. A total of 11,520 genomic DNA samples from individual M_2 plants and 768 DNA samples from M_3 plants were utilized. The mutations were screened in eight fold genomic DNA pools (described above) using 96-well format plates. Two phytochrome genes *viz Phytochrome A* and *Phytochrome B1*

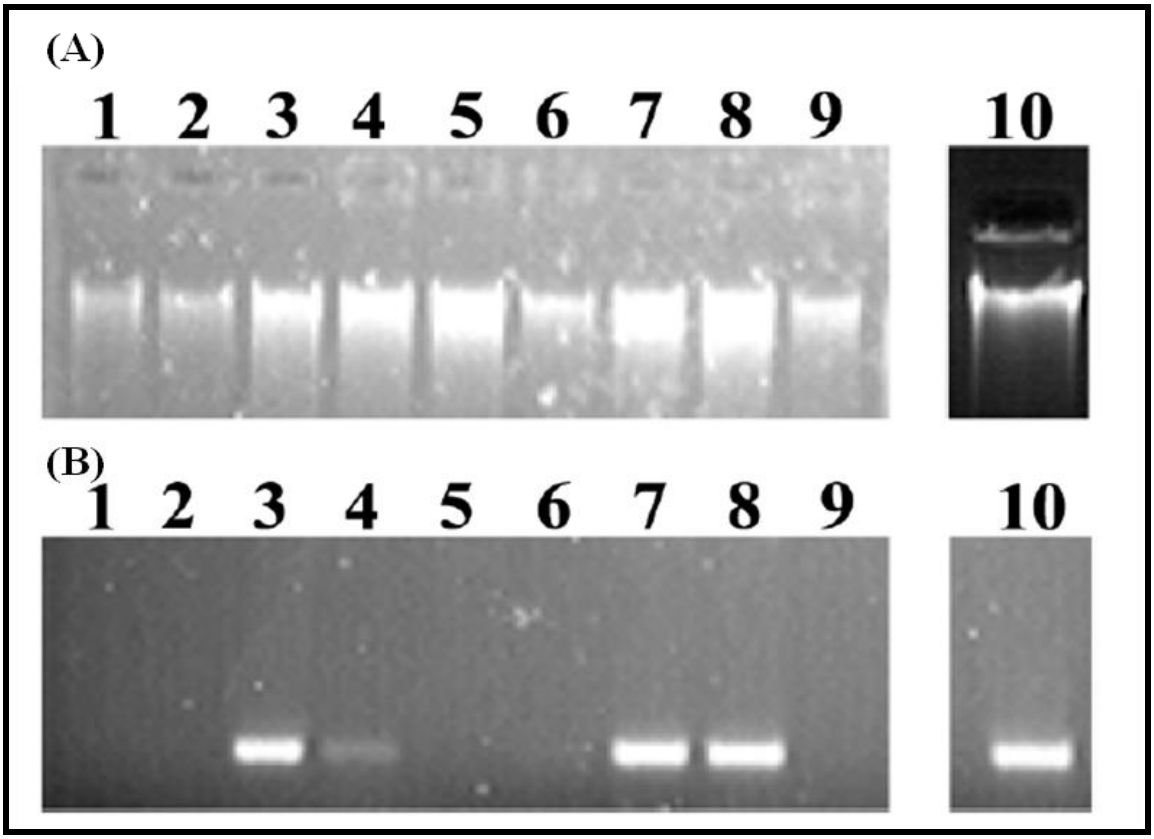

Figure 23. Genomic DNA quality and PCR amplification of DNA isolated using different modifications. (A) Gel electrophoresis of DNA Lane. 1: tissue was homogenized in extraction buffer (0.1 M Tris-HCl, pH 7.5; 0.05 M EDTA, pH 8.0; 1.25% (w/v) SDS), Lane 2: Same as lane 1 with additional step of PCI (25:24:1). The DNA pellet after dissolving in 200 µl of milliQ water was extracted with an equal volume of PCI. The aqueous phase was collected and DNA was reprecipitated and dissolved in milliQ water, Lane 3: Same as lane 1 with inclusion of 2% (w/v) PVP and 0.2 M β-ME during extraction and PCI extraction was done as for lane 2, Lane 4: Same as in lane 3 but without PCI step, Lane 5: Same as in lane 3 but without β -ME, Lane 6: Same as lane 1 with inclusion of 2% (w/v) PVP during extraction, Lane 7: Same as lane 1 with inclusion of 30 mg PVPP and 0.2 M β -ME during extraction and PCI extraction as done for lane 2, Lane 8: Same as lane 1 with inclusion of 30 mg PVPP and 0.2 M β -ME during extraction, Lane 9: Same as lane 1 with inclusion of 30 mg PVPP during extraction, Lane 10: DNA isolated by Qiagen kit. (B) PCR amplification of isolated DNA. The quality of DNA was checked by PCR amplification of actin gene using forward primer.

Abbreviations: PCI-Phenol chloroform isoamyl alcohol, β-ME - β-mercaptoethanol, PVP - Polyvinylpyrrolidone, PVPP - Polyvinylpolypyrrolidone.

were screened to detect mutation caused by EMS treatment. To optimize the detection of mutations that may affect the phenotype, a web-based software CODDLE (http://proweb.org/coddle) was used. CODDLE predicts the regions of a gene that is likely to have the higher density of potentially deleterious mutations caused by treatment with chemical mutagen.

Considering the importance of N-terminal domain of phytochromes in light signaling, first and second exons of *Phytochrome A* and *B1* genes were targeted for TILLING. The potential effect of SNPs on protein function was evaluated using the PARSESNP programs. PARSESNP (http://www.proweb.org/parsesnp/) provides PSSM scores and SIFT values for mutant gene. PSSM or position-specific scoring matrix (PSSM) is a commonly used representation of motif (patterns) in biological sequence. PSSMs enable the scoring of multiple alignments with sequences, structures etc. The conversion of a multiple alignment, such as a block, into a PSSM can use the multiple alignment sequence weights, the expected number of amino acids and the frequencies of unobserved amino acids (pseudocounts). SIFT (Sorting Intolerant From Tolerant) value can predict, whether an amino acid substitution would affect protein function. SIFT prediction is based on the sequence homology and the physical properties of amino acids. For a SNP, a SIFT score < 0.05 and/or a PSSM score >10 is predicted to be damaging to the function of encoded protein.

4.2.8 TILLING for *Phytochrome A*

Two sets of primers were designed using tomato *Phytochrome A* sequence obtained from NCBI GenBank. The *Phytochrome A* gene in tomato consists of 6623 base pairs including four exons and three introns. Fig. 24 shows the overall gene structure of *Phytochrome A* gene. The four exons varied in length from 291 bp (exon 3) for the smallest exon to 2068 base pairs (exon1) for the largest exon. The web-based tool CODDLE (http://proweb.org/coddle) was used to select gene regions that is likely to have highest probability of potentially deleterious

mutations as a consequences of EMS mutagenesis (Fig.25). CODDLE predicted that mutations in exon 1 would have most deleterious effect on function of phytochrome A gene. Considering the importance of N-terminal domain of phytochromes in light signalling we designed two pairs of primer from first and second exons of *Phytochrome A* to cover the two exons. Two primers were designed namely primer A (from bp 2684 to 4104) and primer B (from bp 1304 to 2708) with sizes of the PCR products corresponds to 1420 and 1405 respectively (Fig.24, Table I).

The *fri* mutant (Van Tuinen *et al*., 1995a) that has a lesion on *phytochrome A* gene was used as a positive control to standardize detection of mutation in phytochrome A gene using TILLING protocol. The *fri* mutant of tomato has an A-T substitution at position -2 of 3′ splice site of the intron between exon 1 and 2 at nucleotide 2327. Since the A at position 2 is a highly conserved in plant intron, substitutions at this site are expected to cause in abnormal splicing at the 3′end of this intron. Positive control DNA bearing *fri* mutation was laced with WT DNA and PCR amplified to obtain an 1420 bp amplicon. The PCR and CEL I digestion were carried out using standard protocols described above. The expected position of the CEL I cleaved fragments are 278 bp (bottom left arrow) in 700 channel and 1142 bp (right arrow) in 800 channel. On Li-COR gel electrophoresis the products after cleavage appeared in two channels with fragment size 278 bp (700 channel) and 1142 bp (800 channel) thus confirming that the mutation in positive control can be detected on LICOR DNA analyser (Fig. 26).The sum of size of these two fragments adds up to 1420 bp (total amplicon length of the primer).

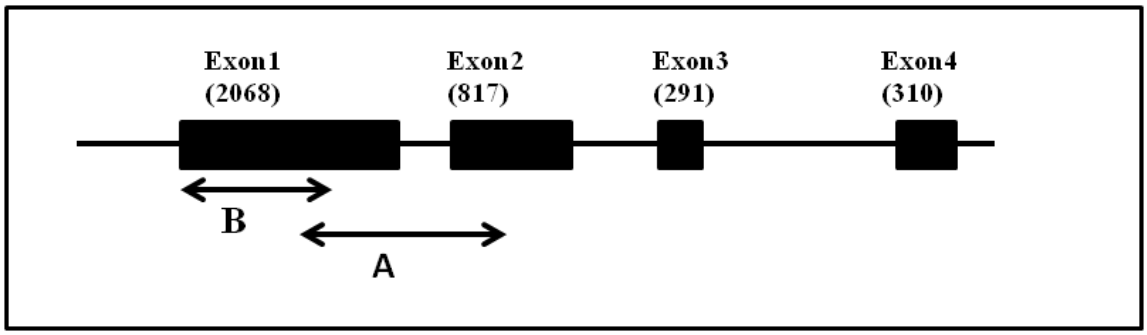

Figure 24. Organization of *Phytochrome A* gene. Exons are shown as boxes; introns are shown as thick black lines. The letter A and B in the figure refers to amplicons amplified by primer set A (from bp 2684 to 4104) and primer set B (from bp 1304 to 2708). Sizes of PCR products were 1420 and 1402 bp, respectively with a 24 bp overlap region between two primer set. Exon numbers are indicated above the gene. The size of each exon is indicated as base pair number given in parenthesis.

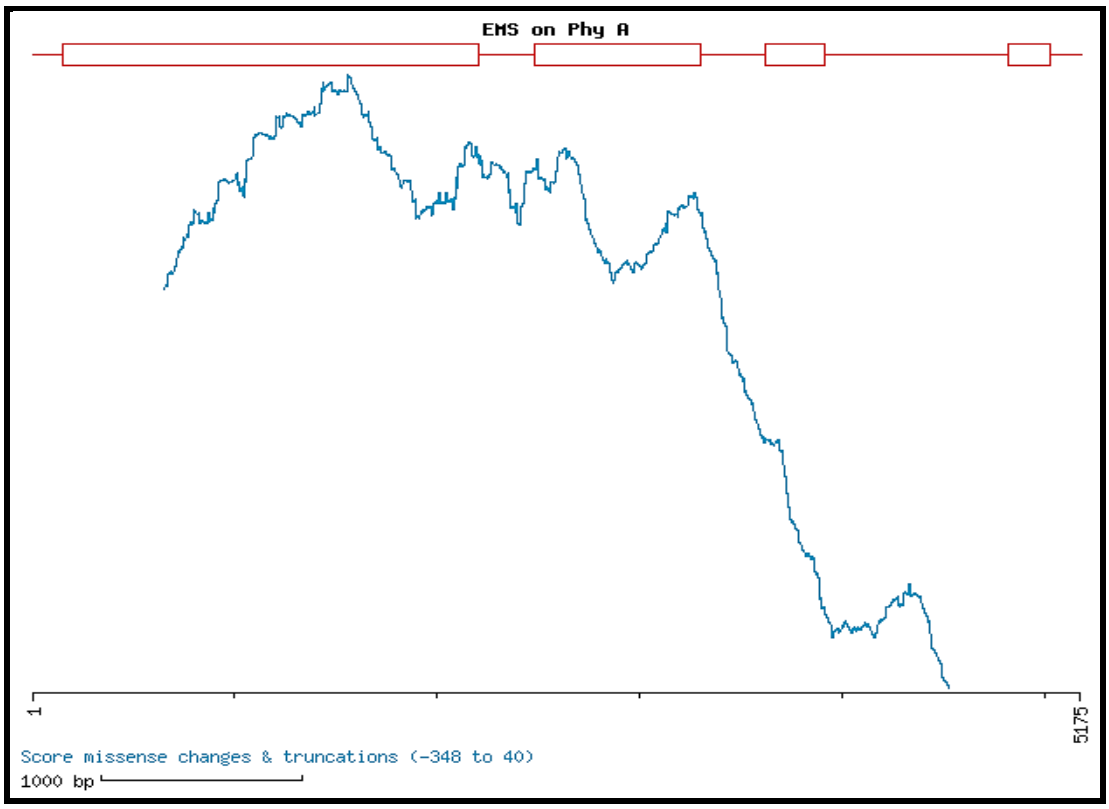

Figure 25. Output of the CODDLE program for *Phytochrome A* genomic sequence. Exons are represented by white boxes and introns by lines. The CODDLE program was used to identify those regions of the gene in which G:C to A:T transitions are most likely to result in deleterious effects on the encoded protein (represented by the probability curve traced in turquoise). The CODDLE algorithm is based on an evaluation of protein sequence conservation from comparison of database accessions of homologous proteins. Note that mutation in exon 1 and exon 2 are expected to be most deleterious.

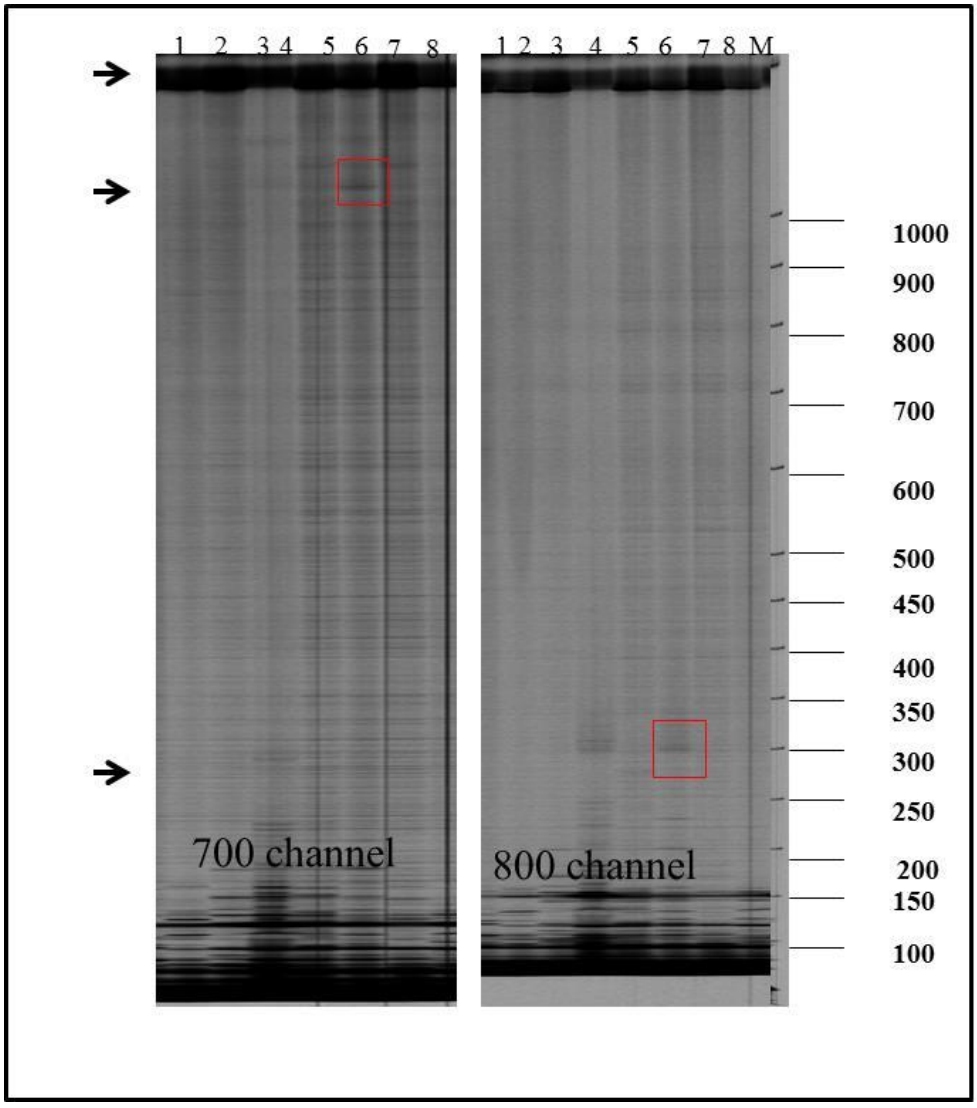

Figure 26. Identification of cleaved fragments after CEL I digestion in Li-COR 4300 DNA Analyzer using DNA heteroduplex consisting of wild type and *fri* mutant DNA. The substrate is a 1420 base pairs heteroduplexed PCR product that includes exon 1, intron 1, and exon 2 of *Phytochrome A*. The expected size of the CEL I cleaved fragments are 1140 bp (top left box) in 700 channel and 280 bp (bottom right box) in 800 channel. Sum of these cut fragments add up to 1420 bp (that is total amplicon length). M on right hand side of the image shows 50-700 bp size standards. The fragments detected specially in the lower portion of either channel images represent the background fragments usually observed in TILLING runs. However these can be distinguished from the CEL I cleaved fragments as these fragments do not show the complementary fragment in the either channel, a characteristic of CEL I cleaved fragments.

Mutation screening for *phytochrome A*: EMS mutagenized populations of tomato were screened for mutations using a PCR product of sizes 1402 bp (primer A) and 1420 bp (primer B) bp respectively for first and second exons. Six lines with putative mutations were detected in the region amplified by primer B, surprisingly no line with a mutation was detected in region amplified by primer A. To find out the exact ID number of positive mutant line, complementary plates (either row or column) was screened simultaneously. Only two lines out of six lines were conclusively identified in the complimentary plate that is M82- M_2 -895 and AV-M_2- 120 mM-2626 (Table III).

Table III. Details of population screened, number of mutations detected and nature of mutation for *phytochrome A*.

Population	No. of individuals screened	No. of mutation detected	Mutation confirmed	Individual mutant plant identified	Nature of base change	Effect of mutations
60 mM AV	1536	-	-	-	-	-
120 mM AV	6144	3	1	-	-	-
M82 M_2	3840	1	1	1	A to G	Non-synonymous
M82 M_3	768	2	-	-	-	-

On Li-COR gel electrophoresis the products of AVM_2-120mM-2626 on CEL-I cleavage were visualized in two channels with fragment size 1140 bp (700 channel) and 280 bp (800 channel). However, fifty seeds from line number AVM_2-120mM-2626 were germinated for finding the individual line containing above mutation, surprisingly none of the above plants

were found to bear the mutation in the expected region. Though we do not know the exact reason, the absence of individual line bearing mutations indicates that the mutation could be of lethal nature and thus it affects the survival of the mutant plants.

The mutation in line M82-M_2-895 was cleaved into two fragments of 1120 bp and 300 bp upon digestion with CEL I enzyme in the first exon of *phytochrome A* gene (Fig. 27). The putative mutant line detected in row plate was identified by screening the complimentary column plate (Fig. 28**)**. Fifteen seeds from line number M82-M_2-895 were germinated for finding individual line containing mutation and only one plant out of a total of fifteen (M82-M_2-895.5) was found to contain above mutation (Fig. 29).

The mutation density was estimated by dividing the total number of identified mutations by the number of base pairs screened (the cumulative length of the amplicons multiplied by the number of samples). The frequency of induced mutation was found to be very low for *Phytochrome A* genes (Table IV).

Table IV. Mutation frequency in *phytochrome* genes.

Gene	No. of mutant individuals screened	Length of fragment screened (bp)	Mutation Frequency
Phytochrome A	12,288	2822	$1.7301*10^{-8}$
Phytochrome B1	13,056	868	$1.764*10^{-7}$

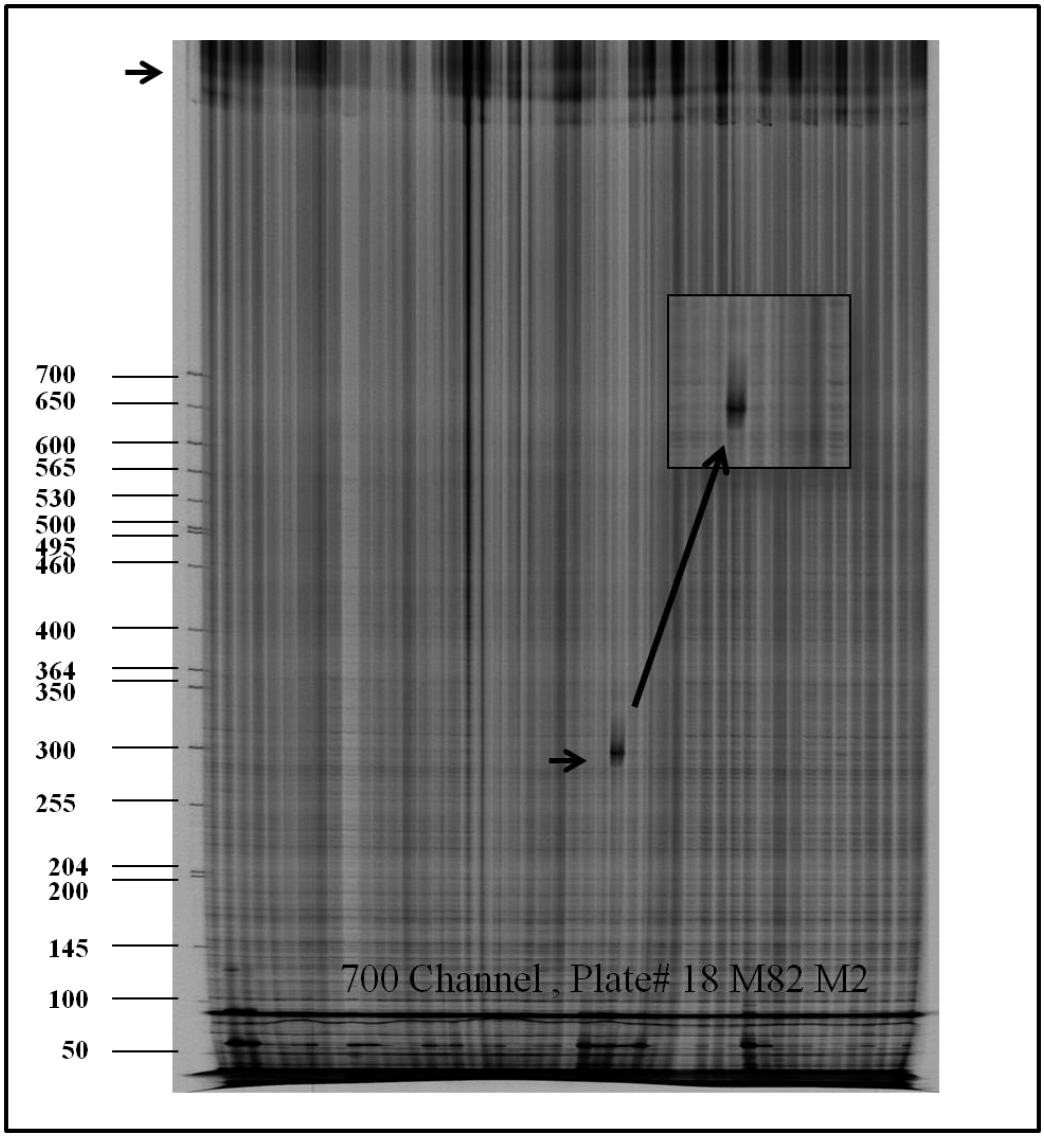

Figure 27. Representative Li-COR gel images showing CEL I-treated PCR products for a 1.4-kb portion of *phytochrome A* gene. The full-length PCR product is visible as a dark line at the top of each of the 48 wells (top arrow). In the lane where amplicon harbours a mutation, PCR product is cleaved into two fragments (300 bp and 1120 bp) labeled with either the 700- or 800-nm IR dye. (Here only 700 channel is shown). Fragment, which corresponds to 300 bp, is clearly visible (arrow) in 700 channel. Inset shows an enlarged view of the fragment. The sizes of the cleavage products from the two dye-labeled DNA strands add up to the size of the full-length PCR product (800 channel is not shown). PCR artefacts are distinguishable from true mutants as they (artefacts) appear at the same size in both channels. The size of the cleavage product (the sizing ladder can be seen at the left of the image) indicates approximately where the single nucleotide polymorphism is located in the fragment. Plate number is given at the bottom of the picture.

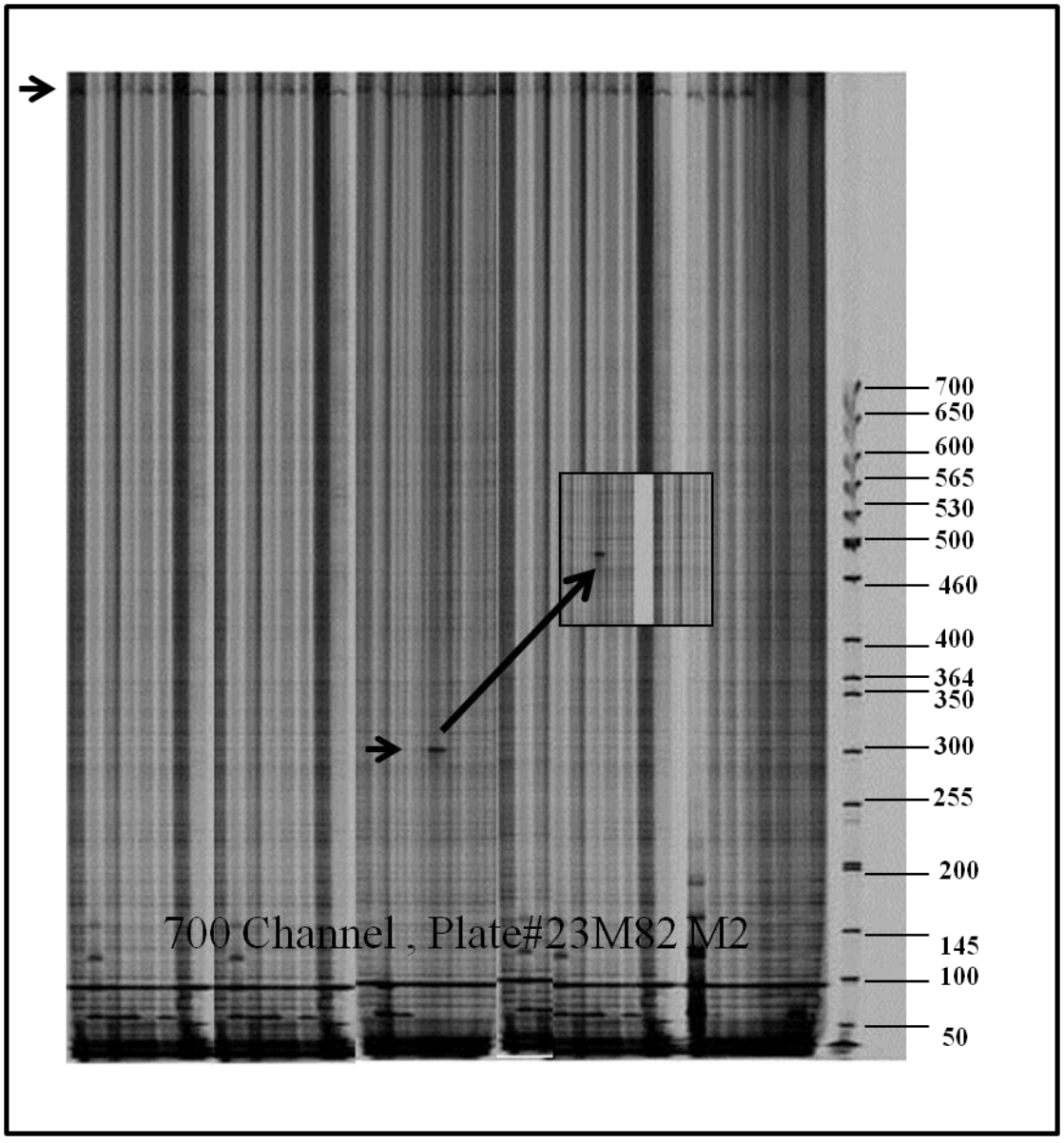

Figure 28. Representative Li-COR gel images showing confirmation of mutation which was detected in plate #18(row). Confirmation of mutation was done by screening the complementary column plate (plate #23) .The full-length PCR product is visible as a dark line at the top of each of the 96 wells (top arrow). In the lane where amplicon harbours a mutation, PCR product is cleaved into two fragments (300 bp and 1120 bp) labeled with either the 700-nm or 800-nm IR dye. (Here only 700 channel is shown). Fragment, which corresponds to 300 bp, is clearly visible (arrow) in 700 channel. Inset showing an enlarged view of the fragment. The sizes of the cleavage products from the two dye-labeled DNA strands add up to the size of the full-length PCR product (800 channel not shown).

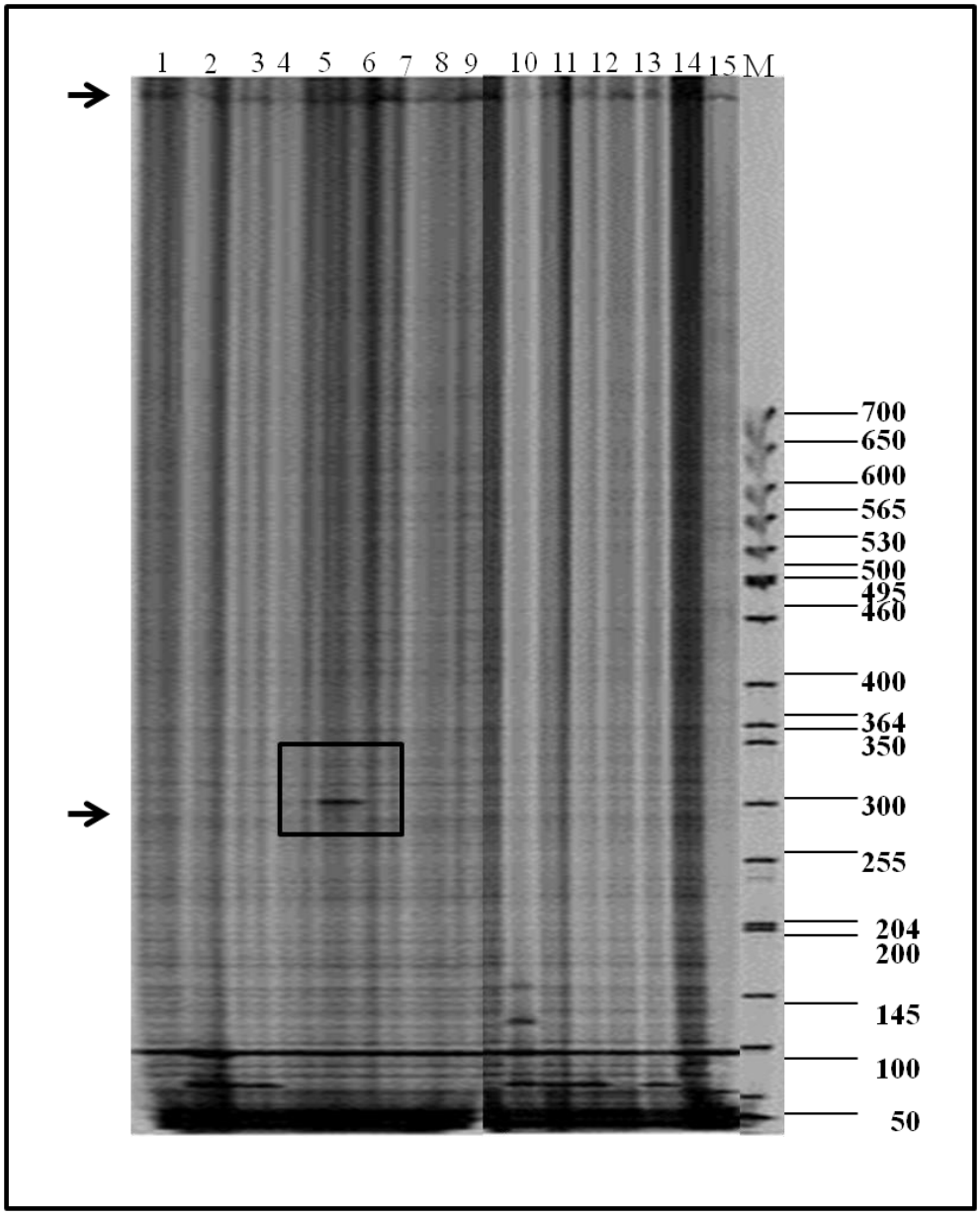

Figure 29. Representative Li-COR gel images showing confirmation of mutation from individual plants of the line M82-M_2-895. Confirmation of mutation was done performing CEL I digestion of genomic DNA of mutant individual (line M82-M_2-895). Lane 1-15 represents DNA sample extracted from 15 individual plants from the line M82-M_2-895. The full-length PCR product is visible as a dark line at the top of each of the 96 wells (top arrow). In the lane where amplicon harbours a mutation, PCR product is cleaved into two fragments (300 bp and 1120 bp) labeled with either the 700-nm or 800-nm IR dye. (Here only 700 channel is shown). Fragment which corresponds to 300 bp is clearly visible (arrow) in Lane 5. Lane 5 represents DNA from the plant M82-M_2-895.5. The size of the cleavage product (the sizing ladder can be seen at the right of the image) indicates approximately, where the single nucleotide polymorphism is located in the fragment. Plate number is given at the bottom of the picture.

Molecular nature of the mutant: The mutant line (accession number M82-M_2-895.5) which was confirmed for mutation in *phytochrome A* gene, was sequenced to identify the molecular nature of the mutation. The precise position and the nature the mutation was determined by sequencing PCR products comprising exons 1 and 2 and intron 1 for above mutant line. Sequencing of phytochrome gene for above mutant line revealed a nucleotide change from Guanine (G) to Adenine (A) at 1486th position of ORF (2986th position of *PHYA* gene) (Fig. 30). On translating to coding amino acid it was found to be a non-synonymous mutation which altered the codon GGG (encoding for Glycine) to AGG (encoding for Arginine). Thus, the overall consequence of mutation was a shift from glycine to arginine at amino acid 496 (G496R) in the PHYA polypeptide (Fig. 31). This change causes the shift from non-polar neutral amino acid to polar positive amino acid in the PHY domain of phytochrome (Fig. 32).

Phenotyping of the mutant: Considering the importance of N-terminal domain in *phytochrome A* function, we further analysed the mutant line M82-M_2-895.5 to ascertain whether the mutation impaired phytochrome function. Though phytochrome affects several facets of plant development, one of the primary effects of it is seen during de-etiolation of the seedlings when it emerges from the soil. Therefore, we examined etiolated and light grown seedling phenotype of above mutant line related to wild type control. To ascertain the effect of above mutation on seedling phenotype, seedlings of the mutant line M82-M_2-895.5 and its wild type control *cv.* AV were grown under continuous blue, red, far red light, white light and absolute darkness. On comparison with the wild type, we found no perceptible difference was found between the WT control and the mutant accession under any light conditions. However, the adult mutant plant exhibited an altered phenotype compared to wild type control. The mutant plant showed slightly elongated internodes with broader leaves (Fig. 33).

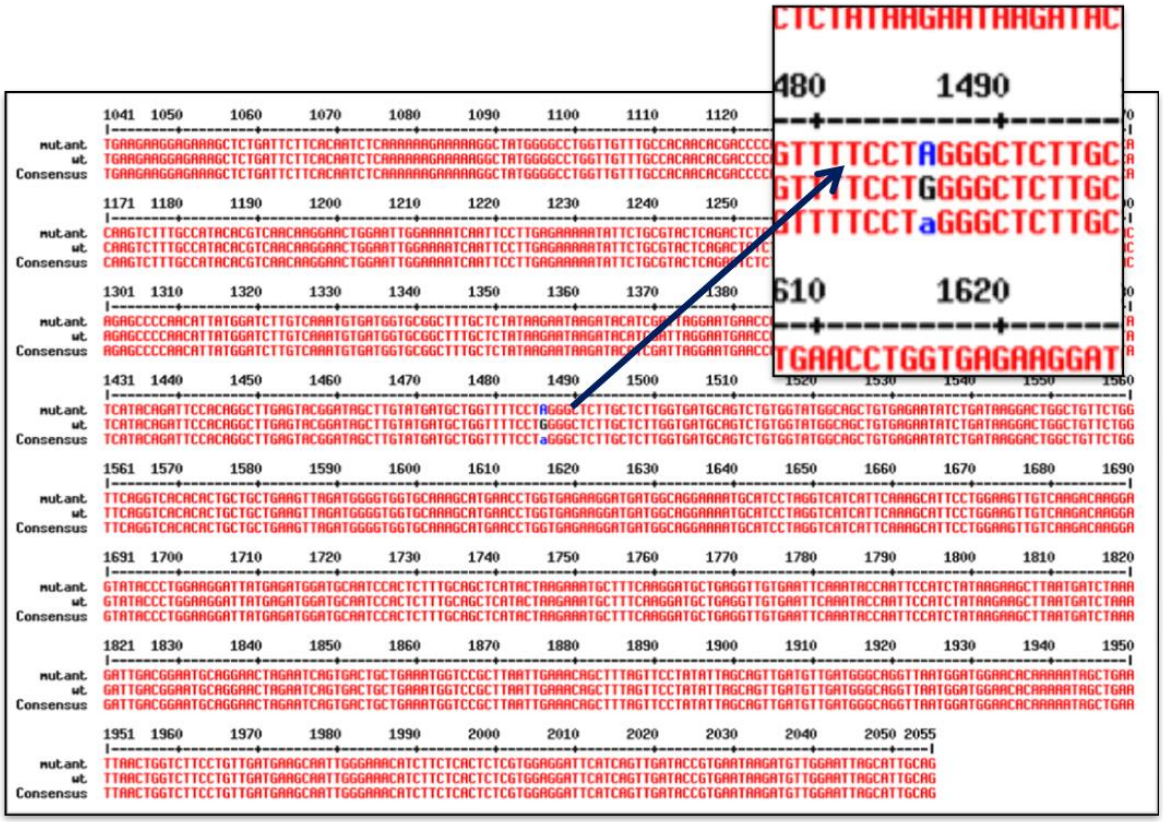

Figure 30. Alignment of *phytochrome A* sequence of amplified from mutant line (M82-M_2-895.5) with wild Arka vikas. Upper sequence is from (M82-M_2-895.5), middle sequence from Arka Vikas and lower sequence is the consensus sequence. Note in accession (M82-M_2-895.5) nucleotide change G to A changes the codon from GGG to AGG. Blue letter indicates a nucleotide change. Inset shows an enlarged view of the nucleotide change.

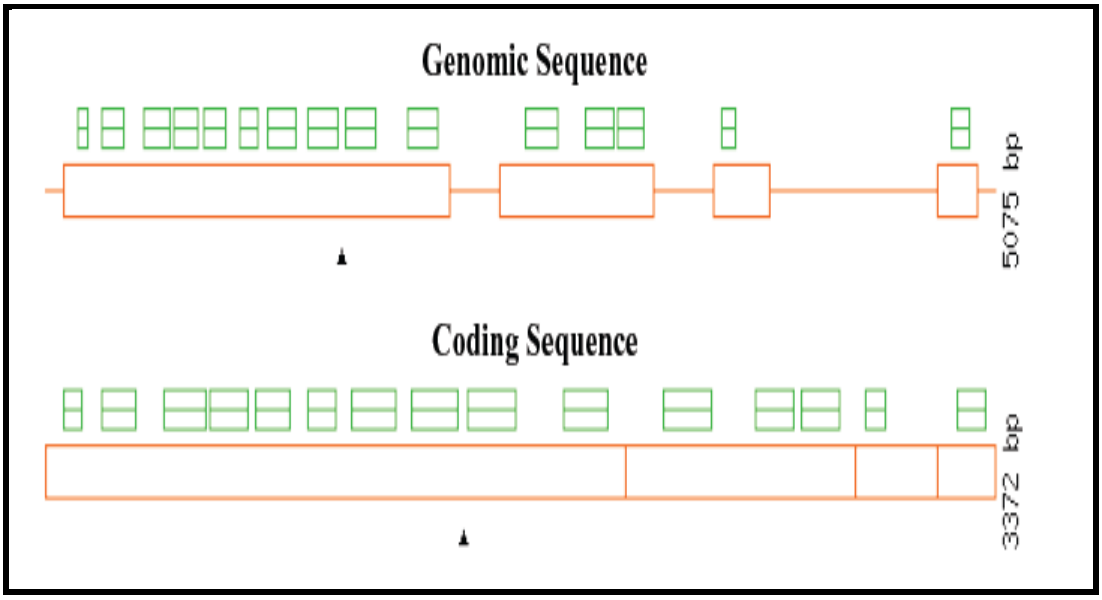

Figure 31. PARSESNP graphical positioning of identified mutation in M82-M_2-895.5. The orange box represents the *phytochrome A* coding sequence. The black triangles represent the position of the mutations.

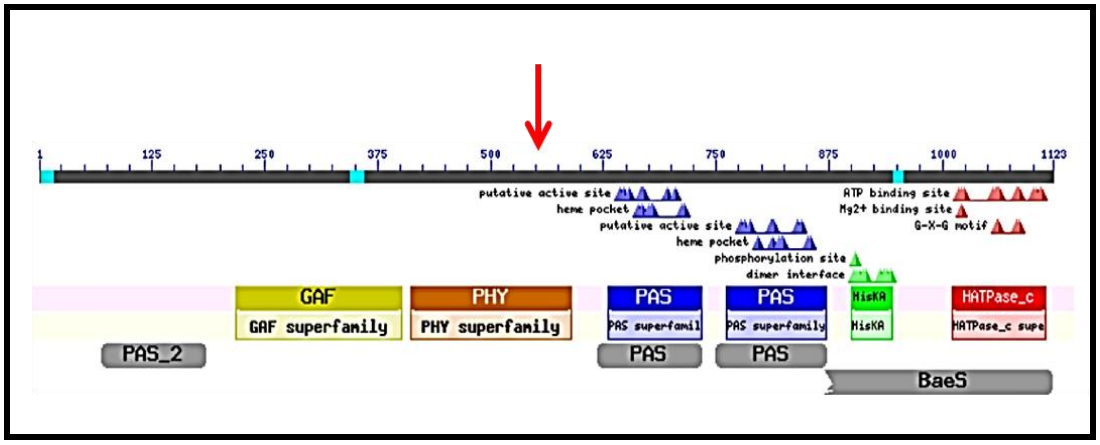

Figure 32. Pictorial representation of putative mutation in PHY domain of phytochrome A in tomato. Lower panel shows functional domain scheme of tomato phytochrome. Red arrows indicating amino acid change.

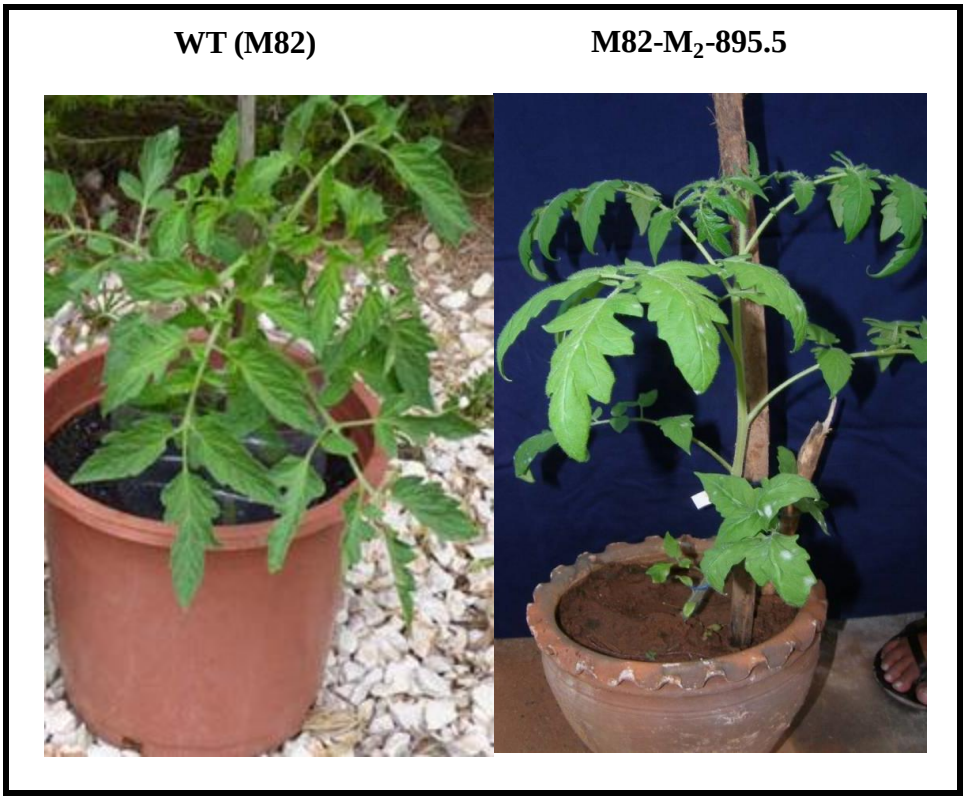

Figure 33. Phenotypes of tomato plants M82 WT and derived M82-M_2-895.5 mutant. The wild-type (WT) and M82-M_2-895.5 mutant plants grown for 35 days in pots in open field.

4.2.9 TILLING for *Phytochrome B1* Gene

One set of primers was designed using tomato *phytochrome B1* sequence obtained from NCBI GenBank. The *phytochrome B1* gene in tomato consists of 10088 base pairs including four exons and three introns. Fig. 34 shows the overall gene structure of *phytochrome B1* gene. The four exons varied in length from 219 bp (exon 4) for the smallest exon to 2074 base pairs (exon 1) for the largest exon. Using CODDLE predictions (Fig. 35) exons 1 of *phytochromeB1* was selected for screening and one pair of primer with amplicon size 868 bp was designed (Fig. 34, Table I).

The *tri* mutant (Tuinen *et al*., 1995) that has a lesion in the *PHYB1*gene was used as a positive control to standardize detection of mutation in *phytochrome B1* gene using TILLING protocol. The *tri* mutant has a single point mutation, which is a C-T substitution at nucleotide 3274, located on the first exon of the *PHYB1* gene. Substitutions at this site would lead to a stop codon at codon 92 which in turn result in the formation of a truncated protein with 92 amino acids.

Positive control DNA bearing *tri* mutation was mixed with WT DNA and PCR amplified to obtain an 868 bp amplicon. The PCR and CEL I digestion were carried out using standard protocols described above. The expected position of the CEL I cleaved fragments are 234 bp (bottom left arrow) in 700 channel and 634 bp (right arrow) in 800 channel. These cut fragments add up to 868 bp (total amplicon length of the primer). On Li-COR gel electrophoresis, the products after cleavage appeared in two channels with fragment size 234 bp (700 channel) and 634 bp (800 channel) (Fig. 36).

Exon 1, that codes for N-terminal region of phytochrome, which is important for its involvement in light signalling was targeted for *phytochrome B1* TILLING. A mutagenized

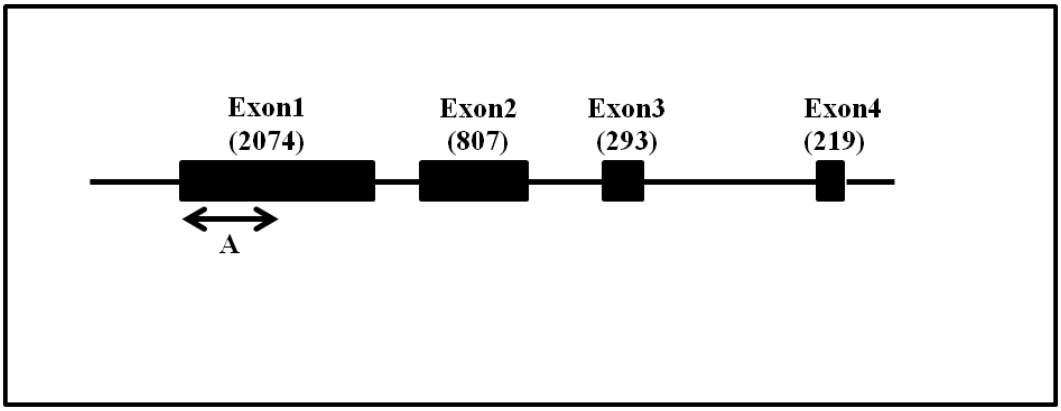

Figure 34. Organization of *phytochrome B1*gene. Exons are shown as boxes; introns are shown as thick black lines. The letter A in the figure refers to amplicon amplified by primer set A (from bp 3041 to 3908). Size of PCR product is 868 bp. Exon numbers are indicated above the gene. The size of each exon is indicated in bp by number given in parenthesis.

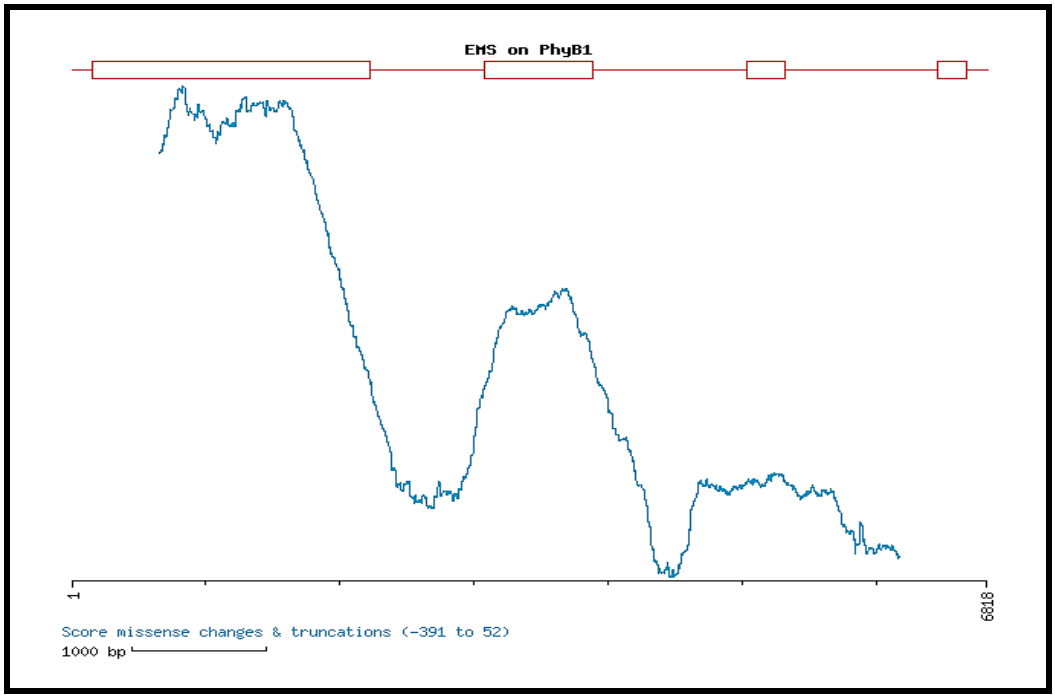

Figure 35. Output of the CODDLE program for *phytochrome B1* genomic sequence. Exons are represented by boxes and introns by lines. The CODDLE program was used to identify those regions of the gene in which G:C to A:T transitions are most likely to result in deleterious effects on the encoded protein (represented by the probability curve traced in turquoise). The CODDLE algorithm is based on an evaluation of protein sequence conservation from comparison of database accessions of homologous proteins. Note that a mutation in exon 1 would be most deleterious.

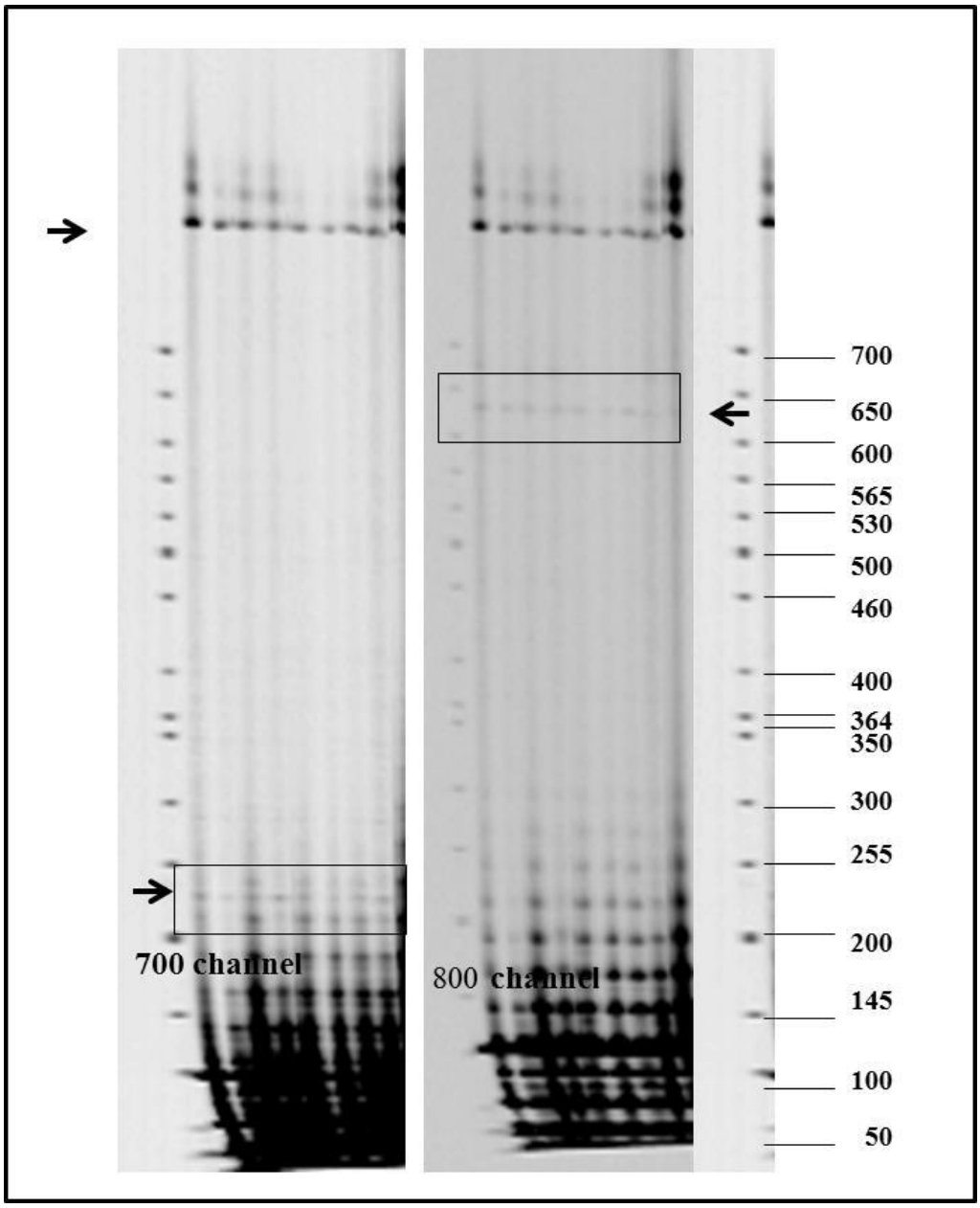

Figure 36. Identification of cleaved fragments after CEL I digestion in Li-COR 4300 DNA Analyzer using heteroduplex consists of wild type and *tri* mutant DNA. The substrate is an 868 bp heteroduplexed PCR product. The expected size of the CEL I cleaved fragments are 234 bp (top right box) in 800channel and 634 bp (bottom left box) in 700 channel. Sum of these cut fragments add up to 868 bp (total amplicon length). M on right hand side of the image shows 50-700 bp size standards. The fragments detected specially in the lower portion of either channel images represent the background fragments usually observed in TILLING runs. However, these can be distinguished from the CEL I cleaved fragments as these fragments do not show the complementary fragment in the either channel, a characteristic of CEL I cleaved fragments.

population of ~10,000 plants were screened for mutation and two putative mutations were identified. Confirmation of mutants was done by screening the complimentary plate. About 50 seed from each mutant family (AV-60mM-888 and AV-60mM-708) were grown to find out the individual line containing mutation. For family AV-60mM-708, mutant individual was not found out even after screening 50 individual lines of the family. The mutant individual for the family AV-60mM-888 was found by screening DNA from ~50 individual lines and mutant line was grown in greenhouse to ascertain the phenotype (Table V).

Table V. Tables showing details of population screened, number of mutations detected and nature of mutation for *phytochrome B1*.

Population	No. of individuals screened	No. of mutation detected	Mutation confirmed	Individual mutant plant identified	Nature of Base change	Effect of mutations
60 mM AV	2304	2	2	1	C to T	Synonymous
120 mM AV	6144	-	-	-	-	-
M82 M2	3840	-	-	-	-	-
M82 M3	768	-	-	-	-	-

The mutant allele for *phytochrome B1* (family AV-60 mM-888) was isolated by screening a mutagenized population of tomato. Upon digestion, the mutation generated two fragments of 360 bp and 508 bp (Fig. 37). The putative mutant line detected in row plate was confirmed by screening the complimentary column plate (Fig. 38). Sequence analysis revealed that a change from Cytosine (C) to Thymine (T), (Fig. 39**)** is a silent or synonymous mutation, as this mutation affected the third base of a codon (CTC to CTT) which does not change the amino acid encoded by that codon (Fig. 40).

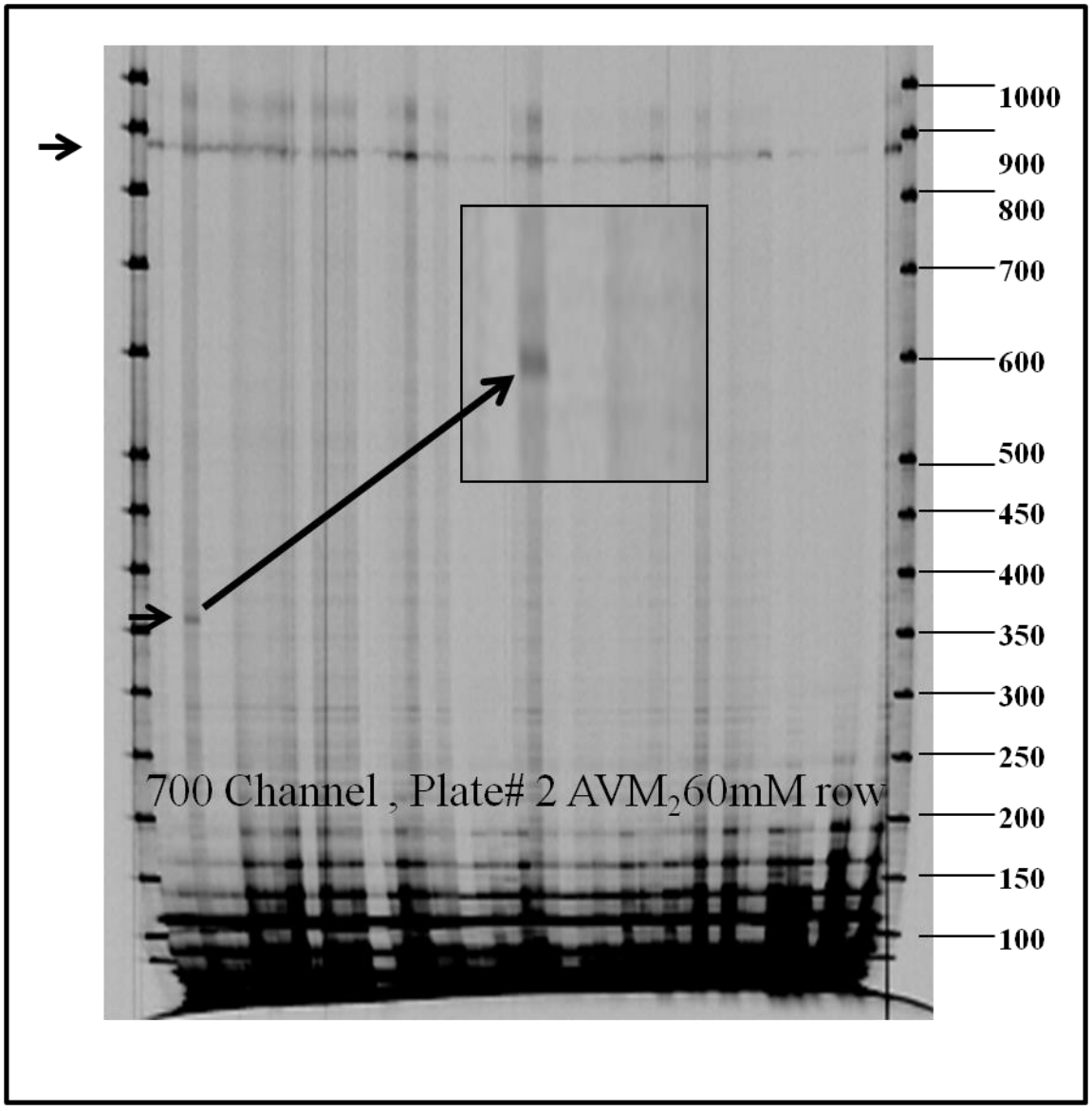

Figure 37. Representative Li-COR gel images showing CEL I-treated polymerase chain reaction (PCR) products for an 868 bp portion *phytochrome B1* gene in tomato. The full-length PCR product is visible as a dark line at the top of each of the 48 wells (top arrow). In the lane where amplicon harbours a mutation, PCR product is cleaved into two fragments (360 bp and 508 bp) labeled with either the 700- or 800-nm IR dye. (Here only 700 channel is shown). Fragment, which corresponds to 360 bp, is clearly visible (arrow) in 700 channel. Inset showing an enlarged view of the fragment. The sizes of the cleavage products from the two dye-labeled DNA strands add up to the size of the full-length PCR product (800 channel is not shown).

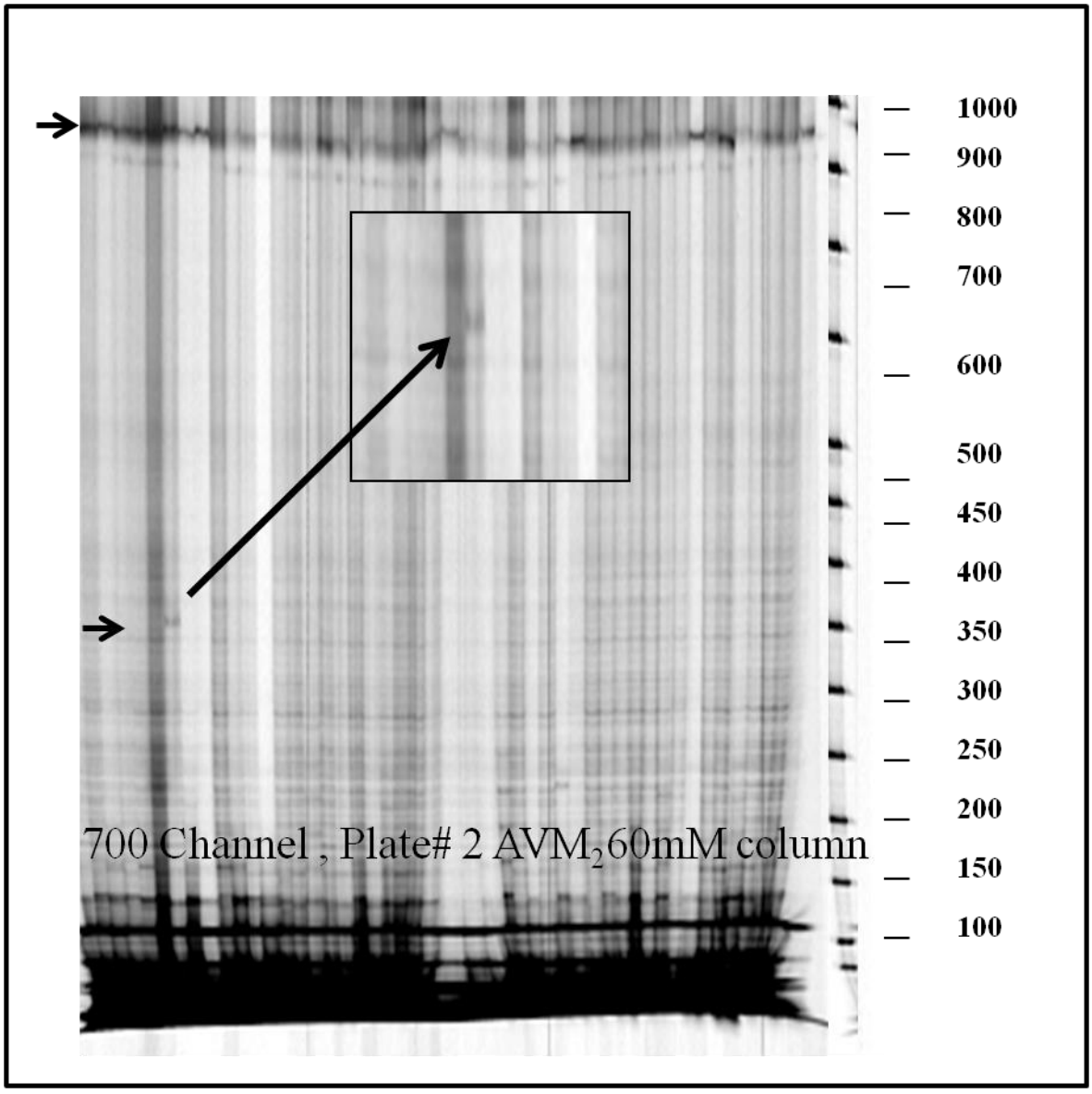

Figure 38. Representative Li-COR gel images showing confirmation of mutation which was already detected in AV-M_2 60mM plate #2(row). Confirmation of mutation was done by screening the complementary column plate (AV-M_2 60 mM plate #2 (column)) .The full-length PCR product is visible as a dark line at the top of each of the 48 wells (top arrow). In the lane where amplicon harbours a mutation, PCR product is cleaved into two fragments (360 bp and 508 bp) labeled with either the 700- or 800-nm IR dye. (Here only 700 channel is shown). Fragment, which corresponds to 508 bp, is clearly visible (arrow) in 700 channel. Inset showing an enlarged view of the fragment. The sizes of the cleavage products from the two dye-labeled DNA strands add up to the size of the full-length PCR product (800 channel is not shown).

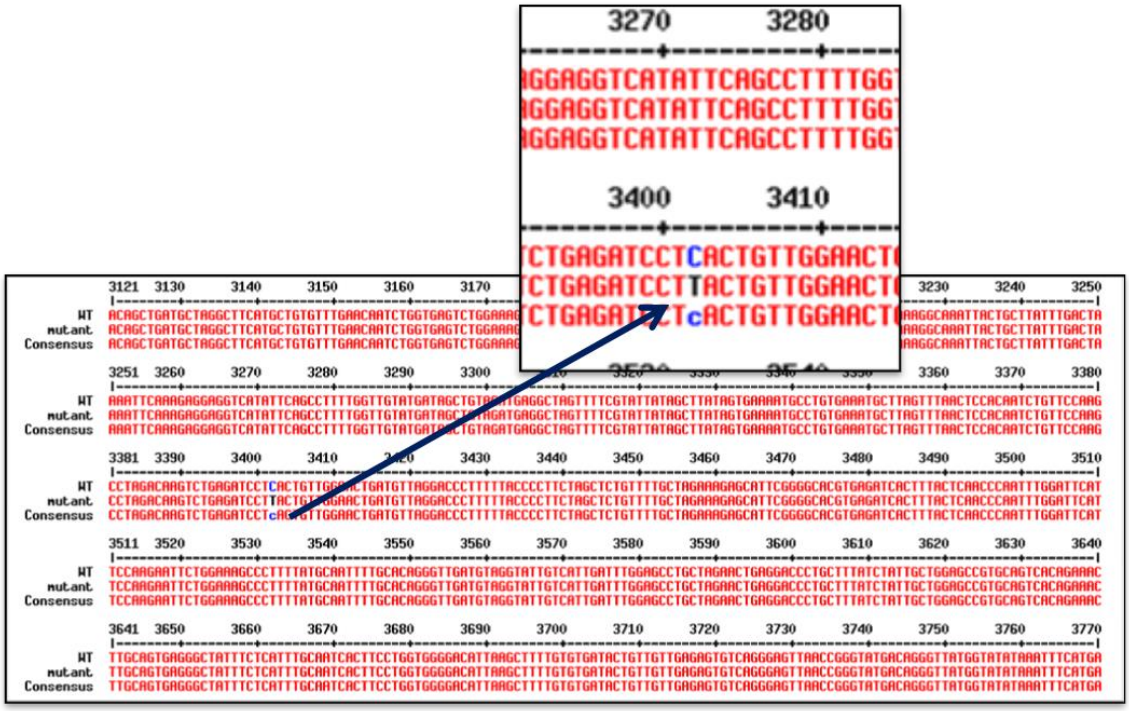

Figure 39. Alignment of *phytochrome B1* sequence of amplified from mutant line (AV-M_2 60mM 888) with wild Arka Vikas. Upper sequence is from Arka Vikas, middle sequence from (AV-M_2 60mM 888) and lower sequence is the consensus sequence. Note in accession (AV-M_2 60mM 888) nucleotide change C to T changes the codon from CTC to CTT. Blue letter indicates a nucleotide change. Inset shows an enlarged view of the nucleotide change.

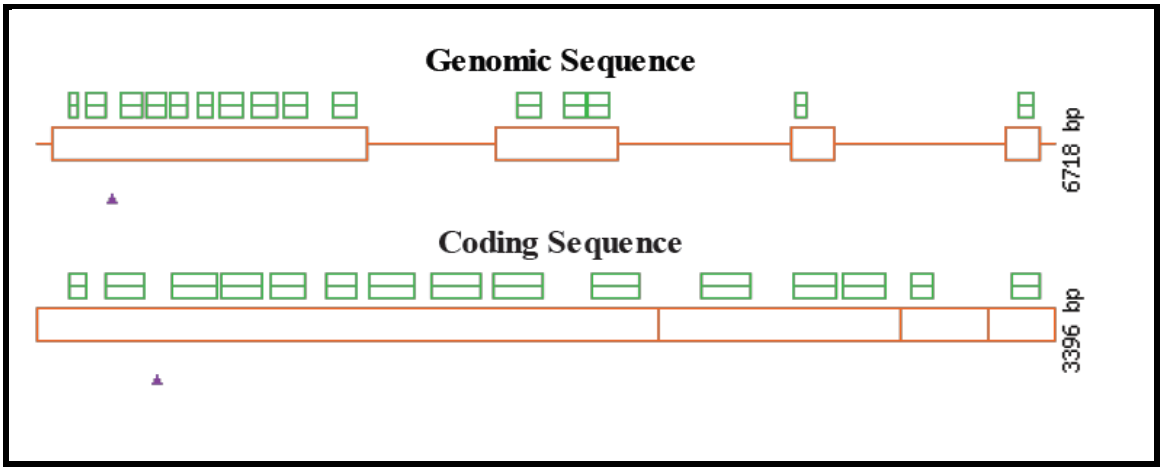

Figure 40. PARSESNP graphical positioning of identified mutation in AV-M_2 60mM 888. The orange box represents the *phytochrome B1* coding sequence. The purple triangles represent the position of the silent mutations.

4.3 EcoTILLING

4.3.1 Tomato EcoTILLING Platform

We examined polymorphism in natural accessions of tomato using EcoTILLING. The key steps of EcoTILLING includes

i) A large collection of natural accessions

ii) Phenotyping of the above accessions

iii) DNA Polymorphism analysis using EcoTILLING

4.3.2 Collection of Accessions and Phenotyping for Architectural Variations

We analysed a total of 605 tomato accessions using EcoTILLING. These accessions were collected from various sources (Table VI). The above accessions were grown in open field at University of Hyderabad campus. At various stages of vegetative growth and flowering these accessions were examined for the phenotypes that were distinct from reference cultivar Arka Vikas using an electronic hand held device PDA. Using PDA loaded with phenome software data under 10 categories (plant size, plant habit, inter nodal length, leaf width, leaf colour, leaf size, leaf complexity, leaf texture, flowering and flower morphology) the morphological data was recorded. Several plants in above population of natural accessions exhibited phenotypes that were distinct from Arka Vikas.

Frequency of the phenotype variations was calculated and overall distribution of different phenotypes was expressed as a percentage of total number of variations. Fig. 41 shows the frequency of occurrence of different morphological categories as a percentage of the observed number of variations. The most abundant variation was in plant habit (50%) followed by leaf morphology (36%), and internodal length (5%). Compared to this only 6% plants showed

variations related to flower morphology. We found some accessions with drastically increased height and some with sharp phenotypes which is related to leaf morphology like serrated leaves and extremely small leaves (Fig.42).

Since plant architecture is influenced by light environment, to evaluate contribution of different SNP of phytochrome we specifically examined leaf architecture. Fig.42 shows that most drastic effect was on plant habit and leaf morphology which together consisted of 86% of total variations.

Table VI. Source of accessions used for EcoTILLING.

Source of accessions	Number of accessions
TGRC, USA	184
NBPGR, INDIA	200
IIVR, INDIA	156
Bejo Sheetal, INDIA	65

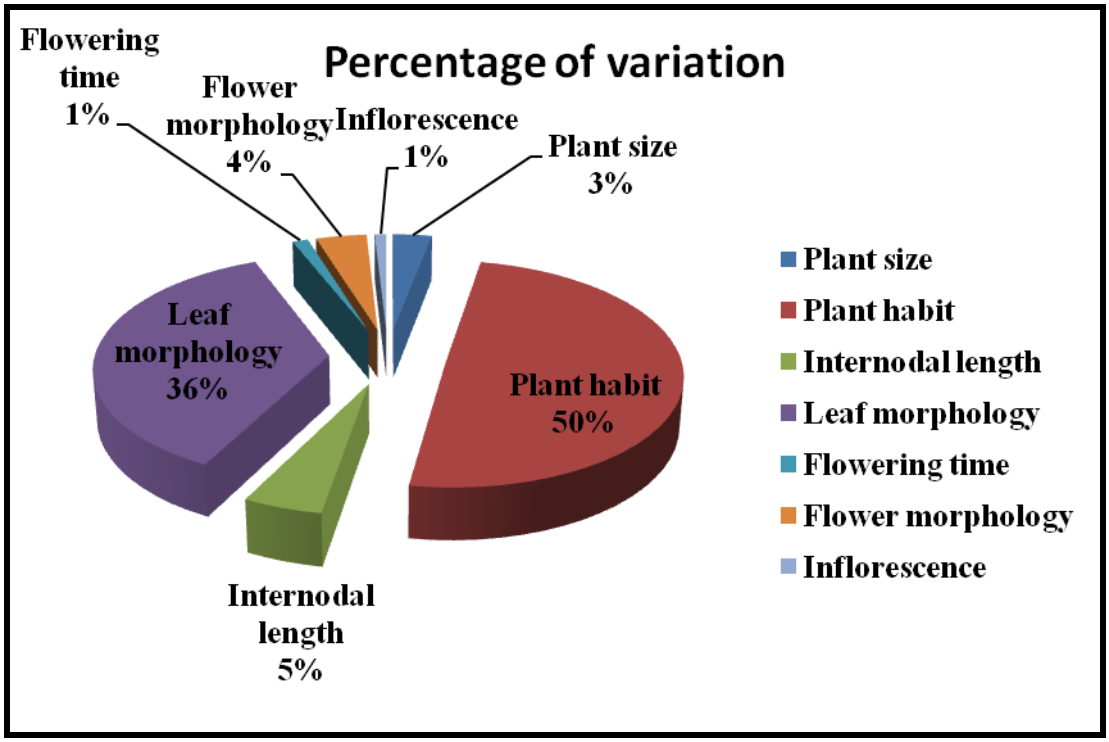

Figure 41. Frequency of distribution of morphological variations in tomato accession. The pie diagram shows 7 phenotypic categories. All the variations in leaf phenotype are grouped together. The values are the percentage of each category in a population of 605 tomato accessions.

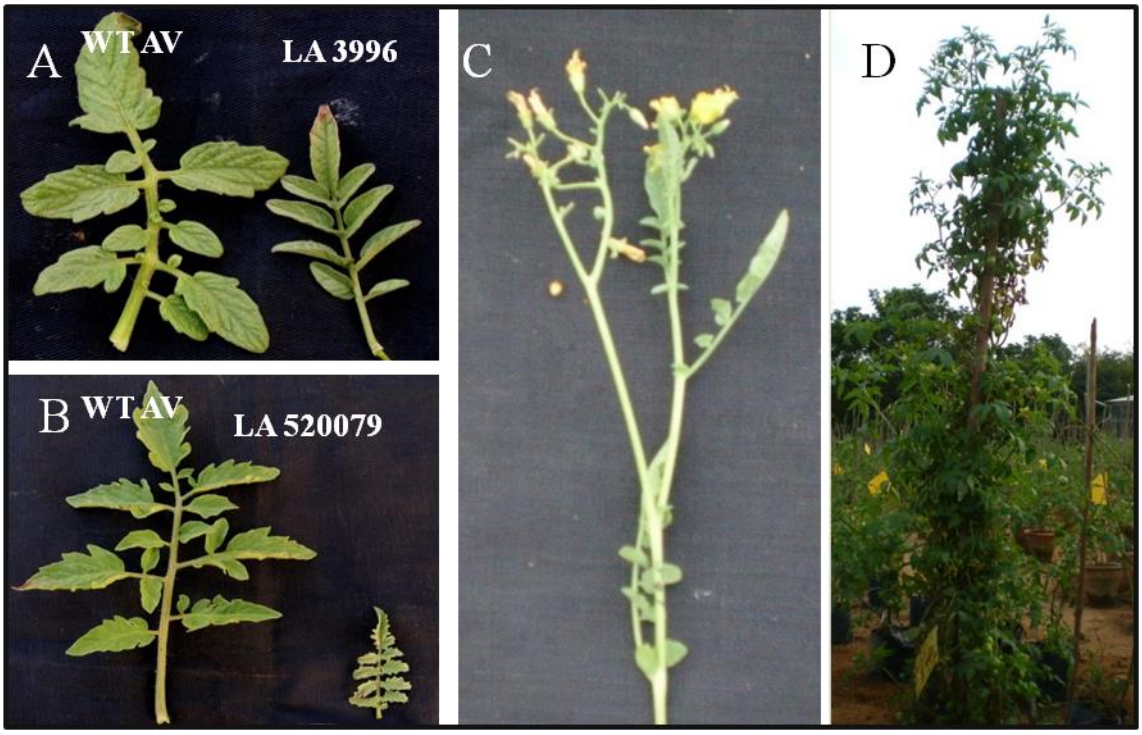

Figure 42. Representative examples of tomato accessions showing variation in plant architecture and leaf morphology (A) Leaves with no serration (LA3996) (B) small leaves (EC520079) (C) Abnormal inflorescence (NBPGR 610) (D) tall plant (IIHR 2201). The number in parenthesis indicates the respective accession number. In A and B Arka Vikas phenotype is shown in left and accession on right.

4.3.3 Polymorphism Analysis using EcoTILLING

Both *phytochrome A* and *phytochrome B1* genes were examined for the detection of SNPs in natural accessions of tomato using the same region of gene that was used for TILLING (Table VII, Figs. 24, 34). For EcoTILLING, genomic DNA from each accession was mixed in 1:1 ratio with genomic DNA from the reference cultivar Arka Vikas. EcoTILLING of above accessions revealed a total of 32 SNPs in *phytochrome A and B1* genes in 605 accessions (Table VIII).

4.3.4 Screening of *Phytochrome A* Polymorphisms by EcoTILLING

The light-sensing N-terminal end of *phytochrome A* gene was scanned for polymorphism using, two pairs of primers (Table VII, Fig. 24) encompassing first exon and first intron, and second exon of the gene. Phytochrome polymorphism was examined in a collection of 605 accessions of tomato. Standard EcoTILLING protocol was essentially the same including

Table VII. Gene targets, target specific inner primer sequences with M13 overhang attached and amplicon lengths used in EcoTILLING. M13 sequence is shown in red letters.

Target name	NCBI gene bank locus	Primer name	Forward primer (5'-3')	Reverse primer (5'-3')	Amplicon size (bp)
PHYA	AJ001913.1	Primer A	TGTAAAACGACGG CCAGTACACGTCA ACAAGGAACTGGA ATTGGAAAATC	TGTAAAACGACGG CCAGTCTGATCAA TTTGGCTGGTGTTC TGAGTGGA	1420
		Primer B	TGTAAAACGACGG CCAGTAGGTAGAG GCTTTACGATAAAT CATCC	TGTAAAACGACGG CCAGTAATTCCAG TTCCTTGTTGACGT GTATG	1402
PHYB1	AJ002281.1	Primer A	TGTAAAACGACGG CCAGTCATCACAA GGTCAAGCTCAAT CTTCAGG	TGTAAAACGACGG CCAGTTCCACAAT CATTCTCACCCTGT CCTGC	868

enzymatic mismatch cleavage of heteroduplexed DNA and fluorescence detection of cut fragment as described earlier for TILLING. In the enzymatic mismatch cleavage reaction PCR products obtained from different accessions were heteroduplexed with PCR products amplified from Arka Vikas, and digested with CEL-I.

Table VIII. Analysis of polymorphism of *phytochrome A* and *phytochrome B1* genes in tomato accession. The total number of SNPs detected and grouping in haplotype is shown below.

Target name	Total number of bp screened	No of Haplotypes detected	Number of SNP identified
PHYA	2822 (from bp 1304 to 2708) and (from bp 2684 to 4104)	5	18
PHYB1	868 (from bp 3041 to 3908)	3	14

Out of 605 accessions, 19 showed polymorphisms in comparison to the Arka Vikas. While several polymorphic sites were identified in both exons 1 and 2 and intron 1 (Fig. 43), the gene region from 2684 bp to 4104 bp amplified by primer set A showed comparatively low degree of polymorphism than the region amplified by primer B. Based on nature and location of polymorphisms, the above accessions were grouped into 4 different haplotypes distinct from Arka Vikas (Fig. 43, Table IX). Almost 580 accessions did not show any polymorphism and they were classified as HT.1 (Haplotype 1) along with Arka Vikas (WT *cv.* AV). The most frequent type of polymorphism was observed for HT.4 (Haplotype.4) and 14 accessions showed this polymorphism (Table IX). These accessions bear two SNPs in exon 2 located at G1870T and at A2053T respectively (Table X). HT.2 (Haplotype.2) included two accessions and showed a polymorphism in second exon (G2614A) (Table X). HT.3 (Haplotype.3) consisted of two accessions, corresponding to a change in first intron. Since it was located in the intron, polymorphism of this haplotype was not examined by sequencing.

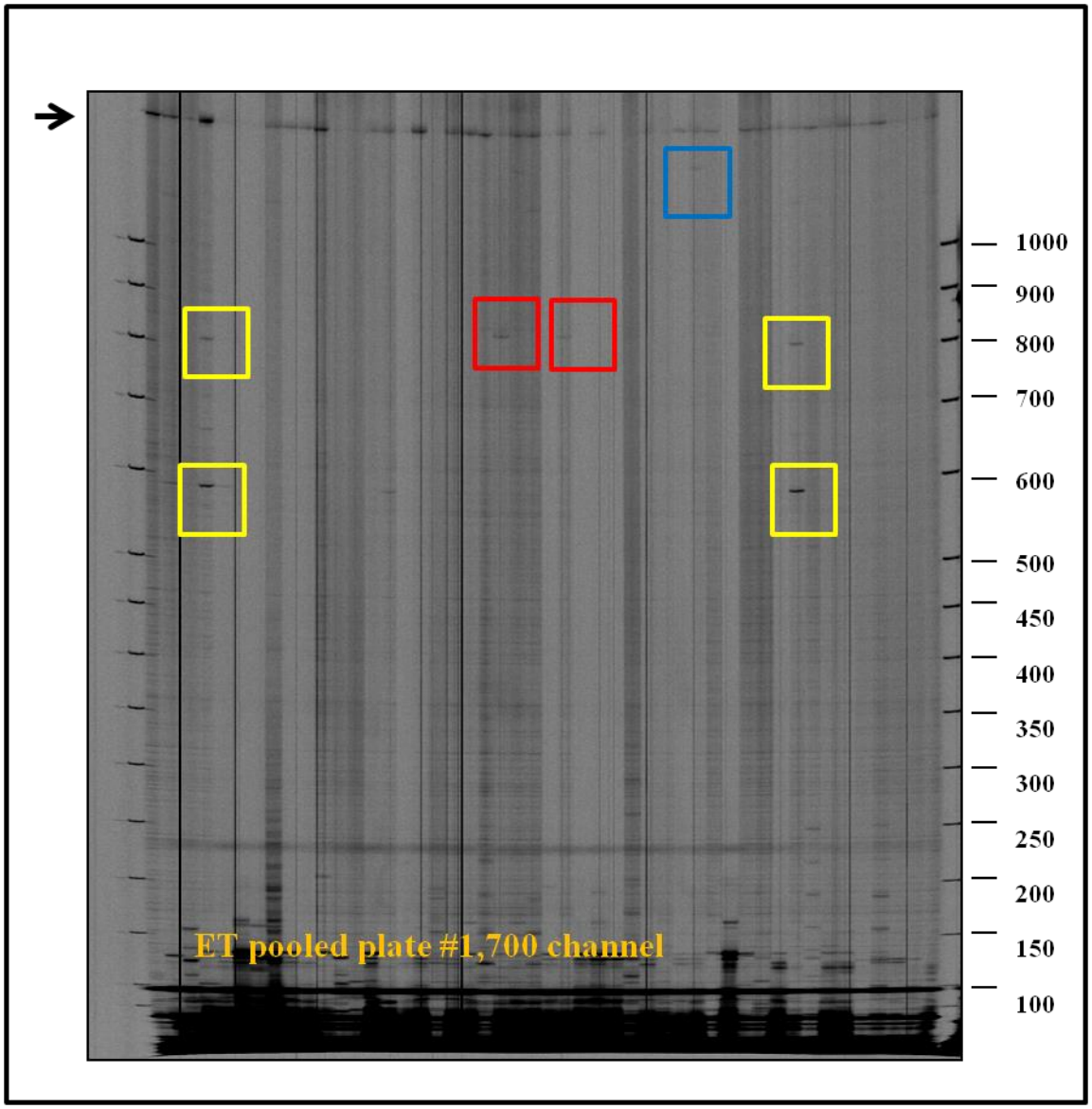

Figure 43. Representative Li-COR gel images of detection of SNPs for a 1.4-kb region *phytochrome A* gene. The arrow at top of gel indicates the full-length PCR product. The cleavage pattern of the different haplotype is shown in the gel only for700 channel. Samples with similar cleavage patterns are classified as same haplotype (samples with the same cleavage patterns are marked by same color box, HT.2 blue, HT.3 red and HT.4 yellow). EcoTILLING plate number is given at the bottom of the picture.

Table IX. Classification of tomato accessions according to their haplotype in EcoTILLING of *phytochrome A*.

Haplotype	Accessions
HT.1	WTAV and other 580 accessions
HT.2	EC 521074,EC 528362
HT.3	EC 398711
HT.4	WIR 3768, EC 521067 B, EC-29933, EC-34480, EC-25563, EC-14073, EC529083, EC-35240, EC-163598, EC-521079, EC20636, EC-163598, EC-521079, EC521067B

Table X. Haplotype showing the location of polymorphism on *phytochrome A* gene, amino acid substitution and PSSM/SIFT score for effect of SNP on function of putative active domains.

Haplotype	No. of polymorphism	Polymorphism	Amino acid change	SIFT	PSSM
HT.1	0	-	-		
HT.2	1	G4014A	E748K	0.05	7.3
HT.3	1	unknown	-		
HT.4	2	A3453T G3270T	L651F E590D	0.00	17.6

The translation of nucleotide sequences showed that there are three non-synonymous changes in the regions screened. Two among three non-synonymous SNPs were located on exon 1, and the remaining one was located on exon 2. Among three non-synonymous changes identified, two were found to lead to an amino acid change.

Molecular nature of the mutants: The precise position and the nature of identified polymorphisms were determined by sequencing of PCR products comprising exons 1 and 2 and intron 1 for the accessions from haplotypes H.2 to H.4. From each haplotype, a single accession was chosen which represents the polymorphism. EC-528362 belonging to Haplotype 2 (HT. 2) showed a nucleotide change G2614A, which was non-synonymous and it corresponded to amino acid change E748K (Glutamic acid to Lysine). Similarly, sequence analysis of WIR 3768, which belongs to Haplotype 4 (HT. 4) revealed two polymorphisms in the region encoded by primer A resulted in nucleotide base change in two positions A2053T and G1870T. Translation of the nucleotide to amino acid showed that above nucleotide changes corresponds to amino acid changes at two positions in Phytochrome A protein sequence *viz* E590D and L651F (Table X).

Characterization of Haplotype 2: Haplotype 2 was further characterized to find out the correlation between amino acid change at position 748 in the Phytochrome A protein and its light response. The nucleotide change from guanine (G) to Adenine (A) (Fig. 44, Table X), at 4014^{th} position of *PHYA* genomic sequence, caused a non-synonymous mutation which altered the codon GAA (encoding for glutamic acid) to AAA (encoding for Lysine) (Fig.45, Table X). With this codon change, the nature of amino acid changed from polar positive to polar negative. This change may affect properties of phytochrome such as the solubility of the polypeptide. In view of this change, we examined whether the change in amino acid affect light response in HT.2.

Several studies in Arabidopsis and tomato have reported that seedlings of mutant plants with defect in PHYA protein showed an elongated phenotype under far red light (Van Tuinen *et al.,* 1995a). To ascertain the effect of above SNP on seedling phenotype, seedlings of the accession EC 528362 and its wild type control *cv.* AV were grown under continuous blue,

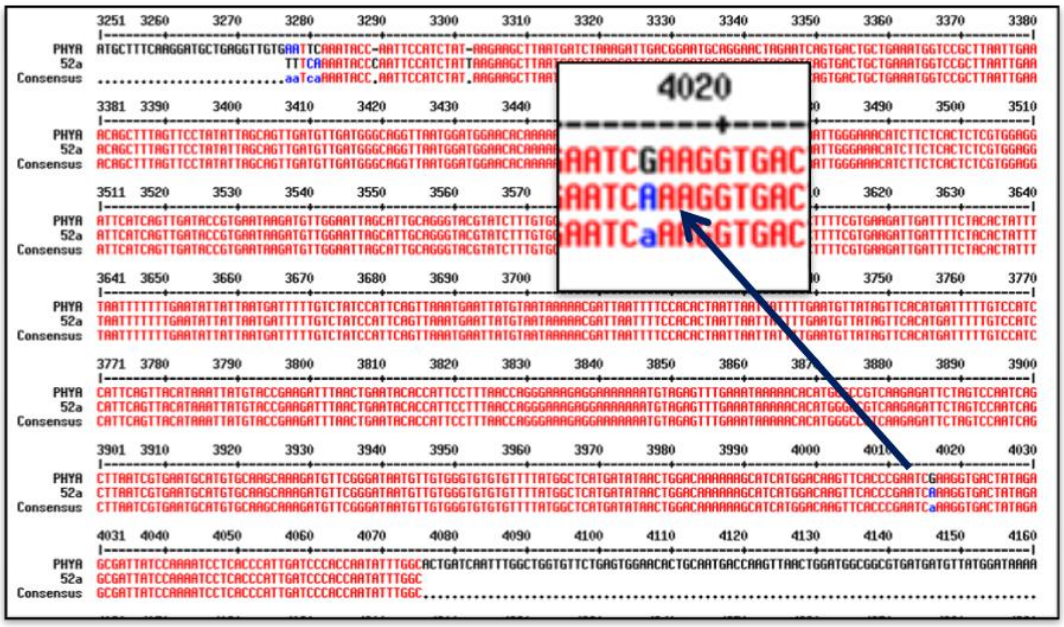

Figure 44. Alignment of *phytochrome A* sequence from EC528362 with Arka Vikas sequence. Upper sequence is from Arka Vikas, middle sequence from EC528362 and lower sequence is the consensus sequence. Note in accession EC 528362 nucleotide change from G to A, which changes the codon from GAA to AAA. Blue letter indicates a nucleotide change. Inset shows an enlarged view of the nucleotide change.

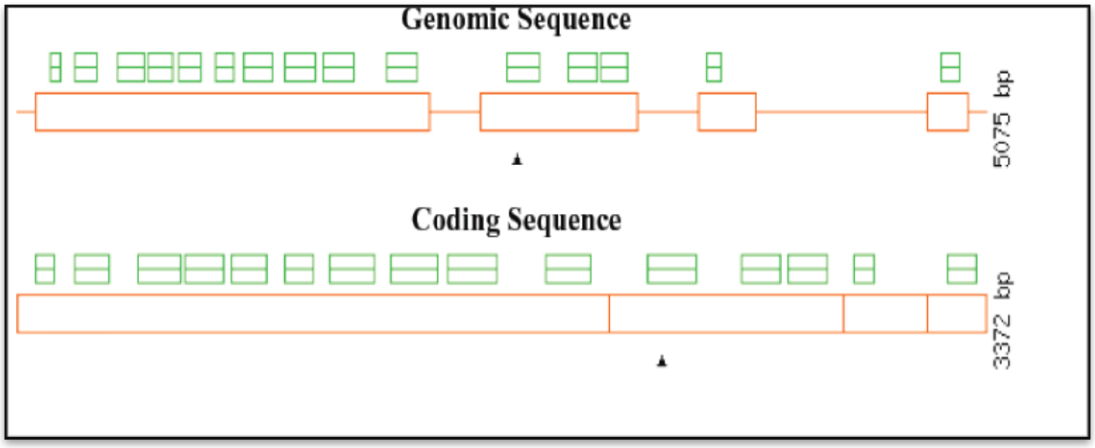

Figure 45. PARSESNP output of SNP found in EC528362. The orange box represents the *Phytochrome A* coding sequence. The black triangles represent the SNP leading to a non-synonymous amino acid change.

red, far red light, white light and absolute darkness. In comparison with the wild type, no perceptible difference was found between Arka Vikas and EC 528362 under all light conditions, except in FR light. In FR light, the hypocotyl of EC 528362 was slightly elongated compared to WT. Interestingly, roots of the accession (EC 528362) exhibited an opposite response, as it displayed a shorter root under FR light compared to WT root **(**Figs. 46, 47**)**. Consistent with altered response to FR light in seedling stage, the field grown plants of this accession also showed a significant change in plant architecture. Compared to WT *cv.* AV plant, above accession EC 528362 exhibited a thinner stem and a large reduction in branching (Fig. 48).

Characterization of Haplotype 4: Considering the presence of two amino acid changes in the accession WIR 3768, which represent haplotype 4, above accession was examined to find the effect of amino acid changes in its light response. Sequence analysis revealed that a nucleotide change from Guanine (G) to Thymine (T) (Fig. 49), at 3270^{th} position and Adenine (A) to Thymine (T), (Fig. 49) at 3453^{th} position of *PHYA* gene corresponds to two non-synonymous changes which alter the codon GAG (encoding for glutamic acid) to GAT (encoding for Aspartic acid), TTA (encoding for Leucine) to TTT (encoding for Phenyl alanine) respectively. Thus, the overall consequence is two amino acid changes that is from glutamic acid to aspartic acid (E590D) and Leucine to Phenyl alanine (L651F) in the PHYA polypeptide (Fig. 50, Table X). Considering the high PSSM score obtained for this amino acid change L651F (Table X), a significant change in phytochrome function is expected. While examining the light response under different wave length of light, the above accession exhibited an altered light response to far red light (Figs. 51, 52). Seedlings grown under far red light displayed a completely opened cotyledon associated with a strong reduction in hypocotyl length. This response was specifically observed under FR light and was absent in other wavelength of light (Figs. 51, 52).

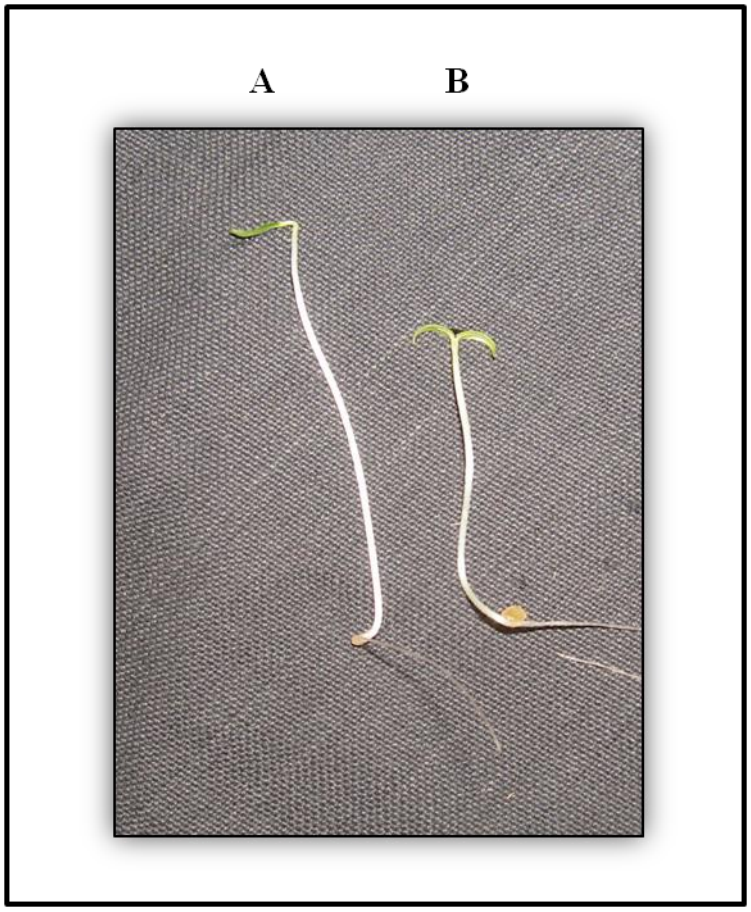

Figure 46. The phenotype of tomato seedlings grown for 7 days after emergence in FR light (5 µmol m^{-2} s^{-1}). The seedling on the left is EC 528362(A) and that on the right is WT *cv.* Arka Vikas (B). Note the increased hypocotyl length of EC 528362 (A) compared to Arka Vikas (B).

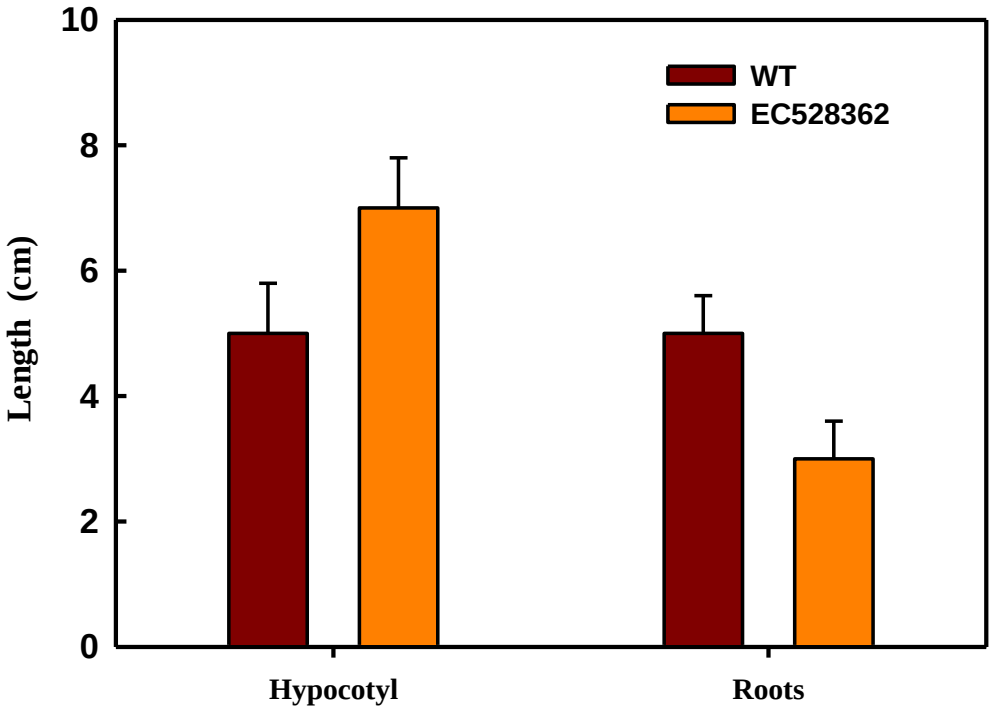

Figure 47. Hypocotyl length and root length of Arka Vikas and the accession EC528362 seedlings after 7 days in continuous FR light (5 µmol m^{-2} s^{-1})

Figure 48. Phenotype of EC 528362 and Arka Vikas. plants were grown for 50 days in pots in open field. Note an altered plant architecture exhibited by EC 528362(B), with thinner stem and reduction in branching compared to Arka Vikas (A).

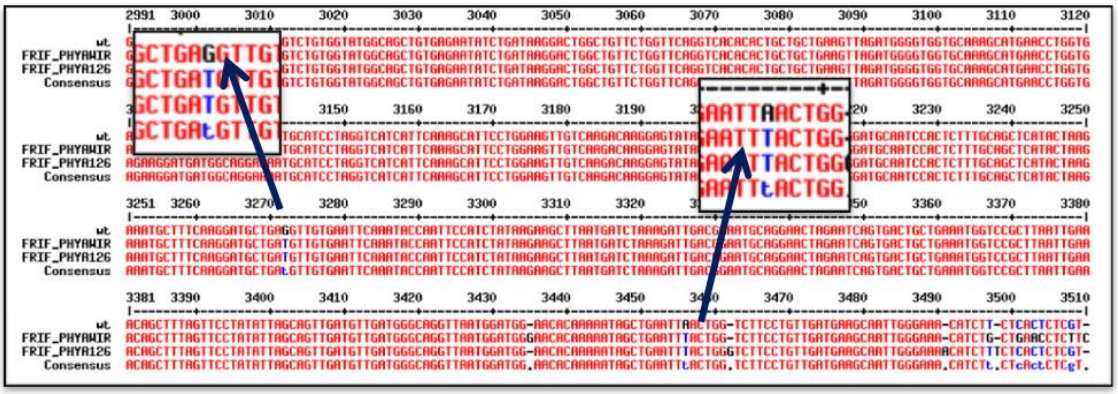

Figure 49. Alignment of *phytochrome A* sequence from (WIR 3767) with Arka Vikas sequence. Upper sequence is from Arka Vikas, middle sequence from (WIR 3767) and lower sequence is the consensus sequence. Note in accession (WIR 3767) nucleotide change from G to T and A to T that changes the codon from GAG to GAT and TTA to TTT respectively. Blue letter indicates a nucleotide change. Inset shows an enlarged view of the nucleotide change.

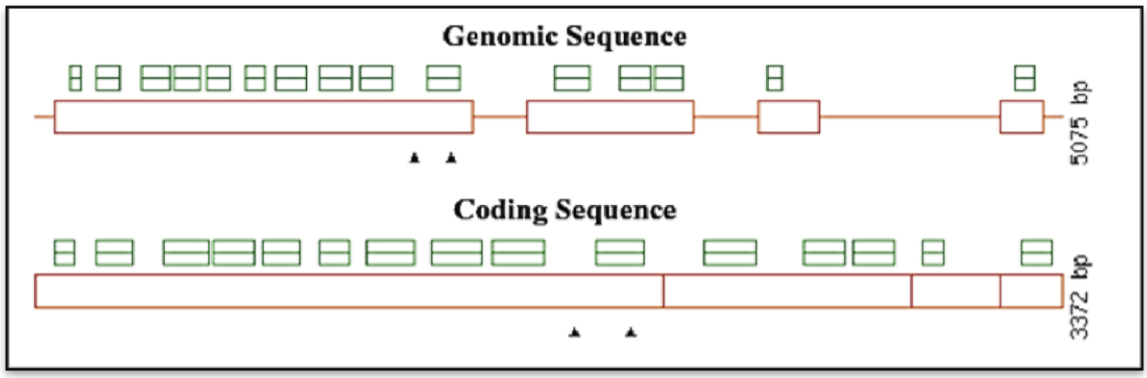

Figure 50. PARSESNP output of identified SNP in WIR 3767. The orange box represents the *phytochrome A* coding sequence. The two black triangles represent the SNP leading to a non-synonymous amino acid changes.

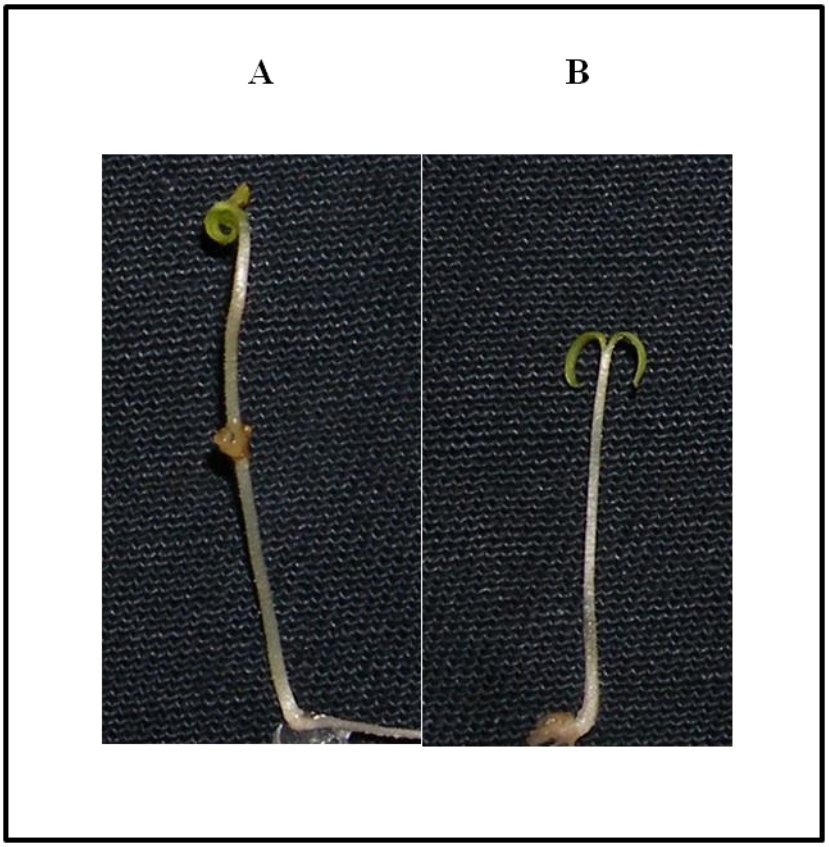

Figure 51. The phenotype of tomato seedlings grown for 7 days after germination in FR (5 µmol m^{-2} s^{-1}). The seedling on the left is WT *cv.* Arka Vikas (A) and that on the right is WIR 3768 (B). Note the decreased hypocotyl length of WIR 3768 (B) compared to Arka Vikas (A).

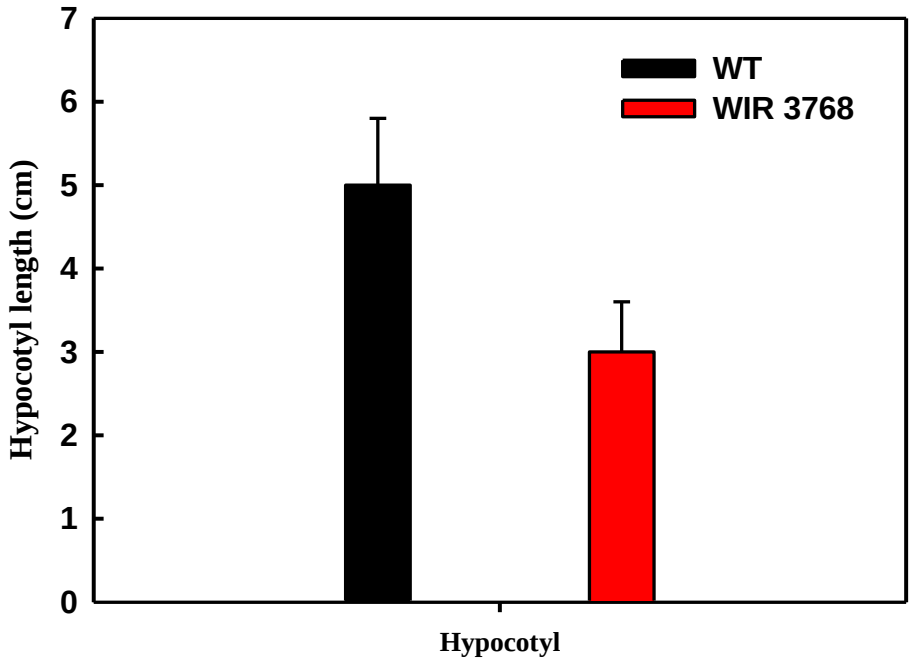

Figure 52. Hypocotyl length of tomato Arka Vikas and EC528362 seedlings after 7 days of continuous FR (5 µmol m^{-2} s^{-1}).

4.3.5 Screening of *Phytochrome B1* Polymorphisms by EcoTILLING

Light-sensing N-terminal end of *phytochrome B1* was screened for natural sequence variation, using a primer set (phytochrome B1 primer set A) designed based on CODDLE. For this gene too, a population of 605 natural accessions of tomato were analysed and standard EcoTILLING was carried out as described earlier. Several accessions showed polymorphic variation in the analysed region (Fig. 53). These accessions were classified into different haplotypes based on the nature of polymorphisms (Table XI, Fig.53). A total of thirteen accessions showed polymorphisms in comparison to Arka Vikas and these were grouped in 3 different haplotypes (Table XI). HT.1 (Haplotype 1) included ~ 592 accessions, which did

Table XI. Classification of tomato accessions according to their haplotype in EcoTILLING of *phytochrome B1*.

Haplotype	Accessions
HT.1	WTAV and other 180 accessions
HT.2	EC 521067B, EC-29933, EC-34480, EC-25563, EC-14073, 529083, EC-35240, EC-163598, EC-521079, EC20636, EC-163598, EC-521079, EC521067B
HT.3	EC-34480

not show any polymorphic site in comparison with WT *cv.* AV. HT.2 (Haplotype 2) consists of 13 accessions which showed multiple polymorphic sites. Haplotype 3 consists of single accession which represents one of the rarest polymorphism for this gene region (Table XII). From each haplotype a single accession was chosen which represents the polymorphism. Sequence analysis revealed that all the nucleotide changes in Haplotype 2 were synonymous (Table XII). Haplotype 3 showed a novel nucleotide change A3164T, which was non-synonymous and corresponded to amino acid change E55V (Glutamic acid to Valine), along

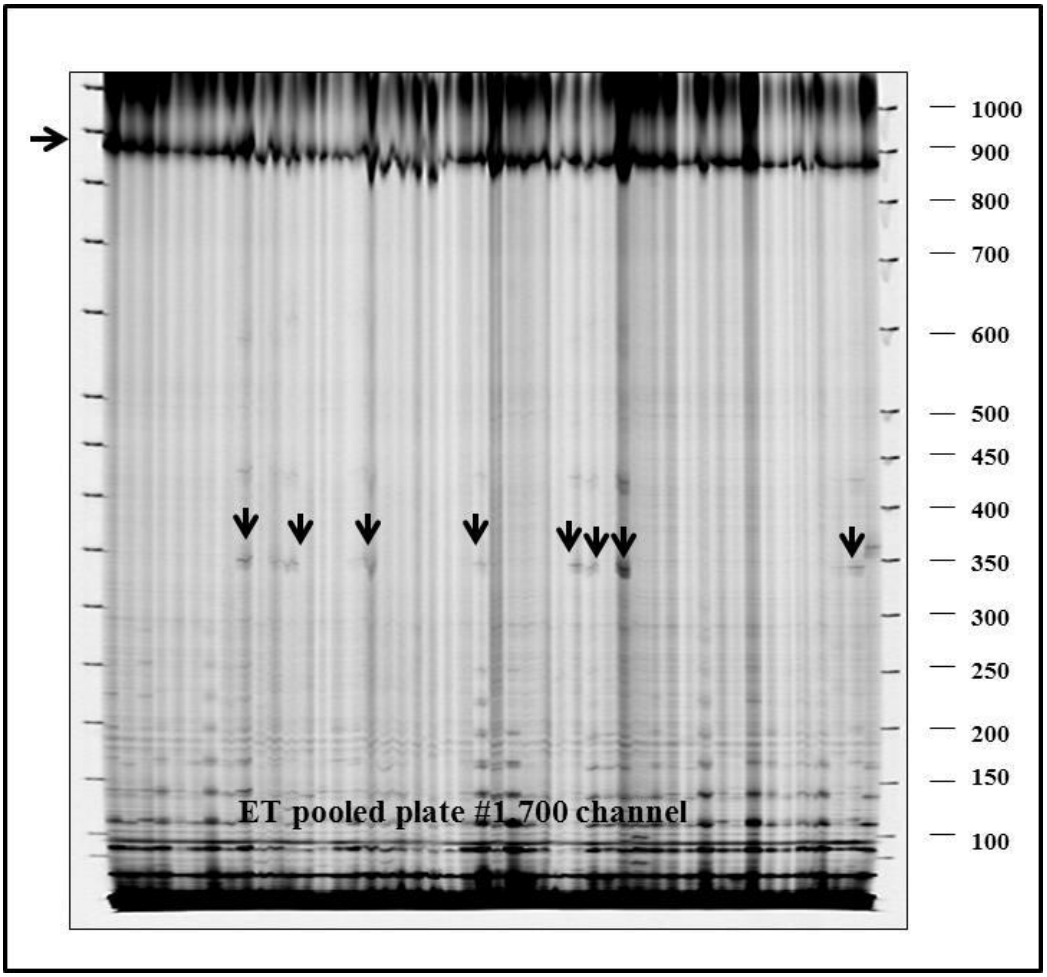

Figure 53. Representative Li-COR gel images of detection of SNPs for a 868 bp region *phytochrome B1* gene. The arrow at top of gel indicates the full-length PCR product. The cleavage pattern of a haplotype (HT.2) is shown in the gel only for 700 channel. Few accessions showed SNPs in genomic DNA are marked by arrows. EcoTILLING plate number is given at the bottom of the picture.

with 3 other synonymous change (Table XII). The three synonymous changes include nucleotide change at A3384T, C3468T, C3624A on *phytochrome B1* sequence.

Table XII. Haplotype showing the location of polymorphism on *phytochrome A* gene, amino acid substitution and PSSM/SIFT score for effect of SNP on function of putative active domains.

Haplotype	No. of polymorphism	Polymorphism	Amino acid change	SIFT	PSSM
HT.1	0	-	-	-	-
HT.2	3	A3384T, C3468T, C3624A	-	-	-
HT.3	4	A3384T, C3468T, C3624A and A3164T	E55V	0.22	7.9

Characterization of new mutant *phytochrome B1* alleles: Though seedlings of EC-34480 did not show any deviation from normal phenotypes with broad spectrum light experiments, but field grown plants showed a strikingly different phenotype. Sequence analysis showed that a nucleotide change from Adenine (A) to Thymine (T), at 3164th position of *PHYB1* genomic sequence (Fig. 54), is a missense mutation which alter the codon GAG (encoding for glutamic acid) to GTG (encoding for valine) . Thus, the overall consequence is the glutamic acid to valine change at amino acid 55 (E55V) in the PHYB polypeptide (Fig. 55, Table XII).

The field grown plants (homozygous for the above non-synonymous SNP) of this accession showed a significant reduction in number of both branches and flowers compared to plants heterozygous for the same non-synonymous SNP). A delay in flowering for almost 30 days also was observed in this accession. The mutant plant also exhibited a retarded growth (Figs. 56, 57).

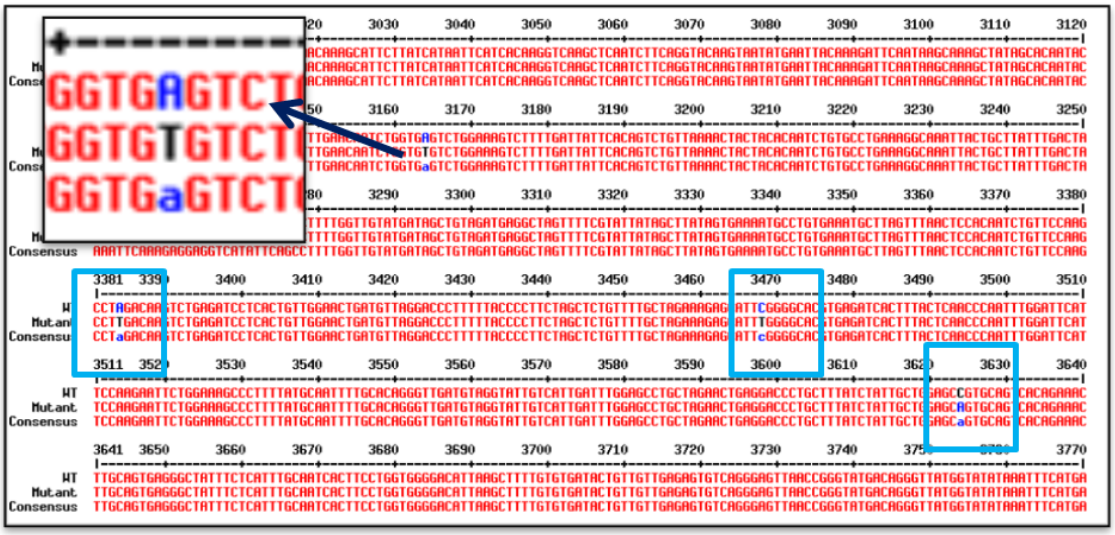

Figure 54. Alignment of *phytochrome B1* sequence from EC-34480 with Arka Vikas sequence. Upper sequence is from Arka Vikas, middle sequence from EC-34480 and lower sequence is the consensus sequence. Note in accession EC-34480 change in 3 position, which include one non synonymous and 3synonymous SNP. Inset showing an enlarged view of the non-synonymous change which is from A to T. Blue squares indicating 3 synonymous changes.

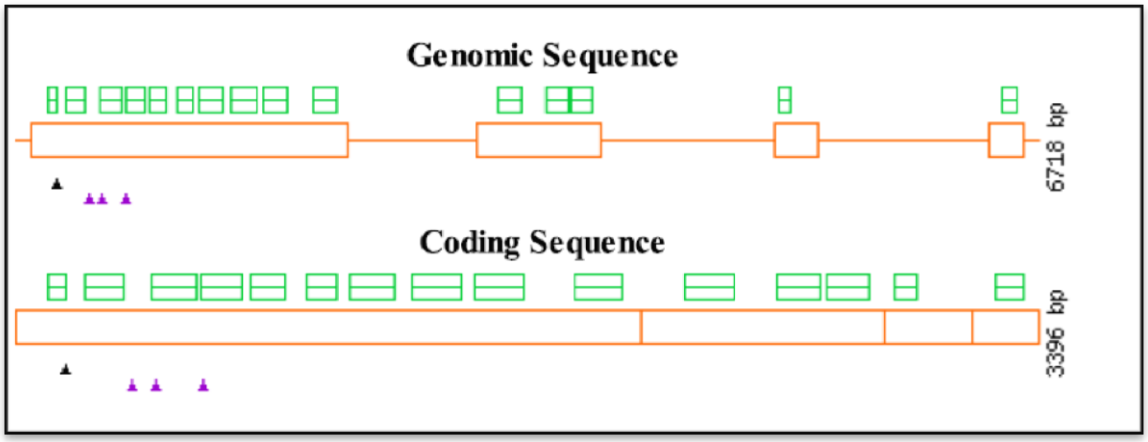

Figure 55. PARSESNP output of the SNP in EC-34480. The orange box represents the *phytochrome B1* coding sequence. The black triangle represent the SNP leading to a non-synonymous amino acid changes, while purple triangle indicating synonymous change.

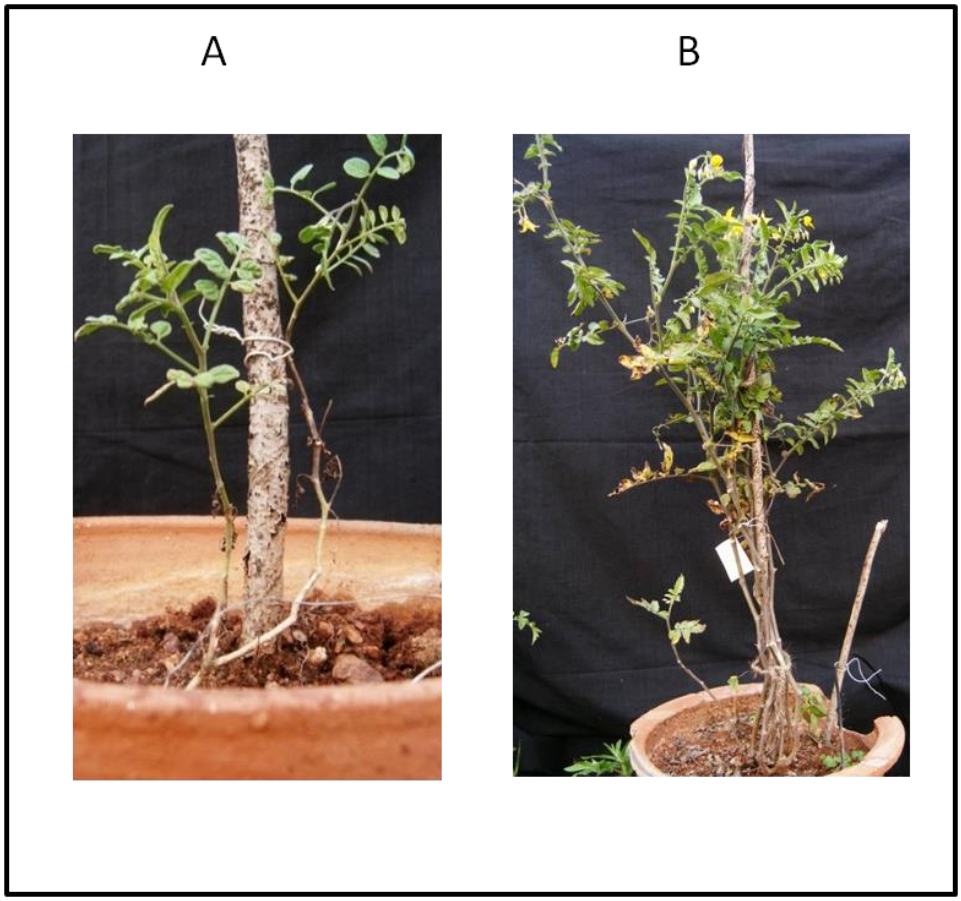

Figure 56. Phenotype of EC-34480 (homozygous for the non-synonymous SNP i.e., A to T at 3164th position of *PHYB1 gene*) (A) and EC-34480 (heterozygous for the same SNP) (B). Plants were grown for 60 days in pots in open field. Note an altered architecture exhibited by EC-34480 (homozygous), with reduction in branching and flower number compared to EC-34480 (heterozygous).

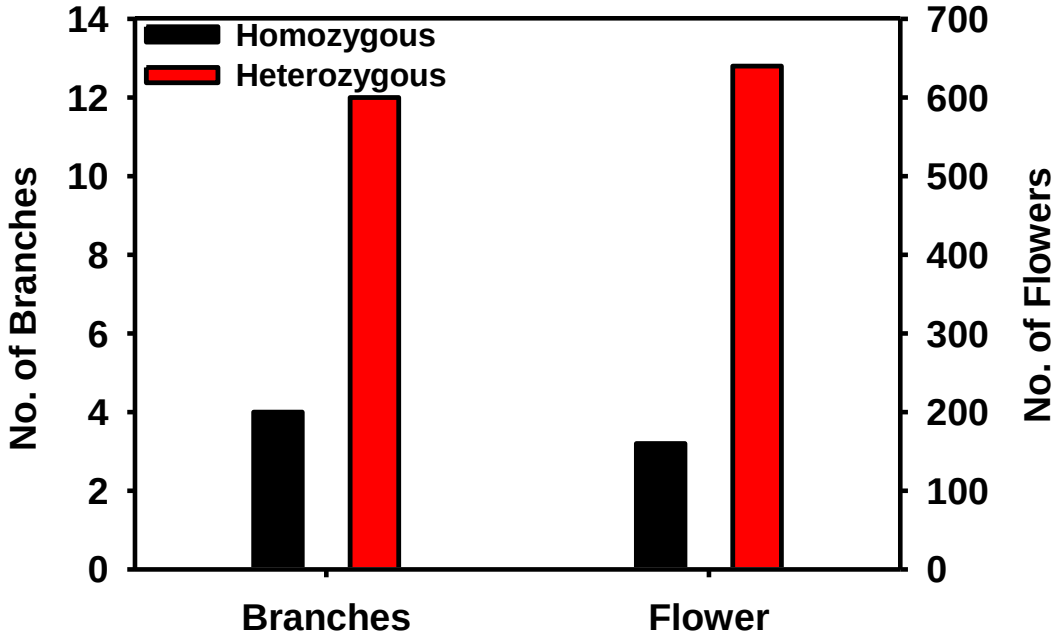

Figure 57. Number of branches and flowers observed for the accession EC-34480. The homozygous ((homozygous for the non-synonymous SNP) and heterozygous ((heterozygous for the same SNP) line were grown for 60 days under field condition.

4.4 Sequences Diversity of *PHY* Genes in Tomato Wild Relatives

4.4.1 Nucleotide Diversity in *PHY* Genes in Tomato Wild Relatives

To evaluate nucleotide diversity and sequence evolution at various phytochrome loci in wild relatives of tomato, we chose 5 different wild relatives (Table.XIII). The oligonucleotide primers amplifying 4 different phytochrome genes used in this study containing amplicons of 750 bp to 850 bp were designed based on sequences in the NCBI databases are shown (Table. XIV, XV). The gene structure, region amplified and the position of detected SNPs are shown in Fig. 58. Sequence analysis showed that all the four phytochromes, analysed in this study, harboured several SNPs (e.g., *PHYA*: 25, *PHYB1*:49, *PHYE*: 56, *PHYF*: 26) (Fig. 59). As expected, more synonymous changes (*PHYA*: 16, *PHYB1*: 45, *PHYE*: 31, *PHYF*: 15) were detected than nonsynonymous changes (*PHYA*: 9, *PHYB1*:4, *PHYE*: 25, *PHYF*: 11) in each

Table XIII. The geographic information of wild relatives of tomato used in this study. Five wild relatives of tomato (*S. habrochaites, S. pimpinellifolium, S. galapagense, S. neorickii, S. chilense)* were selected for this study.

Sample No.	Name	Accession No.	Latitude/Longitude	Area of collection
1	*S. habrochaites*	LA1777	9 °33‘S/77°35‘W	Peru
2	*S. pimpinellifolium*	LA1589	8°22‘S/ 78°43‘W	Peru
3	*S. galapagense*	LA0483	0°22‘S/ 91°33‘W	Ecuador
4	*S. neorickii*	LA2133	3°21‘S/79°10‘W	Ecuador
5	*S. chilense*	LA1969	-17 °33‘S/ -70 °42‘W	Peru

gene (Fig. 60). The ratio of total SNPs to SNPs that were nonsynonymous (dS/dN) ranged from 8% to 45% in various phytochrome members with *PHYE* showing highest ratio (0.45) and other phytochrome genes *viz* *PHYF*, *PHYA* and *PHYB1* showed a ratio of 0.42, 0.36 and 0.8 respectively (Fig. 61). Three species, *S. habrochaites* (71) *S. neorickii* (42) and *S.chilense* (34) harboured several SNPs compared to two other species (Fig. 62 and 63). Sequence analysis of the other two species showed that they possess few (*S. cheesmanii*, 9 SNPs) or no SNP (*S. pimpinellifolium*, 0 SNP) at all (Fig. 62 and 63).

Table XIV. NCBI accession number (codes) for gene targets analyzed in this study.

Gene	NCBI code	No. of base pair
Phytochrome A	AJ001913	6623
Phytochrome B1	AJ002281	10088
Phytochrome E	AF178571	6189
Phytochrome F	U32444	12501

Table XV. Gene targets and primer sequences used in sequencing. Four phytochrome genes (*PHYA*, *PHYB1*, *PHYE* and *PHYF*) were amplified PCR primers were designed based on sequences in the NCBI database.

Gene	Primer Sequence (F) 5'-3'	Primer Sequence (R) 5'-3'
PHYA	ATTTGAGTCGAGATGTCGT	GTGGAATATCTGTAGCAGGATAA
	ATCCTGCTACAGATATTCCAC	GCTTTGAATGATGACCTAGGA
	CCTAGGTCATCATTCAAAGCATTC	CTCAGATTCTTGACCAGTGATAGC
	GCTATCACTGGTCAAGAATCTGAG	CTTGAAATCGTCTTCCACTATAC
PHYB1	AATTACAAAGATTCAATAAGCA	ACCCCATATTTGCCATGTACTG
	CAGTACATGGCAAATATGGG	CAATCTAACCATTTCTCTGGCAA
	GCCAGAGAAATGGTTAGATTG	TTTCCAGATCAACATCCCT
	GTTACAAAGAGTGGGAGACA	GATCATAAGGGATGTTGATCTGG
PHYE	GAGTAGTGAAAACAGAAGAGG	AGGTTCCAAGTCTGATCTCCTTAT
	GATAAGGAGATCAGACTTGGAAC	CTTCCTTAGCTGTGTGAGACCTGA
	TCTGGTTCAGGTCTCACACA	CCGTAAGACGACAAAGACCA
	TGGTGGTCTTTGTCGTCTTACGG	ATTTCGGACCATGTTGTGTAGG
PHYF	TCAAGGGGCAGTTCAGCTA	TGTAGCAGGGTAATGCAAGCCA
	TGGCTTGCATTACCCTGCTACA	TCCGTCATCCTTGTCTCCAGGAA
	ATGCACCCAAGGTCATCATTT	CCAGTTACTCGACCATCGTCAT
	ATGACGATGGTCGAGTAACTGG	AGATACTGGACGGTACCAT

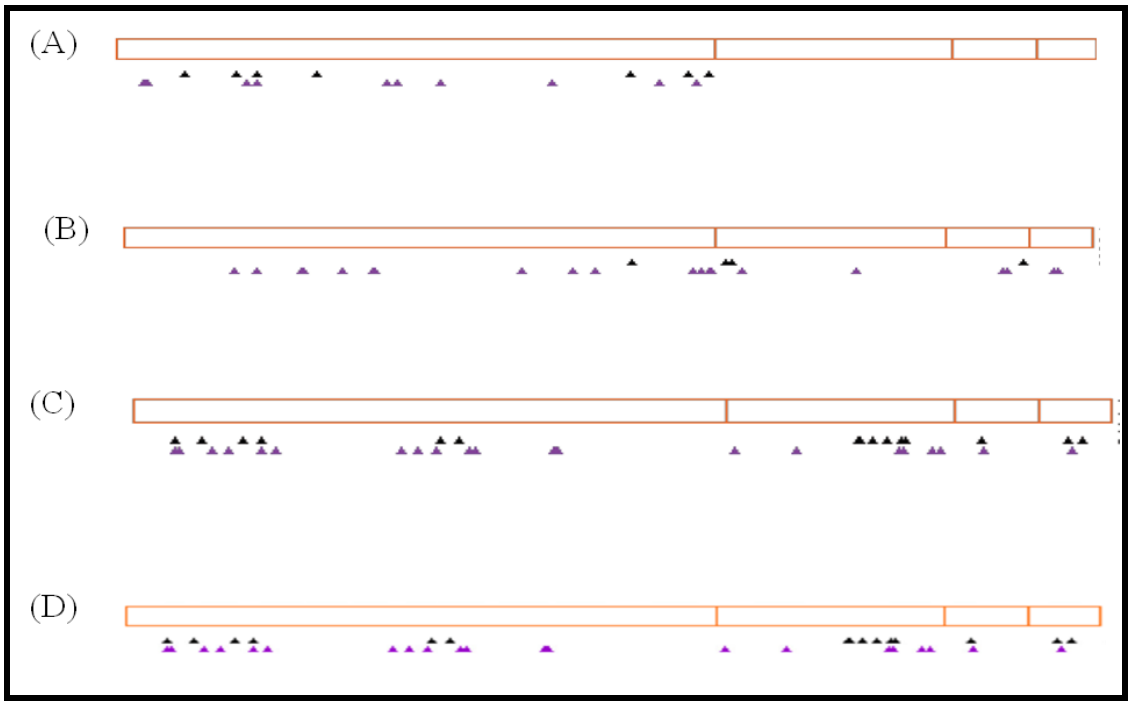

Figure58. Distribution of SNPs on phytochrome genes. Purple and black triangles represent synonymous and nonsynonymous changes, respectively. Sequencing data from five wild relatives of tomato (*S. habrochaites, S. pimpinellifolium, S. galapagense, S. neorickii and S. chilense)* was used to construct the map. (1) *Phytochrome A* (2) *Phytochrome B1* (3) *Phytochrome E* and (4) *Phytochrome F*.

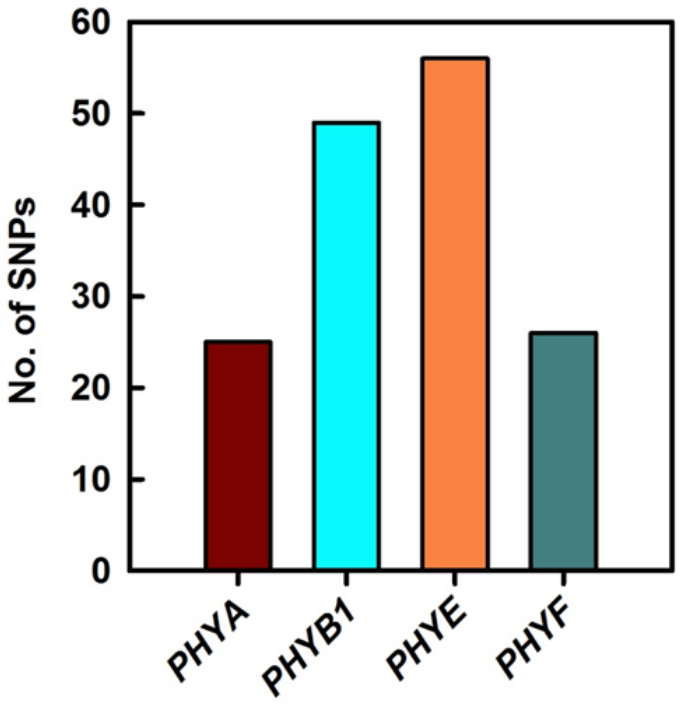

Figure 59. Number of SNPs detected in various *Phytochrome* genes. Sequencing data from five wild relatives of tomato (*S. habrochaites, S. pimpinellifolium, S. galapagense, S. neorickii, and S. chilense*) was used to construct the histogram. The X-axis represents a phytochrome gene and Y axis represents number of SNPs.

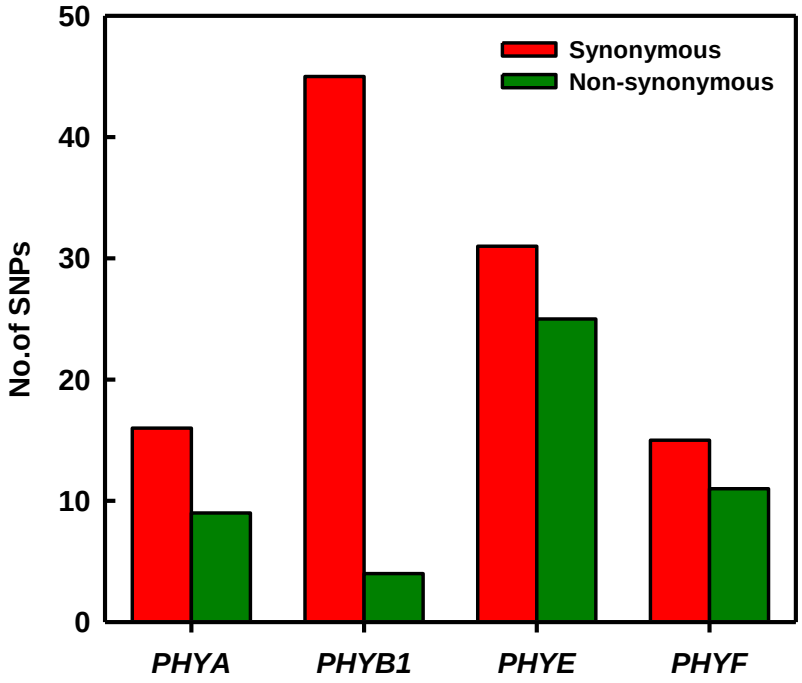

Figure 60. Comparisons of observed synonymous and nonsynonymous SNPs in various *Phytochrome* genes. Red histogram and Green histogram represents synonymous and non-synonymous changes respectively. Sequencing data from five wild relatives of tomato (*S. habrochaites, S. pimpinellifolium, S. galapagense, S. neorickii, and S. chilense)* was used to construct the histogram. The X-axis represents a phytochrome gene and Y axis represents number of SNPs.

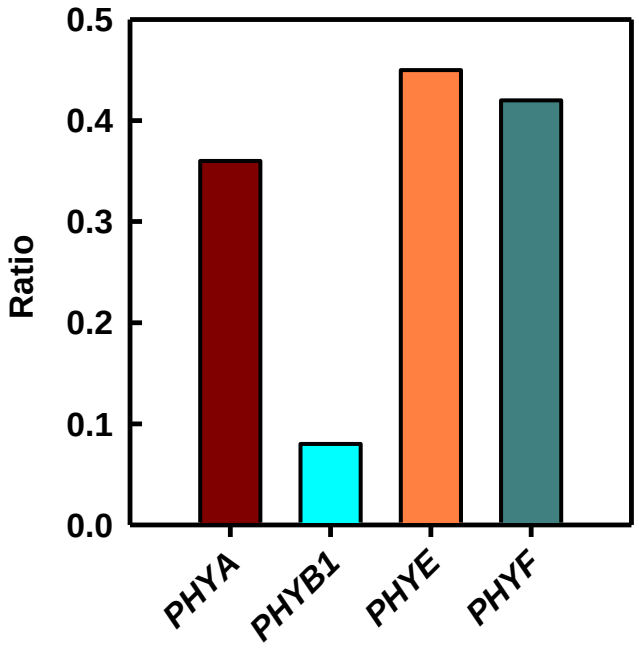

Figure 61. Ratio of observed nonsynonymous to synonymous SNPs in various *Phytochrome* genes. Sequencing data from five wild relatives of tomato (*S. habrochaites, S. pimpinellifolium, S. galapagense, S. neorickii, and S. chilense)* was used to construct the histogram. The X-axis represents a phytochrome gene and Y axis represents ratio of observed non synonymous to synonymous SNPs.

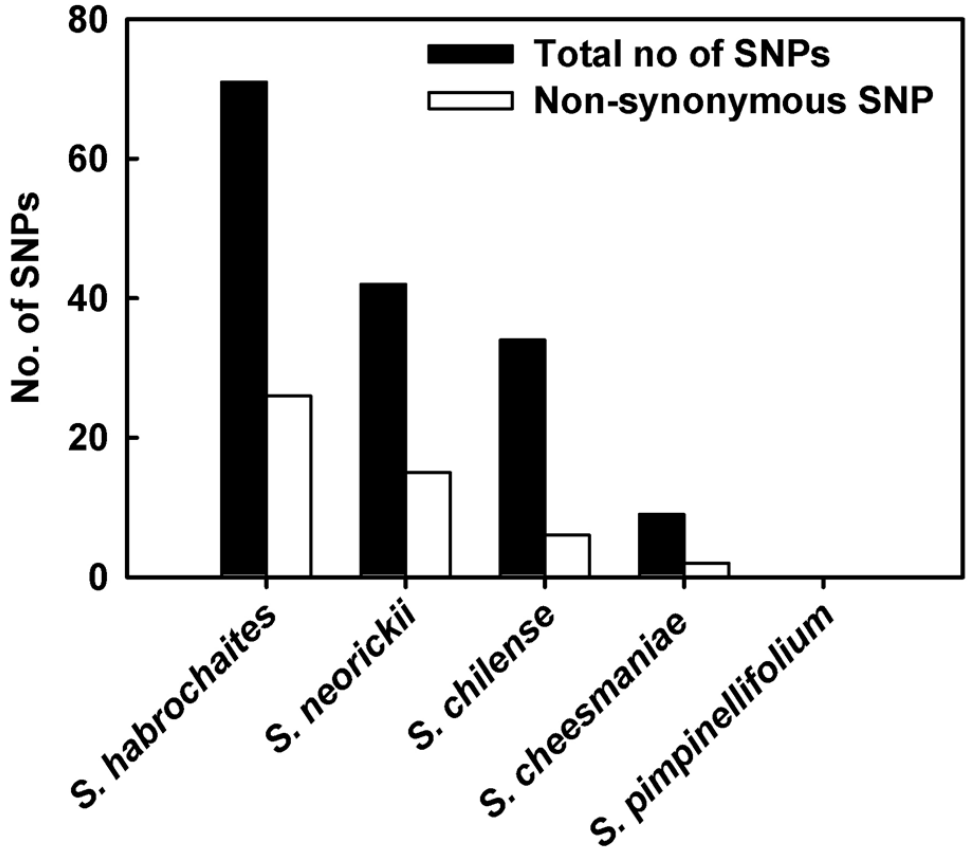

Figure 62. Comparisons of observed SNPs and non-synonymous SNPs in various wild relatives of tomato. Black histogram and white histogram represents total number of SNP and non-synonymous SNPs respectively. Sequencing data from four phytochrome genes (*PHYA, PHYB1, PHYE* and *PHYF*) was used to construct the histogram. The X-axis represents a wild tomato species and Y axis represents number of SNPs.

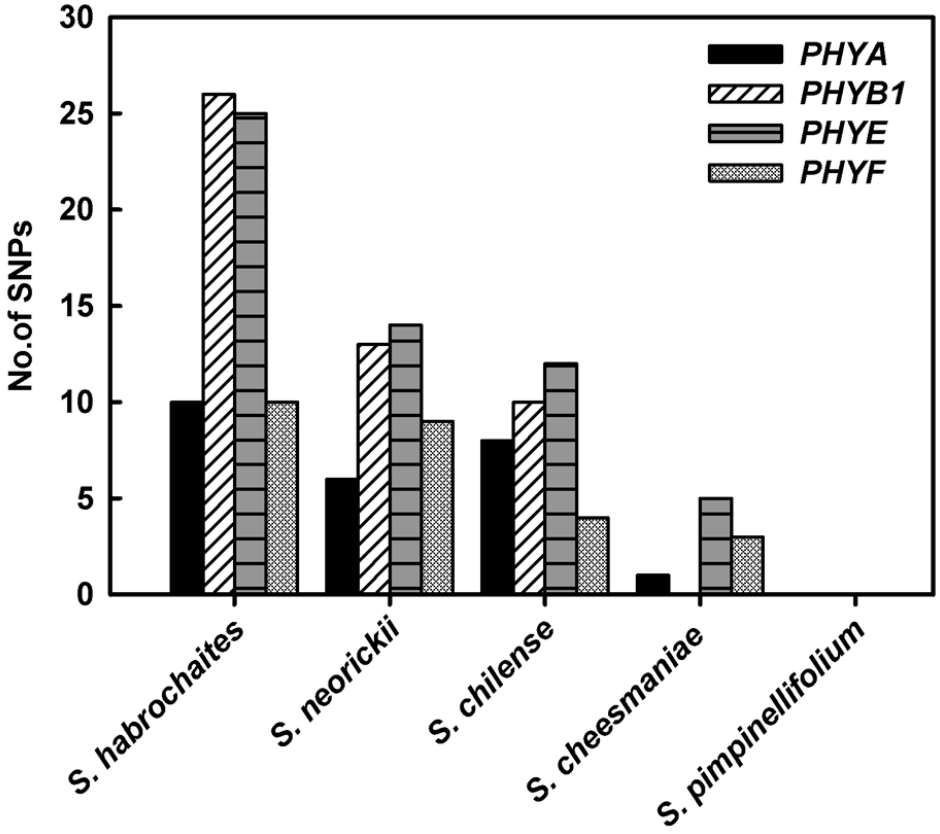

Figure 63. Number of SNPs detected in various wild tomato species for 4 *Phytochrome* genes. Sequencing data from five wild relatives of tomato (*S. habrochaites, S. pimpinellifolium, S. galapagense, S. neorickii, and S. chilense*) was used to construct the histogram. The X-axis represents a wild tomato species and Y-axis represents number of SNPs. Each bar represents number of SNPs detected for each *Phytochrome* gene.

4.4.2 Amino Acid Polymorphisms in Phytochrome in Tomato Wild Relatives

The software PARSESNP (http://www.proweb.org/parsesnp/) was used to find out the amino acid polymorphism in wild tomato species by evaluating the PSSM score and SIFT value. All the four phytochrome genes used in the study showed several amino acid changes (Table. XVI). PARSESNP analysis showed that the major phytochrome molecule like phytochrome A and phytochrome B1 which are considered to have major roles in plant survival harboured relatively few amino acid changes compared to other two phytochrome species that is phytochrome E and F (Table. XVI). Most of the amino acid changes observed for all phytochrome genes showed an insignificant PSSM or SIFT score, with few exceptions (Table. XVI). Among all five wild tomato species, *S. habrochaites and S. neorickii* which are considered as distant relatives of cultivated tomato bore several SNPs compared to other three species (Table. XVI). Most of the amino acid polymorphisms were located outside the functionally important GAF and PHY domain and a large number of polymorphisms were found in the C-terminal end of most of the phytochromes with the exception of Phytochrome F (Fig. 64).

4.4.3 Neutrality and Nucleotide Diversity

To examine the fit of nucleotide polymorphism data to the neutral equilibrium model, each phytochrome gene was subjected to Tajima's D test (Tajima 1989). No significant Tajima's D value was observed at any locus indicating a neutral evolution at this gene locus. D_{total} (entire sequence), D_{nonsyn} (nonsynonymous sites), D_{syn} (synonymous sites), and Pi (nucleotide diversity were calculated for each *phytochrome* gene. It was found that none of the gene showed a significant D value. The nucleotide diversity values of all phytochrome genes were found to be low. Since all the four phytochrome genes analysed by Tajima D test showed a

Table XVI. Sequence validation of polymorphisms identified in various *phytochrome* genes of tomato. The application PARSESNP was used to interpret the amino acid polymorphism, PSSM score and SIFT values of the polymorphisms. Sequencing data from five wild relatives of tomato (*S. habrochaites, S. pimpinellifolium*, *S. galapagense, S. neorickii, and S. chilense)* was used for the analysis. A non-synonymous SNP is predicted to be damaging to the encoded protein if the SIFT score is<0.05 (bold) or the PARSESNP score is>10 (bold).

Amino acid change	Gene	Species	PSSM difference	SIFT score
K78R	*Phytochrome A*	*S. habrochaites*	5.0	0.43
F231S	*Phytochrome A*	*S. habrochaites*	6.5	0.19
E590D	*Phytochrome A*	*S. habrochaites*		
D657V	*Phytochrome A*	*S. habrochaites*	10.6	0.06
L680M	*Phytochrome A*	*S. habrochaites*		
A139T	*Phytochrome A*	*S. neorickii*		
N162S	*Phytochrome A*	*S. neorickii*	4.9	0.58
E590D	*Phytochrome A*	*S. neorickii*		
E590D	*Phytochrome A*	*S. chilense*		
R703K	*Phytochrome B1*	*S. habrochaites*		
V710L	*Phytochrome B1*	*S. habrochaites*		
A1051V	*Phytochrome B1*	*S. habrochaites*		
F593S	*Phytochrome B1*	*S. chilense*		
L49M	*Phytochrome E*	*S. habrochaites*	-0.5	0.10
L79P	*Phytochrome E*	*S. habrochaites*		
Y127F	*Phytochrome E*	*S. habrochaites*	-2.2	0.08
N148T	*Phytochrome E*	*S. habrochaites*		
I358V	*Phytochrome E*	*S. habrochaites*	-9.0	1.00
R845T	*Phytochrome E*	*S. habrochaites*		
E847G	*Phytochrome E*	*S. habrochaites*		
I877V	*Phytochrome E*	*S. habrochaites*		
W893S	*Phytochrome E*	*S. habrochaites*		
V899A	*Phytochrome E*	*S. habrochaites*	-13.3	1.00
L988I	*Phytochrome E*	*S. habrochaites*	1.5	0.16

.....Continuing on next page

Table XVI. (Continue).

Amino acid change	Gene	Species	PSSM difference	SIFT score
A1089S	*Phytochrome E*	*S. habrochaites*	-12.7	
G1105E	*Phytochrome E*	*S. habrochaites*	-10.3	1.00
E1106V	*Phytochrome E*	*S. habrochaites*	-1.5	0.39
Y127F	*Phytochrome E*	*S. chilense*		
I358V	*Phytochrome E*	*S. chilense*	-2.2	0.08
I358V	*Phytochrome E*	*S. cheesmanii*	-9.0	1.00
R380W	*Phytochrome E*	*S. cheesmanii*	25.7	
L79P	*Phytochrome E*	*S. neorickii*		
N148T	*Phytochrome E*	*S. neorickii*		
I358V	*Phytochrome E*	*S. neorickii*	-9.0	1.00
R845T	*Phytochrome E*	*S. neorickii*		
D860N	*Phytochrome E*	*S. neorickii*		
V899A	*Phytochrome E*	*S. neorickii*	-13.3	1.00
N1087S	*Phytochrome E*	*S. neorickii*	-3.5	0.41
E105D	*Phytochrome F*	*S. habrochaites*	5.2	0.22
H188D	*Phytochrome F*	*S. habrochaites*	-4.1	0.61
V428I	*Phytochrome F*	*S. habrochaites*		
K934E	*Phytochrome F*	*S. habrochaites*		
A91E	*Phytochrome F*	*S. neorickii*	-16.1	1.00
S151N	*Phytochrome F*	*S. neorickii*	5.0	0.18
L178V	*Phytochrome F*	*S. neorickii*	5.0	0.21
H188D	*Phytochrome F*	*S. neorickii*	-4.1	0.61
K934E	*Phytochrome F*	*S. neorickii*		
K934E	*Phytochrome F*	*S. cheesmanii*		
A91E	*Phytochrome F*	*S. chilense*	-16.1	
H188D	*Phytochrome F*	*S. chilense*	-4.1	

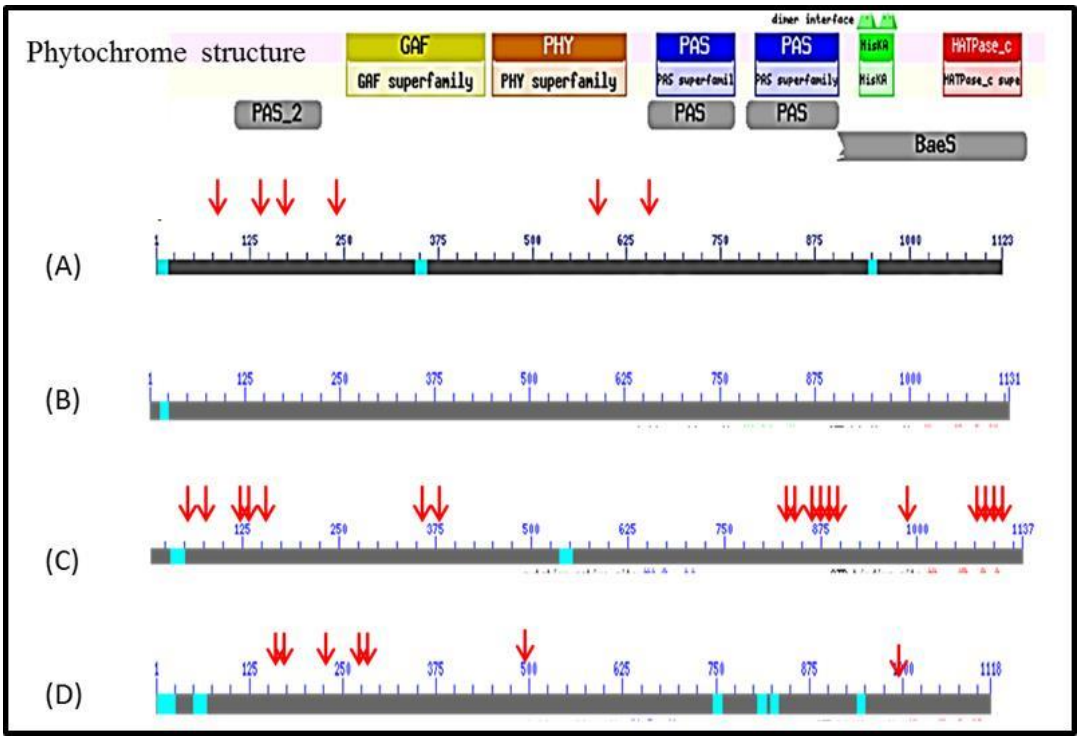

Figure 64. Distribution of amino acid polymorphisms in various domains of phytochromes in tomato. Upper panel shows functional domain scheme of tomato phytochrome. (A) (B) (C) and (D) represent schematic diagrams of PHYA, PHYB1, PHYE and PHYF respectively. Red arrows indicating each amino acid polymorphism. Sequencing data from five wild relatives of tomato (*S. habrochaites, S. pimpinellifolium, S. galapagense, S. neorickii, and S. chilense)* was used to construct the diagram.

negative D value, it indicates a purifying selection for all the four phytochrome genes (Table XVII).

TableXVII. Tajima's D and nucleotide diversity (pi) are shown. Tajima's D and was estimated for the entire (Dtotal) sequence as well as nonsynonymous sites (Dnonsyn) and synonymous sites (Dsyn)) separately. Nucleotide diversity was also estimated for the coding region. None of the genes showed a significant Tajima D value.

Locus	Tajima D(total)	Tajima's D(Syn)	Tajima's D(NonSyn)	Tajima's D (NonSyn/Syn) ratio	Nucleotide diversity: Pi	Type of evolution
PHYA	-0.7597	-0.6120	-0.8841	1.4447	0.0010	Neutral
PHYB1	-0.8354	-0.7713	-1.0199	1.3222	0.0013	Neutral
PHYE	-0.6986	-0.6841	-0.6841	1.0000	0.0025	Neutral
PHYF	-0.6387	0.5946	-1.1571	-1.9464	0.0005	Neutral

4.4.4 Phylogenetic Tree Building

Phylogenetic trees were constructed using nucleotide sequencing data. The dendrograms made from the sequence data followed a topology in which the green-fruited wild tomato used for the study are located at an ancestral position while the coloured fruits in a more closely related position (Fig. 65).

4.4.5 Nucleotide Base Change Analysis

Substitution Patterns observed in various phytochrome genes were evaluated. Frequency of the different types of substitutions is expressed as a percentage of the average substitution rate. As there exists a universal bias towards transition (Ts) over transversion (Tv) in eukaryotes, the type of base substitution pattern in various phytochrome genes was examined. It was found that all phytochromes, except *phytochrome B1* appear to hold the rules of

universal bias over transition quite well (Fig. 66). The point substitution analysis showed that the transition type T-C is the most frequent type of substitution in most of the phytochrome genes. *Phytochrome A* showed 33% T-C substitution whereas *phytochrome B1*, *phytochrome E* and *phytochrome F* showed value of 20%, 12% and 15% respectively. Next prevalent substitution was A-G (17% in *phytochrome A*, 18% in *phytochrome E* and 19% in *phytochrome F*) (Fig. 67). It is interesting to note that *phytochrome B1* showed higher frequencies of rare transversional substitutions like A-T (20 %) and G-T (15%) (Fig. 67).

4.4.6 Differential Response to Light

In view of unavailability of seeds for two wild relatives (*S. neorickii* and *S.chilense*), which are difficult to multiply, the phenotype was analysed only for 3 species, where sufficient seeds were available. To determine whether polymorphisms in phytochrome genes could contribute to variation in light response of a given species, the light response of three wild tomato (*S. habrochaites, S. cheesmanii*, *S. pimpinellifolium*) was examined under different spectral wavelength (WL, FR and R). Compared to tomato (*S.lycopersicum*), there was not much significant difference in phenotype of seedlings under different light condition. One notable exception was *S. habrochaites*, where seedlings under FR light were elongated but surprisingly the apical hooks were not closed and the cotyledons were fully expanded. On the other hand tomato plants grown in FR exhibit less inhibition of hypocotyl growth than *S.habrochaites* (Figs. 68, 69).

4.5 Light Regulation of Root Development

In this study, we found that one of the distinct effects of SNP variation in EC-528362 in *phytochrome A* gene was on phenotype of root particularly under FR light. In view of this we used excision induced lateral root formation as an assay to examine influence of light on this response.

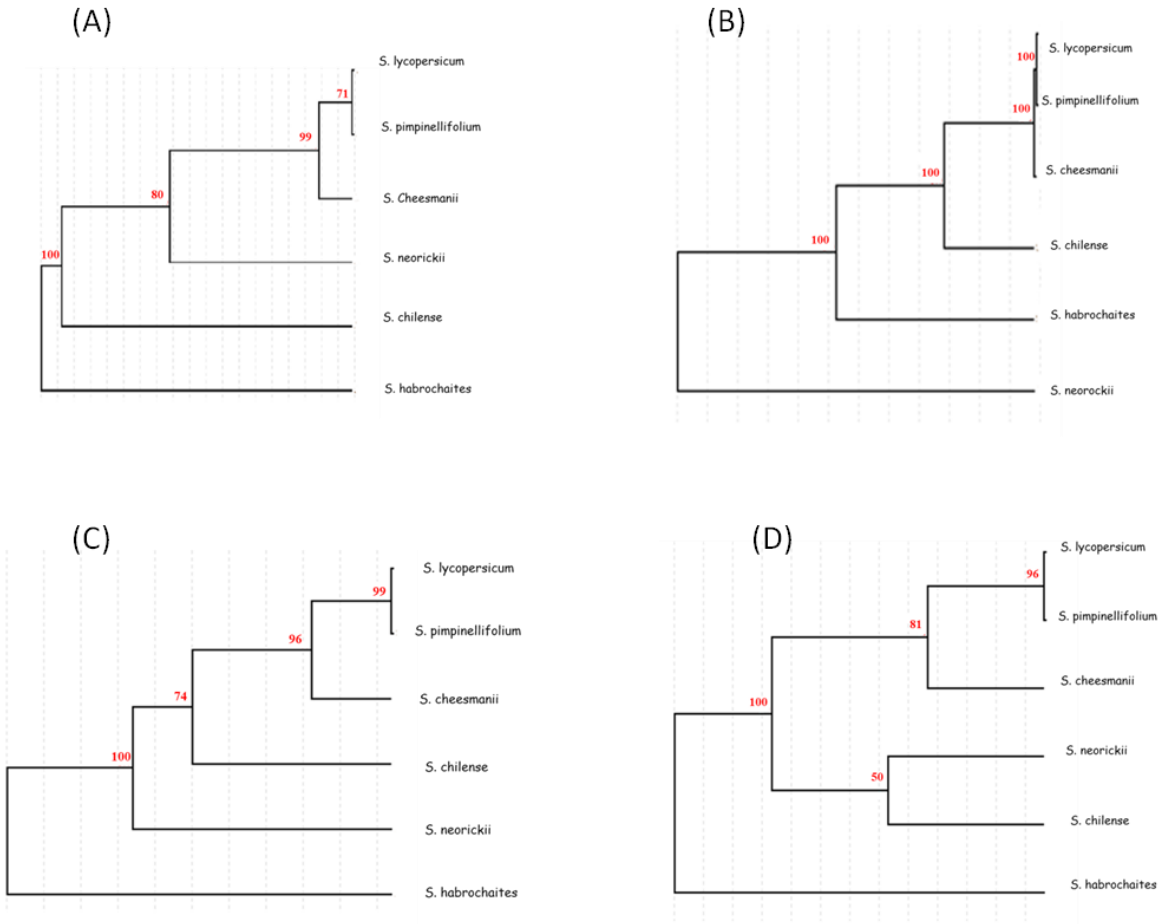

Figure 65. Dendograms, based on nucleotide sequences of four tomato **p**hytochromes, shows the evolutionary distance among phytochrome genes of different wild tomato species. S.lycopersicum was used as an out-group. Percentage bootstrap values are shown above branches. The tree is generated using GeneBee - Molecular Biology Server (http:// www.genebee.msu.su/genebee.html) using neighbor-joining method. The branch length is proportional to the amount of inferred evolutionary change. (A) (B) (C) and (D) represent dendograms of *phytochrome A*, *B1*, *E* and *F* respectively. *S. Cheesmanii* and *S.pimpinellifolium* are closely related to *S.esculentum* invariably in all *phytochrome* genes analysed.

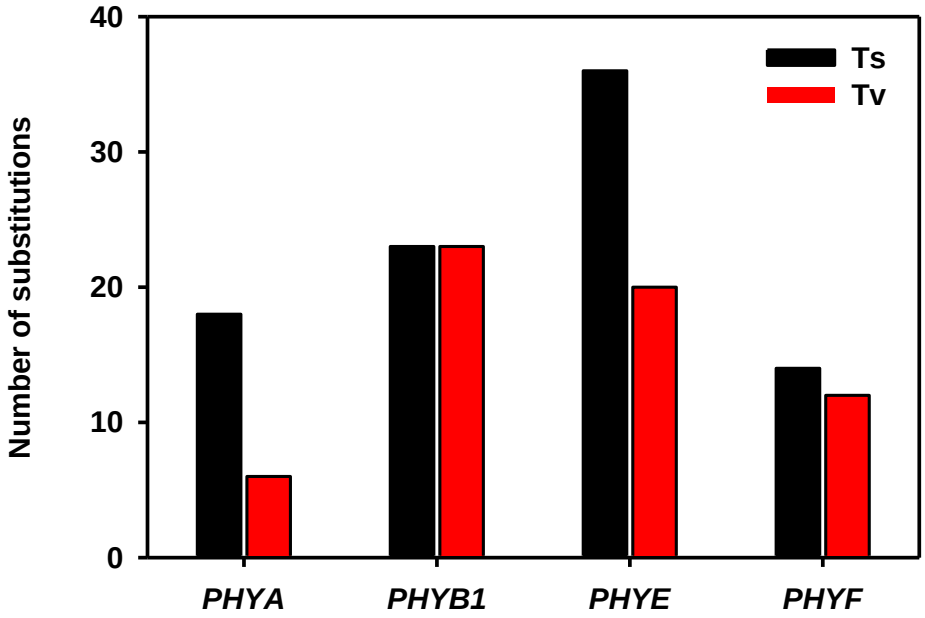

Figure 66. Substitution pattern in 4 different phytochrome genes. The X-axis represents a phytochrome gene and Y-axis represents number of transition or transversion.

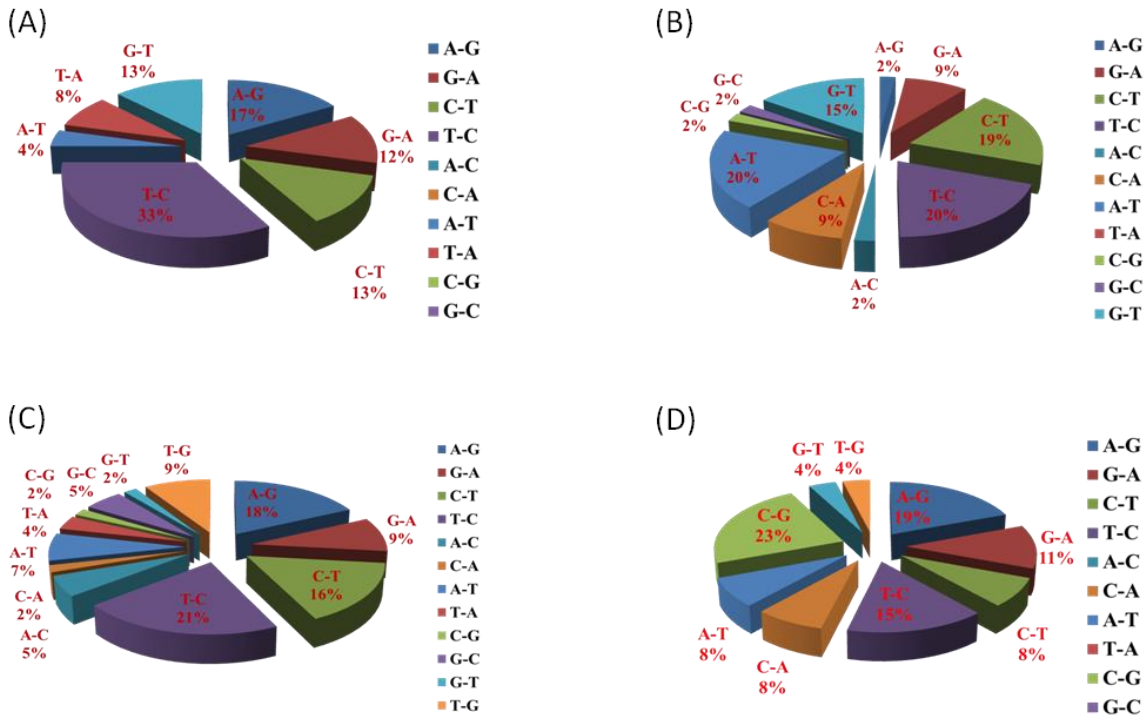

Figure 67. Substitution patterns observed in 4 tomatoes phytochrome genes .Data from five tomato species are included. Frequency of the different types of substitutions is expressed as a percentage of the average substitution rate in the given pie diagram. (A) (B) (C) and (D) represent pie diagrams for *phytochrome A, B1, E* and *F* respectively.

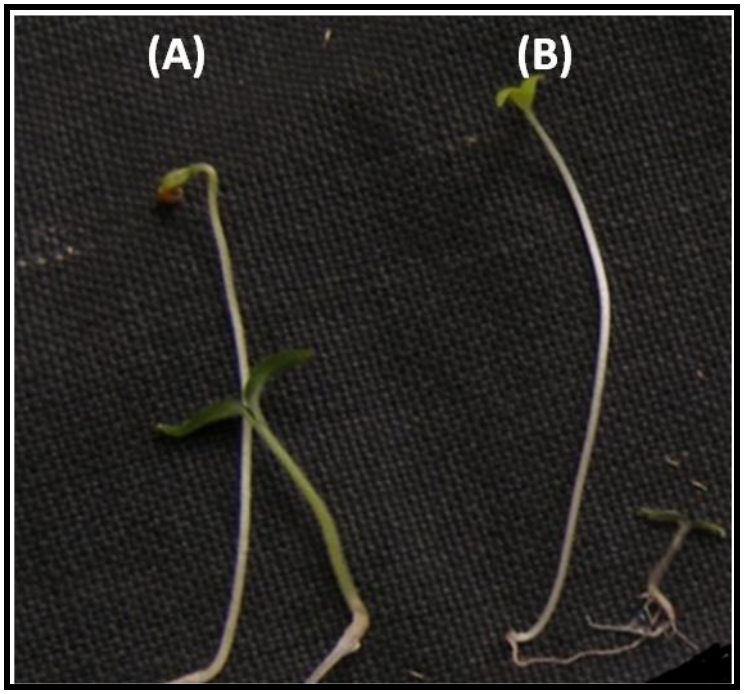

Figure 68. The phenotype of tomato seedlings grown for 7 days after emergence in D and continuous broad-band FR of 5 µmol m^{-2} s^{-1}. The seedling on the left is grown under FR light and that on the right is under WL. (A) *S.lycopersicum* and (B) *S.habrochaites.* Note the increased hypocotyl length of *S.habrochaites* under far red light.

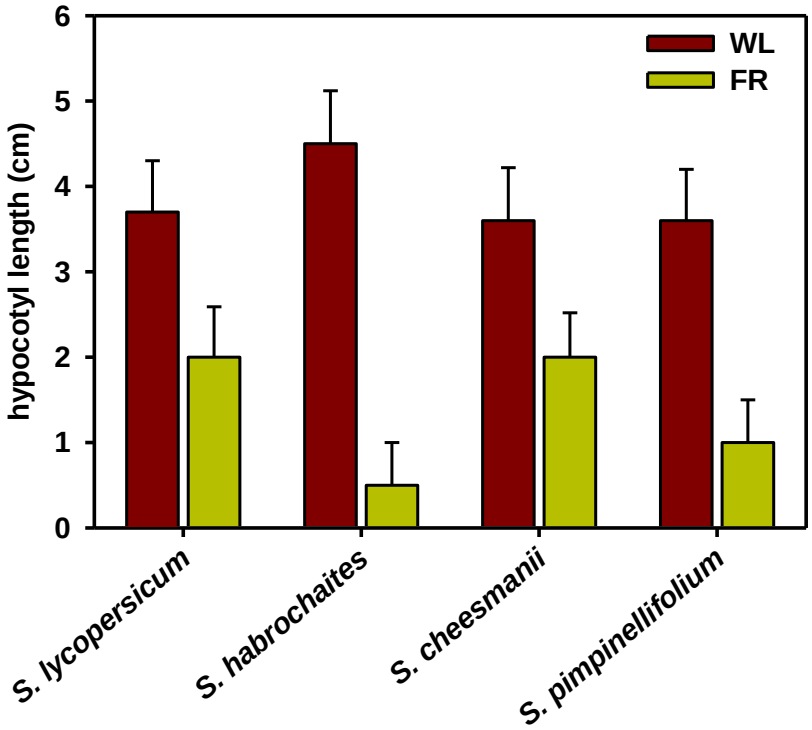

Figure 69. Hypocotyl length of tomato and *wild tomato seedlings* (*S. habrochaites, S. pimpinellifolium*, and *S. galapagense)* after 7 d of continuous FR of 5 µmol m^{-2} s^{-1}. The X-axis represents a tomato species and Y-axis represents hypocotyl length in cm observed in white and FR light condition.

4.5.1 Effect of Excision of Root Tips on Lateral Root Formation (LRF)

To test the hypothesis that lateral roots are induced by excision of root tips, the root tip were excised at different time intervals. About 1cm from distal end of root was excised from seedlings which were grown on vertical agar plates. The tip excision enhanced lateral root formation in the seedlings compared to the control seedlings, where roots were not excised. (Figs. 70, 71). Additionally, the increased lateral root formation after excision of root tip was not linked to increases in hypocotyl or leaf growth. The observation of enhanced lateral root formation is consistent with previous reports of lateral root stimulation by root-tip excision in pea seedlings (Wightman and Thimann, 1980) and in Arabidopsis (Reed *et al.*, 1998).

4.5.2 Role of Developmental Stages on Excision Induced LRF

In a normal tomato seedling grown under WL, the lateral roots are normally initiated only after 5 DAG. This time point could be related to the increased accumulation of auxin in roots of 5 to 7 day old seedlings. To examine the induction of a signal, induced by excision, we performed an experiment in which excision of root tip was carried out at an early stage of root development beginning from 2 days of radicle emergence (2 DAG). The excision of root tips of 2- day old seedlings stimulated lateral root formation compared to the control seedlings where root tips were not excised (Figs. 72, 73). Considering above observations we compared the extent of lateral root formation after excising root tips at different time intervals after emergence of radicle. Interestingly maximum number of lateral root formation was observed when the root tip was excised at a very early stage of development i.e., 2 DAG than when root tip was removed at 4 DAG (Figs 72, 73).

Figure 70. Effect of excision of root tips on lateral roots formation in tomato Seedlings were grown on agar under white light for 4 days then root tip was excised from the seedlings. Seedlings were allowed to grow for an additional 3 days, and the total number of lateral roots was counted. (A) 7 days old control (for which excision was not done) and (B) 7 days old tomato seedlings for which root tip excision was done at 4 days after germination. Note an enhanced lateral root formation in (B).

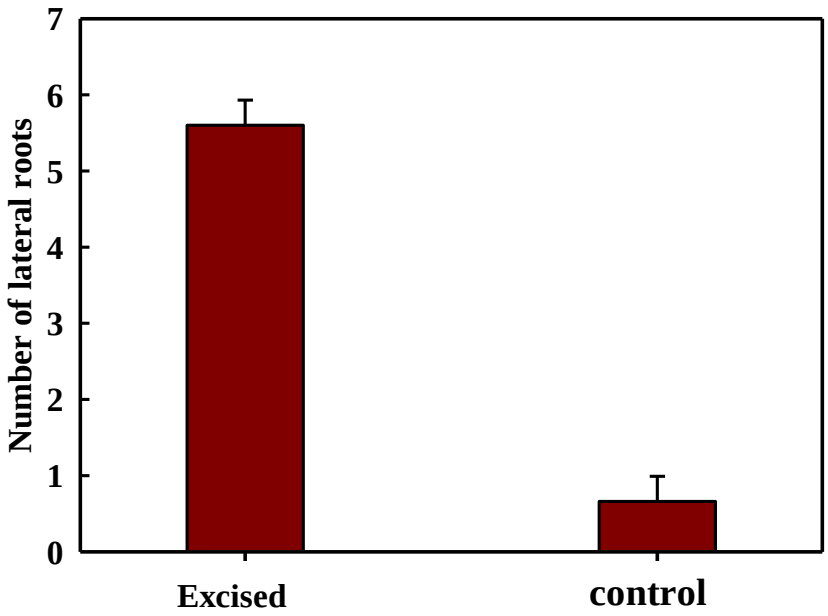

Figure 71. The number of emerged lateral roots at 7 days after germination: Seedlings were grown on 1% (w/v) agar under white light for 4 days then root tip was excised from the seedlings. Seedlings were allowed to grow for an additional 3 days, and the total number of lateral roots were counted. The number of lateral roots was counted for 5 seedlings per treatment.

Figure 72. Comparison of lateral root emerged after root tip excision at different time point of development. Seedlings were grown on agar under white light and, root tips were excised on second day of germination or fourth day of germination and, seedlings were allowed to grow for an additional 5 days or 3 days, respectively. The total number of lateral roots was manually counted. (A) Root tips removed at 2 DAG, (B) root tips removed at 4 DAG, and (C) control for which root tips were not removed.

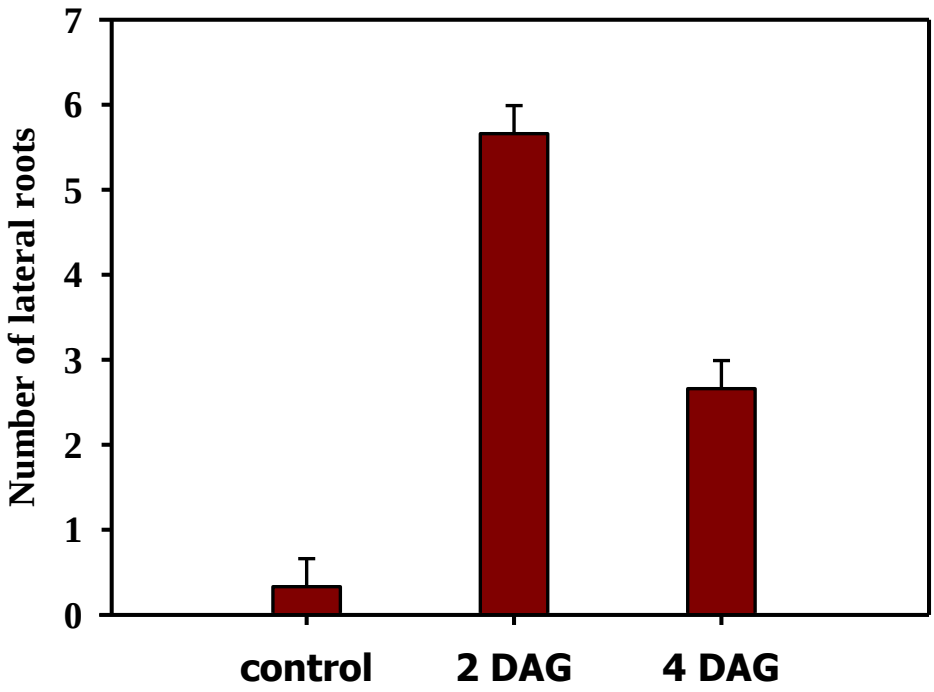

Figure 73. Comparison of lateral root at various time point of development. Seedlings were grown on 1% (w/v) agar under white light and, root tips were excised on second day of germination or fourth day of germination and, seedlings were allowed to grow for an additional 5 days or 3 days, respectively. The total number of lateral roots were manually counted. The number of lateral roots were counted for 5 seedlings per treatment.

4.5.3 Role of Polar Auxin Transport (PAT) on Excision Induced LRF

Several studies have suggested that auxin is required for the emergence of lateral roots (Katekar and Geissler, 1980; Muday and Haworth, 1994), as it establishes a population of rapidly dividing initial cells (Laskowski *et al.,* 1995). Developing lateral root primordia are reported to accumulate auxin via polar auxin transport (Reed *et al.,* 1998). Polar auxin transport inhibitors are known to block lateral root emergence (Casimiro *et al.,* 2001). To investigate role of polar auxin transport in excision induced lateral root development, after excision of root tip at 2DAG agar plates were over layered with (0.5µM TIBA), an inhibitor of auxin transport. Intact seedlings treated with 0.5 µM TIBA were used as controls. These excised seedlings along with controls were grown for 3 days and the number of lateral roots emerging was visually scored. The results showed that upon TIBA addition the number of emerging lateral roots were higher, indicating the partial participation of PAT in the process (Figs. 74, 75).

4.5.4 Role of Shoot-derived Signal on Excision Induced LRF

Previous reports suggest that LRP (Lateral root primordial) emergence is dependent on shoot-derived Auxin. To check the role of shoot derived signal on excision induced lateral root formation, differential excision of shoot tissue was carried out at 2 DAG. If the shoot derived auxin regulates the emergence of lateral roots, then the removal of shoot should abolish this developmental process. We performed two types of shoot excision. In the first case, entire shoot, which includes the hypocotyl and cotyledon along with the root tip, was removed. In this experiment we compared an intact seedling, a root cap excised seedling and a seedling without shoot. In the second case, we excised only cotyledons along with the root tips. So, seedlings consist of hypocotyl and root. Similar to first case, here two treatments were compared namely intact seedlings, seedlings without cotyledon and root tip and seedlings

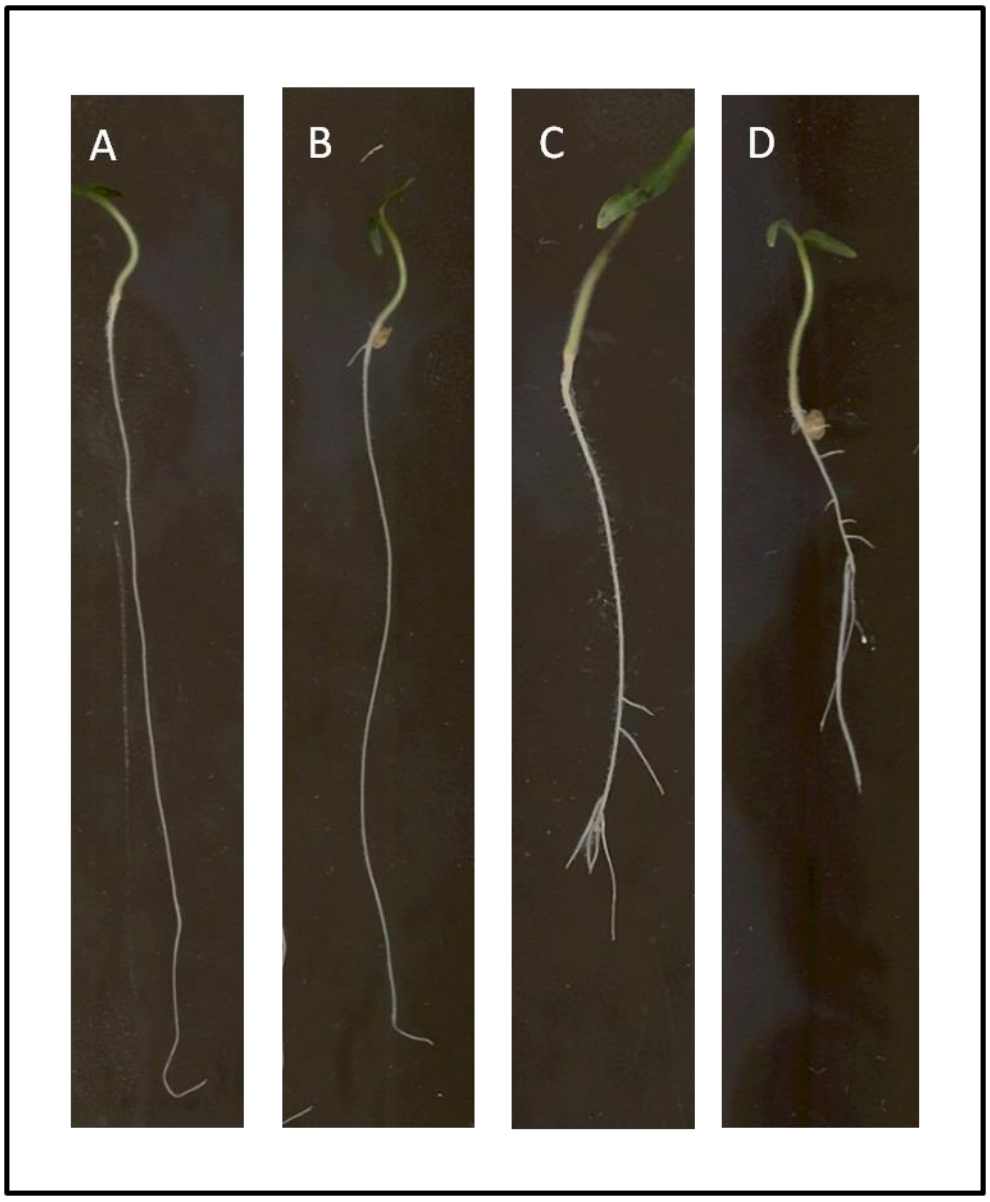

Figure 74. Comparison of lateral root development with or without application 5 µM TIBA. Seedlings were grown on agar under white light, and root tips were excised on second day of germination. A set of seedlings were treated with 5 µM TIBA after excision and, the treated seedlings along with control seedlings were allowed to grow for an additional 5 days. The total number of lateral roots were manually counted. (A) Control seedling, (B) same as A with TIBA added, (C) seedlings with root tip excised, and (D) same as C with TIBA added. Note an enhanced lateral root formation in D.

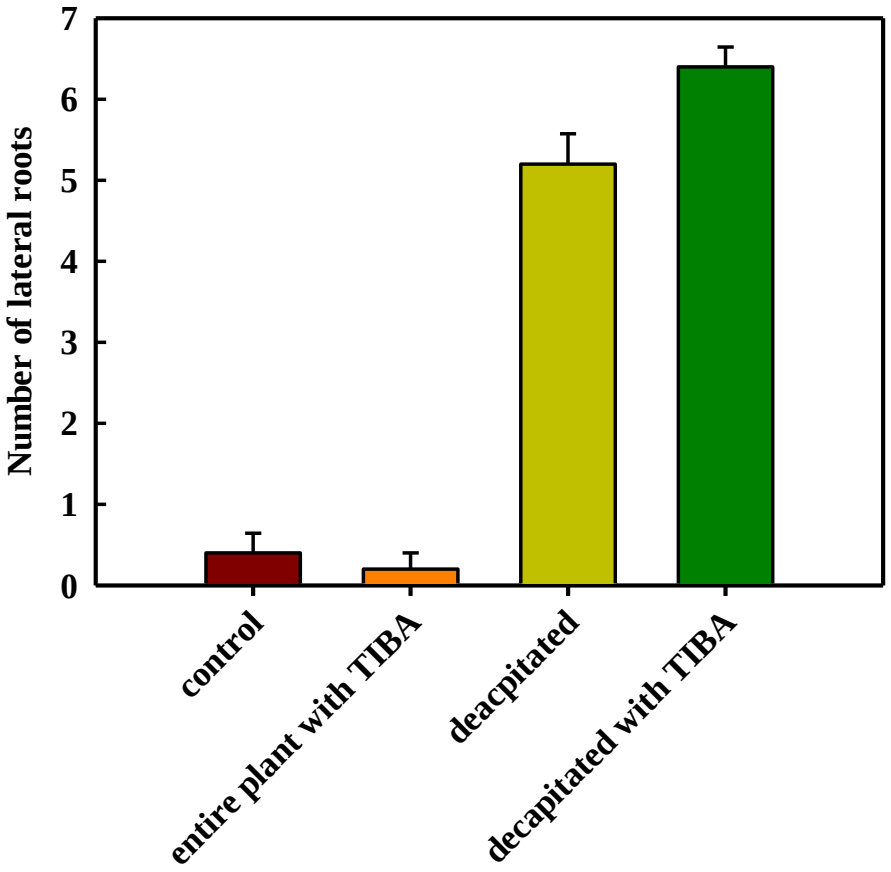

Figure 75. Comparison of lateral root development with or without application 5 µM TIBA: Seedlings were grown on agar under white light and root tips were excised on second day of germination. The seedlings were treated with 5 µM TIBA after excision and the treated seedlings along with control seedlings were allowed to grow for an additional 5 days. The total number of lateral roots were manually counted. The number of lateral roots were counted for 5 seedlings per treatment.

without root tip. The experimental seedlings were grown for a further 3 days and the lateral root formation was recorded. Examination of seedlings showed that root excision on 2DAG led to stimulation of lateral root formation. The excision of cotyledon at 2DAG has no effect on LR F. However the excision of cotyledon along with root tips at 2DAG reduced the number of lateral root formation indicating some influence of cotyledon (Figs. 76, 77).

4.5.5 Role of Ethylene on Excision Induced LRF

Ethylene has an inhibitory role in lateral root formation and elevated ethylene levels inhibit lateral root formation (Negi *et al.*, 2010). To examine the effect of ethylene, we treated seedlings with ACC, a precursor of ethylene. The lateral root formations in excised and intact seedlings were examined in the presence and absence of 20 µM ACC. Figs.78 and 79 show that excision induced lateral root formation was not influenced by ethylene. In the control seedlings ethylene treatment did not show any significant inhibition of lateral root formation. In contrast to this, decapitated seedlings showed more enhanced lateral root formation in presence of ACC (Figs. 78, 79).

4.5.6 Role of Light on Excision Induced LRF

Bhalerao *et al.* (2002) reported that LRF is profoundly affected by light, as light controls transport of auxin to the root. In Arabidopsis, it has been shown that seedlings grown in the dark initiate few lateral roots compared to the seedlings grown in light (Bhalerao *et al.*, 2002). To examine the role of light in excision induced LRF, tomato seedlings were grown under WL and dark. Tomato seedlings germinated in darkness were transferred to different wavelength of light on 2DAG and root excision was performed. The excised seedlings along with control seedlings were grown for 5 more days and in 7 day old seedling the number of lateral root emerging were manually scored. Surprisingly, LRF was observed in the excised seedlings irrespective of the exposure of different light spectra. However LRF formation was

higher in seedlings grown in WL, compared to D. In contrast to seedlings exposed to R and FR light showed intermediate effect indicating that in addition to phytochrome other photoreceptors may be involved (Figs. 80, 81). In future, we would use this effect of light to examine the influence of specific SNPs on mutations on function of phytochrome in regulating this response.

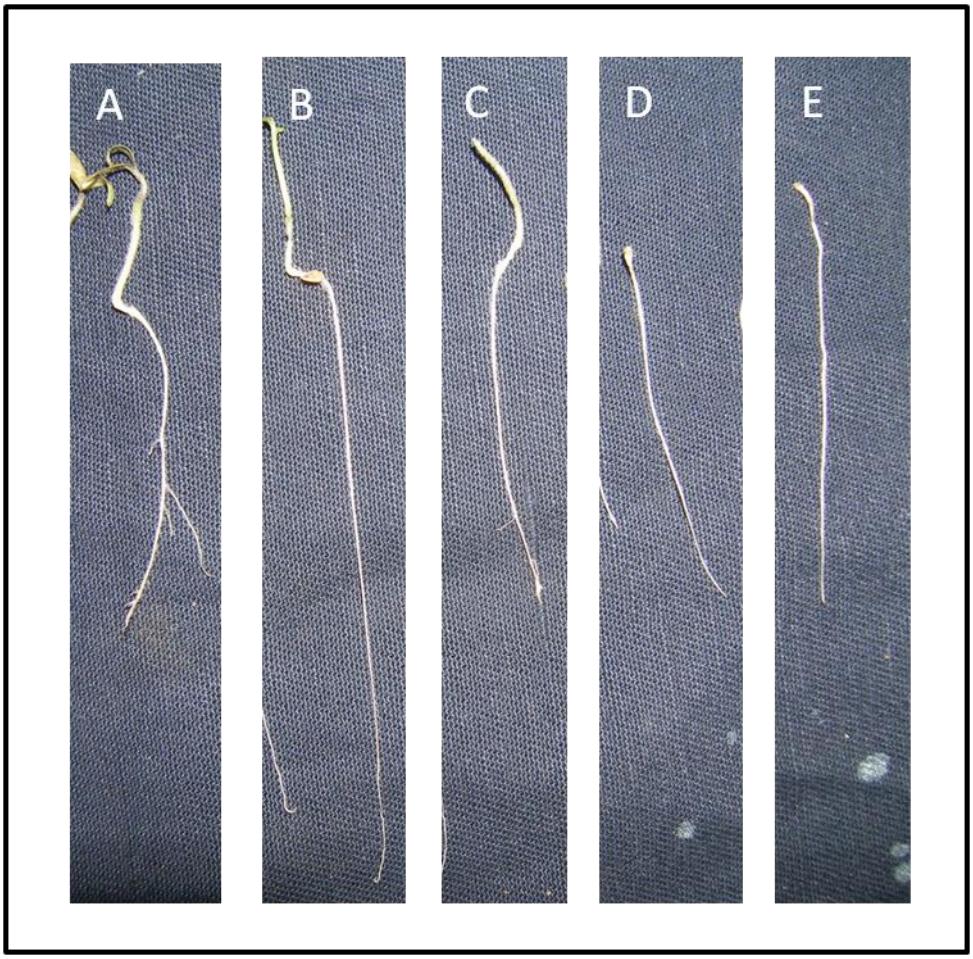

Figure 76. Effect of shoot derived auxin on lateral root formation. Seedlings were grown on agar under white light and root tips and either only the cotyledons or all of the aerial tissues were excised from the seedlings on second day of germination. Root tips excision also performed along with it. Seedlings were allowed to grow for an additional 5 days. The total number of lateral roots was counted manually. (A) Control seedling, (B) cotyledon is excised, (C) both cotyledon and root tip are excised) aerial tissue is excised, and (E) both aerial tissue and root tip were excised.

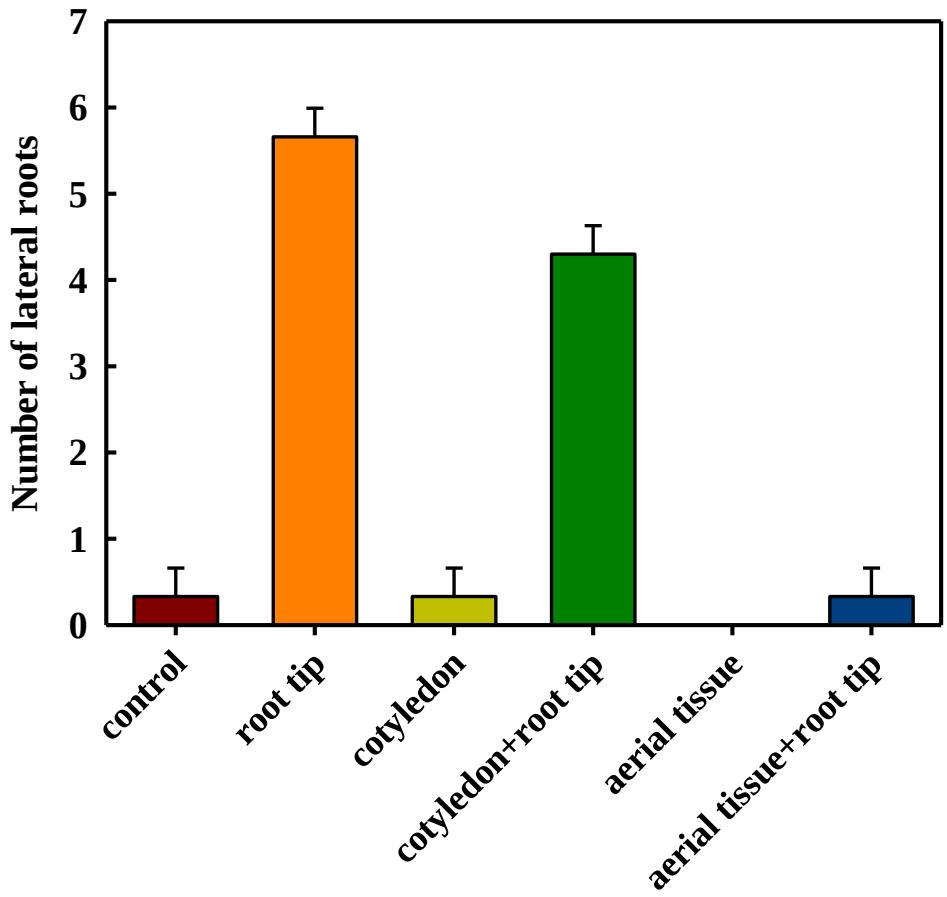

Figure 77. Effect of shoot derived auxin on lateral root formation. Seedlings were grown on agar under white light and root tips and either only the cotyledons or all of the aerial tissues were excised from the seedlings on second day of germination. Root tips excision also performed along with it. Seedlings were allowed to grow for an additional 5 days. The total number of lateral roots were manually counted. The number of lateral roots were counted for 5 seedlings per treatment.

Figure 78. Comparison of lateral root development with or without application of application 20 µM ACC. Seedlings were grown on agar under white light and root tips were excised on second day of germination. The seedlings were treated with 20 µM ACC after excision and the treated seedlings along with control seedlings were allowed to grow for an additional 5 days. The total number of lateral roots was counted manually. (A) control seedling, (B) same as A with 20 µM ACC added, (C) seedlings with root tip excised, and (D) same as C with 20 µM ACC added. Note an enhanced lateral root formation in D.

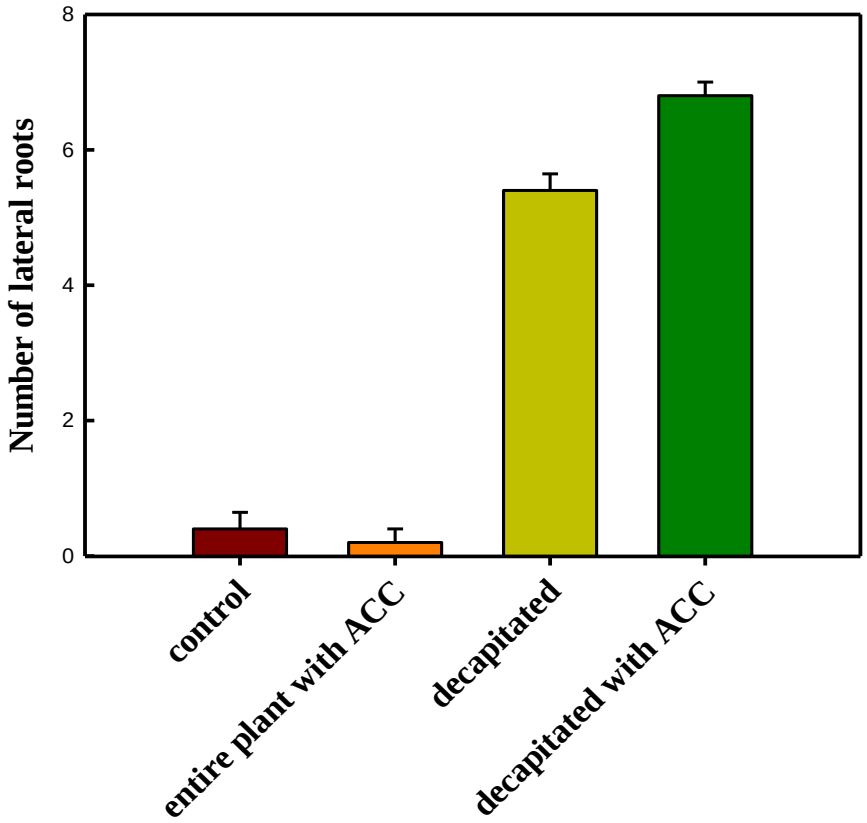

Figure 79. Comparison of lateral root development with or without application 20 µM ACC: Seedlings were grown on 1% agar under white light and root tips were excised on second day of germination. The seedlings were treated with 20 µM ACC after excision and the treated seedlings along with control seedlings were allowed to grow for an additional 5 days. The total number of lateral roots were manually counted. The number of lateral roots were counted for 5 seedlings per treatment.

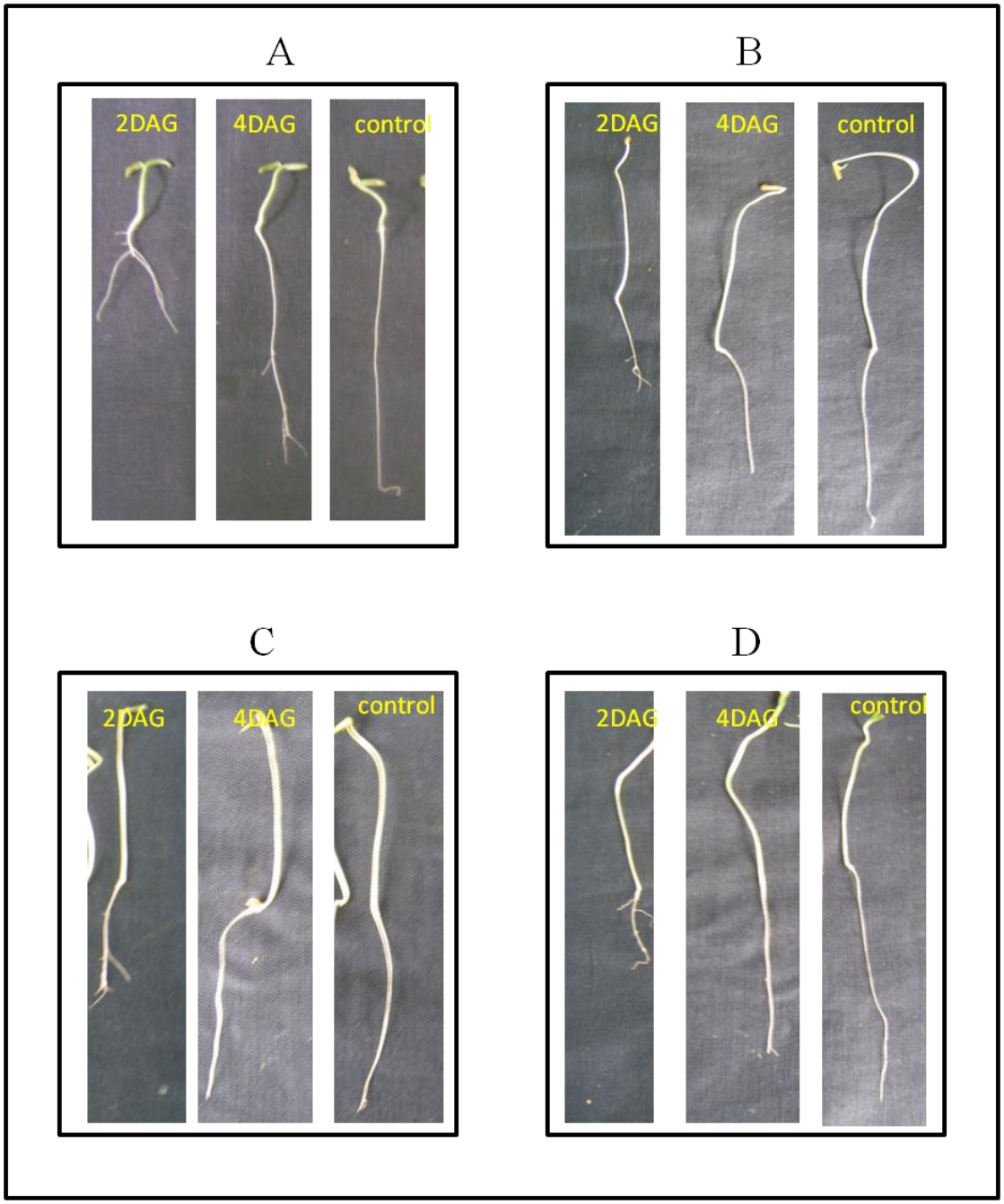

Figure 80. Effect of light on lateral root formation. Seedlings were grown on agar under white light, dark, red, and far red light and, root tips were excised on second day of germination or fourth day of germination and, seedlings were allowed to grow for an additional 5 days or 3 days, respectively. Lateral root formation was assessed by manually counting the number of lateral roots emerged. (A) Seedlings grown under WL, (B) dark, (C) red, and (D) far red.

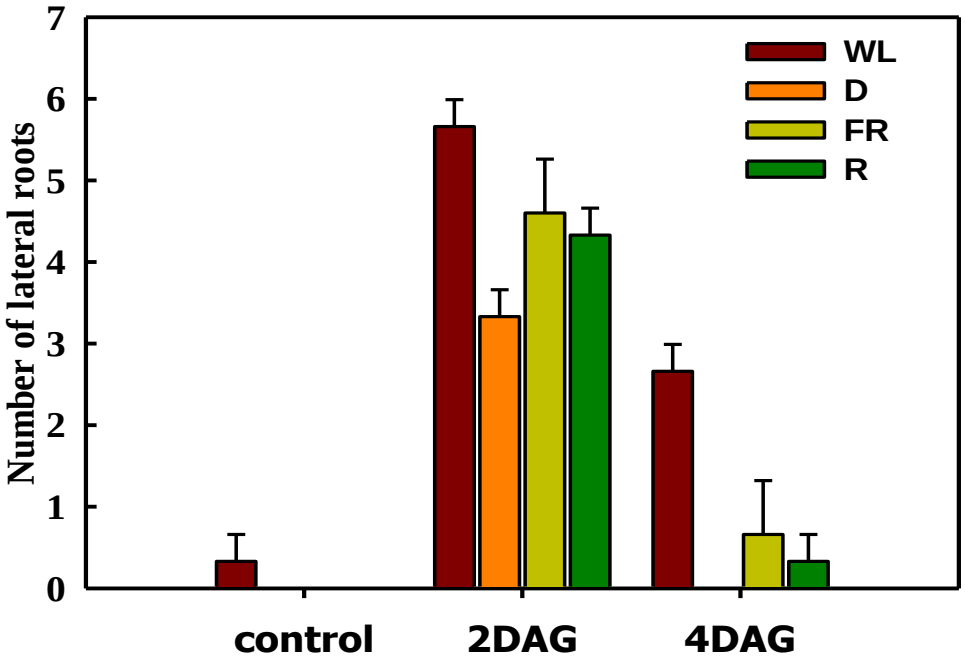

Figure 81. Effect of light on lateral root formation. Seedlings were grown on agar under white light, dark, red, and far red light and, root tips were excised on second day of germination or fourth day of germination and, seedlings were allowed to grow for an additional 5 days or 3 days, respectively. The total number of lateral roots were manually counted. The number of lateral roots were counted for 5 seedlings per treatment.

5. DISCUSSION

5.1 PCR Optimization of *Phytochrome* Genes for TILLING

TILLING is a reverse genetic tool, which allows identification of mutations in a targeted gene. The genomic region to be assessed for mutation is amplified by PCR along with wild type genomic DNA, the heteroduplex present in the DNA is detected by mismatch cleavage by CEL-1 nuclease. The cleavage of PCR product indicates the presence of single nucleotide or small insertion/deletion mutation. As TILLING requires a highly specific and discrete PCR product for CELI digestion, optimization of PCR is one of the most important step for optimal TILLING reaction to identify mutations. Since TILLING method employs stringent parameters to eliminate false positive, the usage of a set of stringent primers with high Tm and high GC content makes the optimization task a major bottleneck.

Considering that PCR optimization is a major bottleneck for TILLING, we optimized PCR for phytochrome genes for TILLING. In most large scale TILLING project, such as maize or Arabidopsis, optimization of PCR is a major issue. The problem assumes a greater significance as these projects also process request from other researchers. Therefore, all major TILLING projects follow stringent parameter for primer design such as high Tm and high GC content. The primers that do not amplify the target region are rejected. The researchers are normally asked to design several primer set so that at least few of them may work in standard TILLING reaction.

Since first described, PCR rapidly become one of the key techniques of molecular biology. However, the amplification of DNA target by the polymerase chain reaction often requires laborious optimization efforts. For several studies, improvement of specificity and increased product formation were the primary and most important targets. The PCR has to be optimized for five parameters (Finckh and Rolfs 1998): (1) specificity, (2) sensitivity, (3) efficiency (yield), (4) reproducibility, and (5) fidelity (polymerization error rate). Since TILLING is a

PCR based technique, the parameters such as specificity (the amount of desired to non-desired PCR product) efficiency (the absolute amount of desired PCR product) and fidelity are vital parameters. In addition to the above parameters, the amount of template DNA needed to amplify PCR product is also crucial for TILLING.

In this study, different procedures and conditions were evaluated for PCR amplification of three different sets of primers used for phytochrome TILLING. After rigorous analysis, an optimal PCR protocol was developed for TILLING for phytochrome gene.

The initial optimization were carried out using unlabeled primers, considering that PCR product generated with unlabeled primers can be visualized on agarose gel electrophoresis compared to fluorescently labeled primers at a much lower cost. The PCR optimization was initiated with a gradient PCR, which determines an appropriate annealing temperature. Based on results annealing temperature of 62ºC was selected for further optimization of PCR. The annealing at 62ºC yielded a better amplification of PCR products. However, using a straight cycle with annealing temperature at 62ºC for PCR in the next step of optimization led to poor PCR yield and suboptimal specificity. Considering this, the modifications in cycling conditions for better PCR amplifications was attempted.

One variant of classical PCR method, namely touchdown PCR was used for next step of optimization. Basically, touchdown PCR employs an annealing temperature that is 5 to 10°C higher than the original Tm of the primer. It has been reported that this improves the specificity of PCR amplification (Don *et al.,* 1991) by avoiding the generation of contaminating PCR products (Wu *et al.,* 2005). Touchdown PCR can be used as a standard practice for any PCR based amplification to enhance specificity and efficiency of the reaction. PCR cycling program for Touchdown involves two steps. In step 1, reaction uses an annealing temperature substantially higher than the Tm of the primer (generally Tm+10°C). This is

followed by step wise decrease to lower annealing temperature during course of successive PCR cycle (1°C decrease per cycle) till annealing temperature becomes equal to the Tm of the primer. Thereafter normal PCR amplification of 20 or 25 cycles at original Tm of the primers is carried out. Usage of touchdown PCR led to threefold increase in PCR product formation compared to the normal straight cycle PCR.

Several studies suggested that, when used in appropriate concentrations various adjuvants like glycerol and BSA (Smith *et al.*, 1990, Kreader, 1996) can effectively improve the PCR amplification efficiency (yield) as well as specificity. However, in our study, many of the reported adjuvants gave inconsistent amplifications in PCR. For all the primers that were used for PCR optimization, addition of glycerol, increased yield, but at the same time decreased specificity. It is believed that glycerol enhances specificity and efficiency by increasing the hydrophobic interaction with protein domain and lowering the strand separation temperature (Wang *et al.*, 1993). Taking together poor specificity and lack of consistency glycerol was found to be unsuitable for TILLING PCR. Compared to glycerol, adjuvant BSA (20 mg/ml) was found to be more effective for TILLING. The inclusion of BSA in reaction mixture considerably increased the efficiency, specificity and sensitivity of the PCR. BSA most likely stabilizes *Taq* polymerase (Nagai *et al.*, 1998) and thus increases the yield of the reaction. PVPP (polyvinyl polypyrolidine) which helps in the removal of flavonoids or polyphenols from a medium, possibly by acting as an adsorbent, was also included as an adjuvant. Though we did not find any change when we used PVPP alone in our reactions, a combination of both PVPP and BSA showed a considerable increase in the product formation.

After attaining optimization of PCR, where PCR product quality was checked by agarose gel electrophoresis, PCR product was also examined for the amplification profile using Li-COR DNA analyser. Surprisingly when the same optimized protocol was applied to mixture

of fluorescently labeled and unlabeled primers it became apparent that agarose gel based optimization was not suitable for above primer combination.

This observation clearly indicated that, inclusion of labeled primers in PCR mixture requires additional optimization than unlabeled primers, and therefore PCR optimization was reinitiated. The next optimization step included the optimization of amount of reaction components. At outset, the amount of *Taq* polymerase, which is the most essential component of any PCR reaction, was optimized for the optimum concentration for a TILLING PCR. Among the concentration examined a volume of 0.18 µl of *Taq* polymerase in a final 20 µl reaction volume led to a better yield with maximum specificity. For catalytic action, *Taq* polymerase requires free magnesium in medium in addition to the magnesium bound by the dNTP and the DNA (Innis *et al.*, 1990). To further improve the profile of product observed on Li-COR DNA analyser, the varying concentrations of components like $MgCl_2$ and dNTP were tested. By combining various amounts of dNTP and $MgCl_2$, a combination of 2.5 mM dNTP with 2 mM $MgCl_2$ was found optimal.

Following this nested PCR was used to enhance the specificity and efficiency of PCR amplification. Nested PCR uses 2 sets of PCR amplification primers namely inner primer set and outer primer set. The target DNA sequence of inner primer is located within the target sequence of outer primer. After completion of first PCR using outer primer set the PCR product of outer primer serve as the template for the second step PCR amplification. Nested PCR increases the efficiency and specificity of PCR amplification by re-amplifying the product of the first PCR step in a second step PCR.

To deal with major challenges related to PCR amplification several groups used nested PCR as a part of their optimization (Wienholds *et al.*, 2003b, Winkler *et al.*, 2005). They perform PCR in two steps, first amplifying individual DNAs, then diluting and pooling 4-fold

and amplifying with nested primers. The initial amplification yields the same approximate final concentration of product regardless of the original concentration of template. Therefore the first step product can be used without careful normalization. The main advantage of this method is that, it avoid the influence of the variation in quality and quantity of the genomic DNA that is used as a template for TILLING PCR (Wienholds *et al.*, 2003b).

The outer unlabeled primers were used to amplify pooled genomic DNA in first PCR. For the second step PCR, the diluted product from first step PCR was used as the template and amplified with an inner target specific primer. The advantage of this method was that the pooled genomic DNA which is present in very a low amount could get amplified and thus improves the possibility of mutation detection. With Nested PCR an improved profile was obtained with good yield, high specificity and sensitivity.

In view of above improvement, detection of mutation on CEL-I digestion, the nested PCR was used for scanning for mutations in TILLING and EcoTILLING population. One advantage of nested PCR was that it amplified the region of interest to sufficiently high level for amplification with M13 based universal primers. The usage of M13 primers considerably reduced the cost of TILLING.

5.2 Use of TILLING as a Mutation Mining Tool in Tomato

TILLING (Targeting Induced Local Lesions IN Genomes) is a reverse-genetic method to identify point mutations in chemically mutagenized populations. The method of TILLING is applicable to all living organisms and has been applied right from *Phythopthora* to mice.

One advantage of TILLING is that it first allows finding of mutations in a given gene and later one can check whether or not the mutations has a phenotype. Compared to forward genetics where mutations with only strong phenotypes are selected, TILLING allows

obtaining multiple alleles of a gene and that can be later scanned for more obvious phenotypic characters. In tomato only few mutants have been isolated for phytochrome using forward genetic screening. In view of limited number of mutants available in tomato, we used TILLING to obtain additional phytochrome mutants mainly in PAS region of tomato phytochrome.

Phytochrome is a plant photoreceptor, which is known to regulate a wide variety of responses of plants to light, including induction of seed germination, modulation of elongation growth, promotion of chloroplast development, and induction of flowering. An understanding of the molecular mechanism of phytochrome action is therefore essential to elucidate the complex processes of plant growth and development. In the present study, a reverse genetic, non-transgenic approach, TILLING, was used for the isolation of induced mutations in *Phytochrome A* genes in an EMS mutagenized population of tomato. N-terminal region of the gene, which codes for photosensory region of the protein, was targeted for mutation mining. In the current study two Phytochrome genes *viz*. *Phytochrome A* and *Phytochrome B1* which are key regulators of light driven plant development were analysed.

5.3 Development of a Mutagenized Tomato Population

EMS (ethyl methane sulfonate) has been used successfully to introduce random single base changes in the genomes of various organisms (Neuffer and Coe 1978). EMS is an alkylating agent that induces chemical modification of nucleotides, which causes in mispairing and base changes during DNA replication. A biased alkylation of guanine (G) results in the formation of O6-methylguanine, which inturn leads to pairing with thymine (T) but not with cytosine (C). In the subsequent DNA repair step, the original G/C pair is replaced with A (adenine)/T (Greene, *et al.,* 2003). Results of many studies suggest that chemical mutagenesis can be used both in search for loss- or gain-of-function mutants which can be used to understand the role

of specific amino acid residues in protein function. Additionally chemically induced mutants also provide useful information for understanding the functions of essential genes by generating weak non-lethal alleles. We initially selected 60 mM (0.75% w/v) concentration of EMS to mutagenize tomato seeds based on the previous reports of the Lethal Dose (LD) values and saturation of mutation in tomato (Menda *et al.*, 2004).

Though there are several methods to evaluate the efficiency of mutagenesis, reduction in germination percentage (embryo lethality), is one of the simplest method. The exposure to EMS led to a reduction in percentage of seedlings compared to untreated one. The reduction in seed germination (40% reduction in germination, LD_{40}) on EMS mutagenesis indicated that above dose was sufficient to induce mutagenesis. As indication of mutagenesis efficiency can be obtained by assessment of phenotypic variation, we examined the phenotypic changes in the M_2 generation of mutagenized population. As the density of mutations in the population was too low, we developed another mutagenized population of *cv.* Arka Vikas by using 120 mM (1.5% w/v) concentration of EMS. Though the increase of EMS did not drastically increase lethality; it affected the survival and phenotypic variability of the plants to a great extent.

5.4 Variability of Phenotypes

Plant architecture is an important parameter that affects plant fitness in the natural environment. Considering that crop plants with desirable architecture are able to produce much higher grain yield, it is essential to understand the mechanism that underlies plant architecture. This understanding is essential for manipulation of plant architecture that in turn can facilitate the breeding of high-yielding crops. Although intrinsic genetic programs are major determinants of architecture, environmental signal also strongly modulate plant form. Light is one of such important factor that regulates plant architecture. It is known that R:FR

ratio perceived by the phytochrome family allows the plants to assess the ambient environment and leads to modulation in plant architecture for better survival. The phytochromes (PhyA to PhyE) sense and transduce light signaling parameters, including the R:FR ratio, with PhyB playing the major role. Reduced R: FR ratio elicits a suite of responses collectively termed the shade avoidance response (Smith, 1995; Franklin and Whitelam, 2005). The resultant phenotype includes rapid elongation of the main shoot, reduced root growth, early flowering, reduced branching, and other effects, which may confer a competitive advantage that allow plants to mount an early response. Reduced R: FR signal indicates competition from neighbouring plants as plants absorb R and reflect or transmit FR (Ballare, 1999). In several studies, the loss of phytochrome functions were reported to result in altered plant architecture (Reed *et al.,* 1993).

Tomato is an important crop and an excellent model system with extensive genome data available (Solanaceae genome network). The advances in genome sequence provide great platform to explore genome information for understanding gene function controlling important traits. Several groups reported approaches attempts to develop mutation library in tomato. Menda *et al.,* (2004) developed an isogenic tomato mutation library in the genetic background of the inbred variety M82. About 13,000 M_2 lines derived from an EMS and fast neutron mutagenized population were phenotyped visually in the field. Similar approaches to develop mutation library in tomato include EMS mutagenesis of *cv*. Redsetter, Tpaadasu, and MicroTom (Gady *et al.,* 2009, Minoia *et al.,* 2010, Saito *et al.,* 2011). The mutants that have been developed through these platforms are currently available to the scientific community. These mutant resources are highly useful in dissecting the mechanism underlying mutant phenotype and such mutagenized population also act as a resource for high throughput reverse genetic strategy to screen for point mutations (Mc Callum *et al.,* 2000a, Colbert *et al.,* 2001).

In our study, we analysed phenotypic variations to investigate the likely interdependence between phytochromes and plant architecture in tomato. We used the mutagenized population that we raised in our lab as a source to study variations related to architecture. While evaluating 10,000 M_2 families for phenotypic variation, we have identified several morphological and developmental mutants. The most abundant category of morphological variation was leaf texture (33%) followed by leaf size (17%), leaf width (13% and leaf colour (11%). In our population phenotypic categories associated with vegetative organs were more prevalent. In fact eight categories related to vegetative organs represented >93% of total phenotype. We found several phenotypes similar to those of previously reported mutations. For example, AV-M_2-120 mM 484C had elongated leaflets without serrations similar to *lanceolate* (Ori *et al.,* 2007), AV-M_2-120 mM 107B showed an inflorescence that were exceptionally large and excessively branched similar to *anatha* (Lippman *et al.,* 2008). AV-M_2-120 mM 230 D exhibited wiry phenotype with reduced leaf complexity (Menda *et al.,* 2004). Some lines were found to be with altered pattern of branching with either a rosette appearance (AV-M_2-120 mM 880C), or showing profuse branching (AV-M_2-120 mM 459D). Furthermore we observed mutants which are very tall (17A) and stunted plants with reduced growth (AV-M_2-120 mM 1498A).

The mutant population generated in our lab is an excellent resource for both forward and reverse genetic studies and we successfully used the population for mining mutations. Though the exact molecular nature of these mutant plants are not known, analysis of these mutations in the future will help, those who seek to identify the functions of tomato genes.

5.5 NEATTILL: A Simplified Procedure for Nucleic Acid Extraction from Arrayed Tissue for TILLING

TILLING which is a reverse genetic, non-transgenic tool of crop improvement, involves generating a large mutant population with the aim of saturating the whole genome with mutations. One essential feature of TILLING is that it needs pooling of genomic DNA of mutant with wild type thus allowing generation of mismatches in heteroduplex. Procedure of TILLING utilizes the multiplex approach i.e. pooling at least two DNA samples, prior to PCR amplification. Since mutagenesis is a random event, it eliminates the need of using wild type DNA for pooling and different numbers of individuals upward of two can be pooled for mutation detection. The upper limit of pooling is determined by the efficiency of mutation detection procedure. One obvious advantage of pooling is the considerable reduction in the number of PCR amplifications to be carried out for mutation detection. Moreover, pooling also reduces the cost of consumables and the time needed for mutation scanning. The choice of pooling is determined by striking a balance between total number of PCR reactions to be carried on population and chances of detection of mutations in the pool. Though various levels of pooling i.e. four, six, eight or even higher folds of DNA pooling can be done, higher folds of pooling beyond 8-fold pool reduce the chances of mutation detection.

In the present study, we adopted a simplified 2-dimensional pooling strategy, NEATTILL **N**ucleic acid **E**xtraction from **A**rrayed **T**issue for **TILL**ING for tomato. Our protocol circumvents isolation of DNA from individual plants by pooling of tissue from different plants followed by DNA isolation from pooled arrayed samples. The scanning of mutations in 2-D pooled plates allows simplified identification of mutant lines as a mutation detected in the row-pooled plate is also represented in the complementary column-pooled plate, allowing direct identification of mutant lines. The pooling of tissue prior to DNA isolation reduces the

total number of extractions with added benefits of cost reduction and time saving. NEATTILL is a convenient procedure that can be applied to all organisms, the genomes of which have been mutagenized and are being scanned for multiple alleles of various genes by TILLING for understanding gene-to-phenotype relationships. It is a time-saving, less labour intensive and reasonably cost-effective method.

Higher eukaryotes offer several possibilities for the starting tissue material for DNA isolation. Choosing the right tissue for arraying and DNA isolation is critical in the overall NEATTILL procedure as it generates the genomic DNA resource for TILLING. Factors such as easy availability, feasibility of culture (in case of microorganisms and cell lines) and growth (in case of plants), minimum post-collection manipulation with samples (such as specific treatments or tissue cleaning, cutting into pieces), age of the tissue sample, absence of secondary metabolites (especially relevant in case of plants) and DNA stability during long term storage can influence one's choice of tissue. Most often genomic DNA is isolated from leaves of plants grown in field or green house. We found that for tomato DNA isolated from mature leaves was of inferior quality due to the presence of secondary metabolites (especially, anthocyanins and polyphenolics). The usage of emerging juvenile leaves, which had less secondary metabolites, yielded better quality DNA. Relatively superior quality DNA was obtained from young cotyledons with minimal interference from secondary metabolites. One advantage of using cotyledons as starting material is that DNA isolation can be done using culture room grown plants at any time of the year.

The tissue arraying gives three options of representing mutant lines of the whole population for screening depending upon the size of the mutagenized population. Large populations having >5000 up to 15000 individual mutant lines can be pooled by combining tissue samples from 6-8 mutant lines to generate 6x – 8x pooled plates as described above in tomato. Population sizes smaller than 1000 individuals can be subjected to in-depth scanning

in which 6-8 individuals of the same mutant line can be pooled together. This improves the chances of detecting the mutation while scanning the whole population particularly for organisms which have "genetically effective cell number" more than one. However, the number of plates to be screened also increases, so this option is practically feasible only with small population. Another manipulation, termed as intermediate scanning, at the level of fold pooling (2x – 8x) can also be attempted. Here pooling can be done by combining 2 lines with 4 individuals each (2x) or 3 lines with 2 individuals each (3x) or 4 lines with 2 individuals each (4x). It is left to the discretion of the researcher to choose either of the options [to attempt vast scanning (8x) or in-depth scanning (1x)] or strike a balance between the two options by manipulating fold pools (2x – 4x) .

NEATTILL, although offers the flexibility of scanning populations in 3 ways: vast, in-depth or intermediate, has one limitation that the fold pooling of DNA is fixed. However, when DNA is isolated separately from individuals, one can try various levels of pooling (2x, 3x, 4x, 5x, 6x or 8x) at any point of time but this flexibility is not possible with tissue pooling. Therefore, fold pooling which works best in a particular organism has to be determined before attempting NEATTILL using a known mutation as a positive control. The protocol of 2-D pooling of tomato cotyledons was proved to be useful for detection of mutation, and also reduced the cost of DNA isolation. Since it also reduces the time to isolate DNA from large population, it was adopted for scanning for mutation in M_2 population of Arka Vikas by TILLING.

5.6 TILLING of *Phytochrome* Genes

Studies on mutants and transgenic plants along with sequence homology analysis have been used to understand several molecular domains associated with phytochrome molecules. Such studies have revealed that N-terminal half of the phytochrome molecules is associated with

photosensory function while the regulatory functions involving transfer of perceived information to downstream components of the signal transduction chain has been assigned to C-terminal domain. The N-terminal domain comprises several subdomains: the N-terminal extension, the Per/Arnt/Sim (PAS) subdomain, the cGMP phosphodiesterase/adenyl cyclase/FhlA (GAF) subdomain, and the phytochrome (PHY) subdomain.

Genetic and molecular analyses have greatly helped in understanding the functions of individual phytochrome family members in plants. Light-labile PhyAs appear to be primarily responsible for mediating photomorphogenic responses to continuous far-red light and sensing very low light fluences and for adaptation to FR-enriched shade environments (reviewed by Casal *et al.,* 1997; Sineshchekov, 2004), while the light-stable phytochromes Phi-E mediate the classic R/FR photoreversible responses and adaptation to elevated fluence rates of R (Reed *et al.,* 1993; Franklin *et al.,* 2003a, b).

Our current understanding of the structure and function of phytochromes has greatly facilitated from the isolation and characterization of photoreceptor mutants (Quail, 1997). To unravel the roles of the different phytochrome species, mutants deficient in one specific type of phytochrome are required. So far, three types of phytochrome mutants have been identified, which include: (a) Mutants with defect in the biosynthesis of the common phytochrome chromophore, like the *hyl* and *hy2* mutants of Arabidopsis (Parks and Quail, 1991) ,the *pew* mutants of *Nicotiana plumbaginifolia* (Kraepiel *et al.,* 1994), and the aurea (*au*) and yellow green-2 (*yg-2*) mutants (Koornneef *et al.,* 1985) of tomato (Sharma *et al.,* 1993; Van Tuinen *et al.,* 1995b). (b) Mutants that lack a light labile phytochrome (PhyA) have been reported in Arabidopsis (Dehesh *et al.,* 1993; Nagatani *et al.,* 1993; Parks and Quail, 1993; Whitelam *et al.,* 1993) in tomato (Van Tuinen *et al.,* 1995a) and in pea (Weller, 1997). (c) Mutant that are deficient in light stable, PHYB-like protein have been reported in severa1 species, including *hy3* mutant in *Arabidopsis* (Reed *et al.,* 1993), *tri* mutant in

tomato (Van Tuinen *et al.,* 1995b), various spectral and signalling mutants in *Arabidopsis* (Oka *et al.,* 2008).

Phytochrome A mutants in various plant species are characterized by their failure to de-etiolate in continuous FR light (absence of a FR-HIR for hypocotyl inhibition and the rather normal phenotype in WL. Similarly, characterization of PhyB deficient mutants in various species revealed that they have difficulty de-etiolating in continuous red light. Additionally adult plant tissues exhibited a reduction in chlorophyll content. A large-scale screen for Arabidopsis *phytochrome B* mutants identified 14 novel missense mutations in the N terminal moiety. Analysis of these new mutations revealed that each subdomain has an important function. Analysis on the spectral properties of these mutants enabled them to be classified into two principal classes: light-signal perception mutants (those with defective spectral activity), and signaling mutants (defective in intracellular signal transfer). Most of the spectral mutants were found in the GAF and PHY subdomains. On the other hand, the signaling mutants tend to be located in the N-terminal extension and PLD (PAS-like domain). These observations indicate that the N-terminal extension and PLD are mainly involved in signal transfer, but that the C-terminal GAF and PHY subdomains are responsible for light perception (Oka *et al.,* 2008).

More recently, Su and Lagarias (2007) reported the isolation of a new class of plant phytochrome mutants that exhibit light-independent signalling. These mutants are reported to have a dominant gain-of function activity caused by mutation of a conserved GAF domain Tyr residue (Y^{GAF}). Y^{GAF} mutants of Arabidopsis phyA and phyB exhibited a light-independent activation of gene expression, and general R/FR insensitivity with a COP (Constitutive photomorphogenesis) phenotype. The above study clearly demonstrates the critical role of the conserved GAF domain in coupling light perception with downstream signaling.

In tomato, only few mutations have been reported for *PHYA*, *PHYB1*and *PHYB2* genes. To understand the function of phytochrome in modulation of plant architecture, there is need for additional alleles, mutated in different domains of phytochrome gene. Considering the importance of tomato as a vegetable plant, and role of phytochrome in regulating fruit ripening we sought to isolate new alleles of *PHYA* and *PHYB1* in tomato. We used TILLING to isolate new allelic variants of *phytochrome A* and *B1* genes. These alleles may influence plant architecture and also provide information on functional importance of respective domains. The mutant lines were also phenotypically characterized for phenotypic aberration. A population of nearly 10,000 EMS mutagenized M_2 plants were screened for mutations in genes encoding the PHYA and PHYB1 proteins. For these genes, the focus of mutation screening was on the regions predicted by CODDLE (Codons Optimised to Discover Deleterious Lesions). The above analysis predicted that mutations in exons 1 and 2 may cause most deleterious effects on Phytochrome A and B1 function. These two exons encodes for the light signalling domains, which consists of core light sensing components like PAS, GAF and PHY. TILLING of *phytochrome A* in the above region yielded six independent point mutations, out of which we could identify only one confirmed individual plant line in subsequent analysis. TILLING of *phytochrome B1* gene yielded two independent point mutations and we could confirm only one mutation at individual plant level.

Though we screened a large population of nearly 10,000 M_2 plants, we could detect only a few mutations in these two phytochrome genes. Though we do not know the reason for the low frequency of mutations in tomato M_2 lines, one probable explanation is recalcitrance of tomato to mutagenesis. The very low frequency of mutation in *phytochrome A* and *B1* suggests the conserved nature of these two phytochrome genes and their importance for plant survival. It is likely that mutation in phytochrome gene may be lethal for plants, and these lines do not survive, thus reducing detection of strong mutations in phytochrome gene. The

mutant line (Accession number M82-M_2-895) which had mutation in phytochrome A gene, was further analysed to detect the molecular nature of the mutation. Sequence analysis of *phytochrome A* gene from the above mutant line revealed the presence of a nucleotide change from guanine (G) to Adenine (A) at 1586th position of open reading frame (ORF). The conversion of amino acid showed that this change causes a missense mutation as it alters the codon GGG to AGG leading to the replacement of glycine with arginine at amino acid 496 (G496R) in the mutant PHYA polypeptide. This change causes the shift from non-polar neutral amino acid to polar positive amino acid in the PHY domain of Phytochrome. Detailed phenotype analysis of the plant revealed that although at the seedling stage any characteristic change was not visible, the adult mutant plant exhibited an altered phenotype compared to wild type control. The observation that mutant plant exhibit altered architecture establishes that the functional consequence of the mutation is the gain of function of the photoreceptors. While the extent of gain of function activities is difficult to predict from our data, the phenotype has promising impact on crop improvement. While field grown plants exhibit a significant change, the seedling phenotype which include hypocotyl elongation and cotyledon expansion, which is present in the previously reported phytochrome were completely absent under continuous far red light. In future, a detailed examination of mutant phytochrome would be carried out to delineate its function in regulating plant architecture and genetic linkage of phenotype with the mutation.

Similar to *phytochrome A* only one mutant allele for *phytochrome B1* (Accession AV 60 mM 888) was isolated from the above mutagenized population of tomato. The sequence of mutant *phytochrome B1*gene revealed a change from cytosine (C) to thymine (T), which leads to a silent or synonymous mutation. This mutation affected the third base of a codon (CTC to CTT) which does not change the amino acid encoded by that codon. Phenotype characterization revealed that the above mutant line did not exhibit any perceptible

phenotypic change either at the seedling stage or at the mature stage. Though synonymous changes should not affect the function of a given protein, it is reported that codon bias for an amino acid may influence the level of protein. In such a case even synonymous mutations have distinct effect on phenotype of plants. Since to evaluate such change, require rigorous examination of plant phenotype and we did not undertake this.

5.7 Use of EcoTILLING as a Polymorphism Discovery Tool in Tomato

EcoTILLING is a rapid, low-cost and efficient method for the discovery and characterization of nucleotide polymorphisms. EcoTILLING was initially used to characterise the variability of collection of Arabidopsis ecotypes (Comai *et al.,* 2004). Later it was adopted as a useful technique to analyse the natural variation in populations *viz* black cottonwood (Gilchrist *et al.,* 2006), and for genotyping in other species. It was also used for the identification of variation in resistance genes of barley (Mejlhede *et al.,* 2006) and *Cucumis species (*Nieto *et al.,* 2007)

A rapid, low-cost and efficient method for the discovery and characterization of nucleotide polymorphisms in tomato would add to understanding its genetic diversity and help in improvement of tomato.

In the current study two phytochrome genes *viz*. *Phytochrome A* and *Phytochrome B1* which are key regulators of light driven plant development were analysed by EcoTILLING. Considering the importance of GAF and PAS domains in phytochrome in signalling, these regions were scanned for polymorphism and a few SNPs were detected. In a population of 605 different accessions, 32 accessions showed with polymorphism in either *phytochrome A* or *B1*. Interestingly 95% of polymorphism in *phytochrome B1* was synonymous SNPs while *phytochrome A* showed several nonsynonymous SNPs which are predicted by either SIFT or PARSESNP or both to be deleterious to phytochrome A function.

5.8 Polymorphisms in *Phytochrome* Genes

The structural motifs of different phytochrome photoreceptors are highly similar (Nagatani, 2010). Functional phytochrome A molecules are dimers of 120-kD monomers, which can be divided into N- and C-terminal halves, connected by a proteolytically vulnerable hinge region (Quail, 1997). The N-terminal half of phytochromes are responsible for defining the functional characteristics of the photoreceptor (Wagner *et al.,* 1996; Mateos *et al.,* 2006). Mutations in the PAS and GAF domains of plant phytochromes that result in altered function *in vivo* have been mapped onto the DrBphP structure (Rockwell *et al.,* 2006). Considering this fact, we targeted the PAS and GAF domain for SNP detection for both Phytochrome A and B1.

Nearly 19 tomato accessions showed polymorphism on Li-COR DNA analyser in target region of *phytochrome A,* in comparison to Arka Vikas. Based on fragment cleavage pattern these accessions were classified into 4 different haplotypes. The precise position and nature of the identified polymorphisms were determined by *phytochrome A* gene sequencing. Haplotype. 2 (HT. 2) showed a nucleotide change G2614A, which was a nonsynonymous mutation. It corresponded to amino acid change E748K (Glutamic acid to Lysine) located at the PAS domain of the amino-terminus of the protein.

Surprisingly GAF domain region of *phytochrome A,* encompassing about first thousand base pair of the first exon of *phytochrome A* of tomato, shows a very low diversity of polymorphism. Only a single SNP was found for this region. Contrastingly the next thousand base pair region of first exon, showed a higher number of SNPs compared to the former region. These accessions with SNPs in *phytochrome A* gene in tomato were examined for any phenotype change.

For *Phytochrome B1*, 13 accessions showed polymorphisms in comparison to Arka Vikas and were grouped in 3 different haplotypes. Sequencing of these three haplotype revealed that that except HT.3, the two other haplotypes did not show any non-synonymous change. HT.3 showed a nucleotide change corresponding to a non-synonymous mutation. Sequencing of *phytochrome B1* gene from the accession EC 34480, belongs to HT.3, exhibited a nucleotide change from Adenine (A) to Thymine (T) at the 164th position of ORF causing amino acid change from glutamic acid to valine.

The fact that most of the SNPs found for *phytochrome B1* gene were synonymous is probably related to the conserved nature of the region screened for polymorphism.

5.9 Effect of Non-synonymous SNPs on Far-red Light Mediated De-etiolation of Seedlings

Seeds after germination under light follows a developmental program known as photomorphogenesis (light development); where seedlings display short hypocotyls and open expanded cotyledons that are capable of photosynthesis (Sullivan and Deng, 2003). The switch between skotomorphogenic growth and photomorphogenic growth or the successful establishment of photoautotrophy require the sensitive detection of light environment by plants.

Phytochromes perform a variety of overlapping roles to detect light environment in combination with other photoreceptors. Seedlings of *phyA* mutants grown under continuous FR light show an elongated hypocotyl contrasting to the wild type seedling, which exhibit a normal de-etiolated short hypocotyl. Studies indicate that phyA plays a unique role in mediating de-etiolation under FR-HIR (Dehesh *et al.,* 1993; Nagatani *et al.,* 1993; Parks and Quail, 1993; Whitelam *et al.,* 1993). Similarly analysis of *phytochrome B* mutant suggested that phyB is the major phytochrome regulating de-etiolation in white or red light and *phyB*

deficient mutants exhibited elongated hypocotyl, reduced cotyledon expansion, and reduced chlorophyll synthesis (Koornneef *et al.,* 1980; Nagatani *et al.,* 1991; Somers *et al.,* 1991; Reed *et al.,* 1993). In this study, polymorphism identified for 2 important phytochrome genes *viz phytochrome A* and *phytochrome B1*, were examined with reference to their effect on de-etiolation of seedlings under far red light.

Among 5 haplotypes identified for *phytochrome A*, two haplotypes, HT.2 and HT.4 exhibited altered response to far red light. Seedlings of tomato accession (EC 528362), belonging to HT.2 showed altered response to far red light. The accession harbours a non-synonymous polymorphism in exon 2 leading to an amino acid change from Glutamic acid to Lysine. It is likely that this particular change located at the PAS domain of the amino-terminus of PHYA protein may be responsible for the observed phenotype of seedling under FR light.

Similarly the accession WIR 3286, belongs to HT.4 exhibited an altered response to far red light. In contrast to other phytochrome mutants, seedlings of WIR 3286 when grown under far red light showed a completely opened cotyledon associated with a strong reduction in hypocotyl length. The sequencing of genomic DNA showed 2 SNPs in exon 1 of phytochrome A. The translation to amino acid sequence showed that these two SNPs alter glutamic acid to Aspartic acid at 590^{th} position and Leucine to Phenyl alanine at 651^{th} position. Between the two amino acid changes, shift from Leucine to Phenyl alanine at 651^{th} position is likely to be deleterious to the phytochrome, and it also showed a high PSSM score (17.6).

5.10 Influence of Phytochrome SNPs on Tomato Plant Architecture

The architecture of plant shoot, though determined by several genes, is also influenced very intensively by the environmental factors especially light. The reduction in PAR

(Photosynthetically active radiation) by shading signified by enrichment of FR light under canopy leads to elongation of plants, a process called shade avoidance. It is expected that attenuation of shade avoidance would allow crop plants to be grown in high density. The enrichment of FR due to shading is detected by plant photoreceptor Phytochrome. In tomato, though five different phytochrome genes are present, the precise role of each member is still not completely known. Seedlings of the accessions bearing non-synonymous SNP in *phytochrome A* and *B* genes showed altered response to FR light. In view of this influence of these SNPs were also examined on adult plant architecture.

Among 5 haplotypes identified for *phytochrome A*, plants belonging to HT.2 exhibited altered plant architecture. Field grown plants of the accession (EC 528362), showed a strikingly different phenotypic changes in plant architecture. The above accession showed a drastic reduction in number of branches with a thin stem compared to Arka Vikas.

Among 3 haplotypes identified for *phytochrome B1*, plants belonging to HT.3 exhibited altered plant architecture. Field grown plants of the accession, EC 34480 showed phenotypic changes such as a drastic reduction in the number of branches and retarded vegetative growth.

5.11 New Phytochrome Alleles with Altered Flowering Response

The transition of vegetative growth to reproductive growth is considered as a major development switch in plant cycle. Several environmental factors are involved in this transition. Photoperiod is recognized as a major environmental factor regulating flowering time in many plants. Phytochromes are principle photoreceptors which are involved in photoperiod detection and floral induction. A key function of phytochrome is monitoring of day length or photoperiod which, together with temperature, provides plants with important seasonal information. Additionally phytochromes are also involved in the detection of relative proportion red and far red light. Sensing the ratio of R/FR light, like photoperiod, provides an

important cue to detect the shading in the plants. The detection of the altered R:FR ratios by phytochrome initiate shade avoidance response in many species (Smith and Whitelam, 1997). Acceleration of flowering is one such response which is induced by shade avoidance. The shade avoidance response helps in the survival of plants under unfavourable condition. Physiological studies of phytochrome mutants of Arabidopsis indicated that phyB is the principle photoreceptor in shade detection (Goto *et al.,* 1991). The early flowering phenotype of *phyB* mutants under altered R:FR indicated the involvement this photoreceptor in flowering in Arabidopsis.

Consistent with above role of phyB in flowering regulation, tomato accession EC 34480 (belongs to HT.3) exhibited a flowering phenotype. One of the characteristic features of this accession was a reduction in the number flowers as well as delayed flowering. The flowering in above accession was delayed of almost by thirty-day compared to Arka Vikas plant.

The above analysis of different accessions reveals that EcoTILLING can be used as a powerful tool for discovering novel SNPs that can be used for their effect on metabolic/physiological/morphological features of plant. In current study, few novel SNPs of *phytochrome A* and *phytochrome B1* were identified. The preliminary study showed that these SNP influence plant architecture. More detailed analyses in future may reveal the precise role of phytochrome molecule.

5.12 Sequence Diversity of Phytochrome in Wild Relatives of Tomato

Plants have evolved an array of photoreceptors for sensing and responding to their light environment. The photo responses of various species native to different habitats exhibit adaptive variation. Understanding the mechanisms of local adaptation of wild species in correlation with photomorphogenic variation is therefore of significant interest. Adaptation can be described as the movement of a population towards a phenotype that facilitates the

highest fitness in a particular environment (Fisher, 1930). Several approaches were developed to detect adaptation in various organisms, though the genetic basis of adaptation in natural populations remains largely unknown (Orr, 2005). These methods, which mainly employ information on DNA variation for adaptation detection, have frequently been applied to plant model systems.

Tomato genome harbours five phytochrome genes, designated *PHYA, PHYB1, PHYB2, PHYE* and *PHYF*. The molecular properties of the photoreceptors, encoded by these genes, enable them to perceive and transduce red light (R) and far-red light (FR) signals to downstream cellular components, ultimately leading to modulation of the expression of genes responsible for photomorphogenesis. Polymorphic variations observed in various phytochrome species have been found to alter light responses. For instance, a single amino acid change in PHYA exhibited a reduced FR sensitivity in *A. thaliana* strain Lm-2, likewise a naturally occurring deletion in *PHYD* increases stem elongation and nucleotide variations in *PHYC* is responsible for differences in both flowering time and hypocotyl elongation, in *A. thaliana* accessions (Maloof *et al.,* 2001, Balasubramanian *et al.,* 2006). It is considered relative to an average plant gene, phytochrome genes evolve faster and previous studies have shown that positive selection might have happened early in the diversification of *PHYA sequence* (Mathews *et al.,* 2003). Among all other members phytochrome B is considered as the most dominant photoreceptor as it plays by far the primary role for white-light responses (Filiault *et al.,* 2008). Moreover, *PHYB* has been proposed as a candidate gene for several quantitative trait loci (QTLs) affecting light mediated physiological response. Phytochrome A is also unique in phytochrome family for its ability to mediate photomorphogenic response to continuous far red light and for the strong photocontrol of its transcript level and protein stability. In tomato, we know very little about function of other phytochrome species like phytochrome B1, E, and F due to the unavailability of mutant alleles for these three species.

The second objective of this study was to unlock genetic potential from the wild relatives. The increased population growth imposes a greater demand on agricultural output than at any time in history. In this scenario, genetic improvement of crops is considered as the most viable approach by which food production can keep pace with the anticipated growth of the human population. To achieve this, it is essential to harness the wealth of genetic variation provided by Nature. Recent findings indicate that, there is significant genetic potential locked up in seed banks and that can be used effectively for crop improvement by searching for superior alleles of genes with the aid of modern technology. It is known that domesticated species represent only a tiny fraction of the variability available among the wild relatives. Plant domestication is an outcome of strong selection pressure exerted by humans, which results in changes in the tissue and organs of greatest interest to humans. The wild tomato species contain several useful traits that can be introgressed into cultivated tomato such as tolerance to drought and salinity (Dehan *et al.*, 1978; Shalata *et al.*, 1998), accumulation of health promoting phytochemicals and resistance to multiple pathogens (Venema, 1999; Stevens 1986; Robert, 2001; Rick *et al.*, 1994).

An exhaustive sequencing approach was used to identify genetic difference responsible for the variability of the different shade response pattern and architectural variation in tomato and its closely related wild relatives. The nucleotide diversity of phytochrome genes was analysed to determine whether polymorphisms in phytochrome genes could contribute to variation in light response. The sequences of five wild relatives of tomato were compared with gene sequence of *S. lycopersicum* (*cv.* Arka Vikas). Using the available genome sequence and annotation data of tomato, bioinformatics analyses are performed to compare various phytochrome genes in these organisms. The sequencing analysis of phytochrome genes showed the presence of numerous SNPs that differentiate the color fruited species from the

green-fruited one. Some non-synonymous substitutions found in this study are potential candidate to be hypo or hypermorphic alleles.

The sequence analysis revealed the presence of 110 synonymous, and 59 nonsynonymous polymorphisms in phytochrome of wild tomato species. The presence of large number of SNPs in three wild tomato species [*S.habrochaites* (71) *S. neorickii* (42) and *S.chilense* (34)] compared to other two species are consistent with the result that these three species are distant relatives of cultivated tomato compared to other two species S. *cheesmanii and S. pimpinellifolium.* The results observed also support the notion that Phytochrome A and B1 plays unique roles in light mediated physiological responses as these two phytochromes showed a very few nonsynonymous SNPs. Comparatively a low dS/dN ratio was observed for both *PhyA* and *PhyB1* (0.36 and 0.08) than the other two phytochrome species (0.42 and 0.45 respectively for *phytochrome E* and *phytochrome F*). Moreover the location of most of the amino acid polymorphism outside the functionally important GAF and PHY domain indicates the due to functional importance of these domains in phytochrome mediated light signalling and the sequence of these domains remains conserved during evolution.

Considering the above results, we examined whether this observed pattern could be explained by selection as this could be due to selection on protein sequence and function. The observed distribution of nonsynonymous sites away from important domains might reflect that the GAF and PHY domains are more highly conserved than the rest of the protein. Tajima's D is a statistical test used to compare observed nucleotide diversity against the expected diversity under the assumption that all polymorphisms are selectively neutral and constant population size. The test finds out whether the evolution of a DNA sequence is neutral (random evolution) or non-neutral (under selection). A randomly evolving DNA sequence contains mutations, which do not affect the fitness and survival of an organism. A negative Tajima's D signifies an excess of low frequency polymorphisms relative to

expectation, indicating population size expansion (e.g., after a bottleneck or a selective sweep) and/or purifying selection. A positive Tajima's D signifies low levels of low and high frequency polymorphisms, indicating a decrease in population size and/or balancing selection.

Above results suggest that all phytochrome genes evolve neutrally as the analysis indicated that none of the phytochrome gene bear a significant Tajima D value (values greater than +2 or less than -2 are likely to be significant). The theoretical distribution of Tajima's D (between -2 and +2) explains that polymorphism ascertainment is not dependent on allele frequency. All the four phytochrome genes showed a negative Tajima D value indicates an excess of rare variation in the region, which can be consistent with population growth, or positive selection or purifying selection. The purifying selection in phytochrome locus strongly suggests that, most amino acid changes are deleterious and therefore, they are selected against the pressure. Alternatively the products of the unique genes are in general more highly conserved. The observed very low nucleotide diversity values for all the four phytochrome genes could be due to a relatively small long-term effective population size rather than any severe bottleneck during tomato evolution.

The phylogenetic relationship analysis data also correlated with SNP distribution data. Phylogram showed a topology where the green-fruited varieties considered for the study (*S.habrochaites, S. neorickii, S.chilense)* were at an ancestral position while the coloured fruits (*S. cheesmanii, S. pimpinellifolium*) were more of closely related position to tomato.

Comparison of DNA sequence of various organisms showed that during evolution there is a universal bias in favour of transition over transversion, although twice as many transversion type substitution i.e. substitution between purines and pyrimidine are possible. Knowledge of the pattern of nucleotide substitution is important as it can help estimating the number of substitutional events between DNA sequence as well as it assists in the phylogenetic

reconstruction that incorporate models of DNA sequence evolution. Part of this bias is due to the relatively high rate of mutation of methylated cytosine to thymine. At low sequence distance, this transition bias results in substitution pattern that is characterized by Ts/Tv ratios typically ranging between 2 and 10. Nucleotide base change analysis for phytochrome genes from wild tomato species showed that, there is no significant difference between transition and transversion in some of the phytochrome genes. The codominance of transition and transversion in *phytochrome B1* sequence is a striking result from our study. While other phytochrome showed a Ts/Tv ratio>1 i.e., *phytochrome A* (3) *phytochrome E* (1.8) and *phytochrome F* (1.1), *phytochrome B1* showed a Ts/Tv ratio of one.

Though the changes in sequence of different phytochrome are difficult to relate to individual function, the seedling phenotype of *S. habrochaites* under FR light was interesting. In this case, effect of FR light was at variance from AV and, it may be related to the ecological niche this particular wild relative is growing. The studies on variation in phytochrome SNPs in relation to geographic distribution may show strong association between certain SNP and ecotypes. However, to relate the SNP to light response or ecotype needs analysis of number of accessions. This aspect can be examined in a future study on tomato similar to Arabidopsis.

5.13 Light Regulation of Lateral Root Formation in Tomato

Lateral roots are derived from the primary roots to optimize primary function of root to acquire water and minerals. Lateral root formation is also a major determinant of root architecture development. The degree of root branching, immensely influence the anchorage by the plants' water and mineral uptake. Understanding the mechanism of lateral root formation is therefore of agronomic importance. Moreover, the role of light on LRF is not

investigated in tomato and this can serve as a good assay to examine the function of phytochrome.

The development of lateral roots is a highly plastic process, which is influenced greatly by both environmental factor and hormonal factor. Lateral root formation is initiated in the pericycle layer cells adjacent to the protoxylem poles of primary root with a highly ordered series of anticlinal divisions, which forms LRP (lateral root primordial). The subsequent development of the LRP involves a precise series of cell divisions that ultimately lead to the emergence of lateral roots (Malamy and Benfey, 1997a, 1997b).

It is a well-known fact that root tip excision can induce lateral roots in plants. Plant breeders take advantage of this attribute by removing the extreme tip of the roots of the plants before transferring them into field. The removal induces numerous lateral roots and thus a proper root architecture that support the plant system. Though the exact reason is not known, the LRF as a result of decapitation (root tip excision) was already observed in pea (Whightman and Thimann, 1980), and in Arabidopsis (Reed *et al.*, 1998).

Our result indicate that root tip exert some level of regulatory effect on lateral root formation. Since excision induces lateral root formation in tomato it is interesting to speculate on the nature of this signal. In addition, it is also worth to examine how this signal interacts with light. At this moment the nature of the signal and the signalling events between the excision of root tip and lateral root formation are unknown.

The root tip excision induced nearly 5-fold increase in lateral root formation in tomato. The result suggests that, in tomato, as in other plant system wound response due to excision of tip does not inhibit lateral root development. Since root tip excision induces LRF, it can be assumed that root tip might be exerting an inhibitory effect on lateral root development.

Several studies have shown that Auxin is necessary for various stages of plant development. Auxin application to growing plants was found to stimulate lateral root development. (Torrey, 1950; Blakely *et al.,* 1982; Muday and Haworth, 1994). Conversely application of Auxin transport inhibitors decreases the number of lateral roots (Muday and Haworth, 1994). Moreover various auxin-related mutants have been reported to arrest lateral root formation in Arabidopsis (Celenza *et al.,* 1995). Auxin is highly required in the initial stage of LRP formation, to establish a population of rapidly dividing cells in the pericycle. In the later stage of development derivatives of the LRP subsequently form hormone-autonomous meristems. The developing lateral root primordia are reported to get auxin via polar auxin transport, before they become hormone autonomous (Reed *et al.,* 1998). Polar auxin transport is regulated auxin delivery system used by the plants to mobilize from the source tissue to the sink tissue (Bennett *et al.,* 1998). Previous studies (Bhalerao *et al.,* 2002) suggests that , auxin synthesis occurs in the first developing true leaves act as a source of auxin for the emergence of first LRP and later in the development , the primordial depends on leaf derived auxin to a lesser degree as the root system autonomously synthesize its own Auxin.

Most literature report on LRF formation supports that at the initial stage of seedling development, auxin, which is synthesised in the developing leaves, is required for LRF and plants depends on polar auxin transport from aerial tissue for the initiation of LRP. In this study, mechanism of LRF as a result of decapitation at a very early stage of development (as young as 2 DAG), is not known. There are two possibilities that may be responsible for this phenomenon.1) Presence of an auxin independent signal that root tip decapitation induce 2) removal of an inhibitory signal that is already there in the root tip and is removed due to excision. Though we do not know the exact reason, we found more number of lateral roots in seedlings, which are decapitated at 2DAG than that of seedlings at 4DAG. This may be

related to a development dependent response as lateral root emergence requires 2-4 days. Therefore late excision at 4 DAG may not lead to visible LRF. To check the possibility of the presence of auxin independent signal in decapitated seedlings, auxin transport was inhibited by supplementing TIBA, an auxin transport inhibitor in decapitated seedlings at the time of excision. The slightly enhanced LRF in TIBA treated seedlings indicate that the signal is auxin independent, as reduction of PAT stimulated LRF. The removal of aerial tissues has an inhibitory effect on LRF. The above studies suggest that, this phenomenon could be because of the removal of the auxin source (developing leaves) for LRP formation (Bhalerao *et al.*, 2002). Interestingly our results showed a reduction of LRF in seedlings from which cotyledons were also excised. Since excision of complete shoot abolish LRF completely, it has to be considered that the reduction may be more related to carbohydrate starvation as developing root depends on shoot for energy.

However, we cannot rule out the role of shoot-derived auxin. In future, we may examine whether after excision of aerial tissue, application of auxin on cut stump can lead to LRF formation.

Recent genetic studies and mutational analysis have shown that ethylene, a gaseous plant hormone; negatively regulate lateral root formation in various plants. Both ethylene overproducing mutants and constitutive ethylene signalling mutants shows decreased lateral root formation (Ivanchenko *et al.*, 2008; Negi *et al.*, 2008; Negi *et al.*, 2010). Moreover, treatment with ethylene or ethylene precursors like, 1-aminocyclopropane carboxylic acid (ACC) also inhibits lateral root formation. The effect of ethylene in excision induced LRF was examined by adding an ethylene precursor and our results show LRF as a result of root tip excision is not related to ethylene. The addition of ACC (an ethylene precursor) stimulated LRF in excised seedlings rather than inhibiting it, as evidently more number of lateral roots in the seedlings which were treated with ACC showed more number of lateral roots as compared to untreated one when the seedlings were subjected to root tip excision.

Little information on role of light in lateral root formation is available. Previous reports showed that, in Arabidopsis dark grown seedlings exhibited a reduced LRF compared to WL grown seedlings (Bhalerao *et al.*, 2002). In addition light also affect the formation of indole-3-acetic acid (IAA) in germinating Arabidopsis seedlings (Bhalerao *et al.*, 2002). Therefore it is possible that in tomato too light may regulate the process of LRF by stimulating auxin synthesis in young leaves. To examine whether LRF as a result of excision also would require a specific light/ photoreceptor, an experiment was done in which seedlings were grown under R, FR, WL and D and subsequently their root tips were removed. The result clearly indicated that WL stimulated LRF as a result of root tip excision.

Since R/FR grown seedlings shown less LRF than WL grown seedlings, it indicate that multiple photoreceptor control the LRF stimulation in tomato. It remains to be examined whether cryptochrome and/or photropins are influencing the response, in addition to phytochromes.

In summary our results show that excision induce a signal that stimulate LRF in tomato seedlings. Since inhibition of PAT stimulates LRF formation, this may be related to auxin accumulation of LR founder cells. It remained to be examined if shoot derived auxin plays a role in the response, but it appears that shoot also contribute to LRF by providing necessary nutrition such as carbohydrate. The role of ethylene in the response appears to be minimal as ACC application did not inhibit LR formation. The light has a modulating role and possibly all photoreceptors play in this response as WL grown root induce more LRF than R and FR light grown seedlings. Since light has a specific modulatory role in this process, effect of R/FR light on excision induced LRF formation can be used to examine the relative role of different phytochrome species in this response.

6. SUMMARY

Phytochrome is a plant photoreceptor, which is known to regulate a wide variety of responses of plants to light, including induction of seed germination, modulation of elongation growth, promotion of chloroplast development, and induction of flowering. An understanding of the molecular mechanism of phytochrome action is therefore essential to elucidate the complex processes of plant growth and development. In the present study, a reverse genetic, non-transgenic approach like TILLING and Eco-TILLING, were used for the isolation of induced mutations in *Phytochrome A* genes in an EMS mutagenized population of tomato. N-terminal region of the gene, which codes for photosensory region of the protein, was targeted for mutation mining. Here we report the isolation of novel mutant alleles of *phytochrome A* and *B1* that would facilitate the functional analyses of different domains phytochromes in tomato.

A population of nearly 10,000 EMS mutagenized M_2 plants were screened for mutations in genes encoding the PHYA and PHYB1 proteins. For these genes, the focus of mutation screening was on the regions predicted by CODDLE (Codons Optimised to Discover Deleterious Lesions). The above analysis predicted that mutations in exons 1 and 2 might cause most deleterious effects on *phytochrome A* and *B1* function. These two exons encodes for the light signalling domains, which consists of core light sensing components like PAS, GAF and PHY. TILLING of *phytochrome A* in the above region yielded six independent point mutations, out of which we could identify only one confirmed individual plant line in subsequent analysis. TILLING of phytochrome B1 gene yielded two independent point mutations and we could confirm only one mutation at individual plant level.

Though we screened a large population of nearly 10,000 M_2 plants, we could detect only a few mutations in these two phytochrome genes. Though we do not know the reason for the low frequency of mutations in tomato M_2 lines, one probable explanation is recalcitrance of tomato to mutagenesis. The very low frequency of mutation in *phytochrome A* and *B1* suggests the conserved nature of these two phytochrome genes and their importance for plant

survival. The mutant line (Accession number $M8_2M2895$) which had mutation in *phytochrome A* gene, was further analysed to detect the molecular nature of the mutation. Sequence analysis of *phytochrome A* gene from the above mutant line revealed the presence of a nucleotide change from guanine (G) to Adenine (A) at 1586^{th} position of open reading frame (ORF). The conversion of amino acid showed that this change causes a missense mutation as it alters the codon GGG to AGG leading to the replacement of glycine with arginine at amino acid 496(G496R) in the mutant PHYA polypeptide. This change causes the shift from non-polar neutral amino acid to polar positive amino acid in the PHY domain of Phytochrome. Detailed phenotype analysis of the plant revealed that although at the seedling stage any characteristic change was not visible, the adult mutant plant exhibited an altered phenotype compared to wild type control.

Similar to *phytochrome A* only one mutant allele for *phytochrome B1* (Accession AV 60 mM 888) was isolated from the above mutagenized population of tomato. The sequence of mutant *phytochrome B1*gene revealed a change from cytosine (C) to thymine (T), which leads to a silent or synonymous mutation. This mutation affected the third base of a codon (CTC to CTT) which does not change the amino acid encoded by that codon. Phenotype characterization revealed that the above mutant line did not exhibit any perceptible phenotypic change either at the seedling stage or at the mature stage.

Both *phytochrome A* and *phytochrome B1* genes were also screened for the detection of SNPs in a population of 600 natural accessions of tomato using the same region that was used for TILLING. A large number of polymorphisms were observed for both *phytochrome A* and *B1* and accessions were classified into different haplotypes based on the nature of polymorphisms.

Nearly 19 accessions showed polymorphism in target region of *phytochrome A*, in comparison to the reference cultivar WT Arka Vikas. These accessions were classified into 4 different haplotypes. The precise position and nature of the identified polymorphisms were determined by *phytochrome A* gene sequencing. Out of 4 haplotypes, 2 haplotypes (HT.2 and HT.4) were confirmed for the polymorphism by sequencing. Haplotype 2 (HT. 2) showed a nucleotide change G2614A, which was a nonsynonymous mutation (missense). It corresponded to amino acid change E748K (Glutamic acid to Lysine) located at the PAS domain of the amino-terminus of the protein.

Considering the importance of PAS domain in *phytochrome A* function we further analysed HT.2 for its impaired phytochrome function and we selected accession EC 528362, which represent HT.2 for further analysis. Several studies have reported that seedlings of mutant plants with defect in Phytochrome A protein showed an elongated phenotype under far red light (van Tuinen *et al.*, 1995a). To ascertain the effect of above SNP on seedling phenotype, seedlings of the accession EC 528362 and its wild type control *cv.* AV were grown under continuous blue, red, far red light, white light and absolute darkness. On comparison with the wild type, we found no difference between the WT control and the mutant accession under all light conditions, except in FR light. In FR light, the hypocotyl of EC 528362 was slightly elongated compared to WT. Interestingly, roots of the accession (EC 528362) exhibited an opposite response, as it displayed a shorter root under FR light compared to WT plant.

For *phytochrome B1*, 13 accessions showed polymorphisms in comparison to Arka Vikas and were grouped in 3 different haplotypes. Sequencing results suggested that except HT.3, the two other haplotypes do not carry any nucleotide change that would bring about a non-synonymous change. HT.3 showed a nucleotide change corresponding to a non-synonymous mutation. It was found that the accession EC 34480, which represents HT.3 exhibited a

nucleotide change from Adenine (A) to Thymine (T) at the 164th position of ORF causing an amino acid change from glutamic acid to valine. In the mutant PHY B1 protein, the above amino acid change (from polar amino acid to non-polar neutral) would affect the functionality of the PHYB1 protein. The structural superimposition of PHYB1 model of EC 34480 and wild type protein showed that the RMSD (Root Mean Square Deviation) for the protein structure superimposition is 5.04 Å and it results in a significant deviation of the mutated protein structure.

Though the accession EC-34480, at seedling stage did not indicate any abnormal phenotypes with broad spectrum light experiments, field grown plants showed a strikingly different phenotypic changes in plant architecture. One of the characteristic features was a drastic reduction in the number of branches and flowers and retarded growth. In addition to this, an almost thirty-day delay in flowering was also observed for this accession.

Given the diversity of ecological niches where different wild relatives of tomato grow in diverse environmental conditions ranging from deserts to high-altitude mountains, we examined sequence variation at the four *Phytochrome loci, PhyA, PhyB1, PhyE and PhyF* in wild tomato species. An exhaustive sequencing approach was applied to understand the structure of this gene family by amplifying as many paralogous and allelic phytochrome sequences as possible. To evaluate nucleotide diversity and sequence evolution at various phytochrome loci in wild relatives of tomato, five different wild relatives (*S. habrochaites, S. neorickii, S. chilense, S. cheesmanii, and S. pimpinellifolium)* were used.

Sequence analysis showed that all the four phytochromes, which were analysed in this study, harboured several SNPs (e.g., *PHYA*: 25, *PHYB1*:49, *PHYE*: 56, *PHYF*: 26). Similar to the results found in EcoTILLING, we found more synonymous changes (*PHYA*: 16, *PHYB1*:45, *PHYE*: 31, *PHYF*: 15) than non-synonymous changes (*PHYA*: 9, *PHYB1:*4,

PHYE: 25, *PHYF*: 11) in each gene. The ratio of total SNPs to SNPs that were non-synonymous ranged from 8% to 45% in different phytochrome members with *PHYE* ranking first (0.45) with more synonymous changes and other phytochromes viz *PHYF*, *PHYA* and *PHYB1* yielding ratios of 0.42, 0.36 and 0.8 respectively. Three species, *S. habrochaites (*71 SNPs*) S. neorickii (*42 SNPs*) and S.chilense (*34 *SNPs)* harboured higher number of SNPs compared to the two other species. Sequence analysis of the other two tomato species revealed that they bear extremely less polymorphic variation (*S. cheesmanii*, 9 SNPs) or none in case of (*S. pimpinellifolium*, 0 SNP)

Tajima's D test showed that all four phytochrome genes evolved in a neutral manner. D_{total} (entire sequence), D_{nonsyn} (nonsynonymous sites), D_{syn} (synonymous sites), and Pi (nucleotide diversity) were calculated for all four phytochrome genes and it was found that none of these genes showed a significant D value indicating that the nucleotide diversity values of all phytochrome genes were low.

Phylogenetic trees were constructed using nucleotide sequencing data. The dendrograms based on sequence data, followed a topology showing the green fruited varieties considered for the study (*S.habrochaites, S. neorickii, and S.chilense)* were at an ancestral position while the coloured fruits (*S. cheesmanii*, *S. pimpinellifolium*,) were more closely related position. This finding indicates the absence of lateral gene transfer events in the process of domestication and the products of the unique genes such as phytochrome that are essential for plant survival are in general more highly conserved.

REFERENCES

Adamse P, Peters JL, Jaspers PAPM, van Tuinen A, Koornneef M and Kendrick RE (1989) Photocontrol of anthocyanin synthesis in tomato seedlings: A genetic approach. *Photochem Photobiol* **50:** 107–111

Ahmad M, Cashmore AR (1993) HY4 gene of A. thaliana encodes aprotein with the characteristics of a blue-light photoreceptor. *Nature* **366:** 162–166

Ahmad M, Lin C, Cashmore AR (1995) Mutations throughout an Arabidopsis blue-light photoreceptor impair blue-light-responsive anthocyanin accumulation and inhibition of hypocotyl elongation. *Plant J* **8:** 653–658

Alba R, Kelmenson PM, Cordonnier-Pratt MM, Pratt LH (2000) The phytochrome gene family in tomato and the rapid differential evolution of this family in angiosperms. *Mol Biol Evol* **17:** 362–373

Aukerman MJ, Hirschfeld M, Wester L, Weaver M, Clack T, Amasino RM, Sharrock RA (1997) A deletion in the PHYD gene of the Arabidopsis Wassilewskija ecotype defines a role for phytochrome D in red/far-red light sensing. *The Plant Cell* **9:** 1317–1326

Bagnall DJ (1993) Light quality and vernalization interact in controlling late flowering in Arabidopsis ecotypes and mutants. *Ann Bot (Lond*) **71:** 75–83

Baker NR, Nogues S, Allen DJ (1997) Photosynthesis and photoinhibition. In: Lumsden PJ, ed. Plants and UV-B: Responses to Environmental Change. *Cambridge University Press*, Cambridge, pp 95–111

Balasubramanian S, Sureshkumar S, Agrawal M, Michael TP, Wessinger C, Maloof JN, Clark R, Warthmann N, Chory J, Weigel D (2006) The PHYTOCHROME C photoreceptor gene mediates natural variation in flowering and growth responses of Arabidopsis thaliana. *Nat Genet* **38:**711-715

Ballaré CL (1999) Keeping up with the neighbours: phytochrome sensing and other signalling mechanisms. *Trends in Plant Science* **4:** 97–102

Ballaré CL, Casal JJ, Kendrick RE (1991) Responses of light-grown wild-type and long-hypocotyl mutant cucumber seedlings to natural amd simulated shade light. *Photochem. Photobiol*. **54:** 819–826

Ballaré CL, Scopel AL, Sa´nchez RA (1990) Far-red radiation reflected from adjacent leaves: an early signal of competition in plant canopies. *Science* **247:** 329–332

Ballesteros ML, Bolle C, Lois LM, Moore JM, Vielle-Calzada JP, Grossniklaus U, Chua NH (2001) LAF1, a MYB transcription activator for phytochrome A signaling. *Genes Dev* **15:** 2613–2625

Baskin TI, lino M (1987) An action spectrum in the blue and ultraviolet for phototropism in alfalfa. *Photochem. Photobiol*. **46:**127-136

Bauer D, Viczián A, Kircher S, Nobis T, Nitschke R, Kunkel T, Panigrahi KC, Adám E, Fejes E, Schäfer E, Nagy F (2004) Constitutive photomorphogenesis 1 and multiple photoreceptors control degradation of phytochrome interacting factor 3, a transcription factor required for light signaling in Arabidopsis. *Plant Cell* **16:** 1433-1445

Beggs CJ, Wellmann E (1994) Photocontrol of flavonoid biosynthesis. In: R. E. Kedrick and G. H. M. Kronenberg (Eds.). Photomorphogenesis in Plants. *Kluwer Academic Publishers. Dordrecht*, pp 733-751

Bennett MJ, Marchant A, May ST, Swarup R (1998) Going the distance with auxin: Unravelling the molecular basis of auxin transport. *Philos Trans R Soc Lond B Biol Sci* **353:**1511–1515

Bhalerao RP, Eklof J, Ljung K, Marchant A, Bennett M, Sandberg G (2002) Shoot-derived auxin is essential for early lateral root emergence in Arabidopsis seedlings. *Plant J* **29:** 325–332

Blakely LM, Durham M, Evans TA, Blakely RM (1982) Experimental studies on lateral root formation in radish seedling roots. I. General methods, developmental stages, and spontaneous formation of laterals. *Bot Gaz* **143**: 341–352

Blumenstein A, Vienken K, Tasler R, Purschwitz J, Veith D, Frankenberg-Dinkel N, Fischer R (2005) The Aspergillus nidulans phytochrome FphA represses sexual development in red light. *Curr Biol* **15:** 1833–1838

Bolle C, Koncz C, Chua NH (2000) PAT1, a newmember of the GRAS family, is involved in phytochrome A signal transduction. *Genes Dev* **14:**1269–1278

Borthwick HA, Hendricks SB, Parker MW, Toole EH, Toole VK (1952) A reversible photoreaction controlling seed germination. *Proc Natl Acad Sci USA* **38:** 662-666

Botto JF, Alonso-Blanco C, Garzaron I, Sanchez RA, Casal JJ (2003) The Cape Verde Islands allele of cryptochrome 2 enhances cotyledon unfolding in the absence of blue light in Arabidopsis. *Plant Physiol* **133:** 1547–1556

Botto JF, Sanchez RA, Whitelam GC, Casal JJ (1996) Phytochrome A mediates the promotion of seed germination by very low fluences of light and canopy shade-light in Arabidopsis. *Plant Physiol* **110:** 439–444

Briggs WR, Christie JM (2002) Phototropins 1 and 2: Versatile plant blue-light receptors. *Trends Plant Sci.* **7:** 204–210

Burrmeijer WF, Roelofs TA, Vredenberg WJ (1987) Some aspects of altered structure and function of the photosynthetic apparatus in phytochrome-less mutants of tomato. In :Progress in photosynthetic research II (J Biggens *ed*). *Marthinus Nijhoff, Dordrecht* pp 383–386

Casal JJ, Davis SJ, Kirchenbauer D, Viczian A, Yanovsky MJ, Clough RC, Kircher S, Jordan-Beebe ET, Schäfer E, Nagy F, Vierstra RD (2002) The serine-rich N-terminal domain of oat phytochrome A helps regulate light responses and subnuclear localization of the photoreceptor. *Plant Physiol* **129:**1127–1137

Casal JJ, Luccioni LG, Oliverio KA, Boccalandro HE (2003) Light, phytochrome signalling and photomorphogenesis in Arabidopsis. *Photochem Photobiol Sci* **2**:625–636

Casal JJ, Sa´nchez RA, Yanovsky MJ (1997) The function of phytochrome A. *Plant, Cell, and Environment* **20:**813–819

Casal JJ, Sanchez RA (1998) Phytochromes and seed germination. *Seed Sci Res* **8:** 317–329

Casimiro I, Marchant A, Bhalerao RP, Beeckman T, Dhooge S, Swarup R, Graham N, Inzé D, Sandberg G, Casero PJ, Bennett M (2001) Auxin transport promotes Arabidopsis lateral root initiation. *Plant Cell* **13**: 843-852

Caspary R (1860) Bulliarda aquatica D.C. *Schrifen KSniglichen Physikalisch-Okonomischen Gesellschaft K6nigsberg* **1:** 66-91

Celenza JL, Grisafi PL, Fink GR (1995) A pathway for lateral root formation in Arabidopsis thaliana. *Genes Dev* **9:** 2131–2142

Chattopadhyay S, Ang LH, Puente P, Deng XW, Wei N (1998) Arabidopsis bZIP protein HY5 directly interacts with lightresponsive promoters in mediating light control of gene expression. *Plant Cell* **10:** 673–683

Chen M, Chory J, Fankhauser C (2004) Light signal transduction in higher plants. *Annu Rev Genet* **38:**87–117

Chu LY, Shao HB, Li MY (2005) Molecular mechanisms of phytochrome signal transduction in higher plants. *Colloids Surf B Biointerfaces* **45:** 154-161

Colbert T, Till BJ, Tompa R, Reynolds S, Steine MN, Yeung AT, McCallum CM, Comai L, Henikoff S (2001) High-throughput screening for induced point mutations. *Plant Physiol* **126:** 480-484

Comai L, Young K, Till BJ, Reynolds SH, Greene EA, Codomo CA, Enns LC, Johnson JE, Burtner C, Odden AR, Henikoff S (2004) Efficient discovery of DNA polymorphisms in natural populations by EcoTILLING. *Plant J.* **37:** 778-786

Crosson S, Rajagopal S, Moffat K (2003) The LOV domain family: Photoresponsive signaling modules coupled to diverse output domains. *Biochemistry* **42:** 2–10

Dehan K, Tal M (1978) Salt tolerance in the wild relatives of the cultivated tomato:Response of solanum pennellii to high salinity. *Irrigation Sci* **1:** 71-76

Dehesh K, Franci C, Parks BM, Seeley KA, Short TW, Tepperman JM, Quail PH (1993) Arabidopsis HY8 locus encodes phytochrome A. *Plant Cell* **5:** 1081–1088.

Devlin PF, Kay SA (1999) Cryptochromes: bringing the blues to circadian rhythms. *Trends Cell Biol* **9:** 295–298

Devlin PF, Patel SR, Whitelam GC (1998) Phytochrome E influences internode elongation and flowering time in Arabidopsis. *The Plant Cell* **10:** 1479–1487

Devlin PF, Robson PRH, Patel SR, Goosey L, Sharrock RA, Whitelam GC (1999) Phytochrome D acts in the shade-avoidance syndrome in Arabidopsis by controlling elongation and flowering time. *Plant Physiol* **119:** 909–915

Dieterle M, Zhou YC, Schafer E, Funk M, Kretsch T (2001) EID1, an F-box protein involved in phytochrome A-specific light signaling. *Genes Dev* **15:** 939–944

Don RH, Cox PT, Wainwright BJ, Baker K, Mattick JS (1991) "Touchdown" PCR to circumvent spurious priming during gene amplification. *Nucleic Acids Res.* **19:** 4008-4008

Duek PD, Fankhauser C (2003) HFR1, a putative bHLH transcription factor, mediates both phytochrome A and cryptochrome signalling. *Plant J* **34:** 827–836

Eckardt NA (2002) Specificity and cross-talk in plant signal transduction: January 2002 Keystone Symposium. *Plant Cell (Suppl)* S9–S14

Eisinger WR, Bogomolni RA, Taiz L (2003) Interactions between a blue–green reversible photoreceptor and a separate UV-B receptor in stomatal guard cells. *Amer. J. Bot.* **90:** 1560–1566

Favory JJ, Stec A, Gruber H, Rizzini L, Oravecz A, Funk M, Albert A, Cloix C, Jenkins GI, Oakeley EJ, Seidlitz HK, Nagy F, Ulm R (2009) Interaction of COP1 and UVR8 regulates UVB-induced photomorphogenesis and stress acclimation inArabidopsis. *EMBO J* **28:** 591–601

Filiault DL, Wessinger CA, Dinneny JR, Lutes J, Borevitz JO, Weigel D, Chory J, Maloof JN (2008) Amino acid polymorphisms in Arabidopsis phytochrome B cause differential responses to light. *Proc Natl Acad Sci U S A* **105:**3157-3162

Finckh U, Rolfs A (1998) PCR optimization strategies. Roche Molecular Biochemicals. Internet address http://206.53.227.20/prod_inf/manuals/pcr_man/pcr_toc.htm

Fisher RA (1930) The genetical theory of natural selection. *Oxford Univ. Press, Oxford, U.K*

Flint LH, McAlister ED (1935) Wave lengths of radiation in the visible spectrum inhibiting the germination of light-sensitive lettuce seed. *Smithson Misc Collec* **94**: 1-11

Frankhauser C, Chory J (1997) Light control of plant development. *Annu. Rev. Cell Dev. Biol.* **13:** 203–229

Franklin KA, Praekelt U, Stoddart WM, Billingham OE, Halliday KJ, Whitelam GC (2003b). Phytochromes B, D, and E act redundantly to control multiple physiological responses in Arabidopsis. *Plant Physiol*. **131:** 1340–1346

Franklin KA, Davis SJ, Stoddart WM, Vierstra RD, Whitelam GC (2003a) Mutant analyses define multiple roles for phytochrome C in Arabidopsis photomorphogenesis. *Plant Cell* **15:** 1981–1989

Franklin KA, Whitelam GC (2004) Light signals, phytochromes and cross-talk with other environmental cues. *J Exp Bot* **55:** 271–276

Franklin KA, Whitelam GC (2005) Phytochromes and shade-avoidance responses in *plants. Ann Bot* **96:** 169–175

Froehlich AC, Noh B, Vierstra RD, Loros J, Dunlap JC (2005) Genetic and molecular analysis of phytochromes from the filamentous fungus Neurospora crassa. *Eukaryot Cell* **4:**2140-2152

Gady AL, Hermans FW, Van de Wal MH, van Loo EN, Visser RG, Bachem, CW (2009) Implementation of two high through-put techniques in a novel application: detecting point mutations in large EMS mutated plant populations. *Plant Methods* **5:** 13

Gil P, Kircher S, Adam E, Bury E, Kozma-Bognar L, Schafer E, Nagy F (2000) Photocontrol of subcellular partitioning of phytochrome-B: GFP fusion protein in tobacco seedlings. *Plant J* **22:** 135-145

Gilchrist EJ, Haughn GW, Ying CC, Otto SP, Zhuang J, Cheung D, Hamberger B, Aboutorabi F, Kalynyak T, Johnson L, Bohlmann J, Ellis BE, Douglas CJ, Cronk QCB (2006) Use of EcoTILLING as an efficient SNP discovery tool to survey genetic variation in wild populations of Populus trichocarpa. *Mol Ecol* **15:**1367-1378

Giliberto L, Perrotta G, Pallara P, Weller JL, Fraser PD, Bramley PM, Fiore A, Tavazza M, Giuliano G (2005) Manipulation of the blue light photoreceptor cryptochrome 2 in tomato affects vegetative development, flowering time, and fruit anti-oxidant content. *Plant Physiol* **137:**199–208

Goto N, Kumagai T, Koornneef M (1991) Flowering responses to light-breaks in photomorphogenic mutants of Arabidopsis thaliana, a long day plant. *Physiologia Plantarum* **83:** 209–215

Greene EA, Codomo CA, Taylor NE, Henikoff JG, Till BJ, Reynolds SH, Enns LC, Burtner C, Johnson JE, Odden AR, Comai L, Henikoff S (2003) Spectrum of chemically induced mutations from a large-scale reverse-genetic screen in Arabidopsis. *Genetics* **164:** 731–740

Guo H, Mockler T, Duong H, Lin C (2001) SUB1, an Arabidopsis Ca^{2+}-binding protein involved in cryptochrome and phytochrome coaction. *Science* **291:** 487–489

Guo H, Yang H, Mockler TC, Lin C (1998) Regulation of flowering time by Arabidopsis photoreceptors. *Science* **279:** 1360–1363

Hall A, Kozma-Bognár L, Tóth R, Nagy F, Millar AJ(2001) Conditional circadian regulation of PHYTOCHROME A gene expression. *Plant Physiol* **127:** 1808–1818

Hangarter RP (1997) Gravity, light and plant form. *Plant Cell Environ* **20:** 796–800

Harmon FG, Kay SA (2003) The F box protein AFR is a positive regulator of phytochrome A-mediated light signaling. *Curr Biol* **13:** 2091–2096

Hasunuma K, Furukawa K, Kubota M, Watanabe M (1987) partial characterization and light-induced regulation of GTP- binding proteins in Lemna paucicostata. *Photochem. Photobiol.* **46:** 531-535

Heijde M, Ulm R (2012) UV-B photoreceptormediated signalling in plants. *Trends Plant Sci*.**17:** 230–237

Heim MA, Jakoby M, Werber M, Martin C, Weisshaar B, Bailey PC (2003) The basic helix-loop-helix transcription factor family in plants: a genome-wide study of protein structure and functional diversity. *Mol Biol Evol* **20:** 735–747

Hennig L, Stoddart WM, Dieterle M, Whitelam GC, Schäfer E (2002) Phytochrome E controls light-induced germination of Arabidopsis.*Plant Physiol.* **128:** 194–200

Hisada A, Hanzawa H, Weller JL, Nagatani A, Reid JB, Furuya M (2000) Light-induced nuclear translocation of endogenous pea phytochrome A visualized by immune cytochemical procedures. *Plant Cell* **12:** 1063-1078

Hoecker U, Tepperman JM, Quail PH (1999) SPA1, a WD-repeat protein specific to phytochrome A signal transduction. *Science* **284:** 496–499

Holm M, Ma LG, Qu LJ, Deng XW (2002) Two interacting bZIP proteins are direct targets of COP1-mediated control of light dependent gene expression in Arabidopsis. *Genes Dev* **16:** 1247–1259

Huala E, *et al.*, (1997) Arabidopsis NPH1: A protein kinase with a putative redox-sensing domain. *Science* **278:** 2120–2123

Hudson M, Ringli C, Boylan MT, Quail PH (1999) The FAR1 locus encodes a novel nuclear protein specific to phytochrome A signaling. *Genes Dev* **13:** 2017–2027

Hudson ME, Lisch DR, Quail PH (2003) The FHY3 and FAR1 genes encode transposase-related proteins involved in regulation of gene expression by the phytochrome A-signaling pathway. *Plant J* **34:** 453–471

Innis MA, Gelfand DH (1990) Optimization of PCRs. In MA Innis, DH Gelfand, JJ Sninsky, TJ White, eds, PCR Protocols. A Guide to Methods and Applications. *Academic Press, San Diego,* p 3-13

Ivanchenko MG, Muday GK, Dubrovsky JG (2008) Ethylene-auxin interactions regulate lateral root initiation and emergence in Arabidopsis thaliana. Plant J **55**: 335-347

Johnson E, Bradley JM, Harberd NP, Whitelam GC (1994) Photoresponses of light-grown *phyA* mutants of *Arabidopsis:* phytochrome A is required for the perception of daylength extensions. *Plant Physiol* **105:** 141-149

Jones AM, Ecker JR, Chen JG (2003) A reevaluation of the role of the heterotrimeric G protein in coupling light responses in Arabidopsis. *Plant Physiol* **131:** 1623–1627

Kaiserli E, Jenkins GI (2007) UV-B promotes rapid nuclear translocation of the Arabidopsis UV-B specific signaling component UVR8 and activates its function in the nucleus. *Plant Cell* **19:** 2662–2673

Karniol B, Wagner JR, Walker JM, Vierstra RD (2005) Phylogenetic analysis of the phytochrome superfamily reveals distinct microbial subfamilies of photoreceptors. *Biochem. J* **392:** 103–116

Katekar GF, Geissler AE (1980) Auxin transport inhibitors. IV. Evidence of a common mode of action for a proposed class of auxin transport inhibitors, the phytotropins. *Plant Physiol* **66:** 1190–1195

Kendrick RE, Kerckhoffs LHJ, Pundsnes AS, van Tuinen A, Koornneef M, Nagatani A, Terry MJ, Tretyn A, Cordonnier-Pratt MM, Hauser B, Pratt LH (1994) Photomorphogenic mutants of tomato. *Euphytica* **79:** 227–234

Kendrick RE, Kerckhoffs LHJ, Van Tuinen A, Koornneef M (1997) Photomorphogenic mutants of tomato. *Plant Cell Environ.* **20:** 746–751

Kendrick RE, Kronenberg GHM (1994) Photomorphogenesis in Plants, Ed2. Kluwer, Dordrecht, Netherlands

Kennis JTM, Crosson S, Gauden M, van Stokkum IHM, Moffat K, van Grondelle R (2003) Primary reactions of the LOV2 domain of phototropin, a plant blue-light photoreceptor. *Biochemistry* **42:**3385–92

Kerckhoffs LHJ, Kelmenson PM, Schreuder CI, Kendrick CI, Kendrick RE, Hanhart CJ, Koornneef M, Pratt LH and Cordonnier MM (1999) Characterization of the gene encoding the apoprotein of phytochrome B2 in tomato, and identification of molecular lesions in two mutant alleles. *Mol Gen Genet* **261:** 901–907

Kerckhoffs LHJ, van Tuinen A, Hauser B, Cordonnier-Pratt MM, Nagatani A, Koornneef M, Pratt LH and Kendrick RE (1995) Molecular analysis of *tri*-mutant alleles in tomato indicates the *tri* locus is the gene encoding the apoprotein of phytochrome B1. *Planta* **164:** 333–344

Kim L, Kircher S, Toth R, Adam E, Schafer E, Nagy F (2000) Light-induced nuclear import of phytochrome-A: GFP fusion proteins is differentially regulated in transgenic tobacco and Arabidopsis. *Plant J* **22:** 125-133

Kircher S, Kozma-Bognar L, Kim L, Adam E, Harter K, Schafer E, Nagy F (1999) Light quality-dependent nuclear import of the plant photoreceptors phytochrome A and B. *Plant Cell* **11:** 1445-1456

Koornneef M, Cone JW, Dekens RG, O'Herne-Robers EG, Spruit CJP, Kendrick RE (1985) Photomorphogenic responses of long hypocotyl mutants of tomato. *J Plant Physiol* **120:** 153-165

Koornneef M, Rolff E, Spruit CJP (1980). Genetic control of lightinhibited hypocotyl elongation in Arabidopsis thaliana (L.). *Z. Pflanzenphysiol. Bd.* **100:** 147−160

Kraepiel Y, Julien M, Cordonnier-Pratt MM, Pratt L (1994) Identification of two loci involved in phytochrome expression on Nicotiana plumbaginifoliu and lethality of the corresponding double mutant. *Mo1 Gen Genet* **242:** 559-565

Kreader CA (1996) Relief of amplification inhibition in PCR with bovine serum albumin or T4 gene 32 protein. *Appl Environ Microbiol* **62:**1102–1106

Lake JV, Slack G (1961) Dependence on light of geotropism in plant roots. *Nature* **191:** 300-302

Laskowski MJ, Williams ME, Nusbaum HC, Sussex IM (1995) Formation of lateral root meristems is a two-stage process. *Development* **121:** 3303-3310

Lazarova GI, Kerckhoffs LHJ, Brandstädter J, Matsui M, Kendrick RE, Cordonnier- PrattMMand Pratt LH (1998a) Molecular analysis of *PHYA* in wild-type and phytochrome A-deficient mutants of tomato. *Plant J* **14:** 653–662

Lazarova GI, Kubota T, Frances S, Peters JL, Hughes MJG, Brandstädter J, Szëll M, Matsui M, Kendrick RE, Cordonnier-Pratt MM and Pratt LH (1998b) Characterization of tomato *PHYB1* and identification of molecular defects in four mutant alleles. *Plant Mol Biol* **38:** 1137–1146

Librado P, Rozas J (2009) DnaSP v5: A software for comprehensive analysis of DNA polymorphism data. *Bioinformatics* **25:** 1451-1452

Lin C (2002) Blue light photoreceptors and signal transduction. *Plant Cell Suppl*. **2002:** 207–225

Lin C, Robertson DE, Ahmad M, Raibekas AA, Jorns MS, Dutton PL, Cashmore AR (1995) Association of flavin adenine dinucleotide with the Arabidopsis blue light receptor CRY1. *Science* **269:** 968–970

Lin C, Shalitin D (2003) Cryptochrome structure and signal transduction. *Annu Rev Plant Biol* **54:** 469–496

Lin C, Yang H, Guo H, Mockler T, Chen J, Cashmore AR (1998) Enhancement of blue-light sensitivity of Arabidopsis seedlings by a blue light receptor cryptochrome 2. *Proc Natl Acad Sci* USA **95:** 2686–2690

Lippman ZB, Cohen O, Alvarez JP, Abu-Abied, M, Pekker I, Paran I *et al.* (2008) The making of a compound inflorescence in tomato and related nightshades. *PLoS Biol* **6:** e288

Liscum E, Briggs WR (1996) Mutations of Arabidopsis in potential transduction and response components of the phototropic signaling pathway. *Plant Physiol.* **112:** 291-296

Liscum E, Hangarter RP (1993) Genetic evidence that the red-absorbing form of phytochrome B modulates gravitropism in Arabidopsis thaliana. *Plant Physiol.* **103:**15–19

Liscum E, Hodgson DW and Campbell TJ (2003) Blue light signaling through the cryptochromes and phototropins.So that is what the blues is all about. *Plant Physiol* **133:** 1429–1436

Lu YT, Hidaka H, Feldman LJ (1996) Characterization of a calcium/calmodulin-dependent protein kinase homolog from maize roots showing light-regulated gravitropism. *Planta* **199:**18–24

Ma L, Li J, Qu L, Hager J, Chen Z, Zhao H, Deng XW (2001) Light control of Arabidopsis development entails coordinated regulation of genome expression and cellular pathways. *Plant Cell* **13:**2589–2607

Malamy JE, Benfey PN (1997a) Organisation and cell in lateral roots of Arabidopsis thaliana. *Development* **124:**33-44

Malamy JE, Benfey PN (1997b) Down and out in Arabidopsis: the formation of lateral roots. *Trends Plant Sci* **2:** 390-396

Malhotra K, Kim ST, Batschauer A, Dawut L, Sancar A (1995) Putative blue-light photoreceptors from Arabidopsis thaliana and Sinapis alba with a high degree of sequence homology to DNA photolyase contain the twophotolyase cofactors but lack DNA repair activity. *Biochemistry* **34:** 6892–6899

Maloof JN, Borevitz JO, Dabi T, Lutes J, Nehring RB, Redfern JL, Trainer GT, Wilson JM, Asami T, Berry CC, Weigel D, Chory J (2001) Natural variation in light sensitivity of Arabidopsis. *Nat Genet* **29:**441- 446

Mandoli DF, Ford GA, Waldron LJ, Nemson JA, Briggs WR (1990) Some spectral properties of several soil types: implications for photomorphogenesis. *Plant Cell Environ* **13:** 287–294

Martinez-Garcia JF, Huq E, Quail PH (2000) Direct targeting of light signals to a promoter element-bound transcription factor. *Science* **288:** 859–863

Mas P, Devlin PF, Panda S, Kay SA (2000) Functional interaction of phytochrome B and cryptochrome 2. *Nature* **408:** 207-211

Mateos JL, Luppi JP, Ogorodnikova OB, Sineshchekov VA, Yanovsky MJ, Braslavsky SE, Gärtner W, Casal JJ (2006) Functional and biochemical analysis of the N-terminal domain of phytochrome A. *J Biol Chem* **281:** 34421–34429

Mathews S, Burleigh JG, Donoghue MJ (2003) Adaptive evolution in the photosensory domain of phytochrome A in early angiosperms. *Mol Biol Evol* **20:** 1087–1097

Mathews S, Lavin M, Sharrock RA (1995) Evolution of the phytochrome gene family and its utility for phylogenetic analyses of angiosperms. *Ann Mo Bot Gard* **82:** 296–321

Mathews S, Sharrock RA (1996) The phytochrome gene family in grasses (Poaceae): a phylogeny and evidence that grasses have a subset of the loci found in dicot angiosperms. *Mol Biol Evol* **13:** 1141–1150

Mathews S, Sharrock RA (1997) Phytochrome gene diversity. *Plant Cell Environ* **20:** 666–671

McCallum CM, Comai L, Greene EA and Henikoff S (2000b) Targeting induced local lesions in genomes (TILLING) for plant functional genomics. *Plant Physiol.* **123:** 439–442

McCallum CM, Comai L, Greene EA, Henikoff S (2000a) Targeted screening for induced mutations. *Nat. Biotechnol.* **18:** 455–457

Mejlhede N, Kyjovska Z, Backes G, Burhenne K, Rasmussen SK, Jahoor A (2006) EcoTILLING for the identification of allelic variation in the powdery mildew resistance genes *mlo* and *Mla* of barley. *Plant Breeding* **125:** 461-467

Menda N, Semel Y , Peled D, Eshed Y, Zamir D (2004) In silico screening of a saturated mutation library of tomato. *Plant J* **38:** 861-872

Migge A, Carrayol E, Hirel B, Lohmann M, Meya G Becker TM (1998) Regulation of the subunit composition of plastidic glutamine synthetase of the wild-type and the phytochrome-deficient aurea mutant of omato by blue-UV-A- or UV-B-light. *Plant Mol. Biol.* **37:** 689–700

Millar AJ (2003) A suite of photoreceptors entrains the plant circadian clock. *J Biol Rhythms* **18:** 217–226

Minoia S, Petrozza A, D'Onofrio O, Piron F, Mosca G, Sozio G *et al.* (2010) A new mutant genetic resource for tomato crop improvement by TILLING technology. *BMC Res. Notes* **3:** 69

Mockler TC, Guo H, Yang H, Duong H, Lin C (1999) Antagonistic actions of Arabidopsis cryptochromes and phytochrome B in the regulation of floral induction. *Development* **126:** 2073–2082

Mohr H (1983) Pattern specification and realization in photomorphogenesis. In W Shropshire Jr, H Mohr, eds, Encyclopedia Plant Physiol New Series, *Photomorphogenesis. Springer, Berlin* **16A:** 336-357

Møller SG, Ingles JP, Whitelam GC (2002) The cell biology of phytochrome signaling. *New Phytol.* **154:** 553–590

Montgomery BL, Lagarias JC (2002) Phytochrome ancestry: sensors of bilins and light. *Trends Plant Sci.* **7:** 357–366

Muday GK, Haworth P (1994) Tomato root growth, gravitropism, and lateral development: correlation with auxin transport. *Plant Physiol Biochem* **33:**193-203

Muramoto T, Kami C, Kataoka H, Iwata N, Linley PJ, Mukougawa K, Yokota A and Kohchi T (2005) The tomato photomorphogenetic mutant, *aurea*, is deficient in phytochromobilin synthase for phytochrome chromophore biosynthesis. *Plant and Cell Physiol* **46:** 661–665

Nagai M, Yoshida A, Sato N (1998) Additive effects of bovine serum albumin, dithiothreitol, and glycerol on PCR. *Biochem Mol Biol Int* **44:**157-163

Nagatani A (2004) Light-regulated nuclear localization of phytochromes. *Curr Opin Plant Biol* **7:**708-711

Nagatani A (2010) Phytochrome: structural basis for its functions. *Curr Opin Plant Biol* **13:** 565–570

Nagatani A, Chory J, Furuya M (1991) Phytochrome B is not detectable in the hy3 mutant of Arabidopsis, which is deficient in responding to end-of-day far-red light treatments. *Plant Cell Physiol.* **32:** 1119–1122

Nagatani A, Reed JW, Chory J (1993) Isolation and initial characterization of Arabidopsis mutants that are deficient in functional phytochrome A. *Plant Physiol* **102:** 269–277

Nagy F, Schafer E (2002) Phytochromes control photomorphogenesis by differentially regulated, interacting signalling pathways in higher plants. *Annu Rev Plant Biol* **53:**329–355

Neff MM, Fankhauser C, Chory J (2000) Light: an indicator of time and place. *Genes Dev.* **14:** 257–271

Negi S, Ivanchenko MG, Muday GK (2008) Ethylene regulates lateral root formation and auxin transport in Arabidopsis thaliana. *Plant J* **55:** 175-187

Negi S, Sukumar P, Liu X, Cohen JD, Muday G K (2010) Genetic dissection of the role of ethylene in regulating auxin-dependent lateral and adventitious root formation in tomato. *Plant J* **61:** 3-15

Nemhauser J, Chory J (2002) Photomorphogenesis. In E Meyerowitz, C Somerville, eds, The Arabidopsis Book. *American Society of Plant Biologists, Rockville, MD,* pp 1–12

Neuffer MG, Coe EH (1978) Paraffin oil technique for treating mature corn pollen with chemical mutagens. *Maydica* **23:**21–28

Neuhas G, Bowler C, Kern R and Chua NH (1993) Calcium/calmodulin-dependent and-independent phytochrome signal transduction pathways. *Cell* **73:** 27–35

Ni M, Tepperman JM, Quail PH (1998) PIF3, a phytochrome-interacting factor necessary for normal photoinduced signal transduction, is a novel basic helix-loophelix protein. *Cell* **95:** 657–667

Nieto C, Piron F, Dalmais M, Marco CF, Moriones E, Gomez-GuillamonML , Truniger V, Gomez P, Garcia-Mas J, Aranda MA, Bendahmane A (2007) EcoTILLING for the identification of allelic variants of melon eIF4E, a factor that controls virus susceptibility. *BMC Plant Biol* **7:**34

Ohno Y, Fujiwara A (1967) Photoinhibition of elongation growth of roots in rice seedlings. *Plant Cell Physiol.* **8:** 141-150

Oka Y, Matsushita T, Mochizuki N, Quail PH, Nagatani A (2008) Mutant screen distinguishes between residues necessary for light-signal perception and signal transfer by phytochrome *B. PLoS Genet* **4**: e1000158.

Okada K, Shimura Y (1992) Mutational analysis of root gravitropism and phototropism of Arabidopsis thaliana seedlings. *Aust. J. Plant Physiol.* 1**9:** 439-448

Ori N, Cohen AR, Etzioni A, Brand A, Yanai O, Shleizer S *et al.* (2007) Regulation of LANCEOLATE by miR319 is required for compound-leaf development in tomato. *Nat. Genet.* **39:** 787–791

Orr HA (2005) The genetic theory of adaptation: a brief history. *Nature Reviews Genetics* **6:** 119-127

Parks BM, Quail PH (1991) Phytochromedeficient *hy1* and *hy2* long hypocotyl mutants of Arabidopsis are defective in phytochrome chromophore biosynthesis. *Plant Cell* **3:** 1177–86

Parks BM, Quail PH (1993) hy8, a new class of Arabidopsis long hypocotyl mutants deficient in functional phytochrome A. *Plant Cell* **3:** 39–48.

Parks BM, Spalding EP (1999) Sequential and coordinated action of phytochromes A and B during Arabidopsis stem growth revealed by kinetic analysis. *Proc. Natl Acad. Sci. USA* **96:** 14142–14146

Peralta IE, Spooner DM (2005) Morphological characterization and relationships of wild tomatoes (Solanum L.Section Lycopersicon) *Monogr. Syst. Bot. Missouri Bot Gard*. **104:** 227-257

Perry JA, Wang TL, Welham TJ, Gardner S, Pike JM, Yoshida S Parniske M (2003) A TILLING reverse genetics tool and a web-accessible collection of mutants of the legume *Lotus japonicus*. *Plant Physiol*. **131:** 866–871

Poppe C, Hangarter RP, Sharrock RA, Nagy F Schäfer E (1996) The light-induced reduction of the gravitropic growth-orientation of seedlings of Arabidopsis thaliana (L.) Heynh. is a photomorphogenic response mediated synergistically by the far-red-absorbing forms of phytochromes A and B. *Planta* **199:** 511–514

Poppe C, Schäfer E (1997) Seed germination of *Arabidopsis thaliana* phyA/phyB double mutants is under phytochrome control. *Plant Physiol* **114:** 1487–1492

Pratt L H, Cordonnier-Pratt M.-M, Kelmenson PM, Lazarova G I, Kubota T, Alba RM (1997) The phytochrome gene family in tomato (Solanum lycopersicum L.). *Plant Cell Environ.* **20:** 672–677

Quail PH (1991) Phytochrome: A light-activated molecular switch that regulates plant gene expression. *Annu. Rev. Genet.* **25:** 389-409

Quail PH (1997) An emerging molecular map of the phytochromes. *Plant Cell Environ.* **20:** 657–666

Quail PH (2002) Phytochrome photosensory signalling networks. *Nat Rev Mol Cell Biol* **3:** 85–93

Quail PH, Boylan MT, Parks BM, Short TW, Xu Y, Wagner D (1995) Phytochromes: Photosensory perception and signal transduction. *Science* **268:**675–680

Reed JW, Nagatani A, Elich TD, Fagan M, Chory J (1994) Phytochrome A and phytochrome B have overlapping but distinct functions in *Arabidopsis* development. *Plant Physiol* **104:** 1139-1149

Reed JW, Nagpal P, Poole DS, Furuya M, Chory J (1993) Mutations in the gene for the red/far-red light receptor phytochrome B alter cell elongation and physiological responses throughout Arabidopsis development. *Plant Cell* **5:** 147–157

Reed RC, Brady SR, Muday GK (1998) Inhibition of auxin movement from the shoot into the root inhibits lateral root development in Arabidopsis. *Plant Physiol* **118:** 1369-1378

Rick CM, Uhlig JW, Jones AD (1994) High alpha tomatine content in ripe fruit of Andean Lycopersicon esculentum var. cerasiforme: Developmental and genetic aspects. *Proc Natl Acad Sci USA* **91:**12877-12881

Rizzini L, Favory JJ, Cloix C, Faggionato D, O'Hara A, Kaiserli E, Baumeister RE, Nagy F, Jenkins GI, Ulm R (2011) Perception of UV-B by the Arabidopsis UVR8 protein. *Science* **332:** 103-106

Robert VJM, West MAL, Inai S, et al. (2001) Marker assisted introgression of black mold resistance QTL alleles from wild Lycopersicon cheesmanii to cultivated tomato (L. esculentum) and evaluation of QTL phenotypic effects. *Molecular Breeding* **8:** 217-223

Robson PRH, Smith H (1996) Genetic and transgenic evidence that phytochromes A and B act to modulate the gravitropic orientation of Arabidopsis thaliana hypocotyls. *Plant Physiol*. **110:** 211–216

Rockwell NC, Su YS, Lagarias JC (2006) Phytochrome structure and signaling mechanisms. *Annu. Rev. Plant Biol.* **57:** 837 – 858

Saijo Y, Sullivan JA, Wang H, Yang J, Shen Y, Rubio V, Ma L, Hoecker U, Deng XW (2003) The COP1-SPA1 interaction defines a critical step in phytochrome A-mediated regulation of HY5 activity. *Genes Dev* **17:** 2642–2647

Saito T, Ariizumi T, Okabe Y, Asamizu E, Hiwasa-Tanase K, Fukuda N *et al.* (2011) TOMATOMA: a novel tomato mutant database distributing Micro-Tom mutant collections. *Plant Cell Physiol.* **52:** 283–296

Sakamoto K, Briggs W (2002) Cellular and subcellular localization of phototropin1. *Plant Cell* **14:** 1723–1735

Sakamoto K, Nagatani A (1996) Nuclear localization activity of phytochrome B. *Plant J* **10:** 859-868

Salisbury FJ, Hall A, Grierson CS, Halliday KJ(2007) Phytochrome coordinates Arabidopsis shoot and root development. *The Plant Journal* **50:** 429–438

Sancar A (2000) Cryptochrome: the second photoactive pigment in the eye and its role in circadian photorecpetion. *Annu. Rev. Biochem*. **69:** 31–67

Sancar A (2003) Stucture and function of DNA photolyase and cryptochrome blue-light photoreceptors. *Chem. Rev.* **103:** 2203−2237

Seo HS, Watanabe E, Tokutomi S, Nagatani A, Chua NH (2004) Photoreceptor ubiquitination by COP1 E3 ligase desensitizes phytochrome A signaling. *Genes Dev* **18:** 617-622

Seo HS, Yang JY, Ishikawa M, Bolle C, Ballesteros ML, Chua NH (2003) LAF1 ubiquitination by COP1 controls photomorphogenesis and is stimulated by SPA1. *Nature* **424**: 995–999

Shalata A, Tal M (1998) The effect of salt stress on lipid peroxidation and antioxidants in the leaf of the cultivated tomato and its wild salt-tolerant relative *Lycopersicon pennellii* P*hysiologia Plantarum* **104:** 169–174

Sharma R, López-Juez E, Nagatani A and Furuya M (1993) Identification of photoinactive phytochrome A in etiolated seedlings and photo-active phytochrome B in green leaves of the aurea mutant of tomato. *Plant J* **4:** 1035–1042

Sharrock RA, Clack T (2002) Patterns of expression and normalized levels of the five Arabidopsis phytochromes. *Plant Physiol* **130:** 442–456

Sharrock RA, Quail PH (1989) Novel phytochrome sequences in Arabidopsis thaliana: structure, evolution, and differential expression of a plant regulatory photoreceptor family.*Genes Dev* **3:** 1745–1757

Shinkle JR, Atkins AK, Humphrey EE, Rodgers CW, Wheeler SL, Barnes PW (2004) Growth and morphological responses to different UV wavebands in cucumber (Cucumis sativum) and other dicotyledonous seedlings. *Physiol Plant* **120:** 240–248

Shinomura T, Nagatani A, Hanzawa H, Kubota M, Watanabe M, Furuya M (1996) Action spectra for phytochrome A- and B-specific photoinduction of seed germination in *Arabidopsis thaliana*. *Proc Natl Acad Sci USA* **93:** 8129–8133

Simon MI, Strathmann MP, Gautham N (1991) Diversity of the G proteins in signal transduction. *Science* **252:** 802-808

Sineshchekov VA (2004) Phytochrome A: functional diversity and polymorphism. In: Braslavsky S (ed) Biological photosensors, special issue. *Photochem Photobiol Sci* **3:** 596–607

Slade AJ, Fuerstenberg SI, Loeffler D, Steine MN Facciotti D (2005) A reverse genetic, nontransgenic approach to wheat crop improvement by TILLING. *Nat. Biotechnol*. **23:** 75–81

Smith H (1982) Light quality, photoperception, and plant strategy. *Annu Rev Plant Physiol* **33:** 481-518

Smith H (1995) Physiological and ecological function within the phytochrome family. *Annu Rev Plant Physiol Plant Mol Biol* **46:** 289–315

Smith H (2000) Phytochromes and light signal perception by plants: an emerging synthesis. *Nature* **407:** 585–591

Smith H, Whitelam GC (1990) Phytochrome: A Family of photoreceptors with multiple physiological roles. *Plant Cell and Environment* **13:** 695-708

Smith H, Whitelam GC (1997) The shade avoidance syndrome: multiple responses mediated by multiple phytochromes. *Plant Cell Environ* **20:** 840–844

Smith TK, Long CM, Bowman B, Manos MM (1990) Using cosolvents to enhance PCR amplification. *Amplifications* **5:** 16-17

S**mits BMG, Mudde J, Plasterk RHA , Cuppen E** (2004) Target-selected mutagenesis of the rat. *Genomics*, **83**, 332–334

Somers DE, Sharrock RA, Tepperman JM, Quail PH (1991). The hy3 long hypocotyl mutant of Arabidopsis is deficient in phytochrome B. *Plant Cell* **3:** 1263–1274

Sreelakshmi Y, Gupta S, Bodanapu R, Chauhan VS, Hanjabam M, Thomas S, Mohan V, Sharma S, Srinivasan R, Sharma R (2010) NEATTILL: A simplified procedure for nucleic acid extraction from arrayed tissue for TILLING and other high-throughput reverse genetic applications. *Plant Methods* **6:**3

Stevens MA, Rick CM (1986) Genetics and breeding. In JG Atherton J Rudich, eds, The omato Crop: A scientific basis for improvement. *Chapman and Hall, London*, pp 36-109

Su YS, Lagarias JC (2007) Light-Independent Phytochrome Signaling Mediated by Dominant GAF Domain Tyrosine Mutants of *Arabidopsis* Phytochromes in Transgenic Plants *Plant Cell* **19:** 2124–2139

Sullivan JA, Deng XW (2003) From seed to seed: the role of photoreceptorsin Arabidopsis development. *Dev Biol* **260:** 289–297

Sullivan JH, Rozema J (1999) UV-B effects on terrestrial plant growth and photosynthesis. In J. Rozema (Ed.), Stratospheric Ozone Depletion: The Effects of Enhanced UV-B Radiation on Terrestrial Ecosystems Leiden. *Backhuys Publishers, The Netherlands*, pp 39-57

Suzuki T, Eiguchi M, Kumamaru T, Satoh H, Matsusaka H, Moriguchi K, Nagato Y and Kurata N (2008) MNU-induced mutant pools and high performance TILLING enable finding of any gene mutation in rice. *Mol. Genet. Genomics*, **279:** 213–223

Tajima F (1989) Statistical method for testing the neutral mutation hypothesis by DNA polymorphism. *Genetics* **123:** 585–95

Takano M, Kanegae H, Shinomura T, Miyao A, Hirochika H, Furuya M (2001) Isolation and characterization of rice phytochrome A mutants. *Plant Cell* **13:** 521–534

Takemiya A, Inoue S, Doi M, Kinoshita T, Shimazaki K (2005) Phototropins promote plant growth in response to blue light in low light environments. *Plant Cell* **17:** 1120-1127

Talamè V, Bovina R, Sanguineti MC, Tuberosa R, Lundqvist U, Salvi S (2008) TILLMore, a resource for the discovery of chemically induced mutants in barley. *Plant Biotechnol J* **6:** 477-485

Taylor BL, Zhulin IB (1999) PAS domains: internal sensors of oxygen, redox potential, and light. *Microbiol Mol Biol Rev.* **63:** 479–506

Tepperman JM, Zhu T, Chang HS, Wang X, Quail PH (2001) Multiple transcription-factor genes are early targets of phytochrome A signaling. *Proc Natl Acad Sci USA* **98**: 9437–9442

Terry MJ, Kendrick RE (1996) The aurea and yellow-green-2 mutants of tomato are deficient in phytochrome chromophore synthesis. *J. Biol. Chem.* **271:** 21681–21686

Terry MJ, Kendrick RE (1999) Feedback inhibition of chlorophyll synthesis in the phytochrome chromophore-deficient aurea and yellow-green-2 mutants of tomato. *Plant Physiol.* **119:** 143–152

Terry MJ, Ryberg M, Raitt CE, Page AM (2001) Altered etioplast development in phytochrome chromophore-deficient mutants. *Planta* **241:** 314–325

Till BJ, Cooper J, Tai TH, Colowit P, Greene EA, Henikoff S Comai L (2007b) Discovery of chemically induced mutations in rice by TILLING. *BMC Plant Biol*. **7:** 19.

Till BJ, Reynolds SH, Greene EA, Codomo CA, Enns LC, Johnson JE, Burtner C, Odden AR, Young K, Taylor NE, Henikoff JG, Comai L, Henikoff S (2003) Large-scale discovery of induced point mutations with high-throughput TILLING. *Genome Res* **13:** 524-530

Till BJ, Reynolds SH, Weil C, Springer N, Burtner C, Young K, Bowers E, Codomo CA, Enns LC Odden AR (2004) Discovery of induced point mutations in maize genes by TILLING. *BMC Plant Biol*. **4:** 12

Till BJ, Zerr T, Comai L, Henikoff S (2006) A protocol for TILLING and Ecotilling in plants and animals. *Nat. Prot* **1:** 2465-2477

Toledo-Ortiz G, Huq E, Quail PH (2003) The Arabidopsis basic/helix-loop-helix transcription factor family. *Plant Cell* **15:** 1749–1770

Torrey JG (1950) The induction of lateral roots by indoleacetic acid and root decapitation. *Am J Bot* **37:** 257–264

Torrey JG (1952) Effect of light on elongation and branching in pea roots. *Plant Physiol.* **27:** 591-602

Trewavas A, Gilroy S (1991) Signal transduction in plant cells. Trends Genet **7:** 356-361

Triques K, Sturbois B, Gallais S, Dalmais M, Chauvin S, Clepet C, Aubourg S, Rameau C, Caboche M, Bendahmane A (2007) Characterization of *Arabidopsis thaliana* mismatch specific endonucleases: application to mutation discovery by TILLING in pea. *Plant J*. **51**: 1116–1125

Usami T, Matsushita T, Oka Y, Mochizuki N, Nagatani A (2007) Roles for the N- and C-terminal domains of phytochrome B in interactions between phytochrome B and cryptochrome signalling cascades. *Plant and Cell Physiology* **48:** 424–433

van Tuinen A, Cordonnier-Pratt MM, Pratt LH, Verkerk R, Zabel P and Koornneef M (1997) The mapping of phytochrome genes and photomorphogenic mutants of tomato. *Theor Appl Genet* **94:** 115–122

Van Tuinen A, Kerckhoffs L, Nagatani A, Kendrick RE, Koornneef M (1995b) A temporarily red light-insensitive mutant of tomato lacks a light-stable, B-like phytochrome. *Plant Physiol* **108:** 939-947

Van Tuinen A, Kerckhoffs LHJ, Nagatani A, Kendrick RE, Koomneef M (1995a) Far-red light-insensitive, phytochrome A- deficient mutants of tomato. *Mo1 Gen Genet* **246:**133-141

Vankadavath RN, Hussain AJ, Bodanapu R, Kharshiing E, Basha PO, Gupta S, Sreelakshmi Y, Sharma R (2009) Computer aided data acquisition tool for high-throughput phenotyping of plant populations. *Plant Methods* **5:**18 doi:10.1186/1746-4811-5-18

Venema JH, Posthumus F, De Vries M, Van Hasselt PR (1999)Differential response of domestic and wild *Lycopersicon* species to chilling under low light: growth, carbohydrate content, photosynthesis and the xanthophyll cycle**.** Physiologia Plantarum **105:** 81–88

Vierstra RD(1993) Illuminating Phytochrome Functions. *Plant Physiol* **103:** 679–684

Von Arnim AG, Deng XW (1996) Light control of seedling development. *Annu Rev Plant Physiol Plant Mo1 Biol* **47:** 215-243

Wagner D, Fairchild CD, Kuhn RM, Quail PH (1996) Chromophorebearing NH2-terminal domains of phytochromes A and B determine their photosensory specificity and differential light lability. *Proc Natl Acad Sci USA* **93:** 4011–4015

Wagner JR, Brunzelle JS, Forest KT, Vierstra RD (2005) A light-sensing knot revealed by the structure of the chromophore binding domain of phytochrome. *Nature* **438:** 325-331

Wang C, Altieri F, Ferraro A, Giartosio A, Turano C (1993) The effect of polyols on the stability of duplex DNA. *Physiol Chem Phys Med NMR* **25:** 273-280

Wang H, Deng XW (2002) Arabidopsis FHY3 defines a key phytochrome A signaling component directly interacting with its homologous partner FAR1. *EMBO J* **21:**1339–1349

Wang H, Ma L, Habashi J, Li J, Zhao H, Deng XW (2002) Analysis of far-red lightregulated genome expression profiles of phytochrome A pathway mutants in Arabidopsis. *Plant J* **32:** 723–33

Wang YC, Cordonnier-Pratt MM, Pratt LH (1993) Spatial distribution of three phytochromes in dark-and light-grown Avena sativa L. *Planta.***189:** 391–396.

Weller JL, Murfet IC, Reid JB (1997) Pea Mutants with Reduced Sensitivity to Far-Red Light Define an Important Role for Phytochrome A in Day-Length Detection. *Plant Physiol* **114:** 1225-1236

Whitelam GC, Johnson E, Peng J, Carol P, Anderson ML, Cowl JS, Harberd NP (1993) Phytochrome A null mutants of Arabidopsis display a wild-type phenotype in white light. *Plant Cell* **5:** 757–76.

Whitelam GC, Patel S, Devlin PF (1998) Phytochromes and photomorphogenesis in Arabidopsis. *Phil. Trans. Roy. Soc. Lond. B.* **353:** 1445–1453

Wienholds E, van Eeden FJ, Kosters M, Mudde J, Plasterk RH, Cuppen E (2003b) Efficient target-selected mutagenesis in zebrafish. *Genome Res* **13:** 2700–2707

Wightman F, Thimann KV (1980) Hormonal factors controlling the initiation and development of lateral roots. I. Sources of primordia-inducing substances in the primary root of pea seedlings. *Physiologia Plantarum* **49:** 13-20

Winkler S, Schwabedissen A, Backasch D, Bökel C, Seidel C, Bönisch S, Fürthauer M, Kuhrs A, Cobreros L, Brand M and González-Gaitán M (2005) Target-selected mutant screen by TILLING in Drosophila.*Genome research* **15:** 718-723

Wong YS, McMichael RW Jr, Lagarias JC (1989) Properties of a polycation-stimulated protein kinase associated with purified Avena phytochrome. *Plant Physiol.* **91:** 709–718

Wu SH, Lagarias JC (2000) Defining the bilin lyase domain: lessons from the extended phytochrome superfamily. *Biochemistry* **39:**13487–13495

Wu WM, Tsai HJ, Pang JH, Wang HS, Hong HS, Lee YS (2005) Touchdown thermocycling program enables a robust single nucleotide polymorphism typing method based on allele-specific real-time polymerase chain reaction. *Anal. Biochem.* **339:** 290–296

Xiong LM, Stomacher KS, Hi FK (2002) Cell singling during cod, drought, and calf saffron. *Plant Cell (Suppl)* S156–S183

Yamaguchi R, Nakamura M, Mochizuki N, Kay SA, Nagatani A (1999) Light-dependent translocation of a phytochrome B–GFP fusion protein to the nucleus in transgenic Arabidopsis. *J Cell Biol* **145:** 437-445

Yamashino T, Matsushika A, Fujimori T, Sato S, Kato T, Tabata S, Mizuno T (2003) A Link between circadian-controlled bHLH factors and the APRR1/TOC1 quintet in Arabidopsis thaliana. *Plant Cell Physiol* **44:** 619–629

Yanovsky MJ, Kay SA (2002) Molecular basis of seasonal time measurement in Arabidopsis. *Nature* **419:** 308–312

Yeh KC, Lagarias JC (1998) Eukaryotic phytochromes: light-regulated serine/threonine protein kinases with histidine kinase ancestry. *Proc Natl Acad Sci USA* **95:**13976–13981

Zhang J, Stankey RJ, Vierstra R D (2013) Structure-guided engineering of plant phytochrome B with altered photochemistry and light signaling. *Plant Physiol* **3:** 1445-1457

Zhang ZB, Xu P, Zhang JH, Wang J (2002) Advance on study of molecular marker and gene cloning and transgenes in drought resistance and water saving in crops. *Acta Bot Boreal-Occident Sin* **22:** 1537–1544